THE EFFECT OF CLAY CONTENT AND TYPE ON OIL RECOVERY FROM SANDSTONE CORES USING HIGH PH CHELATING AGENTS

BY

AHMED ABDULHAMID AHMED MAHMOUD

A Thesis Presented to the

DEANSHIP OF GRADUATE STUDIES

KING FAHD UNIVERSITY OF PETROLEUM & MINERALS

DHAHRAN, SAUDI ARABIA

In Partial Fulfillment of the
Requirements for the Degree of

MASTER OF SCIENCE

In

PETROLEUM ENGINEERING

May 2015

KING FAHD UNIVERSITY OF PETROLEUM & MINERALS

DHAHRAN- 31261, SAUDI ARABIA

DEANSHIP OF GRADUATE STUDIES

This thesis, written by **AHMED ABDULHAMID AHMED MAHMOUD**, under the direction his thesis advisor and approved by his thesis committee, has been present and accepted by the Dean of Graduate Studies, in partial fulfillment of the requirements for the degree of **MASTER OF SCIENCE IN PETROLEUM ENGINEERING.**

Dr. Hasan S. Al-Hashim
(Advisor)

Dr. Abdullah S. Sultan
Department Chairman

Dr. Ahmet U. Dogan
(Member)

Dr. Salam A. Zummo
Dean of Graduate Studies

Dr. Mohamed A. Mahmoud
(Member)

14/6/15
Date

This work is dedicated to my lovely parents, sister, brother, and my fiancée

ACKNOWLEDGMENTS

Glory and praise be to Allah the almighty, first and foremost, for every success I found, and knowledge been developed throughout this work.

Acknowledgement is due to King Fahd University of petroleum & minerals for the scholarship I have been given to pursue my master degree in petroleum engineering.

My sincere gratitude goes to my thesis advisor, Dr. Hasan Salman Al-Hashim, for allowing me to join his research activities and for the trust he put in me, and for his professional guidance during the course of my thesis work. I would like to extend my thanks to my committee members, Prof. Ahmet U. Dogan and Dr. Mohamed Mahmoud for their valuable comments, contributions and guidance.

I also would like to thank the department of petroleum engineering represented by the chairman, Dr. Abdullah Sultan, for allowing me to use the department's laboratories and equipment to carry out my work, and for his valuable support during ordering of the consumables and materials for my thesis work through the Center for Petroleum & Minerals of the Research Institute.

TABLE OF CONTENTS

LIST OF TABLES

LIST OF FIGURES

LIST OF ABBREVIATIONS

CEOR	:	Chemical Enhanced Oil Recovery
EDTA	:	Ethylenediaminetetraacetic Acid
EOR	:	Enhanced Oil Recovery
FESEM	:	Field Emission Scanning Electron Microscope
ICP	:	Inductively Coupled Plasma
Na_2EDTA	:	Di-Sodium Ethylenediaminetetraacetic Acid
NMR	:	Nuclear Magnetic Resonance
PPM	:	Parts Per Million
PXRD	:	Powder X-Ray Diffraction
SEM	:	Scanning Electron Microscope
SFB	:	Synthetic Seawater
SSW	:	Synthetic Formation Brine
TDS	:	Total Dissolved Solids
TO	:	Tetra-Octa Clay Minerals
TOT	:	Tetra-Octa-Tetra Clay Minerals
UTMN	:	Uthmania Crude Oil
XRF	:	X-Ray Fluorescence

ABSTRACT

Full Name : Ahmed Abdulhamid Ahmed Mahmoud

Thesis Title : The Effect of Clay Content and Type on Oil Recovery from Sandstone Cores Using High pH Chelating Agent

Major Field : Petroleum Engineering

Date of Degree : May 2015

In this study the effect of the presence of clay minerals on oil recovery from sandstone reservoirs using EDTA chelating agent was investigated. Two different sandstone types with different mineralogical composition were used in this study; those are Gray Berea and Gray Bandera sandstones.

Core flooding experiments were carried out on both sandstone core samples using composite cores to optimize the concentration of the chelating agent required to maximize the oil recovery in the presence of clay minerals. The pressure drop and pH were monitored during the coreflood experiments and the effluent samples were collected as a function of pore volume, the collected effluent samples were analyzed using ICP and IC analyses to determine the change of the concentration of the different elements to understand the mechanism of the interaction of the EDTA solutions with the rock constituents specifically the clay minerals.

The effect of different clay minerals present in the rock samples used in this study on the ultimate oil recovery as well as on the different reservoir properties is presented and the

effect of the EDTA chelating agent on the composition of the clays and their main layers is also investigated.

The effect of EDTA chelating agent solutions on the change of the wettability of the sandstone samples and the stability of the water film around the rock surfaces were studied through the zeta-potential measurements at rock/brine surface using crushed rock samples in the presence and absence of the crude oil. The effect of the change of the pH on the stability of the water film was also studied for both seawater and chelating agent solutions.

The effect of the EDTA chelating agent on the forces between this chemical and the crude oil phases was studied through the interfacial tension measurements, and the enhancement introduced by those chemicals was compared to that achieved by the seawater.

The 5wt% EDTA in seawater solution was found to be the optimum concentration which resulted in the highest recovery without effecting the rock integrity. The maximum oil recovered from Gray Berea sandstone with the 5wt% EDTA solution was slightly higher than 15.00% of OOIP compared to about 6.30% of OOIP recovered from Gray Bandera sandstone samples this is due to the very low permeability of Gray Bandera cores due to the presence of high amount of illite and a considerable quantity of kaolinite in those samples. Addition of 5wt% of EDTA in seawater reduced the IFT from 20.58mN/m in case of seawater to 5.29mN/m in case of 5wt% EDTA solution. Zeta potential of the 5wt% Na_4EDTA/crushed rock samples at pH of 12.00 were -21.07 mV and -28.02 mV for Gray Berea and Gray Bandera respectively.

ملخص الرسالة

الاسم الكامل : أحمد عبدالحميد أحمد محمود

عنوان الرسالة : دراسة تأثير المعادن الصلصالية على المستخلص النهائي من النفط الخام بإستخدام العوامل المخلبية عند درجات الحموضة العالية

التخصص : هندسة نفط

تاريخ الدرجة العلمية : مايو 2015

تهدف هذه الرسالة لدراسة تأثير وجود المعادن الصلصالية علي الإنتاج الزيت (النفط) من المكامن الرملية بإستخدام العامل المخلبي EDTA. في هذه الدراسة تم إستخدام نوعين من الصخور الرملية القياسية مختلفين من حيث التركيب المعدني بالأخص من حيث نسبة المعادن الصلصالية.

تم إجراء تجارب الحقن على النوعين من الصخور الرملية المستخدميتن في هذه الدراسة في محاولة لتحديد التركيز المثالي من المركب الكيميائي اللازم لإنتاج أكبر قدر من النفط المتبقي داخل المكامن الرملية بعد فترة الإزاحة بالماء، خلال هذه التجارب تمت مراقبة تغير فرق الضغط خلال العينات المستخدمة، كما تم تجميع السوائل المنتجة والتي تم قياس تغير درجة الحموضة لها فيما بعد وكذلك أستخدمت هذه العينات من السوائل لمعرفة الآلية التي أدت لزيادة إنتاج النفط الخام بإستخدام هذه العوامل المخلبية وذلك من خلال دراسة تغير التركيب الأيوني لهذه السوائل المنتجة خلال هذه التجارب ومقارنته بالتركيب الأيوني للمواد التي تم حقنها. هذا التغير في التركيب الكيميائي كذلك يمكن من خلاله معرفة آلية التفاعل بين المواد الكيميائية المستخدمة والمعادن الصلصالية المكونة للصخور.

كذلك تم دراسة تأثير وجود المعادن الصلصالية على الخواص المختلفة للمكامن الرملية ومدى تأثير ذلك على المستخلص النهائي من الخام. وكذلك تمت الإشارة إلى مدى التفاعل بين العوامل المخلبية المستخدمة في هذه الدراسة مع المعادن الصلصالية المختلفة الموجودة في الصخور المستخدمة في هذه الدراسة.

كما أيضا تمت دراسة تأثير تغيير نسبة العوامل المخلبية علي درجة تبلل الصخور الرملية وعلى درجة ثبات الطبقة المائية المحيطة بالجزيئات الصخرية من خلال إجراء قياسات شحنة الصخور على الأسطح الفاصلة بين الصخور

والطبقة المائية من خلال دراسة الشحنات في هذه الأسطح عند غياب ووجود الزيت. كذلك تم إختبار تأثير درجة حموضة المركب الكيميائي على درجة إستقرار هذه الطبقة المائية.

أجريت قياسات التوتر السطحي لمقارنة تأثير إستخدام المركبات المخلبية وماء البحر على قوة الترابط بين هذه المركبات والخام النفطي.

أثبتت نتائج هذه الدراسة بأن التركيز 5% (تركيز وزني) هو التركيز المثالي من الناحية الإقتصادية وكذلك من ناحية تأثيره علي سلامة الصخور. أقصى زيادة في الإنتاج النفطي بإستخدام هذا التركيز كانت أكثر بقليل من 15.00% من الصخور Gray Berea بينما كانت الزيادة حوالي 6.30%عند إستخدام صخور Gray Bandera. إضافة 5% (تركيز وزني) من العامل المخلبي EDTA لماء البحر أدت لتقليل القوة الرابطة بين النفط وماء البحر من 20.58 ملي نيوتن/متر إلى5.29 ملي نيوتن/متر. كما وجد أن شحنة الصخور عند السطح الفاصل بين الصخور و 5% تركيز وزني من العامل المخلبي EDTA عند درجة الحموضة 12.00 كانت (21.07-) ملي فولت و (28.02-) ملي فولت عند إستخدام Gray Berea و Gray Bandera على التوالي.

CHAPTER 1

INTRODUCTION

Oil recovery operations have been subdivided into three stages: primary recovery, secondary recovery, and tertiary recovery or enhanced oil recovery (EOR). During the primary recovery stage, the reservoir is depleted naturally depending on its natural forces. The sources for those natural reservoir forces are: the expansion of fluids and compaction of rocks, solution gas drive, the gravity drainage and the influx of water from aquifer (Willhite, 1986; Green and Willhite, 1998).

As the reservoir pressure start declining and its natural forces are depleted, the gas dissolved into the liquid will start liberating. At this stage another recovery method must be used to help moving the remaining oil through porous media toward the production wells. So shifting to the secondary recovery period (or waterflooding) to maintain the reservoir pressure, to keep the gas phase dissolved into the liquid phase (oil), and to push the oil toward the producing wells is must, several authors attributed the success of this stage of oil recovery to the quality of the injected water rather than its quantity (McGuire et al., 2005; Austad et al., 2010; Rezaeidoust et al., 2010).

After a period of time and with the increase of water to oil ratio the oil production rate will become economically invisible; so switching to the third stage become mandatory to keep producing the field economically. During this stage different fluids like: miscible gas, chemicals or thermal energy are introduced into the reservoir to recover additional oil from the reservoirs. For example, lowering the interfacial tension (IFT) between crude oil and

brine phases, oil swelling, oil viscosity reduction, water viscosity increase or rock surface wettability modification to more water-wet conditions (Willhite, 1986).

Some researchers consider the quality of the injected water rather than its quantity has a major role in changing the wettability and hence increasing the oil recovery. Depending on that they consider the low salinity water injection as an EOR technique (Bernard, 1967; Tang and Morrow, 1997; Morrow et al., 1998; Tang and Morrow, 1999; Loahardjo et al., 2007).

Injection of fluids (especially chemicals) into sandstone oil reservoirs is a very crucial and sensitive decision since those kind of reservoirs are dominated by different minerals: quartz, carbonates, feldspars, oxides, and clays. Because of their sheet morphology, surface area, very small grain size and their distribution through the pore system clay minerals surfaces are considered as the most dominant reactive surfaces seen by oil particles (Shehata and Nasr-el-din, 2014). Different types of clays are present in sandstone reservoirs such as: illite, chlorite, kaolinite, smectite and vermiculite.

Also clay minerals sometimes show extreme reactivity toward water especially smectite clays group: montmorillonite, beidellite, nontronite, saponite, and hectorite clays (Moore and Reynolds, 1997). Although illite and kaolinite group clay minerals are not swellable clays but also they could be effected by the quality of the injected water and its compatibility with those clays (Moore and Reynolds, 1986; Abbasi et al., 2011).

Clay minerals are very sensitive to the injected fluids. Injection of low salinity water into clayey sandstone reservoir may result in a favorable or unfavorable results depending on the type of clay, clay swelling may results in plugging the pores and significantly reduce

the permeability of the reservoir and increase the pressure drop (Bernard, 1967). On the other hand injection of low salinity water in certain reservoirs may results in better oil recovery (Cissokho et al., 2010).

Chemical enhanced oil recovery fluids are usually diluted with seawater before they injected into reservoirs, the seawater is usually treated before mixing with those chemicals to remove some of the active cations present in it which are responsible for some problems usually encountered in oil fields such as: equipments corrosion due to high salinity, precipitation of salts from seawater at high temperature and pressure conditions, and formation of fogies and some organic components which are responsible for plugging of the pore system.

The process of seawater treatment is costly but it is required to prevent the problems of already mentioned, on the other hand, treatment of the seawater before injection into oil reservoirs and the decrease in the salinity of the injected brine than that of the initial formation brine could effect on the swellable clay minerals.

Clay minerals and the relationship between their presence and distribution inside the pore system and the in-situ adsorption of crude oil was a debatable issue. Several authors attributed the increase in oil recovery at secondary or tertiary modes to the presence of the kaolinite and its very large size which increase its surface contact area with the crude oil and result in adsorbing higher amounts of the crude oil (Lebedeva and Fogden, 2011; Fogden, 2012; Hematfar et al., 2013). Tang and Morrow (1999) considered the dispersion of kaolinite after low salinity injection as the main mechanism for increasing oil recovery. On the other hand, Cissokho et al. (2010) confirmed that the increase in the ultimate oil

recovered by injecting alkaline/surfactant/polymer solutions although it requires the presence of clay minerals but it does not necessary requires the presence of kaolinite type clays.

Chelating agents were first introduced as chemical enhanced oil recovery by Attia (2013) and Abdelgawd (2013). These chemicals have the ability to be injected at high pH which could result in breaking down the equilibrium initially stablished between crude oil and rock, also they could be mixed with the seawater without any pretreatment needed for the seawater, the chelating agents could prevent problems like corrosion and precipitation since they have the ability to deactivate the active cations from interaction with other materials.

1.1 Objectives

The main objective of this study is to develop a fundamental understanding about the role of the clay minerals on oil recovery from sandstone core samples when flooded with EDTA chelating agent as a chemical enhanced oil recovery (CEOR) fluid. To achieve this objective, the following objectives are specified.

1. To evaluate the impact of different clay content on oil recovery using Na_2EDTA chelating agent.
2. To determine the optimum Na_2EDTA concentration leading to the highest oil recovery from sandstone core samples in the presence of clays.

3. To understand the mechanism leading to additional oil recovery using Na_2EDTA chelating agents.
4. To understand the role of iron (Fe) on oil recovery using Na_2EDTA chelating agent.

1.2 Thesis Organization

This thesis is organized into five chapters as follows:

Chapter one: This chapter presents a prelude to this research and the different objectives of this study.

Chapter two: Summarizes the literature review related to clay minerals composition, classification, different physical and chemical properties and how the interaction of these clay minerals with the injected fluids will effect on different sandstone reservoir properties. This chapter also present a review of different chelating agents and the chelation chemistry of these chemicals. The suggested mechanisms of oil recovery from sandstone reservoirs were also discussed.

Chapter three: The different materials used in this study as well as the work methodology followed and both constant and variable parameters considered in different experiments are reported in this part of the report.

Chapter four: This chapter contains all the results of different experiments conducted during this study and the explanation of those outcomes and how they are logically related to each other.

Chapter five: The fifth chapter presents the conclusions and recommendations for further studies in this area of research.

CHAPTER 2

LITERATURE REVIEW

2.1 Rock Wettability Concept and Its Impact on Oil Recovery

"Wettability is the tendency of one fluid to spread on or adhere to a solid surface in the presence of other immiscible fluids", and applying this term to reservoir engineering, oil and gas are the fluids and the reservoir rocks are the solid surface (Craig, 1971).

At first the reservoir rocks are saturated with water "wetted with water" after oil migration into the reservoir the possibility for alteration of the reservoir rocks wettability to more oil wet condition will increase as a result of adsorption and deposition of polar compounds and organic materials from crude oil (Fogden, 2012; Anderson, 1986).

The interaction of oil components, the chemistry of the brine water and the minerals at the rocks surface are the main factors those are controlling the process of wettability alteration. Because of its control on the location, distribution and flow of fluids inside the reservoir layer pores the wettability has an important role in determining the oil recovery efficiency and the residual oil saturation after waterflooding process (Anderson, 1986).

Beside oil composition, surface rock and aqueous phase chemistry, the temperature, pressure, and the contact time can be considered as important parameters affecting the rock wettability. Any wettability modification will affect the capillary pressure between oil and water, and hence, the effective permeability of fluids in the reservoir and waterflooding behavior (Alotaibi et al., 2011).

The fluids displacement effectiveness and hence the ultimate oil recovery by drive fluids (e.g. water) is mainly controlled by the reservoir rocks wettability. The smallest and most resistive pore channels are occupied by the most wetting phase while the least wetting phase occupies the largest pore channels as shown in Figure 2.1. In case of multiphase flow, phase trapping are critically controlled by the reservoir rock wettability (Craig, 1971; Abdallah et al., 2007).

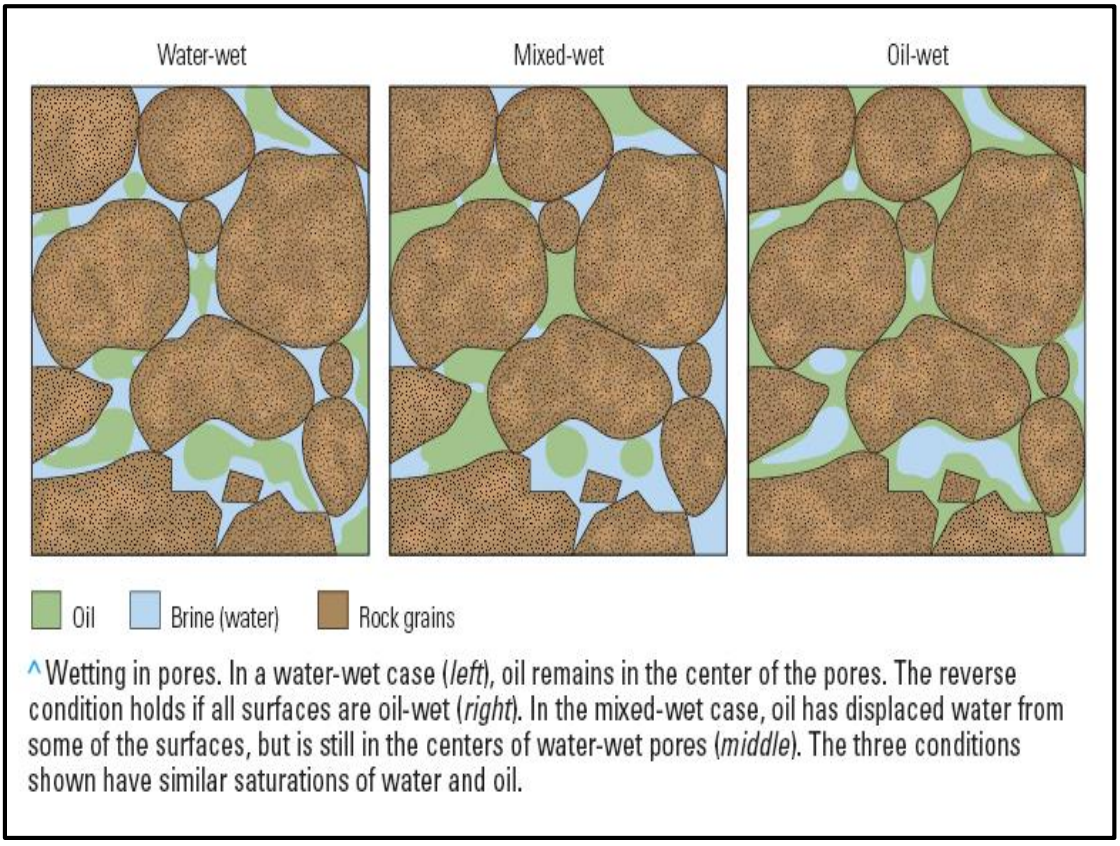

^Wetting in pores. In a water-wet case (*left*), oil remains in the center of the pores. The reverse condition holds if all surfaces are oil-wet (*right*). In the mixed-wet case, oil has displaced water from some of the surfaces, but is still in the centers of water-wet pores (*middle*). The three conditions shown have similar saturations of water and oil.

Figure 2.1: Fluids Distributions in Pores, Water-Wet "Left", Mixed-Wet "Middle" and Oil-Wet "Right" (Abdallah et al., 2007).

The change in rock wettability could be indicated through different measurements including zeta-potential (ζ), interfacial tension and contact angle measurements.

2.1.1 Zeta-Potential (ζ)

"Zeta potential, or as sometimes called electrokinetics, measures the difference in electrical charge between the dense layer of ions surrounding the particle and the charge of the bulk of the suspended fluid surrounding the particles", (Strand et al., 2006).

The rock surface is surrounded by water film and then crude oil layer, the stability of this film is the main factor controlling the rock wettability. The stability of the water film itself depends on the surface electrical charges at the interfaces of surface rock/water and water/crude oil. (Hirasaki, 1991; Dubey and Doe, 1993; Nasralla and Nasr-El-Din, 2011).

Oil-wet rock is the result of unstable water film so to change the rock wettability toward more water-wet conditions a stable water film should be developed, thus if a water with salinity differ than the formation brine is injected into the reservoir it may result in improving or suppressing the oil recovery. This depends on the trend of the change of the electrical charges at oil/brine and rock/brine interfaces caused by the injected water. Adsorption of crude oil to the rock surfaces is controlled by the charges signs at the oil/brine and rock/brine interfaces and their magnitude, when the same sign is present at both interfaces then they will repulse each other and as the magnitude of the charge increases this repulsion force will increase, and vice versa. As the repulsion forces increase the rock wettability is change to more water-wet rock due to the stability and the increase in the thickness of water film surrounding the rock (Nasralla and Nasr-El-Din, 2011).

Nasralla and Nasr-El-Din (2011) studied the impact of cations type and concentration on the electrical surface charges at both surface rock/brine and brine/crude oil interfaces, on their work they used Berea sandstone, two different crude oils and three different synthetic

solutions of NaCl, $CaCl_2$, and $MgCl_2$ at three different concentrations of 5wt%, 1wt%, and 0.2wt% as bines. They reported that zeta potential at both interfaces strongly depends on the cations type and concentration, the charges at crude oil/brine interface are negative for both crude oils they used with all brines except 5wt% $CaCl_2$. At Berea sandstone surface/different brines interfaces, the NaCl solution unlike other solutions showed strong negative charge with Berea sandstone even at higher concentration, the positive charge was noticed only for 5wt% calcium chloride solution while the MgCl solution has a weakly negative charge at the same concentration.

Nasralla and Nasr-El-Din (2011) repeated the same measurements on different types of clay minerals (kaolinite, illite, chlorite, and montmorillonite), the results of those measurements are shown in Figure 2.2 which indicates that all clays behave similarly as Berea sandstone. 0.2wt% NaCl solution results in the highest negatively charge, the magnitude of the negative charge resulted from using 5wt% NaCl is higher than that of 0.2wt% of $CaCl_2$ or $MgCl_2$ with all clays types; which indicate that the effect of the type of cation on electrical surface is the dominant effect. Also the surface charge is positive for kaolinite with all concentrations of $CaCl_2$ and $MgCl_2$ solutions except for 0.2wt% solution, which mean that the rock surface also has an impact on the charge.

Nasralla and Nasr-El-Din (2011) concluded that the NaCl solution has the highest repulsion forces between the oil/brine and solid/brine interfaces among the studied solutions; because the same sign "negative" is present at both interfaces and its magnitude is high.

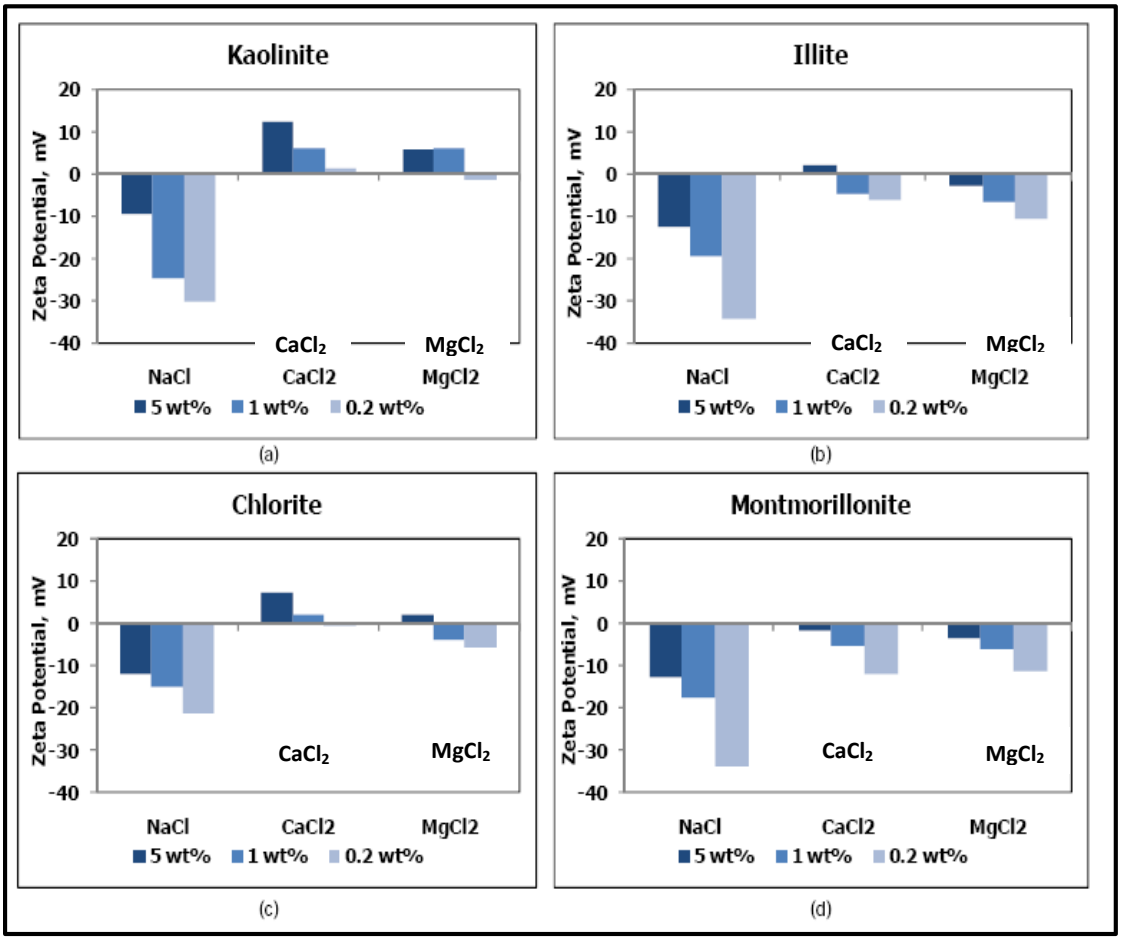

Figure 2.2: Zeta Potential at Various Clays/Brines Interfaces (Nasralla and Nasr-El-Din, 2011).

Nasralla and Nasr-El-Din (2012) studied the effect of changing the injected brine pH on zeta potential of Berea sandstone by using two different brines 5 Kmg/L NaCl and the 10 times diluted aquifer water (10% AQ), they found that increasing the pH of the injected water will result in increasing the stability of the water film due to the reduction in the negative magnitude of the surface charges at both oil/brine and rock/brine; as a result the rock wettability will be changed into more water wet conditions.

2.2 Clay Minerals

Clay minerals are hydrous aluminum phyllosilicates. A large fraction of sedimentary rocks (especially sandstones) are occupied by clay minerals, these minerals are considerably different in their physical and chemical properties, but all of them are less than two micrometers (except of kaolinite group clays with size of up to 10 micrometers). (Moore and Reynolds, 1997).

Clay minerals are composed of two types of sheets shown in Figure 2.3; the tetrahedral sheet (T) with the dominant Si^{+4}, Al^{+3}, and/or Fe^{+3} cations forming four-fold coordination with O^{-2}, and the octahedral sheet (O) with dominant Mg^{+2}, Mn^{+2}, Li^{+2}, Ti^{+2}, Fe^{+2}, Fe^{+3}, and Al^{+3} cations forming six-fold coordinations with O^{-2} and/or OH^{-} anions. According to their structure clay minerals are divided into two types: TO or 1:1 layers type clay minerals which contains the kaolinite group, and the TOT or 2:1 layers type clay minerals which contains smectite, illite, chlorite, and vermiculite clay minerals groups. TO clay minerals are uncharged clays while TOT clays contain an interlayer sheet to compensate for the charge deficiency at TOT layer. Table 2.1 summarizes the classification of clay minerals (Moore and Reynolds, 1997).

The primary cause of the petroleum bearing formation damage is the interaction of brine (specially injected water) with clay minerals. There are two main interactions of rock-fluid in sedimentary formations: "(1) chemical reactions resulting from the contact of rock minerals with incompatible fluids, and (2) physical processes caused by excessive flow rates and pressure gradients" (Mahmoud et al., 2011a).

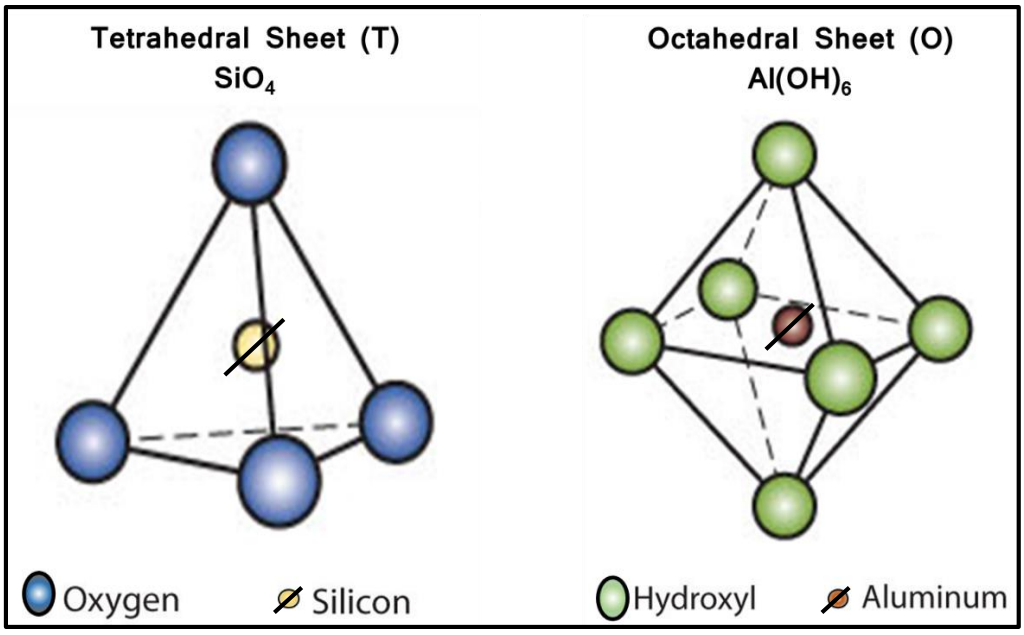

Figure 2.3: The Tetrahedral and Octahedral Sheets of Clay Minerals.

Table 2.1: Clay Minerals Classification (Moore and Reynolds, 1997).

Layer Type	Group	Subgroup	Species
1:1 (TO)	Kaolinite	Kaolinite (Di)	Kaolinite, dickite, nacrite, halloysite.
2:1 (TOT)	Smectite	Di smectite	Montmorillonite, beidellite, nontronite.
		Tri smectite	Saponite, hectorite.
	Illite	Di illite	Illite.
		Tri illite?	-
	Chlorite	Di, Di chlorite	Donbassite, gibbsite.
		Di, Tri chlorite	Sudoite, cookeite, bracite.
		Tri, Tri chlorite	Brucite, clinochlore.
	Vermiculite	Di vermiculite	Not common
		Tri vermiculite	-

2.2.1 The Impact of Clay Minerals on Oil Reservoirs Rock Properties

The presence of clay minerals in pore spaces of oil reservoirs will effect on the different reservoir properties especially porosity and permeability. This is related to the behavior of clay minerals in the pore spaces, according to Neasham (1977) clay minerals behave in three different ways in porous media as summarized bellow.

1. Pore filling: Some clay minerals specially kaolinite which is a highly dispersible and large sized clay with size of about 10 micrometers is preferentially deposited inside the pore or at the entrance to the pore throat; as a result they will decrease the system permeability or in many cases they will totally damage it as illustrated in Figure 2.4.a. Presence of chlorite and smectite also may cause this problem especially Fe rich chlorite which has the ability to form a gel when it reacts with the injected fluids, the ability of these clay minerals to block or fill the pores is depends on the size of clay minerals as well as the pore throat diameter (Moore and Reynolds, 1986).
2. Pore lining: Chlorite has a higher ability to line the grains surfaces and reduces the effective porosity, as a result it will effect on the total reserve in oil reservoirs. Illite and smectite also effect the system porosity as indicated in Figure 2.4.b.
3. Pore bridging: In this situation the clay particles will make bridges in the pore body, this will result in significant reduction in both porosity and permeability (e.g., illite) as shown in Figure 2.4.b.

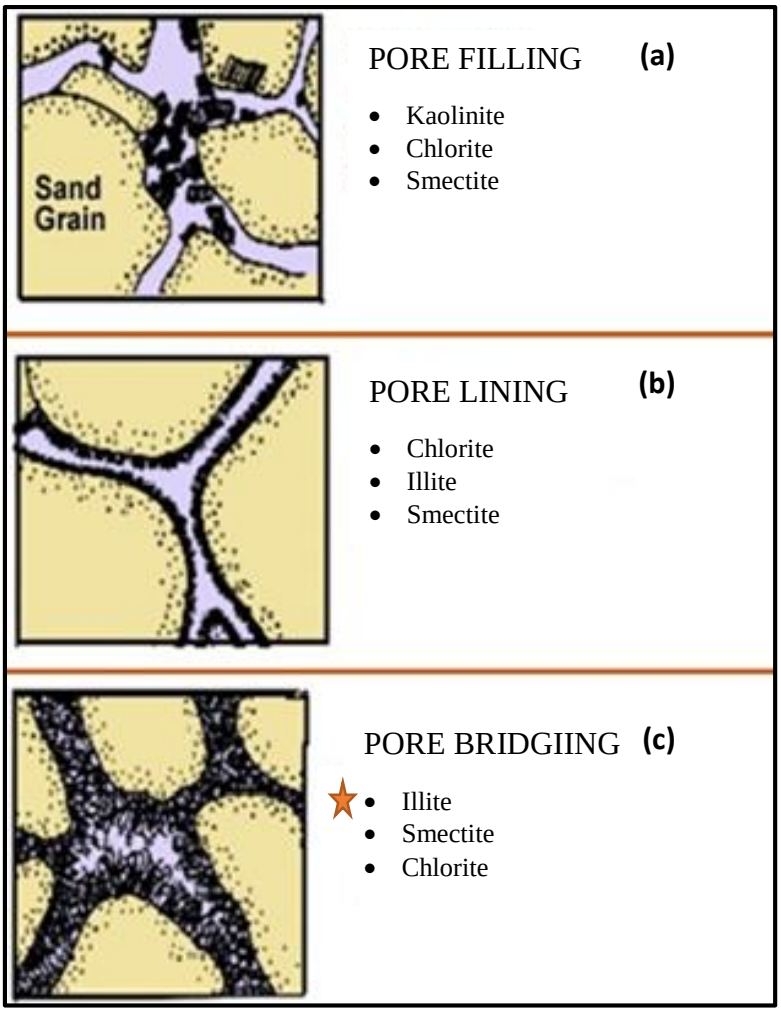

Figure 2.4: The Behaviors of the Clay Minerals inside the Pore Spaces (Neasham, 1977).

The worst situation is usually encountered in the case of the presence of both pore filling large sized kaolinite clays and pore bridging illite clays within the same pore system; in this case although both clays are not expandable but the movement of highly dispersible kaolinite and its accumulation on illite bridges may totally block the pore system and effect on the porosity and oil effective permeability.

2.2.2 Clay/Oil Attraction by Divalent Cations

There are different mechanisms proposed for oil attraction onto clay minerals surfaces. Lager et al. (2008) explained the four main mechanisms proposed for the adsorption of crude oil polar components onto the clay minerals surfaces as a result of oil interaction with clays through the interlayer cations. Figure 2.5 below shows schematically these four mechanisms.

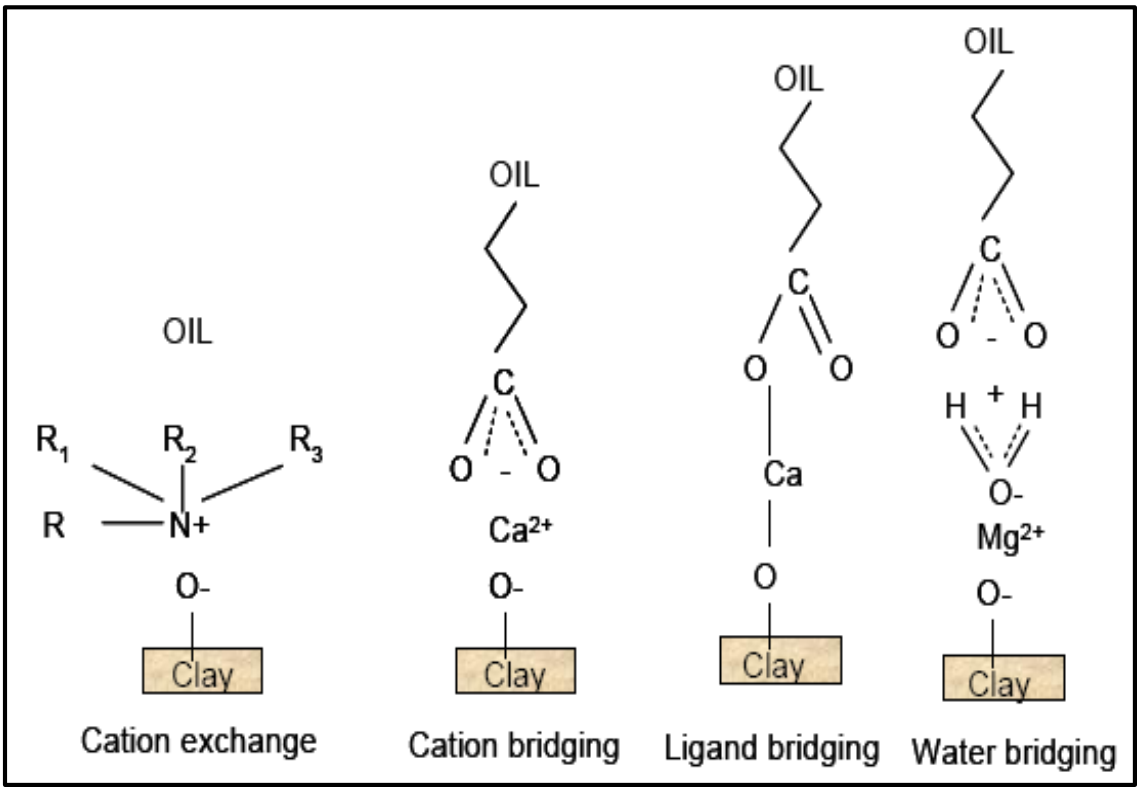

Figure 2.5: The Suggested Mechanisms of Crude Oil Adsorption onto the Surface of Clay Minerals (Lager et al., 2008).

These mechanisms are based on the reaction of interlayer cations with the crude oil which occur in the following forms:

Cation exchange: This usually happens when an oil molecule containing a quaternized nitrogen or heterocyclic ring replaces an interlayer cation initially bond to the clay surface; as a result the oil molecule will be adsorbed onto the clay surface.

Cation bridging: A weak adsorption of oil particles onto the surface of clay is occurred through the interaction with the interlayer cations.

Ligand bridging: When the interlayer cation has a strong covalent bond with both the oil polar molecule and the clay minerals, it results in oil adsorption onto clay surface.

Water bridging: If an interlayer cation is solved into water molecules, the complexation between both the water molecules solved an interlayer cation and oil molecules will lead into oil attraction onto clay.

Alkan et al. (2005) explained how cations and crude oil molecules will be arranged around clay particles. Figure 2.6 shows many cations specially Ca, Mg, Al and Fe will tend to adsorb onto the negatively charged clay surfaces to compensate for its negative charge. As a result they will form what is called the stern layer which is a layer containing only the cations adsorbed onto the clay surface. Another layer of both positively and negatively charged particles called the diffuse layer will surround the stern layer, some negatively charged molecules including hydrocarbons from the diffuse layer will tend to adsorb onto the positively charge layer. These oil molecules are bonded into the layer of cations through one of the mechanisms explained earlier, and to be able to produce those adsorbed oil particles either the bond between the clay/cations or cations/oil should be broken.

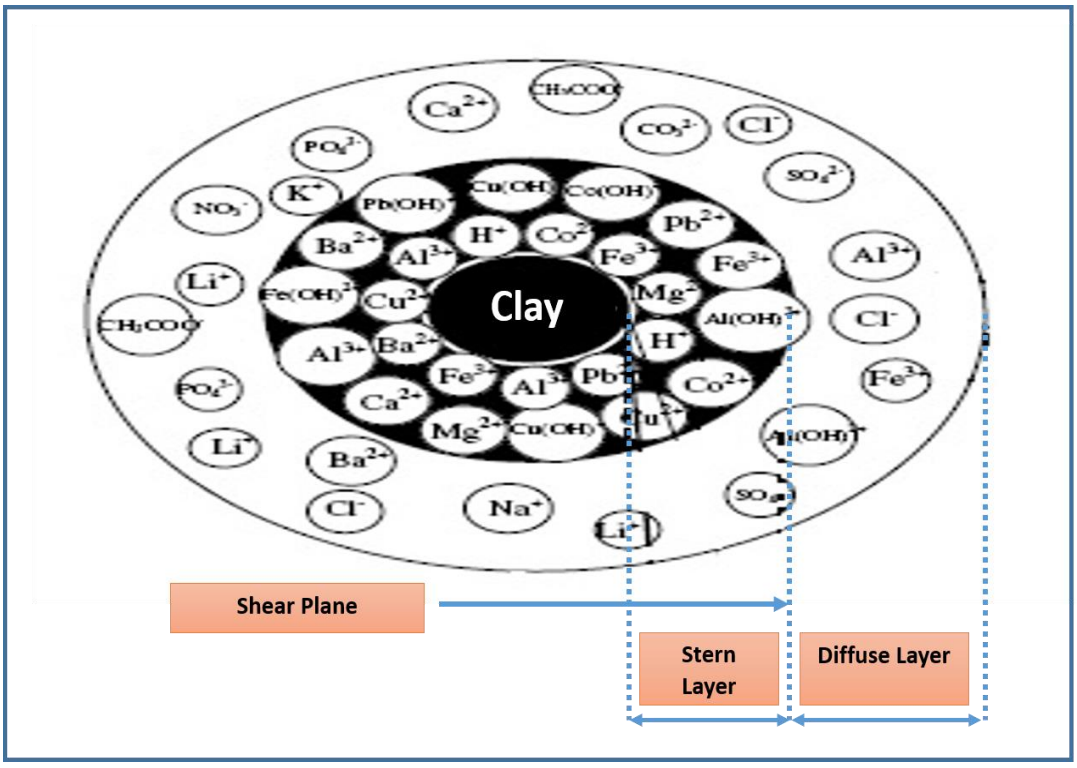

Figure 2.6: The Distribution of Different Cations, Anions and Crude Oil around Clay Minerals (Alkan et al., 2005).

2.2.3 The Effect of Clay Minerals on Oil Recovery from Clayey Sandstone Reservoirs

Shaw et al. (1991) investigated the effect of firing on Berea sandstone cores; they examined the mineralogy and petrography of both fired and unfired samples using powder XRD, SEM-EDS, binocular and petrography analyses. Results of those analyses indicate that there was significant mineralogical transformations occur when Berea is fired at 1000°C, all clay minerals (kaolinite and illite) were changed to amorphous, fused alumino-silicates those changes are indicated by the powder XRD analyses, there is an increase in the amount of the amorphous material in the fired Berea sandstone while the clay minerals and carbonate disappeared after firing, also firing did not effect on quartz and feldspar grains.

From the results of SEM studies Shaw et al. (1991) found that there was simultaneous clay grains (kaolinite and illite) shrinkage of about 10 to 20 vol % and reduction in the space between clay particles when the sample is fired, SEM also showed that there is no grain shattering as a result of firing and the effect of firing on quartz and feldspar appearance is very little. From the thin-section studies they noticed that Fe-rich cements (Fe-sulfide, siderite, and Fe-dolomite) are converted to Fe-oxides after firing, in addition Ca oxide are formed as a result of trace amount of $CaCO_3$ conversion. EDS analysis also confirm the presence of these oxides in the fired Berea and they showed the amount and distribution of those oxides in the fired Berea using thin-section studies because it was very small to be measured by powder XRD analysis.

Shaw et al. (1991) also carried out a set of alkaline/surfactant/polymer flooding experiments; as results of these experiments they reported that there is an increase in the oil recovery after fired Berea at 1000°C. The authors attributed this increase to the changes in pore geometry and rock/fluid interaction. There was also an increase in the pH values for the produced effluents after firing which was the result of the reaction of soluble metal oxides (formed from the destruction of carbonate during firing) and the injected fluid which will form an alkaline solution as an output this solution will react with the acidic components of the crude oil to form surfactant.

Alotaibi and Naser-El-Din (2009) reported that after brine injection the kaolinite clay fraction is the main factor controlling the residual oil saturation reduction and this fact could be attributed to the large particles sizes of those clays.

On the other hand, Tang and Morrow (1999) reported that the presence of kaolinite clay and its fines migration is the main mechanism for increasing oil recovery as a result of injecting low salinity brines, after injecting the low salinity brine it has the ability to detach and move the kaolinite particles through the pore system. As a result the oil particles were originally adsorbed to the kaolinite surfaces could be moved with the detached particles through the pore system up to the core samples outlet.

Cissokho et al. (2010) studied the oil recovery mechanism by low salinity water injection into clayey outcrop sandstone containing 9.2% clay without kaolinite in the secondary and tertiary recovery modes and they reported that the increase in oil recovery could be achieved even in the absence of kaolinite. Cissokho et al. (2010) concluded that while the presence of clays seems to be necessary, the presence of kaolinite is not must develop the mechanism that lead to the increase in oil recovery, and the increase in the system pH and pressure drop due to the interaction of clays with the injected low salinity brines is responsible for the increase in oil recovery.

2.2.4 The Effect of Clay Concentration on Chelating Agents Solutions Stability and Oil Recovery from Sandstone Rocks

The fact that the clays in the reservoir is reacting with water of different salinity in different ways depending on the salinity of the water has been known for a long time. By adjusting the salinity of the injected water properly the ultimate oil recovery could be increased. (Bernard, 1967).

Bernard (1967) found that injecting fresh water into sandstone core samples results in higher oil recovery than injecting NaCl brine. He also reported that the increase in oil recovery was escorted by the increase in the pressure drop. He explained those reaction mechanisms to happen as a result of one of the following two scenarios: In the first scenario, oil recovery is increased by the swelling of clays in the rock caused by fresh water injection which resulted in decreasing the available pore space to both oil and water and eventually cause the increase in the ultimate oil recovery. In the second scenario the authors suggest that after injecting the fresh water, clays will disperse to very fine particles which migrated along the current flow paths and finally result in plugging them. This will result in establishing a new flow channels and increase the oil recovery.

Mahmoud et al. (2011a) carried out stimulation experiments on Berea and Bandera sandstone core samples at 11 and 4 pH units using three chelating agents. They concluded that the EDTA, GLDA, and HEDTA are compatible with both Berea sandstone with "1% illite" and Bandera sandstone with "10% illite" but HEDTA at low pH value of 4 has very low compatibility with illitic-Bandera sandstone compared to GLDA. The authors attributed this to the fact that HEDTA will dissolve more Fe ions than Ca ions which indicate that HEDTA attacks the clays minerals more than the carbonates in the core sample, and the EDTA in not soluble at low pH values. The authors also mention that fines migration will reduce the permeability enhancement as a result of attacking the clays.

Mahmoud et al. (2011b) carried out a set of experiments on sandstone core samples with different illite percentages to compare the performance of GLDA and HEDTA chelating agents in terms of removing formation damage at low pH. They used four different sandstones (Berea 1% illite, Bandera 10% illite, Kentucky 14% illite, and Scioto 18%

illite). They reported that at low pH of 4 the GLDA was compatible with all the sandstone cores with illite content up to 18% illite and it outperformed HEDTA and HCl in the stimulation of sandstone cores; as mentioned by Mahmoud et al. (2011a) this is because the HEDTA at low pH is attacking the clays more than carbonate and causing clay swelling.

2.3 Oil Recovery from Sandstone Reservoirs Using Low Salinity Water

In the past, the chemistry of the injection water has not considered as a primary variable in determining the ultimate oil recovery. Many recent studies have shown that injecting low salinity water rather than injecting high salinity seawater or brine could increase the oil recovery from sandstone rocks. For a long time, LoSal water injection was considered as an EOR technique (McGuire et al., 2005; Austad et al., 2010; Rezaeidoust et al., 2010).

More water-wet conditions and hence increasing oil recovery from sandstone rock could be achieved by injecting low salinity water. The mechanisms that lead to this wettability alteration is a debatable issue. Several studies were carried out and conclude that the main mechanisms for this alteration are: pH increase, double layer effect, multi component ionic exchange, and fines migration. But the question is: are those mechanisms work together to help on recovering more oil or they work separately?, and what are the optimum conditions for each mechanism to effectively enhance the oil recovery?

2.3.1 PH Effect

McGuire et al. (2005), based on four sets of a single well chemical tracer tests (SWCTT) conducted in Alaska's North Slope reservoir, they concluded that the main mechanism for LoSal water recovery is the surfactant generation at elevated pH from the polar components of oil. When the oil is contacted by the elevated-pH LoSal water, the polar components in the oil are saponified by the reaction described by Equations 2.1 to 2.4. They noticed that the LoSal reduces the IFT between oil and water (just like alkaline flooding) and the elevated pH will change the wettability of the reservoir rocks to more water-wet state, so increasing the oil recovery.

$$(RCOO)_3C_3H_5 + 3NaOH \rightarrow 3(RCOONa) + C_3H_5(OH)_3 \quad \text{Equation 2.1}$$

$$Fat + Alkali \rightarrow Soap + Glycerol \quad \text{Equation 2.2}$$

$$2(RCOONa) + Ca(HCO_3)_2 \rightarrow (RCOO)_2Ca + 2(NaHCO_3) \quad \text{Equation 2.3}$$

$$Soap + \text{Hardness} \rightarrow Insoluble\ Soap\ Curd \quad \text{Equation 2.4}$$

The previous equations show that another advantage of using low salinity waterflooding "without divalent ions like: Ca^{2+} and Mg^{2+} or with lower concentrations of these ions" is that it will prevent surfactants precipitation; since the LoSal is quite soft the surfactants remain effective.

At initial reservoir conditions of pressure, temperature, and pH a chemical equilibrium will be established between the adsorbed polar components of oil and formation brine cations. Initially both basic and acidic materials of crude oil will be adsorbed onto the clay surfaces through the inorganic materials of formation brine (especially Ca^{2+}), due to the dissolved

CO_2 and H_2S the formation brine is initially at 5 pH units and this low pH is the main reason for adsorption of oil components (both acidic and basic) onto the clay surfaces. When injection low salinity water into the reservoir, the equilibrium between the brine and rock will be disturbed; as a result the Ca^{+2} ions start to escape from the rock surface. To compensate the loss of Ca^{2+}, H^{+} ions from water adsorb onto the negative site of the clay. This creates an increase in pH value close to the clay surface as shown by Equation 2.5. (Austad et al., 2010).

$$clay - Ca^{2+} + H_2O \rightarrow clay - H^{+} + Ca^{2+} + OH^{-} \qquad \text{Equation 2.5}$$

This increase in the pH value will result in a reaction between adsorbed acidic and basic hydrocarbon materials. And as a result the acidic and basic components of the oil phase will be free, as shown by Equations 2.6 and 2.7 bellow:

$$clay - NHR_3^{+} + OH^{-} \rightarrow clay + R_3N + H_2O \qquad \text{Equation 2.6}$$

$$clay - RCOOH + OH^{-} \rightarrow clay + RCOO^{-} + H_2O \qquad \text{Equation 2.7}$$

The mechanism suggested by Austad et al. (2010) is schematically illustrated in Figure 2.7.

On the other side Lager et al. (2008) studied the effect of injecting LoSal water on a reservoir scale. Based on the results they found that there is no change in the value of pH and it is almost the same as before injecting the LoSal water, so they concluded that this is not the effective mechanism to recover more oil as suggested by Austad et al. (2010).

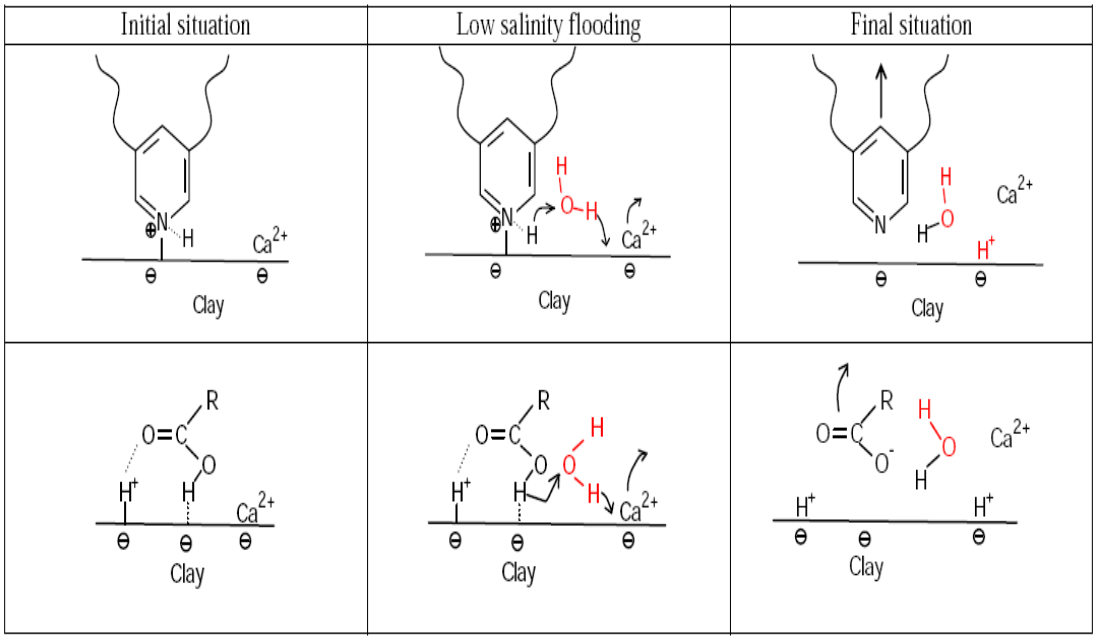

Figure 2.7: LoSal Water Mechanism for EOR. Upper: Description of Basic Material. Lower: Description of Acidic Material (Austad et al., 2010).

2.3.2 Multi Component Ionic Exchange

Lager et al. (2006) demonstrated that flooding with low salinity water into a reservoir containing connate brine which has multivalent cations will increase the oil recovery as a result of cation exchange between the invading low salinity water and the rock surfaces. On the other hand, if the connate water is free of divalent ions the residual oil saturation did not decrease if the reservoir is flooded with high or low salinity water, or if the low salinity water was used in tertiary low salinity flood to displace the low salinity connate brine which was used during the secondary recovery mode.

Lager et al. (2008) studied the effect of injecting low salinity water and its active mechanism that is responsible for increasing the oil recovery for Alaskan reservoir. As a result they found that there is a sharp decrease in the Mg^{+2} concentration in the produced

water which mean that there is an ionic exchange between the clay minerals surfaces and the injected brine. They also found that the timing of the effect was fast, despite being a tertiary flood.

Austad et al. (2010) found that the Mg^{+2} ions concentration change in the produced water was due to the $Mg(OH)_2$ precipitation as a result of the local pH increase caused by injection of low salinity water and not due to the multicomponent ionic exchange (MIE) mechanism.

Nasralla and Nasr-El-Din (2011) injected different brines into dry Berea sandstone core samples to eliminate the interaction between the formation brine and the injected solutions. As a result they found that there was no change on the ions concentrations in the injected brines and produced effluents (Na^+, Ca^{+2}, Mg^{+2}, and SO_4^{-2}), this result confirms that there is no ions exchange between the injected brine and the rocks.

Figure 2.8 shows the result of injecting 5wt% NaCl solution into Dry Berea Sandstone core sample. Nasralla and Nasr-El-Din (2011), as shown in this figure, the concentration of Na^+ ions was constant with NaCl solution injection, while the Ca^{+2} concentration was very high (constant about 60 mg/l) and Mg^{+2} concentration was low (about 9 mg/l) although the injected solution was free of Ca^{+2} and Mg^{+2}, in addition the SO_4^{-2} concentration is decreasing with the increase of the injected pore volume; these results clearly demonstrate cation exchange due to the interaction of injected brine and rocks.

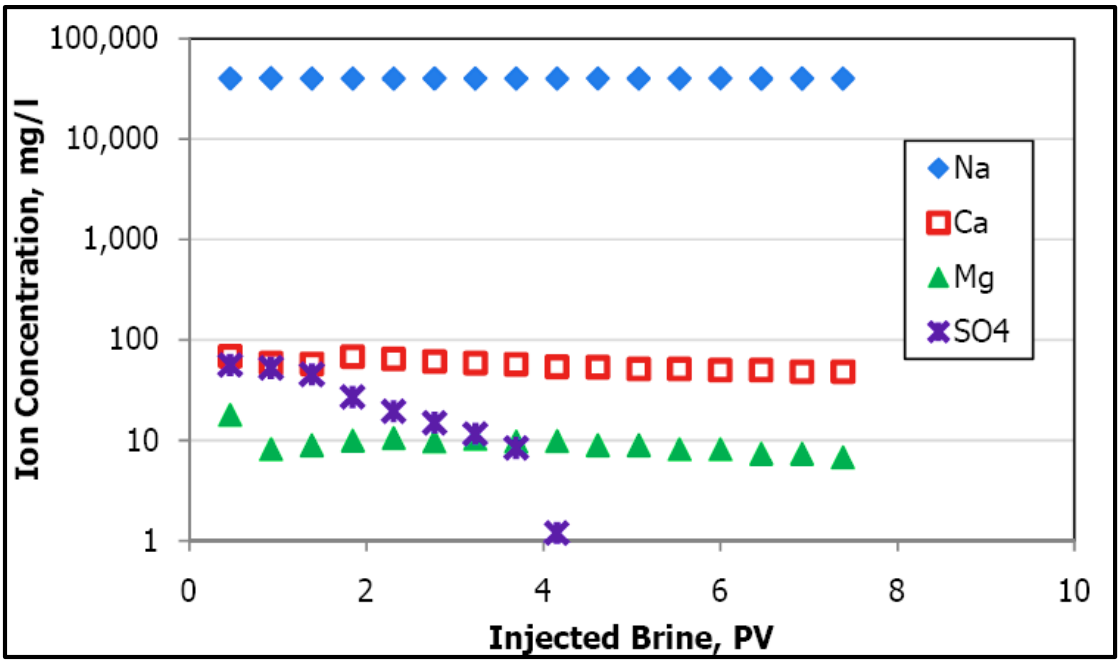

Figure 2.8: Effluent Analysis for Experiment of Injection 5wt% Sodium Chloride in a Dry Berea Sandstone Core (Nasralla and Nasr-El-Din, 2011).

Also for enhancing the ultimate oil recovery the type of ions and their concentrations in the injected water are more important than the total salinity of the water (Nasralla and Nasr-El-Din, 2011).

2.3.3 Fines Migration

Lager et al. (2008), from the results of their study for Alaskan reservoir they notice that the injectivity index did not change or reduced considerably so the reservoir permeability did not reduce which indicates that there is no any fines migration.

Nasralla and Nasr-El-Din (2011) performed waterflooding experiments using Berea sandstone cores and three different synthetic brine solutions NaCl, $CaCl_2$, and $MgCl_2$ at different concentrations of (5wt%, 1wt%, and 0.2wt%). As a result they reported that injection of low salinity synthetic brines increases the pressure drop with the increase in

the volume of the injected brines indicating that there is a formation damage caused by fines migration as result of injecting those low salinity brines. Figure 2.9 shows the increase in the pressure drop with the increase of the injected sodium chloride solution (0.2wt%) into Berea sandstone core saturated with crude oil after the first two injected pore volumes.

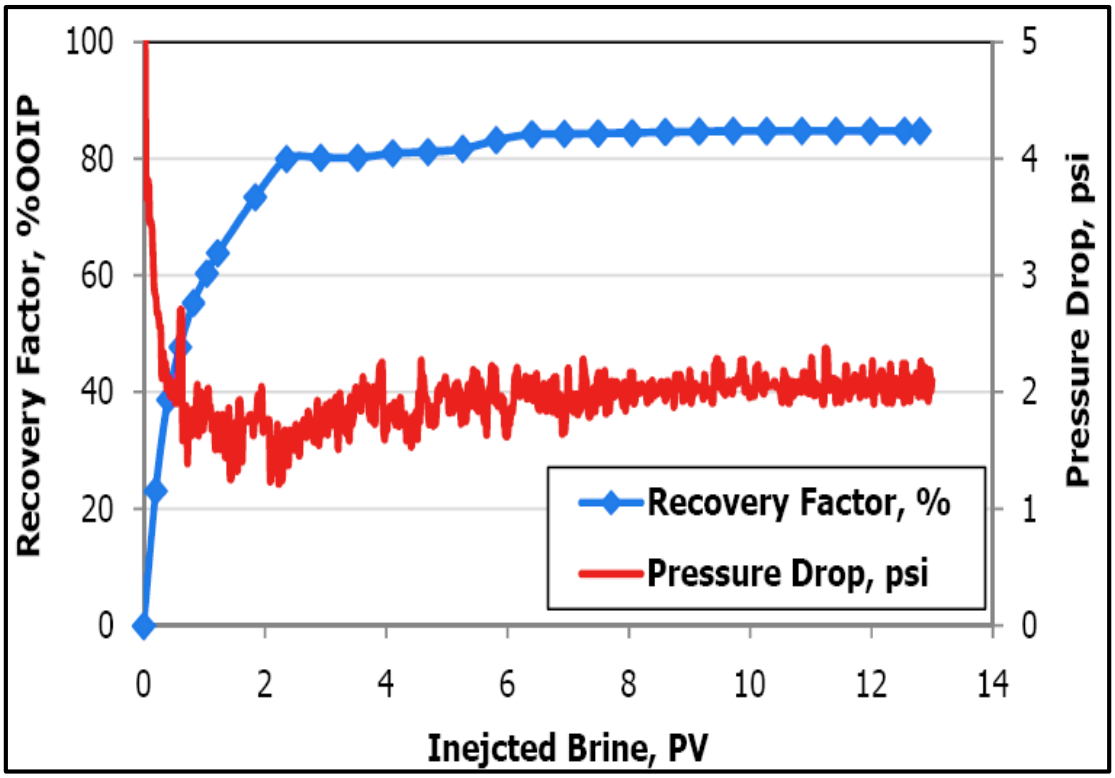

Figure 2.9: Oil Recovery and Pressure Drop for Experiment of Injecting 0.2wt% Sodium Chloride in Berea Sandstone (Nasralla and Nasr-El-Din, 2011).

2.3.4 Double Layer Effect

Nasralla et al. (2011) used both zeta potential technique and the contact angle measurements to examine the rock wettability alteration due to LoSal water injection into sandstone reservoirs to investigate the main reasons of wettability alteration caused by injection of LoSal water. They reported that the injection of LoSal water results in changing the electric charge at oil/brine and brine/rock interfaces and they attributed this adjustment

in the charges is the main reason for wettability modification. The repulsion force between rock and oil increases when the charges at those interfaces become more negative which will result in forming a stable water film around the rock and change the rock wettability to more water-wet conditions.

Nasralla et al. (2011) also found that the rate of wettability alteration is a function of the amount of change in the electrical charge at the oil/brine and brine/rock interfaces; as the magnitude of the surface charge increases the repulsive force increases and hence wettability alteration increases.

2.4 Chelating Agents

Aimnopolycarboxylic acid chelating agents are the most popular kind of chelating agents used in oil industry as stimulation fluids. They are negatively charged organic molecules and have the ability to combine with metal ions (M^{+n}) through coordination bounds with the amino and carboxyl groups. Aminopolycarboxylic acids are one of a few classes of chelating agents that are capable of forming stable chelates with alkaline-earth metals such as Ca, Mg, and Fe (Fredd and Foglar, 1997).

Chelating agents could be used to decrease the salinity of the seawater without any processing since they have the ability to soften the water by chelation of ions like Ca, Mg, and Fe. Chelation of ions will also increase the viscosity of the injected fluid. There are different types of chelating agents Figure 2.10 shows the chemical structure of the most common chelates used in the oil industry.

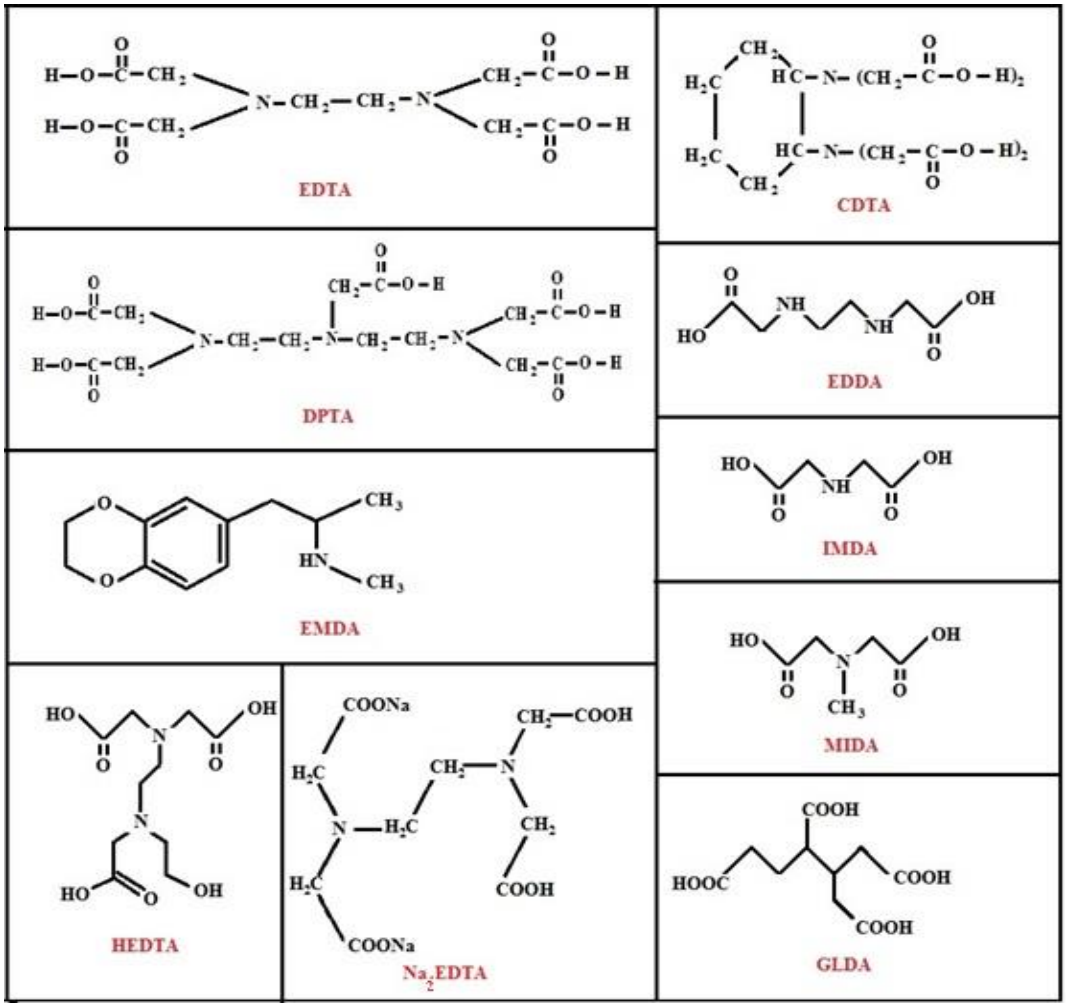

Figure 2.10: Structure of Different Types of Chelating Agents (Szilágyi, 2007; Mahmoud et al., 2010).

Chelating agents were first introduced as stimulating fluids by (Fredd and Foglar, 1997). Matrix acidizing by using HCl at low injection rate will prevent formation fracturing and it is required in heterogeneous formation with low-conductivity zones which accept acid at low rates; since the problem of quick acid spending drastically limits the acid penetration at those low rates and result in only face dissolution or complete dissolution of formation rock, which will results in consuming a large volume of acid and provide a negligible increase in the formation conductivity (Fredd and Foglar, 1997).

Fredd and Foglar (1997) found that the use of EDTA will wormholes even if it injected at low injection rate and at low pH values, also it will not lead to the precipitation of asphaltic sludge, beside that EDTA has the ability to chelate metal ions even if it used under non-acidic conditions.

Shaughnessy and Kline (1983) applied the Na_2H_2EDTA chelating agent at Prudhoe Bay reservoir for stimulation purposes of sandstone formation; this field has 25 damaged wells which exhibited annual decline rate higher than the anticipated one. So they were subjected to matrix acidizing with HCl several times which result in a short-lived productivity increase followed by a dramatic drop that encourage the owners to look for a stimulation fluid which has the ability to stimulate and keep this improvement for long time.

The scale precipitated and resulted on this productivity decline was found to be due to accumulation of $CaCO_3$ and $FeCO_3$ deposited naturally from the reservoir brine and after conventional acid treatment HCl spends on $CaCO_3$ and $FeCO_3$ to produce a concentrated solution of $CaCl_2$ and $FeCl_2$ which result in precipitation of $CaCO_3$ (Shaughnessy and Kline, 1983).

Before the field implementation Shaughnessy and Kline (1983) subjected the Na_2H_2EDTA chelating agent to several lab tests to establish the important design parameters such as: EDTA concentration, treatment volume and additive compatibility. After all those parameters established experimentally, then the stimulation processes were carried out for 25 wells, in which 19 of them the productivity was restored to almost the same level before the onset of decline. Analysis of the wells where productivity was not restored showed the

problem of an incorrect candidate selection; the damage of those wells was not as a result of $CaCO_3$ precipitation.

De Wolf et al. (2014) whose found that for chelating agent to improve the permeability in sandstone formation the formation should contain calcite, dolomite or siderite naturally or be damaged with $CaCO_3$.

Ali et al. (2008) carried out a set of experiments to compare the ability of stimulating a high temperature sandstone formation core samples from West Africa using chelating agent-based fluids (Na_3HEDTA at pH = 4) and 9:1 HCl/HF fluids. From the results of acid solubility tests and slurry reactor tests analyzed using ICP, the authors noticed that the chelating agent and HCl/HF solutions have the same $CaCO_3$ dissolution capacity; however, acidic chelates showed a minor tendency for secondary precipitation compared to HCl/HF fluids. Figure 2.11 shows the results of ICP for 12% carbonate samples with both Na_3HEDTA and HCl/HF solutions. This figure clearly shows that for the sample treated with Na_3HEDTA the percentage of the dissolved ions (Ca, Si, Al, and Mg) increased continuously with time without any decrease, while that stimulated with 9:1 mud acid slurry showed an early increase in Ca, Mg, and Si followed by a latter decrease of those ions as a result of secondary reaction and precipitation. From ICP analysis of samples with different $CaCO_3$ content treated by acidic Na_3HEDTA the authors also noticed that as the $CaCO_3$ concentration decreases the Na_3HEDTA fluids were free to dissolve more clays and other alominosilicates.

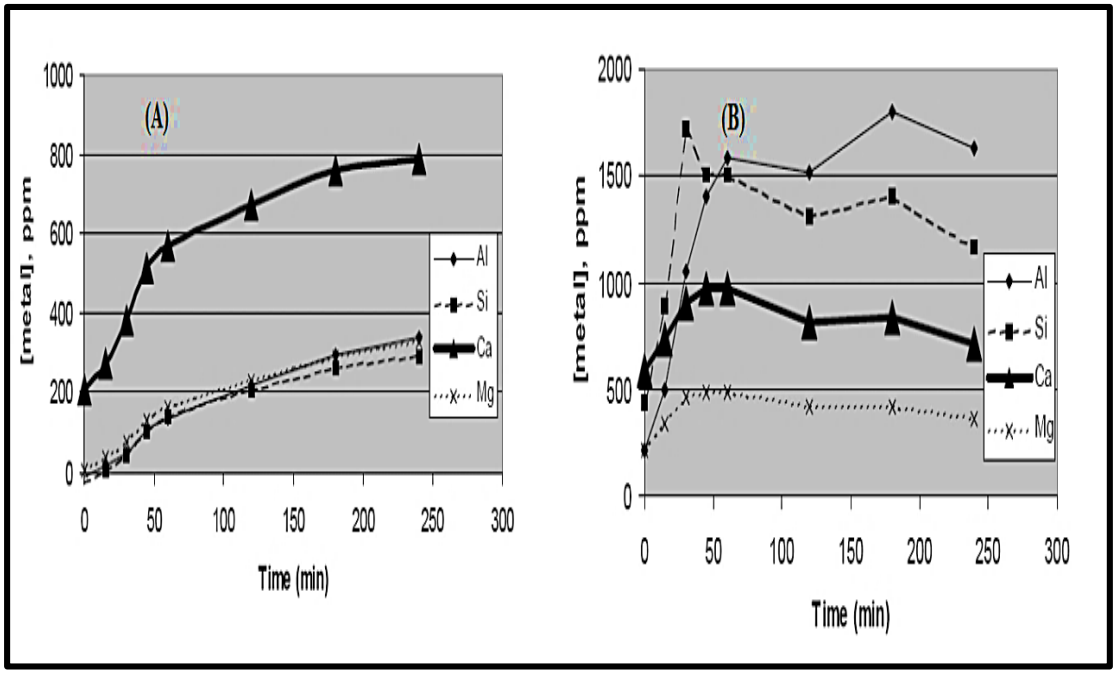

Figure 2.11: ICP Analysis of Solution during Reaction of 12% Carbonate Rock at 149°C with (A) Na_3HEDTA at pH = 4 (B) HCl/HF (Ali et al., 2008).

Ali et al. (2008) also from the results of linear core flood reported that the Na_3HEDTA could be considered as a good alternative for conventional acidizing fluids which are problematic at high temperature, at a temperature of 149°C acidic Na_3HEDTA fluid was quite effective in stimulating moderate carbonate content field core samples.

De Wolf et al. (2014) carried out a set of experiments on Indiana limestone, and Berea and Bandera sandstones to evaluate the performance of four amino ploycarboxylic acid type chelating agents including: glutamic acid N,N-diacetic acid (GLDA), aspartic acid N,N-diacetic acid (ASDA), methyl glycine diacetic acid (MGDA), and ethanoldiglycine (EDG) on a number of properties including: solubility as a function of pH, solubility on acids, iron control, thermal stability, corrosion, $CaCO_3$ dissolution and effectiveness in coreflood tests.

De Wolf et al. (2014) found that GLDA is better soluble among the others at low pH, better soluble in acids, its corrosion rate is the lowest – lower than the acceptable rate – more effective in improving the permeability of the sandstone core samples and has a higher $CaCO_3$ dissolution capacity. Figure 2.12 shows the comparison between the four chelating agents in stimulating Berea and Bandera sandstone cores; as shown in this figure GLDA is the most powerful chelant among the others in stimulating both sandstone core samples at low pH. Figure 2.13 shows the results of effluent analysis for Berea sandstone coreflood experiments carried with both GLDA and ASDA chelating agents; as it is clearly seen that the amount of the chelated Mg and Al ions are very low compared to those of Ca and Fe ions which confirm that this chelating agents are not attacking siliceous materials like quartz and clays but attacking calcite, dolomite, and siderite as indicated by the high amount of the dissolved Ca and Fe.

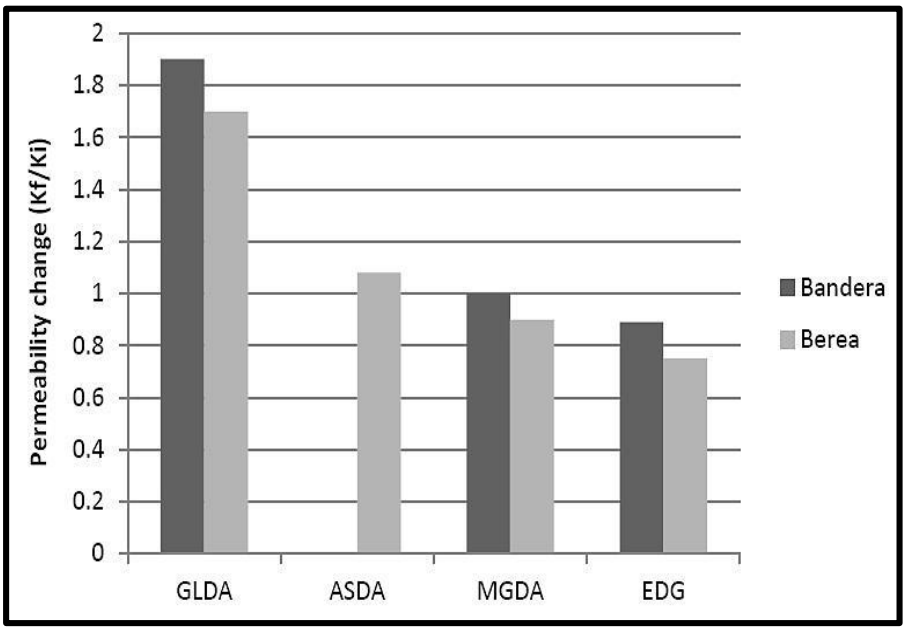

Figure 2.12: Comparison between the Chelating Agents in Stimulating Berea and Bandera sandstone cores at 300°F and 5 cc/min (De Wolf et al., 2014).

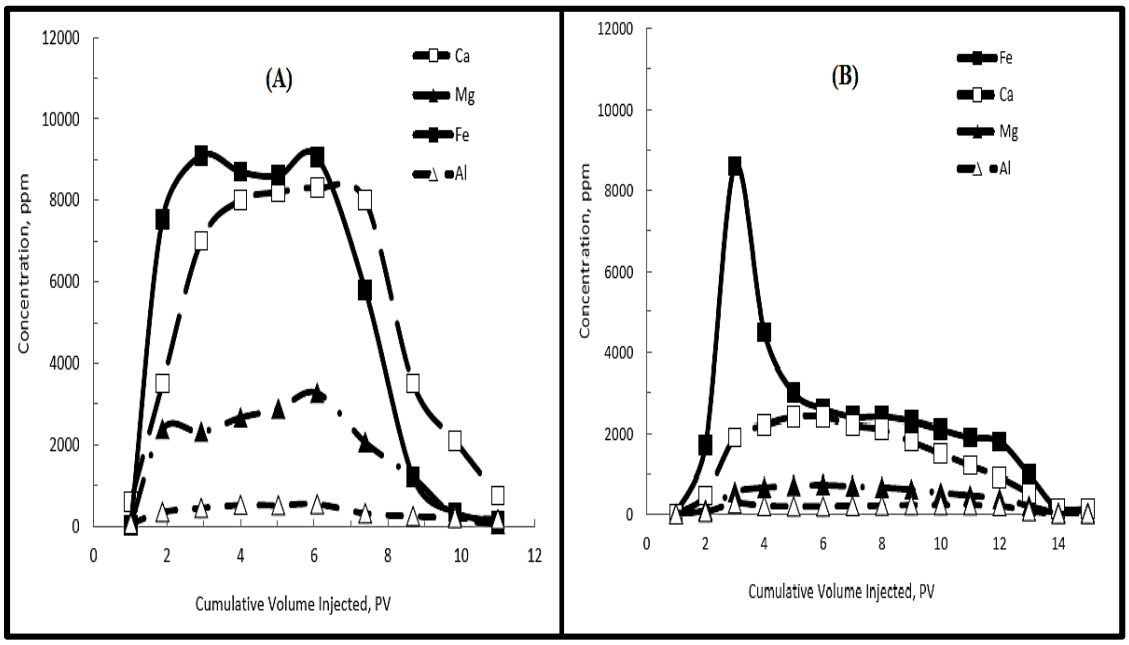

Figure 2.13: Effluent Analysis for Berea Sandstone Treated with 0.7M (A) GLDA and (B) ASDA, at pH 3.8 at 300°F and 5 cc/min (De Wolf et al., 2014).

To stimulate sandstone formations with an acidic chelate, it should contain calcite, dolomite, or siderite naturally or be damaged with $CaCO_3$ for example; since chelating agents are not capable of dissolving quartz or clay minerals those are the main constituents of sandstone formation (De Wolf et al., 2014).

Nasr-El-Din et al. (2014) evaluated the results of the first field application with a fluid based on the chelating agent to acidize a vertical sour oil well in an offshore sandstone reservoir (target zone = 125 ft, temperature = 261°F), with a substantial amount of corrosive gases in the form of seven percent H_2S and three percent CO_2. This field is under seawater injection and a gas lift is used to produce the well under study, the injected gases contain N_2, CO_2 and small concentration of H_2S. The authors used in their study 25wt% GLDA chelate at pH of 4.3, 1 vol% corrosion inhibitor and 0.2 vol% water-wetting

surfactant, and they evaluated the treatment based on the analysis of the produced fluid after treatment. The collected flowback samples did not contain any sand particles or fines; which indicates the compatibility between the GLDA and sandstone minerals, also there was no asphaltene or emulsions in the produced fluids; which indicates the compatibility between this chelant and this crude oil so there was no any loss of productivity and oil production rate increased by 60% while no increase in the water cut observed, the concentration of Fe and Mn in the produced fluids is also very low; which indicates that this treatment has no effect on the integrity of the well tubulars, this result also indicates that it will not result in corrosion problems.

2.4.1 Chelation Chemistry

Chelating agents has the ability to form a stable one or more ringed structure -with high stability constant- with metal ions (M^{+n}) -through coordination bonds with the amino and carboxyl groups- which surround the metal ions and occupy all of their coordination sites. The high stability of those chelates agents reduces the reactivity of metal ions toward other species, and make uses of chelating agents efficient for applications of inactivation of metal ions, water softening and titration of metal ions.

Table 2.2 compares the stability constants for different chelating agents with different divalent ions. As shown in Table 2.2 those different chelating agents could form stable structures with Ca and Mg with stability constants greater than eight.

Table 2.2: The Stability Constants for CDTA, DTPA and EDTA Chelates with Different Divalent Ions (Fredd & Foglar, 1997).

	Log K_{MY}		
Chelates / Metal Ion	CDTA	DTPA	EDTA
Calcium	12.30	10.34	10.59
Magnesium	11.34	8.92	8.69
Strontium	9.84	9.34	8.63
Barium	7.63	-	7.76

The structure of aminopolycarboxylic acid chelating agents can be abbreviated in H_nY where the n hydrogen's are from the carboxylic acids. Equations 2.8 to 2.11 show how EDTA and CDTA undergo a step wise loss of protons to reach their fully ionized state.

$$H_4Y \rightleftharpoons H_3Y^{-1} + H^+ \qquad \text{Equation 2.8}$$

$$H_3Y^{-1} \rightleftharpoons H_2Y^{-2} + H^+ \qquad \text{Equation 2.9}$$

$$H_2Y^{-2} \rightleftharpoons HY^{-3} + H^+ \qquad \text{Equation 2.10}$$

$$HY^{-3} \rightleftharpoons Y^{-4} + H^+ \qquad \text{Equation 2.11}$$

The equilibrium constants of the dissociation reactions as well as the solution pH are the main factors controlling the distribution of different ionic species. Figure 2.14 shows the ionic species distribution at room temperature for CDTA, DPTA, and EDTA.

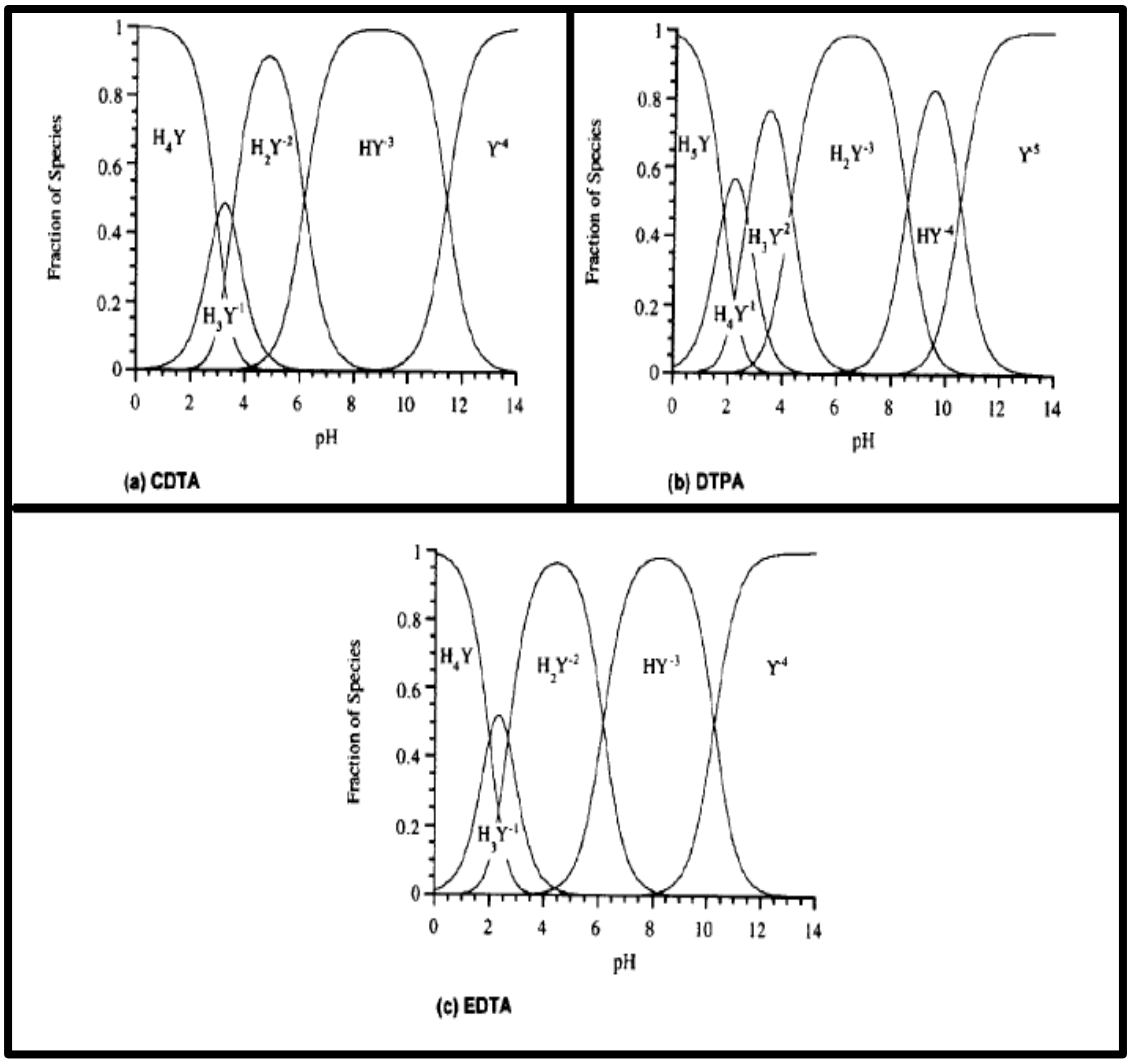

Figure 2.14: Distribution of Ionic Species of: (a) CDTA, (b) DTPA, and (c) EDTA at Room Temperature (Fredd & Foglar, 1997).

2.4.2 Carbonate Dissolution by EDTA

In neutral environment, the dissolution of carbonate is dependent on the mass transfer of the medium and the kinetics of the heterogeneous reaction at the calcite surface (Fredd and Foglar, 1997). Under these environmental conditions three simultaneous reactions shown by Equations 2.12 to 2.14 are occurring:

$$H^+ + CaCO_3 \rightleftharpoons Ca^{+2} + HCO_3^- \qquad \text{Equation 2.12}$$

$$H_2CO_3^* + CaCO_3 \rightleftharpoons Ca^{+2} + 2HCO_3^- \qquad \text{Equation 2.13}$$

$$H_2O + CaCO_3 \rightleftharpoons Ca^{+2} + HCO_3^- + OH^- \qquad \text{Equation 2.14}$$

Where $H_2CO_3^*$ represents $H_2CO_3 + CO_2$ (aq).

When EDTA chelating agents are present, the free calcium ions are sequestered by EDTA as shown below by Equation 2.15.

$$Ca^{+2} + Y^{-4} \rightleftharpoons CaY^{-2} \qquad \text{Equation 2.15}$$

EDTA has been used for removal for $CaCO_3$ scale from sandstone formations because it has an advantage of chelating the ions of the dissolved scale over the conventional acid stimulation, thus preventing scale reprecipitation, and also used for removal of minerals from clay assemblages at high pH values of 10-12 to avoid destroying the clay species (Fredd and Foglar, 1997).

The overall reaction for calcium carbonate dissolution by EDTA at pH of 8.5 is shown in Equation 2.16.

$$HY^{-3} + CaCO_3 \rightleftharpoons CaY^{-2} + HCO_3^- \qquad \text{Equation 2.16}$$

2.4.3 Chelating Agents as a New Chemical Enhanced Oil Recovery (CEOR) Fluids for Sandstone Reservoirs

Attia et al. (2014) were first to introduced using chelating agents as a chemical enhanced oil recovery technique for sandstone reservoirs, they studied the possibility of using Na_4EDTA chelate to improve the oil recovery and as a result the showed that an additional 5-30% of OOIP could be recovered when sandstone core samples originally flooded with

seawater and then flooded by Na_4EDTA solution with high pH of 12.2 as shown in Figure 2.15.

From the effluent analysis Attia et al. (2014) found that this increase of recovery as a result of clay minerals and rock dissolution (not double layer expansion) and it is well correlated to the ions chelation especially chelated iron as shown in Figure 2.15.

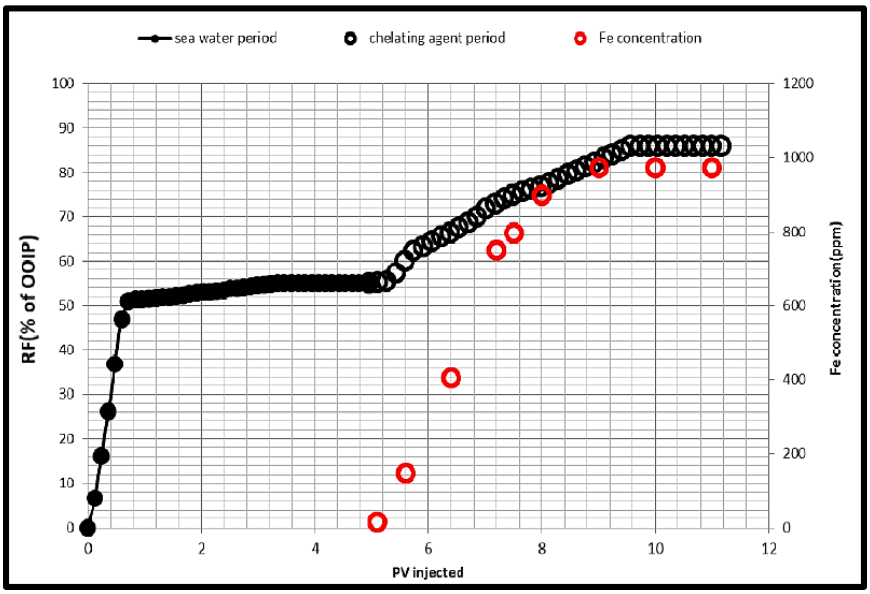

Figure 2.15: Comparison between Iron Concentration in Case of 5wt% Na_4EDTA and the Oil Recovery with the Injected Pore Volume (Attia et al., 2014).

CHAPTER 3

MATERIALS AND METHODOLOGY

3.1 Experimental Materials

3.1.1 Brines

Two different synthetic brines were used in this study; the synthetic formation brine (SFB) with total dissolved solids (TDS) of 172,923.4 ppm which was used to establish the initial water saturation. This brine was also used to measure the core samples porosity as well as the absolute permeability of the samples before and after flooding to examine the effect of the injected fluids on the rocks dissolution, the other brine used in this study was the synthetic seawater (SSW) with 58,270.70 ppm TDS. The SFB and SSW were prepared by dissolving different amounts of reagent chemicals supplied by Panreac ITW companies in deionized water, then the solutions stirred for 6 hours and filtered through 0.22 μm Millipore filter to remove undissolved impurity materials, the solutions were characterized through inductively coupled plasma (ICP) and (IC) analyses. Table 3.1 summarizes the composition of the brines used in this study.

3.1.2 Crude Oil

Dead Uthmania crude oil (UTMN) was used in this study as a reservoir crude oil. The composition, viscosity and density of this crude oil are shown in Table 3.2.

Table 3.1: Composition of the Synthetic Formation Brine and Seawater Used in This Study, by ICP and IC analyses.

Ions	Seawater (ppm)	Formation Brine (ppm)
Na^{+}	24,158.0	54,400.0
Ca^{+2}	615.1	9,378.0
Mg^{+2}	2,085.1	1,505.0
Al^{+3}	20.0	30.6
Fe^{+3}	24.8	25.0
Si^{+4}	6.5	8.6
Mn^{+2}	0.5	1.3
K^{+}	10.0	28.9
Cl^{-}	27,390.0	107,000.0
HCO_3^{-}	173.0	176.0
SO_4^{-2}	3787.8	370.0
TDS (ppm)	58,270.7	172,923.4

Table 3.2: Dead UTMN Crude Oil Composition and Properties.

Component	**Mole**	**Mole %**
C5	0.0021	1.18
C6	0.0074	4.18
C7	0.0185	10.40
C8	0.0278	15.63
C9	0.0256	14.39
C10	0.0254	14.26
C11	0.0201	11.30
C12+	0.0510	28.67
Density	0.8835 gm/cc (29.66 °API) @ 25°C	
Viscosity	17.59 cp @ 25°C	

UTMN crude oil viscosity was measured as a function of temperature as shown in Figure 3.1.

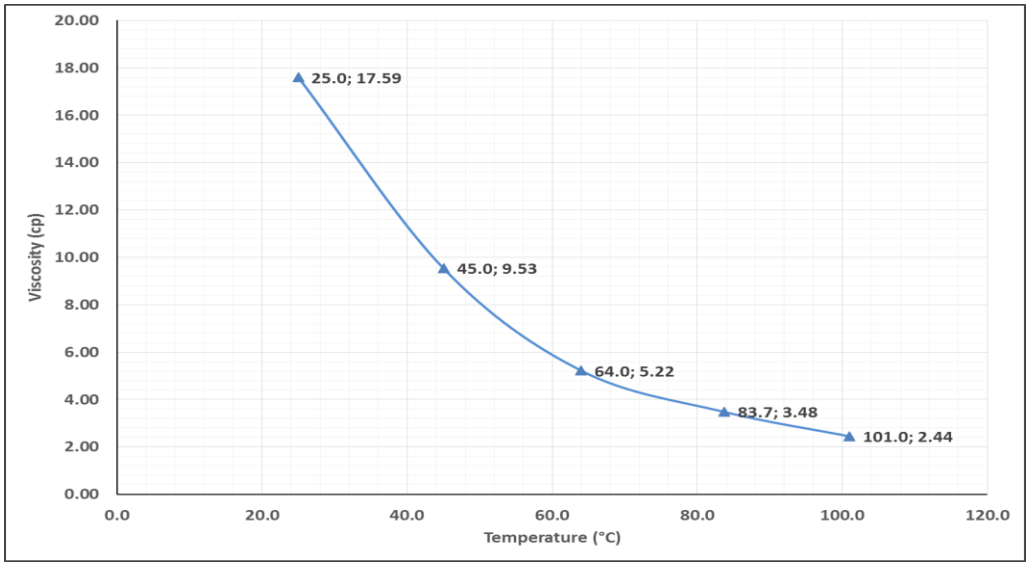

Figure 3.1: UTMN Crude Oil Viscosity as a Function of Temperature.

The percentages of saturates, aromatics, resin and asphaltene (SARA) components for UTMN crude oil are summarized in Table 3.3.

Table 3.3: SARA Analysis Results for UTMN Crude Oil Used in this Study.

Components	Percentage (wt%)
Saturates	42.20 ± 5.0
Aromatics	36.10 ± 3.68
Resin	16.18 ± 0.83
Asphaltene	5.51 ± 0.08

3.1.3 Chelating Agents

Different concentrations of EDTA chelating agent solutions were used in this study. The following steps summarize the procedure followed in preparing EDTA solutions from a powder Na_2EDTA.

3.1.3.1 Preparation of EDTA Chelating Agent Solutions

The EDTA chelating agent solutions used in this study were prepared from a powder Na_2EDTA supplied by Scharlau (purity > 99%) with molecular weight of 372.24 grams/mole as follows:

1. One liter of deionized water was introduced into a flask and its pH was adjusted at 13.00 by adding NaOH pellets and mixing the solution continuously.
2. 300 grams of Na_2EDTA was added into the flask gradually while the solution was mixed.
3. Addition of Na_2EDTA caused a decrease in the solution pH and precipitation of Na_2EDTA powder was observed as a result of this decrease in pH so more NaOH pellets were added to the solution to increase its pH again and dissolving the precipitated powder, the pH was increased finally to about 12.5.
4. Then the solution was mixed for 24 hours to insure its homogeneity.
5. After that it was filtered through 0.22 μm Millipore filter to remove any undissolved materials.
6. Finally the solution of (30-x/10) wt% Na_4EDTA @ pH of 12.50 is ready, where x is the weight of the precipitated Na_2EDTA solids in grams.
7. After preparation of this solution then depending on the required EDTA solution concentration in seawater Equation 3.1 was used to find the required amount of the (30-x/10) wt% Na_4EDTA solution to be mixed with the seawater.

$$X_1 \times W_1 = X_2 \times W_2 \qquad \text{Equation 3.1}$$

Where:

$X_1 \equiv$ the concentration of Na_4EDTA solution before dilution (%).

$W_1 \equiv$ the required weight of (30-x/10) wt% Na_4EDTA solution (grams).

$X_2 \equiv$ the concentration of EDTA solution after dilution (%).

$W_2 \equiv$ the required amount of the EDTA solution with the targeted concentration (grams). The seawater required in this case was calculated as $W_2 - W_1$.

3.1.3.2 Thermal Stability of EDTA Chelating Agent

After the EDTA solutions were prepared with different concentrations of EDTA in seawater, the stability of the 5wt% Na_4EDTA in seawater solution at pH of 12.00 and 250°F was studied through both Fourier Transform Infrared Spectroscopy (FTIR) technique and viscosity measurements.

The 5wt% Na_4EDTA in seawater solution at pH of 12.00 was divided into eight different samples, one of the samples was characterized directly after preparation, the remaining seven samples were carefully sealed in different vials and stored in an oven at 250°F, after every 24 hours one vial was removed from the oven and kept until the solution has cooled down, then the FTIR technique was applied to that sample to generate the pattern representing the bonds exist in the sample, after that the viscosity of the sample was measured to compare the effect of heating on the fluid viscosity.

The important notice about all the samples used in the thermal stability study is that there was no precipitation noticed for all of them as indicated in Figure 3.2 for the last sample which was stored in the oven for one week at 250°F.

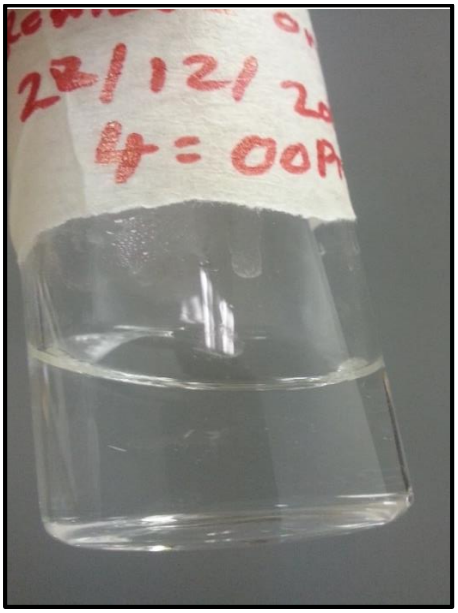

Figure 3.2: No Precipitation Noticed for 5wt% Na_4EDTA Solution at pH of 12.00 kept at 250°F for Seven Days.

Figure 3.3 shows the FTIR patterns for the 5wt% Na_4EDTA in seawater at pH of 12.00 before heating and after heating up to 250°F for one, two, … , seven days. The identical patterns for the sample directly after preparation (before heating) and after heating indicates that this solution is thermally stable up to 250°F for one week and there was no any change in the existing bonds; since all of them have the same FTIR pattern as the original solution.

The effect of the temperature on the viscosity of the EDTA solution was studied, Figure 3.4 compares between the viscosity measurements of 5wt% EDTA solutions before and after heating for one week. This figure shows that there was unremarkable change in the

viscosity of this solution after heating up to 250°F for seven days which indicate that there was no change in the internal structure and bonds of this solution after heating as suggested before by FTIR results.

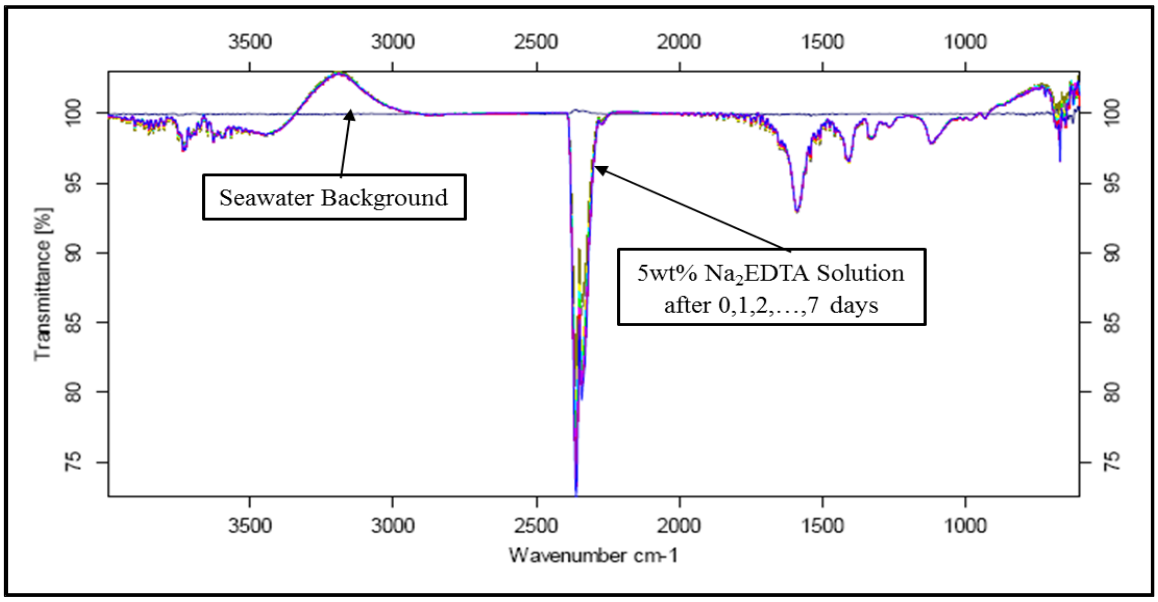

Figure 3.3: FTIR Patterns for 5wt% Na_4EDTA Solutions at pH of 12.00 after Zero, One, Two, …, Seven Days of Heating at 250°F.

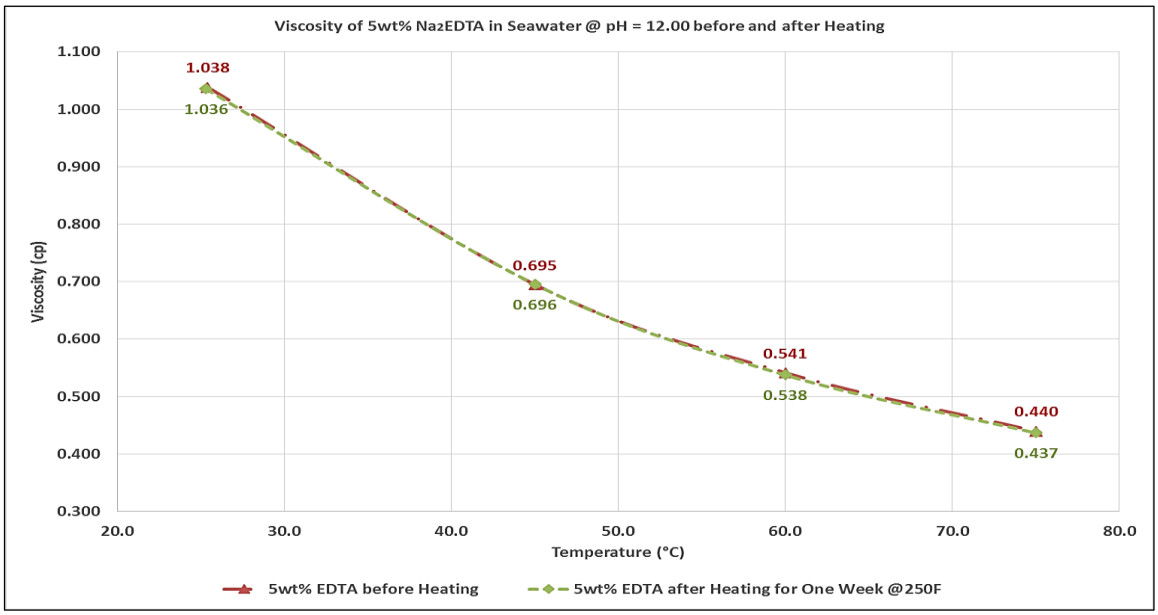

Figure 3.4: 5wt% Na_4EDTA Solution Viscosity before and after Heating at 250°F.

3.1.3.3 Compatibility Test

Since the injection of the chelating agent solutions was preceded by seawater injection, a region where both seawater and chelating agent solutions were mixed in different concentrations was developed inside the core samples, the possibility of $CaCl_2$ precipitation from the seawater will increase due to the increase in the pH level for the seawater in the interference layer. The objective of this test is to check for the possibility of the formulation of this precipitation inside the core samples. Figure 3.5 shows the distribution of the injected fluids in three different zones, the seawater zone, the mixture (interference) zone where both seawater and the chelating agent's solutions are present in different concentrations, and the chelating agent solution zones. The concentration of chelating agent solution decreases in the direction from the inlet to the outlet. Nine solutions were prepared in different concentrations of seawater and 1wt% Na_2EDTA solution @ pH of 9.70 for compatibility study the concentration of those fluids are summarized in Table 3.4. After preparing the samples they were kept in oven for 24 hours at 100°C, then they were removed out of the oven and allowed to cool down before examining the development of precipitations formulation.

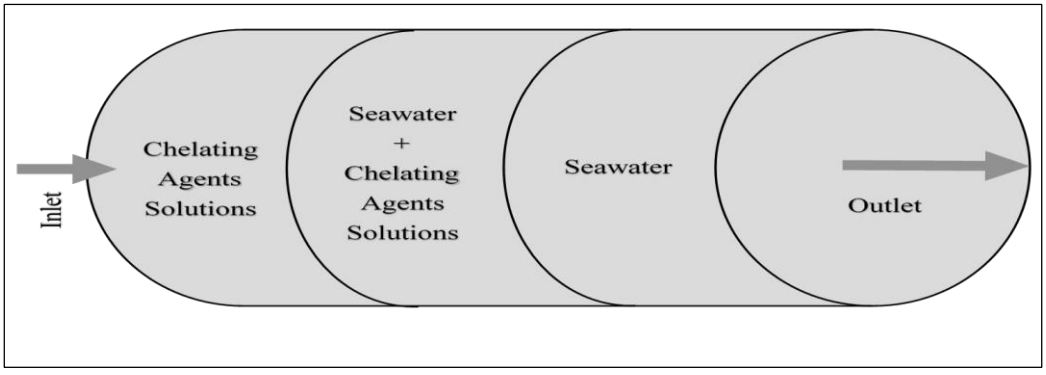

Figure 3.5: The Distribution of the Injected Seawater and Chelating Agents Solutions after Chelating Agent Solution Injection and before Breakthrough.

Table 3.4: The Composition and Concentration of Different Fluids Prepared for Compatibility Test

Sample ID	1wt% Na_2EDTA Concentration (wt%)	Seawater Concentration (wt%)
1	90	10
2	80	20
3	70	30
4	60	40
5	50	50
6	40	60
7	30	70
8	20	80
9	10	90

Figure 3.6 shows the nine samples used in the compatibility test, no precipitation noticed for all samples which confirm the ability of the 1wt% Na_2EDTA chelating agent solution to chelate the Ca^{+2} cations and prevent development of salts precipitation inside the reservoir.

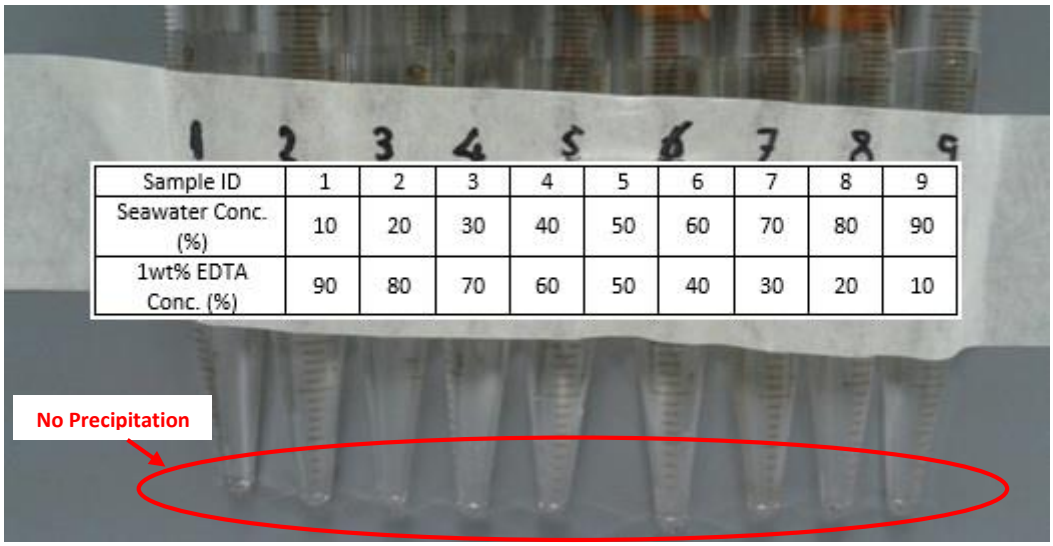

Figure 3.6: The Compatibility Test Results.

3.1.4 Core Samples

Gray Berea and Gray Bandera sandstone core samples with different mineralogical composition (specially the clay content) were used in this study.

The following tests were performed for both sandstone cores:

1. Powder X-Ray Diffraction (PXRD) Analysis

PXRD analysis was performed on both Gray Berea and Gray Bandera sandstones to identify their mineralogical composition. Table 3.5 shows PXRD results of the mineralogical composition of Gray Berea and Gray Bandera sandstone samples.

Table 3.5: Mineralogical Composition of Gray Berea and Gray Bandera Sandstones, by PXRD Analysis conducted at Backer Huges and King Fahd University of Petroleum and Minerals (KFUPM).

Minerals	Gray Berea (wt%)	Gray Bandera (wt%)
Quartz	89.0	61.0
Calcite	0.08	-
Albite	1.47	23.2
Kaolinite	4.80	2.40
Illite	2.29	7.01
Chlorite	1.02	2.50
Ankerite	0.38	3.70

2. X-Ray Fluorescence (XRF) Analysis

The XRF analysis was conducted for both sandstone samples to investigate the difference in the percentages of elements, specifically the active cations those are usually form the

clay minerals and they may have a role in changing the sandstone wettability and increasing the oil recovery as a result of their interaction with the injected chemicals. Table 3.6 shows the elemental composition of both sandstone samples under study in weight percentages and Figure 3.7 compares the concentration of Al, Fe, Ca, Mg, Na, and K cations which are related to the presence of clay minerals in Gray Berea and Gray Bandera sandstones.

Table 3.6: Elemental Composition of Berea Gray and Bandera Gray Sandstone, by XRF Analysis.

Elements	Berea Gray (wt%)	Bandera Gray (wt%)
Si	40.40	30.89
Al	4.18	6.61
Fe	0.76	2.64
Ca	0.29	5.31
Mg	0.35	2.25
Mn	0.02	0.19
Na	0.33	1.26
K	1.51	1.47
Ti	0.35	0.53
Cr	0.03	0.03
Zr	0.06	0.05
P	0.03	0.09
S	0.04	0.06
Cl	0.14	0.35
O	51.52	48.27
Sum	**100.00**	**99.98**

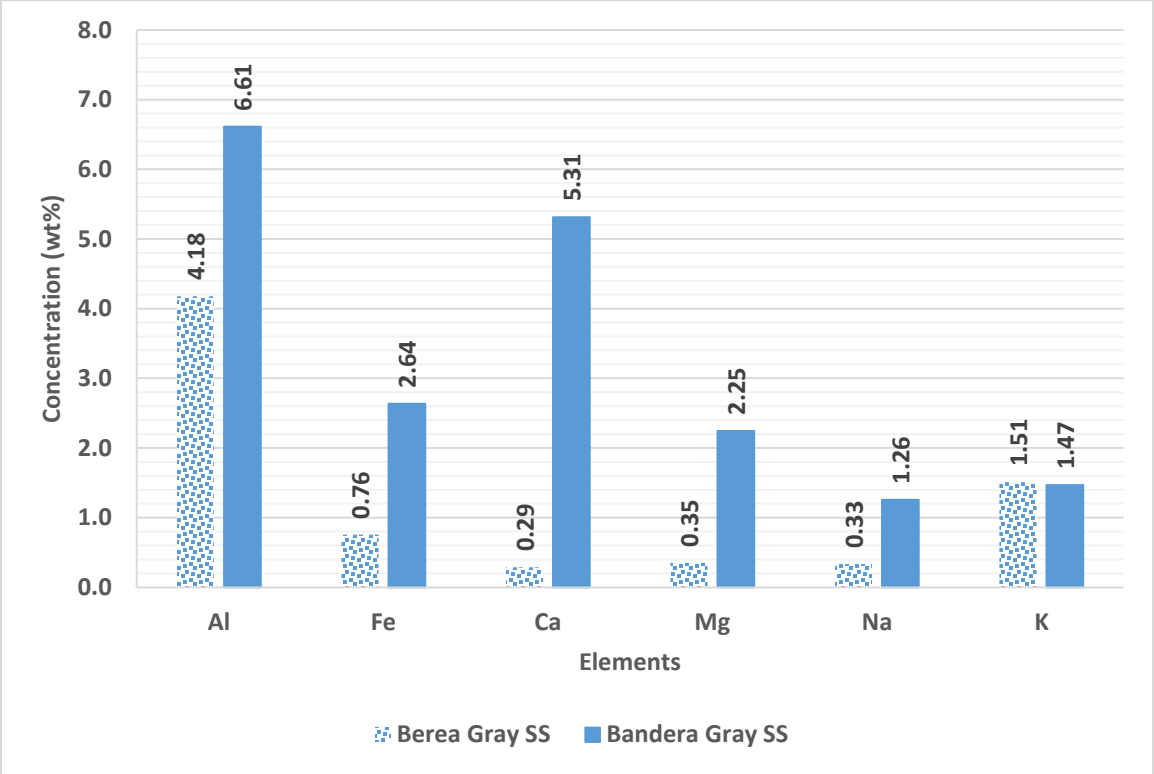

Figure 3.7: Comparison of the Concentrations of Al^{+3}, Fe^{+3}, Ca^{+2}, Mg^{+2}, Na^{+}, and K^{+} Cations in Gray Berea and Gray Bandera Sandstone Samples.

3. SEM-EDX and FESEM-EDS Analyses

The analyses were used to identify the presence of clay minerals and to give information about the distribution of clay minerals within the pore system.

The tested samples of Gray Berea sandstone did not show the presence of any clay particles as shown in Figure 3.8, this result does not necessarily means that there are no clay minerals in Berea samples; since this needs to be confirmed with the results of XRD analysis. On the other hand, the Gray Bandera sandstone samples shows the presence of some particles which are most likely to be clay minerals. Figure 3.9 shows the SEM images of Bandera

sandstone which shows clearly the presence of kaolinite and chlorite types clay minerals in this sample. Figure 3.10 shows the result of FESEM-EDS analysis conducted on Bandera sandstone. This figure indicates the presence of some particles which looks like illite clay mineral, to confirm this result the EDS technique was and although it did not show the presence of any K^{+} but it showed 7.99% of Al^{+3} particles as well as the presence of Si^{+4} and O^{-2} which increase the possibility of those particles to represent clay minerals.

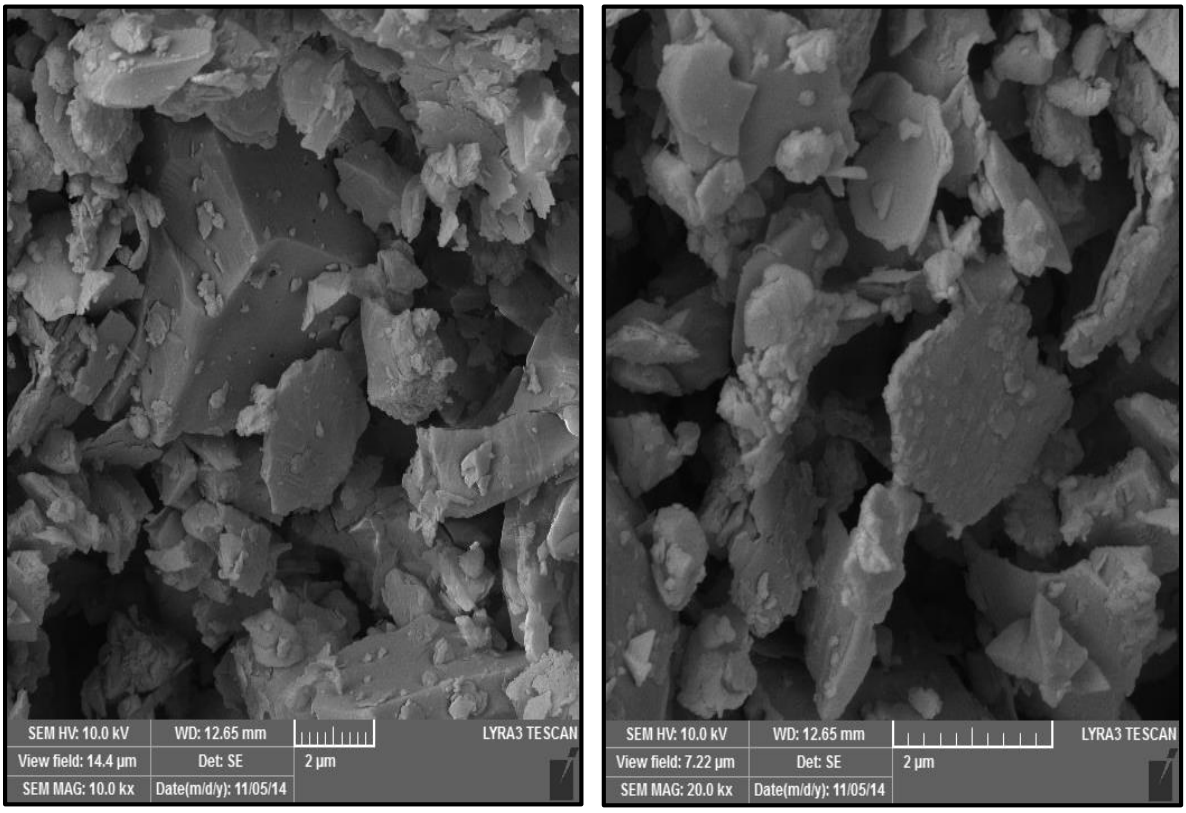

Figure 3.8: FESEM Images for Gray Berea Sandstone Sample.

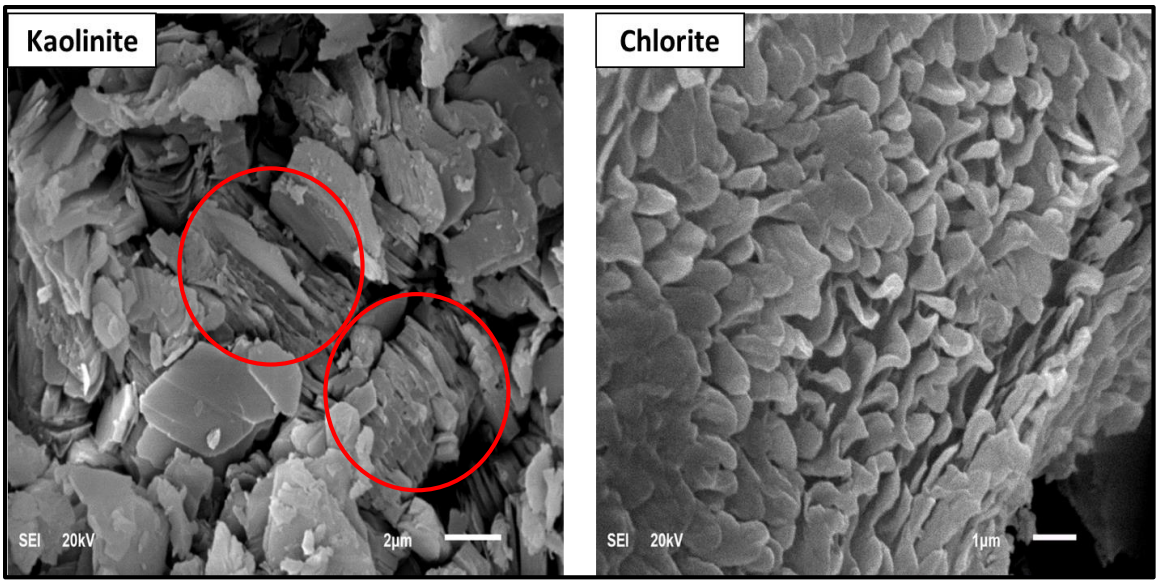

Figure 3.9: SEM Images for Gray Bandera Sandstone Sample.

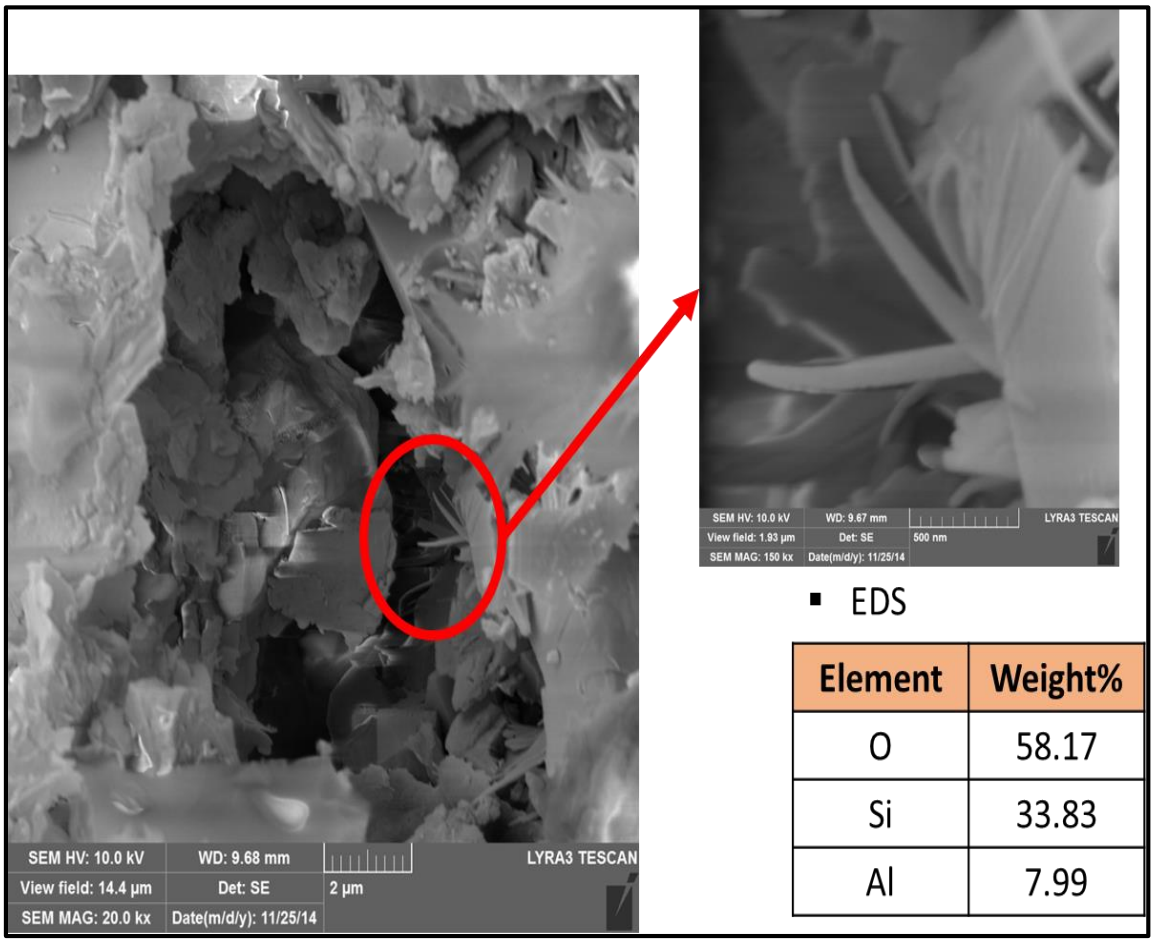

Figure 3.10: FESEM-EDS Results for Gray Bandera Sandstone Sample.

3.2 Interfacial Tension Measurements Procedures

The effect of EDTA chelating agent on decreasing the force between crude oil and brines was studied through interfacial tension measurements. Theta OneAttension Optical Tensiometer was used to measure the IFT in this study.

Table 3.7 below summarizes the constant and variable parameters used during interfacial tension measurements.

Table 3.7: Constant and Variable Parameters for IFT Measurements.

Constant Parameters	
Parameters	**Description/Values**
Light Phase	Uthmania Crude Oil
Oil Density	0.8835 (29.66 API)
Needle Type	Hocked Needle
Tip Size	40 µL
Drop Size	4.0 µL
Measuring Technique	Pendent Drop Technique
Variable Parameters	
Parameters	**Description/Values**
Heavy Phase	Different EDTA Solutions
EDTA Concentration	1wt%, 3wt%, 5wt%, and 7wt%
Temperature	25, 50, and 75 °C

For interfacial tension measurements the following procedures were followed:

1) Before starting every measurement the instrument was calibrated by the calibration ball and its magnetic and also through measuring the IFT between deionized water and air.
2) 5 ml of the heavy phase (EDTA solution) were introduced into the measuring glass cube before it placed onto the sample stage.
3) After that the syringe was filled with the light phase (UTMN crude oil).
4) Then the syringe's needle is inserted into the heavy phase.
5) A drop of 4.0 µL of light phase is injected from the needle tip into the middle of the heavy phase.
6) The temperature is then adjusted to the required level.
7) After that the live analysis mode was activated to monitor the change in interfacial tension with time throughout the dynamic interfacial tension period until the kinematic interfacial tension value is reached (time to reach stabilized interfacial tension measurement).

3.3 Zeta Potential Measurement Procedures

Different zeta-potential measurements were conducted in this study using Brookhaven ZetaPALS (Phase Analysis Light Scattering) instrument to investigate the effect of adding EDTA chelating agent on changing particles charge for both Gray Berea and Gray Bandera sandstone rock samples.

3.3.1 Sample Preparation

Zeta-potential measurements at rock/fluid interface requires preparing a powder of the rock samples; about 1cm in length and 1.5" in diameter pieces were cut from each sample, after that those samples were crushed to make a very fine powder (less than 5.0 µm), and then those samples were kept in labeled bottles.

The following procedures were followed to compare the effect of EDTA chelating agent on zeta-potential and hence the wettability change:

1. Firstly for measuring zeta potential at brine/rock interface in absence of oil different solutions were prepared each one is a mixture of: 0.5wt% of the Gray Berea or Gray Bandera sandstones powder dissolved in one of the following:
    a) Only seawater, diluted seawater or deionized water.
    b) Different concentrations of EDTA (5wt%, 7wt%, and 10wt%) in seawater.
2. And for measuring zeta-potential at crude brine/rock interface in presence of oil the same solutions were again prepared but this time 0.5wt% Uthmania crude oil was added to those solutions.
3. Then the solutions prepared in steps (1) and (2) were shaken for two days, after removed from the shaker the samples kept for 20 minutes to allow all the large particles to settle down, the upper part of the sample was separated from the samples and filtered through 5 µm filter.
4. After that ZetaPALS instrument was used to measure the Electrophoretic mobility value from which zeta potential was calculated.

Table 3.8: Constant and Variable Parameters for Zeta-Potential Measurements.

Constant Parameters	
Parameter	**Description/Value**
Oil	Uthmania Crude Oil
Oil Density	0.8835 (28.66 API) @ 25°C
Oil Viscosity	17.59 cp @ 25°C
Solid to Liquid Ratio	0.5wt%
Oil to Brine Ratio	0.5wt%
Temperature	25°C
Pressure	Atmospheric Pressure (14.7 psi)
Conditioning Time	48 hours
Zeta Potential Model	Smoluchowski Model
Variable Parameters	
Parameter	**Values**
Na_4EDTA Concentration	5wt%, 7wt%, and 10wt%
pH	4.00 to 12.00

3.4 Core Flooding Experiments Procedure

A composite core samples of Gray Berea and Gray Bandera sandstones were used in core flooding experiments, each composite core consists of two core plugs with the dimensions of 2" in length and 1.5" in diameter. Figure 3.11 shows some of the core plugs used in this study.

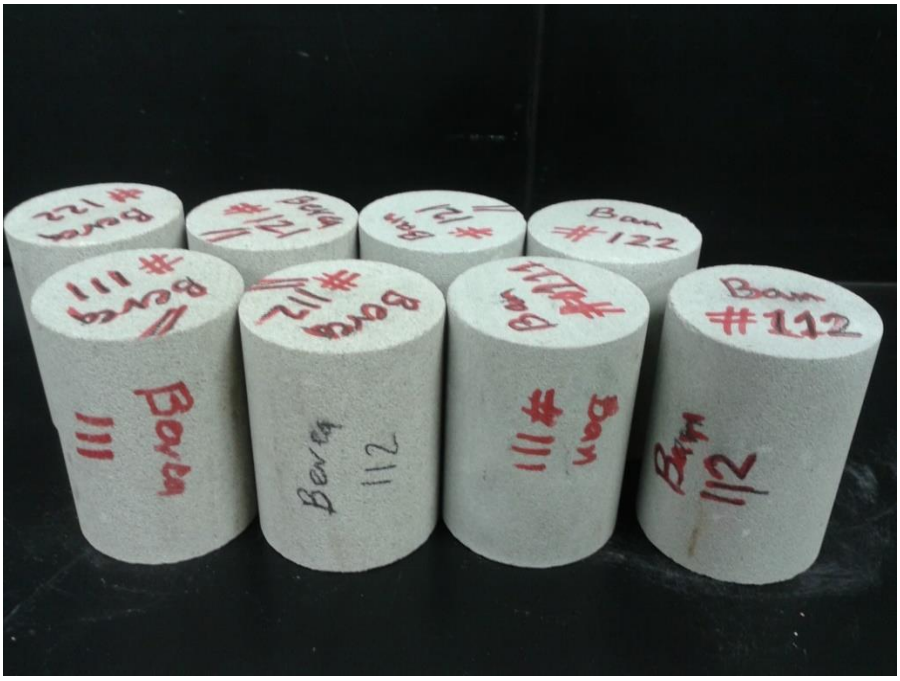

Figure 3.11: Some of Core Plug Samples Used in this Study.

Table 3.9: The Constant and Variable Constants Variables Used for Core Flooding Experiments.

Constant Parameters	
Parameters	**Description/Values**
Aging Period	15 Days
Aging Temperature	100°C
Aging Pressure	2500 psi
Overburden Pressure	2500 psi
Back Pressure	1500 psi
Flowrate	0.5 cc/min
Flooding Temperature	100°C
Variable Parameters	
Parameters	**Description/Values**
EDTA Concentration	1wt%, 3wt%, 5wt%, 7wt%, and 10wt%
Rock Samples	Standard Gray Berea and Gray Bandera Sandstones

The core flooding experiments were carried out as follows:

1. The core plugs were cut with the dimensions summarized in Table 3.1.
2. Then cleaned in soxhlet unit for one day with the methanol and dried in the oven at 40°C for 3 hours before they weighted dry.
3. After that the core samples were saturated with the formation brine under vacuum.
4. Saturation method was used to determine the core plugs porosity.
5. The formation brine injected through the core samples at different flowrates to calculate the samples original absolute permeability before core flooding test.
6. The residual water saturation S_{wi} was established for all plugs through centrifuging at 5000 rpm for 24 hours by using air as a displacing fluid.
7. Then the samples were saturated under vacuum with filtered oil and aged for two weeks.
8. The samples were then loaded into the core holders, and an overburden pressure of 2500 psia and back pressure of 1500 psia were applied at the core samples.
9. Then the effective oil permeability at initial water saturation was measured.
10. After that the core samples were flooded with seawater till no more oil recovery. During the flooding effluent was collected and pressure values were recorded as a function of the injected pore volume (PV_{inj}).
11. When no more oil was recovered by seawater, the EDTA solution with the lowest concentration along those wanted to be injected in the experiment was used again until no more oil recovery is noticed.
12. Then the solution with the middle concentration was injected until all possible oil is produced before start injecting the EDTA solution with highest concentration which

was also injected until it was not contribute by increasing the oil recovery. Again the effluent produced at different stages of EDTA solutions injection was collected and the pressure drop was recorded as a function of PV_{inj}.

13. After the core flooding experiment was finished the core samples were cleaned in the soxhlet unit using toluene until all the remaining oil is removed and then with the methanol for one day, after that the sample were dried in oven at 45°C for three hours.
14. Finally, the core samples were saturated with formation brine again and their absolute permeability after flooding is measured to study the effect of EDTA on rock permeability.

Table 3.1 below summarizes the different properties of the core samples used in this study.

Table 3.1: Different Properties of Core Plug Samples Used in This Study.

Experiment #	Sample ID	Core Length (cm)	Core Diameter (cm)	Dry Sample Weight (g)	Saturated Sample Weight (g)	Bulk Volume (cc)	Pore Volume (cc)	Grain Density (g/cc)	Porosity (%)	Brine Permeability (md), See Appendix B	Swi (%)
1	Berea 1	5.080	3.799	120.3	133.20	57.61	11.49	2.6085	19.94%	119.78	12.40%
	Berea 2	5.000	3.799	118.8	131.40	56.70	11.22	2.6122	19.79%	119.05	11.90%
2	Berea 3	5.030	3.799	119.8	132.23	57.04	11.07	2.6062	19.41%	116.25	12.87%
	Berea 4	5.100	3.799	121.9	134.47	57.83	11.19	2.6135	19.35%	116.66	12.33%
3	Berea 5	5.128	3.799	122.1	133.70	58.15	10.33	2.5534	17.76%	80.85	15.52%
	Berea 6	5.096	3.799	121.6	133.30	57.79	10.42	2.5671	18.03%	84.35	16.24%
4	Bandera 11	5.025	3.799	126.2	136.47	56.98	9.14	2.6380	16.04%	10.62	17.21%
	Bandera 12	5.060	3.799	126.8	137.00	57.38	9.08	2.6255	15.83%	9.35	19.12%
5	Bandera 13	5.151	3.799	129.8	138.40	58.41	7.70	2.5590	13.19%	8.92	20.32%
	Bandera 14	5.059	3.799	127.3	136.80	57.37	8.46	2.6028	14.75%	9.03	20.02%

CHAPTER 4

RESULTS AND DISCUSSION

4.1 Zeta-Potential Measurements

Zeta-potential experiments were carried out to study the effect of EDTA chelating agent on of double layer in the presence and absence of crude oil, the results are shown in Figure 4.1 which compares the effect of the seawater dilution and the increase of chelating agent concentration on the electric double layer charge between the brine and both Gray Berea and Gray Bandera sandstones, the charge is negative for all cases shown in Figure 4.1; in case of seawater, the negative magnitude is higher in case of Gray Berea than Gray Bandera; and this is due to the lower concentration of different cations (Fe^{+3}, Al^{+3}, Ca^{+2}, K^{+}, Mg^{+2}, and Mn^{+2}) in Gray Berea sandstone, and as illustrated earlier the source of those cations in the sandstone reservoirs is the interlayer of clay minerals.

Figure 4.1 shows that the increase of the negative magnitude of zeta-potential with the diluted seawater is higher in case of Gray Bandera sandstone than Gray Berea sandstone; this is due to release of higher amount of different cations from the surface of clay minerals (especially Ca^{+2} and Mg^{+2}) in case of Gray Bandera sandstone.

Uses of Na_4EDTA chelating agents in this study showed that this chemical has the ability to increase the negative magnitude of zeta-potential for both sandstones samples under study (the negative magnitude in case of using the 5wt% Na_4EDTA chelating agent

solution in seawater is even higher than that of using deionized water at the same pH; indicating the ability of the EDTA solution of 5wt% to chelate higher amount of different cations than the deionized water) and again the rate of the increase is higher for Gray Bandera for the same reasons explained earlier, the ability of Na_4EDTA chelating agents solutions to increase the negative magnitude is due to the nature of those chemicals which has high ability to chelate different cations from the surface of rock when they interact, and since Gray Bandera sandstone has plenty of cations compared with those present in Gray Berea sandstone rocks; Na_4EDTA solutions has an opportunity to release higher amount of those cations when they mixed with Gray Bandera sandstone reservoirs than those in case of Gray Berea.

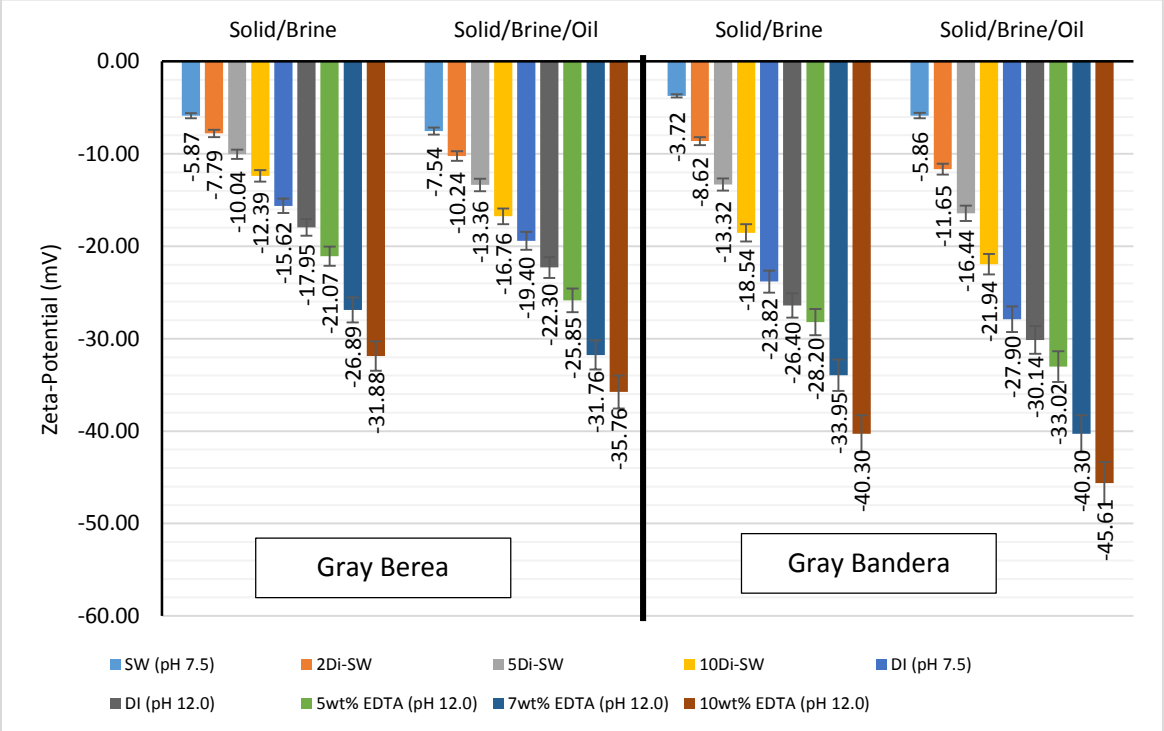

Figure 4.1: The Effect of the Injected Water Salinity and Different Concentrations of Na_4EDTA Chelating Agent on Zeta-Potential for Gray Berea and Gray Bandera Sandstone Samples in the Absence and Presence of Oil at 25°C.

Figure 4.1 shows the values of zeta-potential in the presence of oil; it shows clearly that for all cases the zeta-potential values in the presence of oil have more negative value than that in absence of oil, which could be to attributed to adsorption of negatively charged polar components of the crude oil onto the suspended particles. This result is in agreement with Kassim (2012) for the case of carbonate.

The seawater and Na_4EDTA solutions used in the study showed in Figure 4.1 have pH values of 7.50 and 12.00, respectively, and hence the pH has a significant effect on chemical enhanced oil recovery (CEOR) efficiency and wettability change, the effect of pH on zeta-potential was studied also and the results of this study for both seawater and EDTA solutions with both Gray Berea and Gray Bandera sandstones are shown in Figure 4.2. The pH for the EDTA is ranging from 4.94 up to 12.00 and for seawater it was from 4.67 to 9.00; the pH of the seawater did not increased more than 9.00 pH unit since increasing the seawater pH higher than this value will result in $CaCl_2$ salt precipitation as indicated by the XRF result in Table 4.1.

Figure 4.2 shows that the negative value of zeta-potential in case of EDTA solution is increased at the interface of both sandstones with the increase of the solution pH, while for that of seawater the increase of the negative magnitude is in a decreasing rate, this is due to the saturation of the seawater at high pH with the cations especially the Ca^{+2} as indicated by the XRF results of the salt precipitated from seawater at high pH ($CaCl_2$) tabulated in Table 4.1, which make the seawater unable to take more cations from the rock, this is why the zeta-potential at rock/sweater interface at high pH could not be increased more.

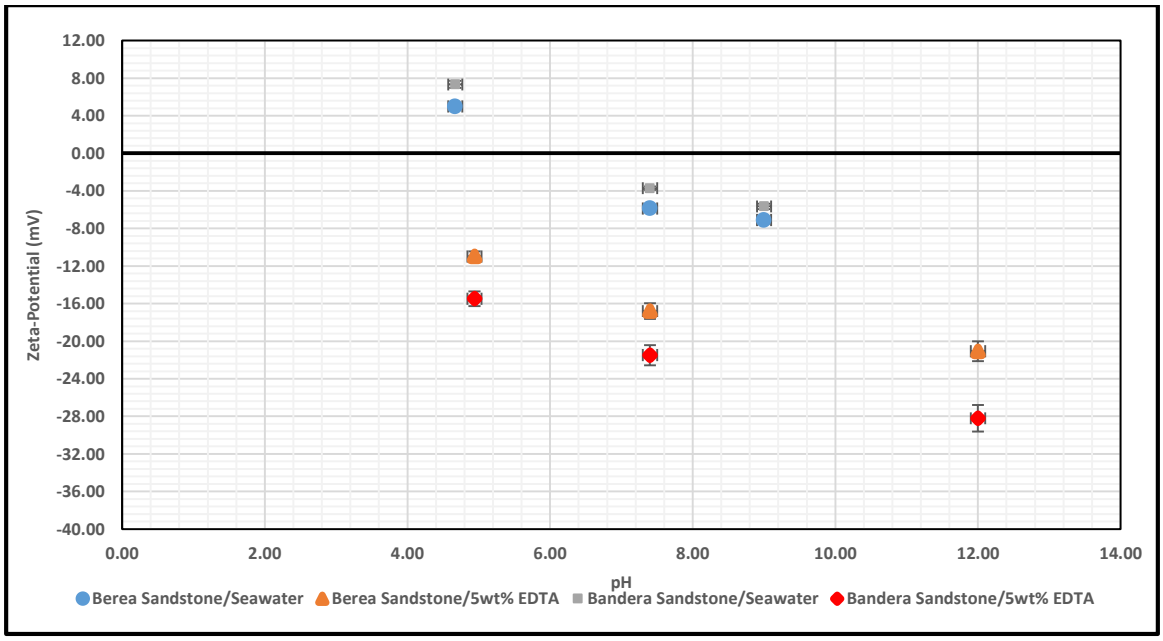

Figure 4.2: The Effect of pH on Zeta-Potential Measurements at Brine/Rock Interface for Seawater and 5wt% Na_4EDTA in Seawater.

Table 4.1: XRF Results of the Precipitated Salt from the Seawater (58 k ppm) at pH Higher than 9.0.

Element	Weight (%)
Ca	33.33
Cl	66.66
Si	Trace
S	Trace
K	Trace
Fe	Trace
Ni	Trace
Cu	Trace
Rb	Trace
Sum	**99.99**

4.2 Interfacial Tension (IFT) Measurements

The IFT between the different concentrations of Na_2EDTA solutions used in this study and UTMN crude oil was studied, one of the most important thing must be considered during those measurements is the stability of the IFT since it is changing with time until it reached stabilized IFT value when the oil droplet and the continues phase (Na_2EDTA solution) reach equilibrium. Figure 4.3 shows the change of the IFT for the 5wt% EDTA solution from the time the oil droplet introduced inside the solution until the stability is reached.

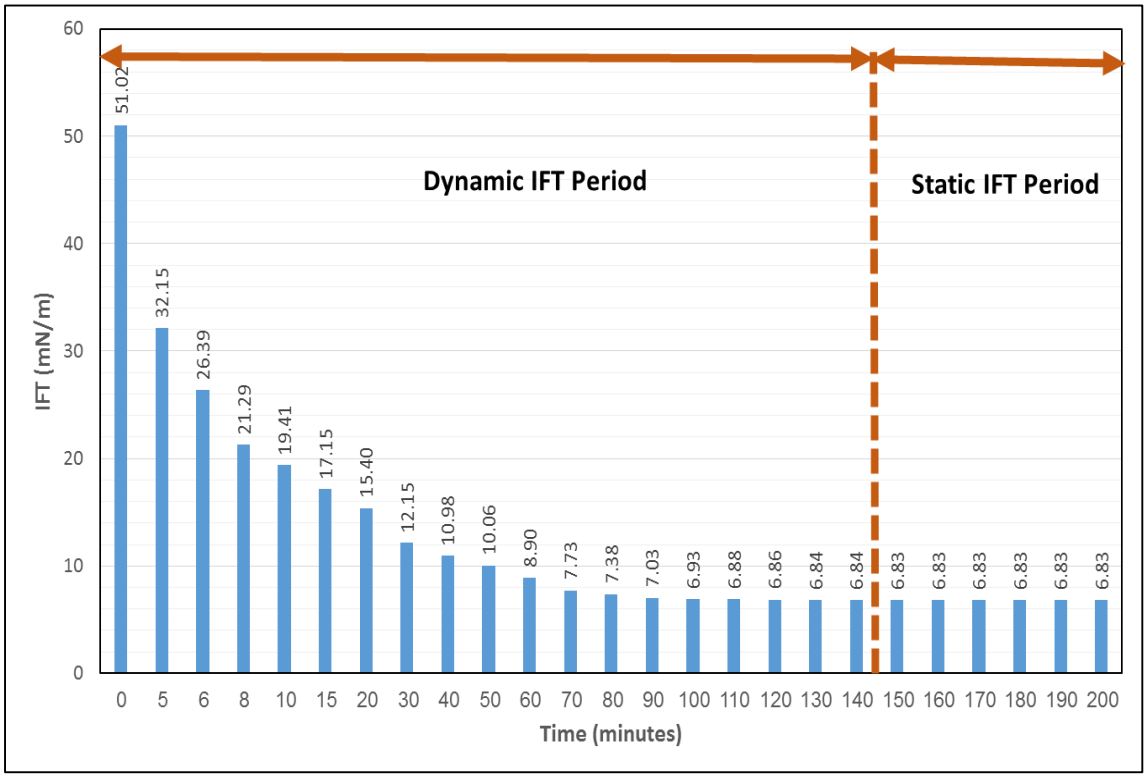

Figure 4.3: The Time Required to Reach the Static Interfacial Tension between 5wt% Na_4EDTA at pH = 12.00 and Uthmania Crude Oil @ 25°C.

The IFT was measured for the four concentrations of Na_2EDTA solutions included in this study, Figure 4.4 compares between the IFT values for all those concentrations as a function of temperature, it is clearly seen that the increase in the temperature will reduce the force between the oil and those chemicals, the increase in the chemical concentration also decreased the IFT values. Figure 4.5 compares between the IFT value between seawater and UTMN crude oil with those between this oil and different concentrations of EDTA at 75°C, increasing the concentration from 1wt% to 7wt% decreased the IFT almost linearly from 6.31 to 4.37 mN/m.

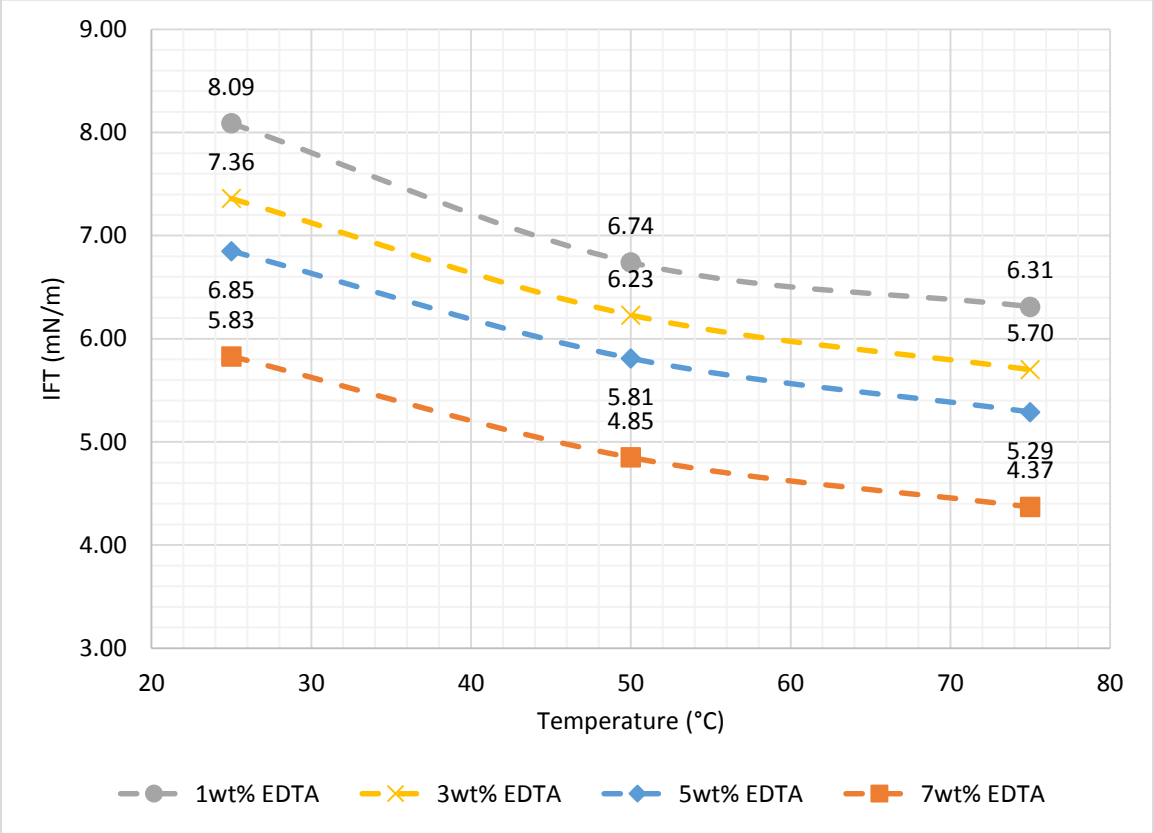

Figure 4.4: The Effect of Temperature of the IFT between UTMN Crude Oil and Different Concentrations of Na_2EDTA Solutions.

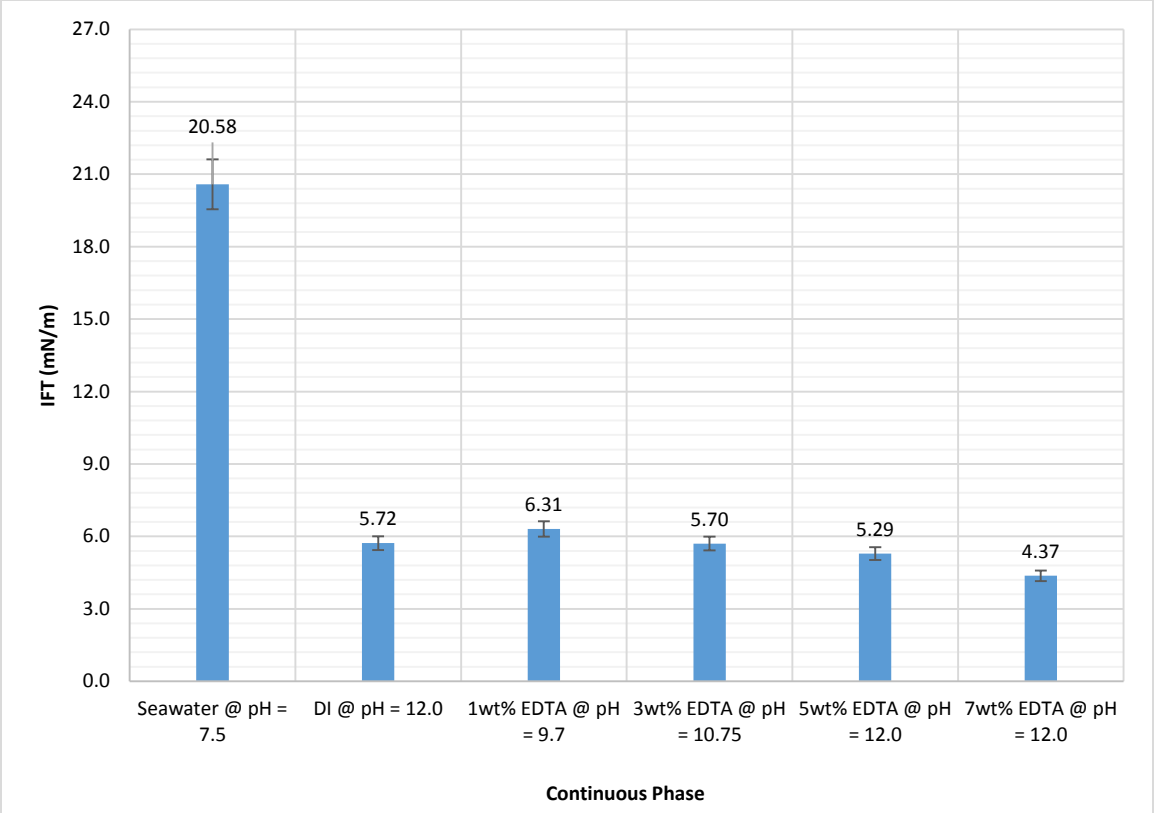

Figure 4.5: The Effect of Increasing the Na_2EDTA Concentration on the IFT at 75°C.

4.3 Coreflood Experiments

4.3.1 Coreflood Experiments for Gray Berea Sandstone Samples

Three sets of coreflood experiments were conducted using Gray Berea sandstone core samples. In the first experiment (Experiment #1) the flooding started with seawater injection followed by 1wt% then 3wt% and 5wt% of EDTA solutions prepared in seawater and finally the sample flooded with seawater again, the results of recovery factors, pressure drop as well as the pH change throughout this experiment are plotted in Figures 4.6 and 4.7, in those figures the seawater produced 50.50% of the original oil in place (OOIP) and

extra 15.36% of OOIP was recovered by injecting the different concentrations of the Na_2EDTA chelating agent solutions.

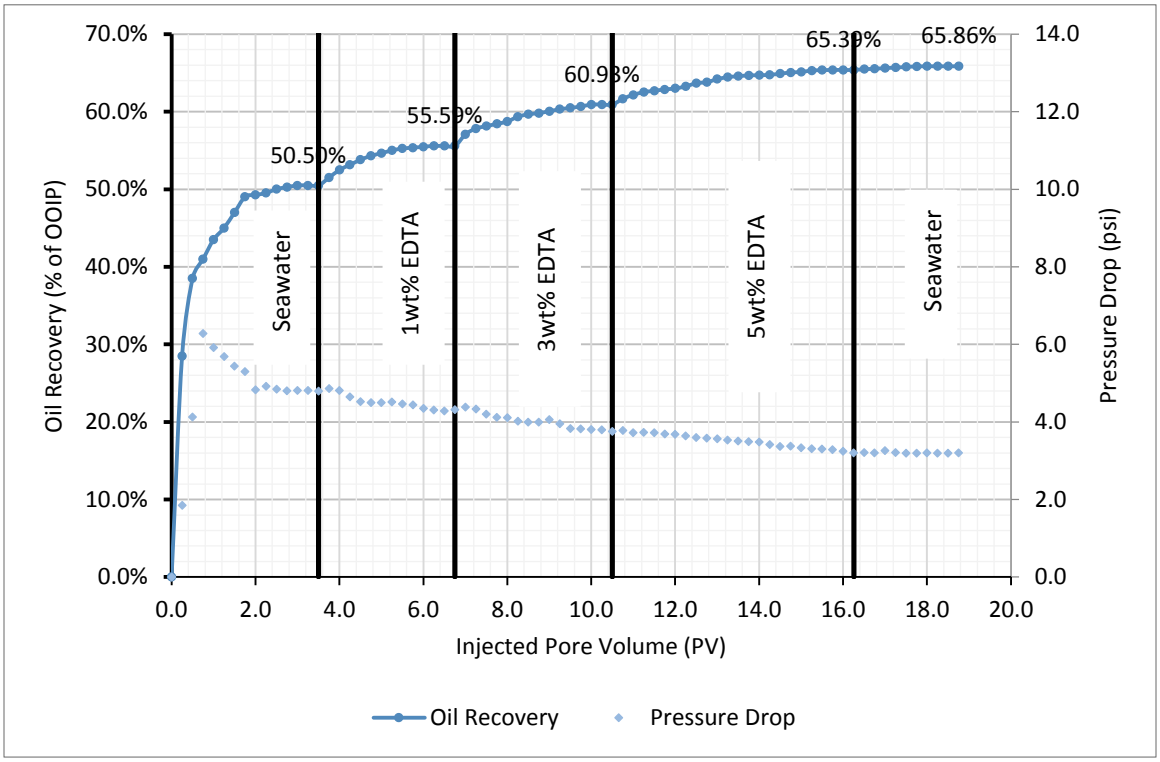

Figure 4.6: Recovery and Pressure Drop as a Function of Injected Pore Volume, Experiment #1.

Figure 4.7 shows that switching from seawater to 1wt% EDTA (at pH of 9.70) resulted in an increase in the pH of the produced effluent by 0.5 pH unit (from about 7.5 in case of injecting the seawater to 8.0 during the 1wt% flooding period); this is as a result of injecting solution with higher pH and the desorption of the active cations from clay minerals (mainly Ca^{+2}) as indicated in Figure 4.8. Injection of one pore volume of 3wt% EDTA at pH of 10.75 increased the produced fluid pH again by 0.2 pH units; again this increase in the pH is a results of chelating more active cations from the interlayer of clay minerals especially Ca^{+2} and Fe^{+3}. Shifting to 5wt% EDTA (pH = 12.00) increased the pH by 1.0 unit to about

9.20 after injection of almost one PV of this concentration. As indicated in Figure 4.7 the increase of oil recovery was well correlated to the increase of the produced fluid pH which results from injecting high pH solution, during all the EDTA flooding stages the produced fluid pH is less than the injected fluid pH indicating the loss of protons from the injected fluids and adsorption of the protons by clays which will lead to alkaline conditions close to clays surfaces. Developing this alkaline condition is considered by Rezaeidoust et al., (2010) and Aksulu et al., (2012) to be the main reason for breaking down the equilibrium of the system which is responsible for adsorption of the components of the crude oil onto clay minerals surfaces through different interlayer cations.

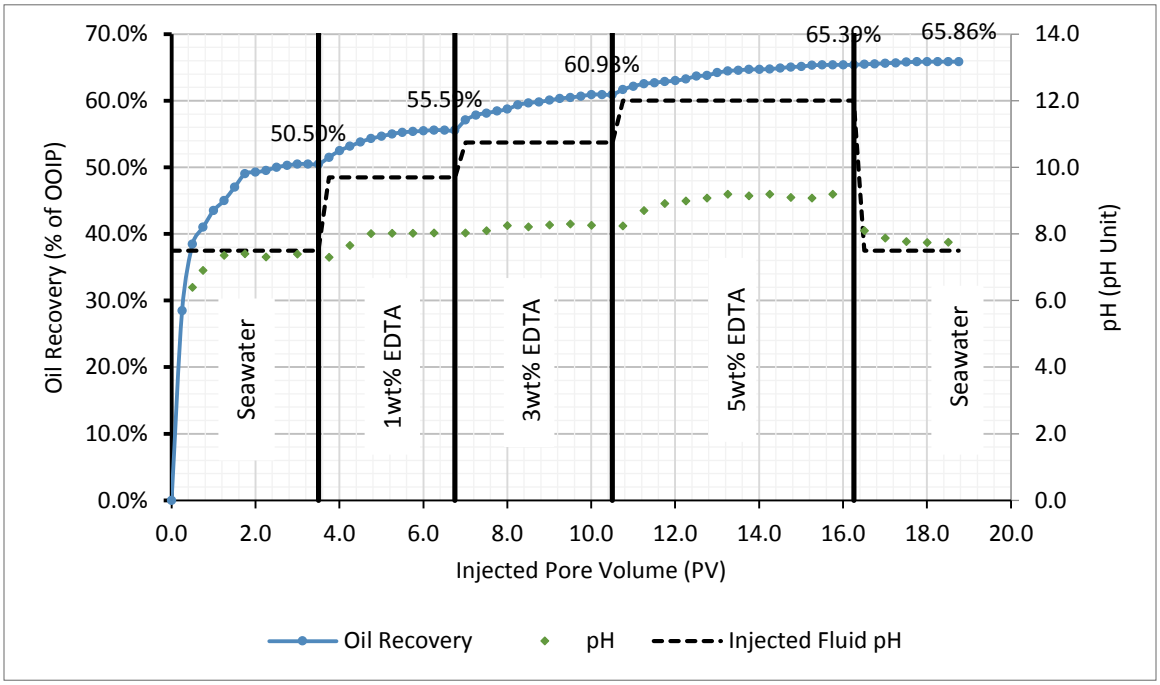

Figure 4.7: The Change of the pH with the Change of EDTA Concentration during Experiment #1.

Figure 4.7 also showed that there was a decrease in the produced effluents pH compared to the injected fluids, this is due to the increase in the Ca^{+2} (pH buffer) concentration in the

produced fluids as explained by Equation 4.1; this equation shows how the interaction between chelated Ca^{+2} and OH^- from the injected solutions could contribute on reducing the produced effluents pH. The increase in the Ca^{+2} concentration will be explained in the following section.

$$Ca^{+2} + OH^- = [\ Ca - OH\ ]^+ \qquad \text{Equation 4.1}$$

Figures 4.8 to 4.15 show the change of Ca^{+2}, Mg^{+2}, Fe^{+3}, Si^{+4}, Al^{+3}, K^+, Mn^{+2}, Cl^-, and SO_4^{-2} concentration during the first and second stages of experiment #1 with change of both oil recovery and pH, those figures indicate the following:

- There was a good correlation between oil recovery and the chelated Ca^{+2} and Fe^{+3}, as can be seen from Figures 4.8 and 4.10 and reported before for low salinity water recovery mechanism Austad et al., (2010) and Attia et al., (2014), respectively.
- The Ca^{+2} and Cl^- concentrations in the produced effluent started with values higher than those in the injected seawater concentration; due to the mixing of the Ca^{+2} and Cl^- from the formation brine which has higher amount of both Ca^{+2} and Cl^- than the injected fluids, as can be seen from Figures 4.8 and 4.15.
- On the other hand, both Mg^{+2} and SO_4^{-2} concentrations in the produced fluids started with lower values than those in the injected fluids; on their way to balance with those Mg^{+2} and SO_4^{-2} originally present in the formation brine, and then increased toward their concentrations in the injected fluids, as can be seen from Figures 4.11 and 4.14.
- When the 1wt% solution is injected the Ca^{+2} concentration and pH increased; this is related to replacement of Ca^{+2} from the interlayer of clays those are in a direct contact with oil molecules by protons. There was a good correlation between Ca^{+2}

concentration , pH, and Oil recovery as reported by Rezaeidoust et al., (2011) and Aksulu et al., (2012), as can be seen from Figure 4.9.

- Fe^{+3} concentration also increased at first steps of 1wt% solution injection when the oil recovery was increasing as reported by (Attia et al., 2014), but the Fe^{+3} concentration also kept increasing when no more oil was recovered indicating that the relationship between the oil recovery and Fe^{+3} chelation is an indirect relationship, as can be seen from Figure 4.10.
- During the first two PV's after shifting to 1 wt% EDTA the concentration of Mg^{+2} decreased again in the produced effluent, as can be seen from Figure 4.11; this decreased in Mg^{+2} started directly with the increase in the produced Ca^{+2} and Fe^{+3} to compensate for the detached Ca^{+2} and Fe^{+3} and the loss of those positively charged particles from the system, as can be seen from Figures 4.8 and 4.10, respectively. Lager et al., (2006) and Lager et al., (2008) reported Mg^{+2} concentration decrease in the produce effluent at both laboratory and reservoir scale.
- There was no significate release of Si^{+4} and Al^{+3} (the cations forming the base for the layers of clay minerals) from the rock samples, which indicates that this chemical does not attack clays at this concentration, same result concluded by (De Wolf et al., 2014), as can be seen from Figure 4.12.

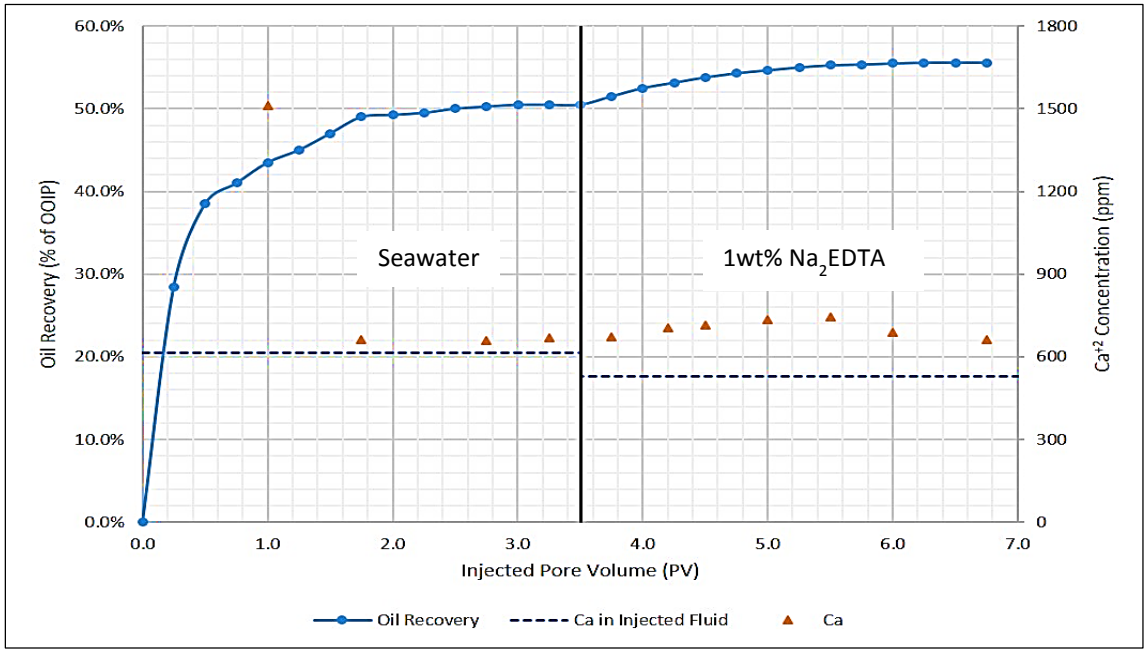

Figure 4.8: Ca^{+2} Concentration in the Produced Effluents during Seawater and 1wt% Na_2EDTA Injection into Gray Berea Sandstone and Oil Recovery, Experiment #1.

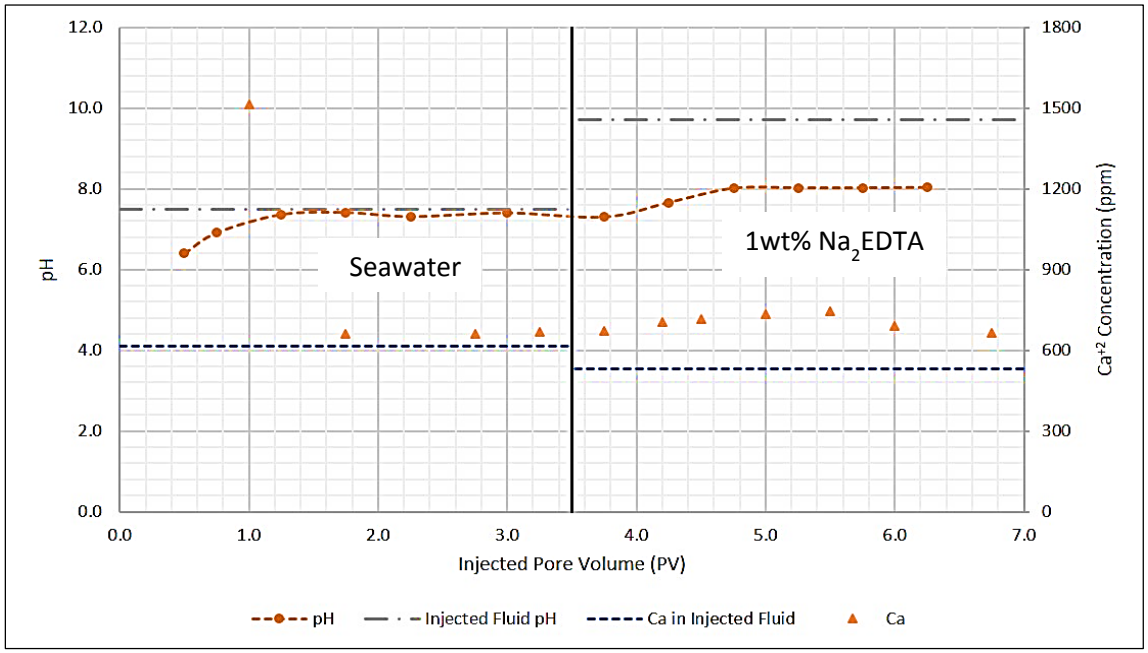

Figure 4.9: Ca^{+2} Concentration in the Produced Effluents during Seawater and 1wt% Na_2EDTA Injection into Gray Berea Sandstone and the pH, Experiment #1.

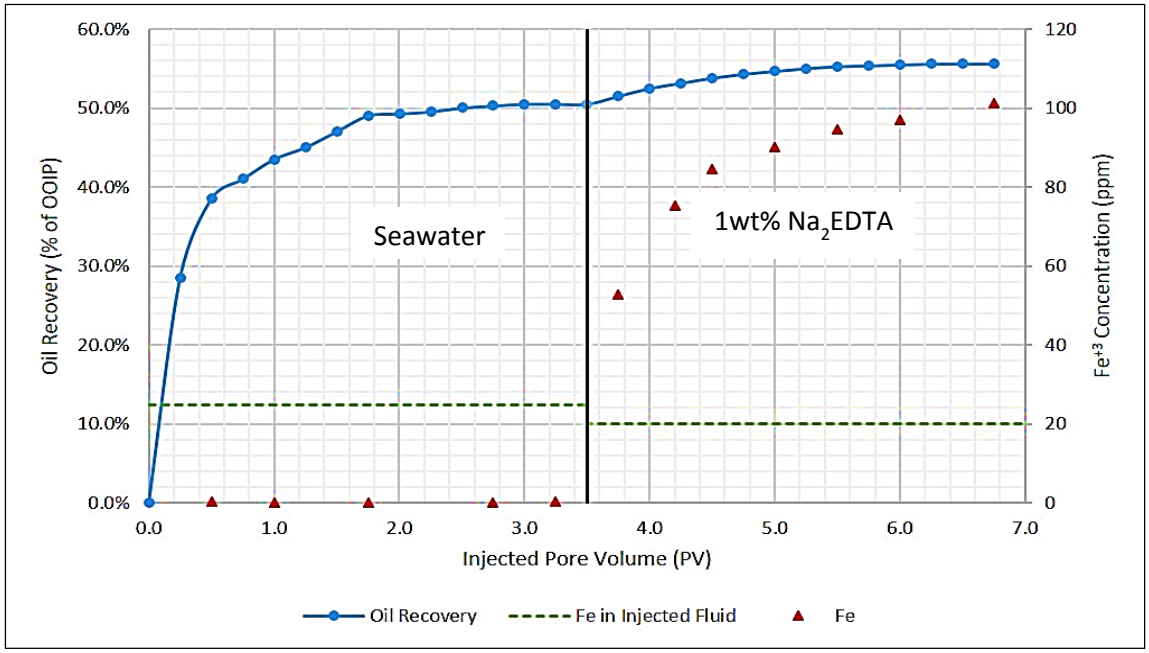

Figure 4.10: Fe^{+3} Concentration in the Produced Effluents during Seawater and 1wt% Na_2EDTA Injection into Gray Berea Sandstone and Oil Recovery, Experiment #1.

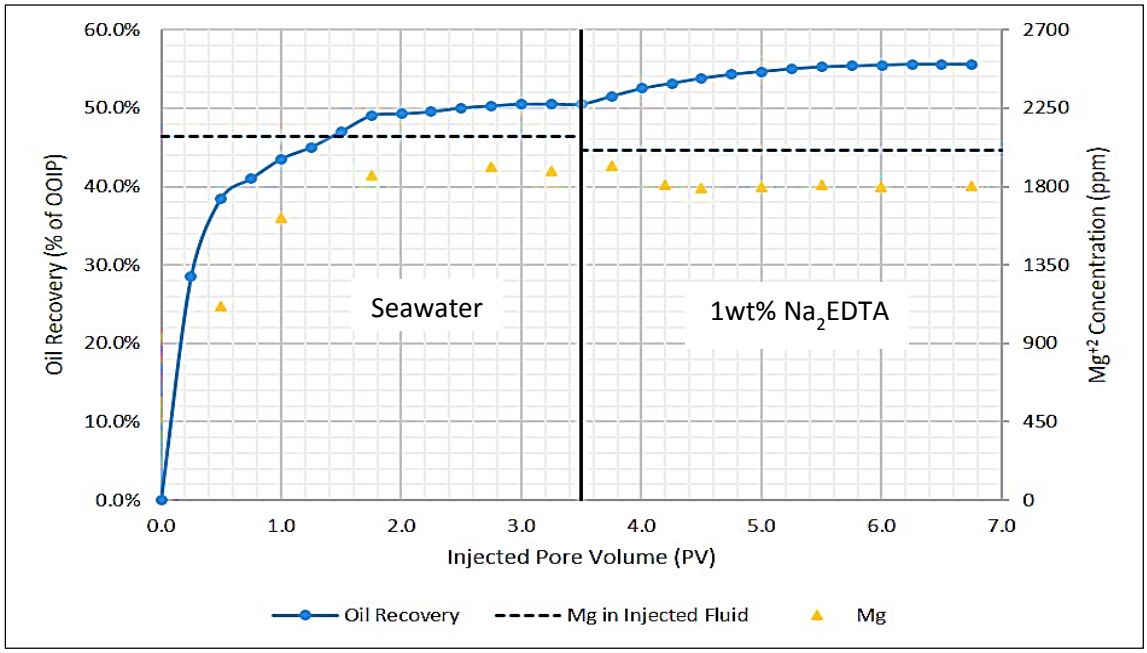

Figure 4.11: Mg^{+2} Concentration in the Produced Effluents during Seawater and 1wt% Na_2EDTA Injection into Gray Berea Sandstone and Oil Recovery, Experiment #1.

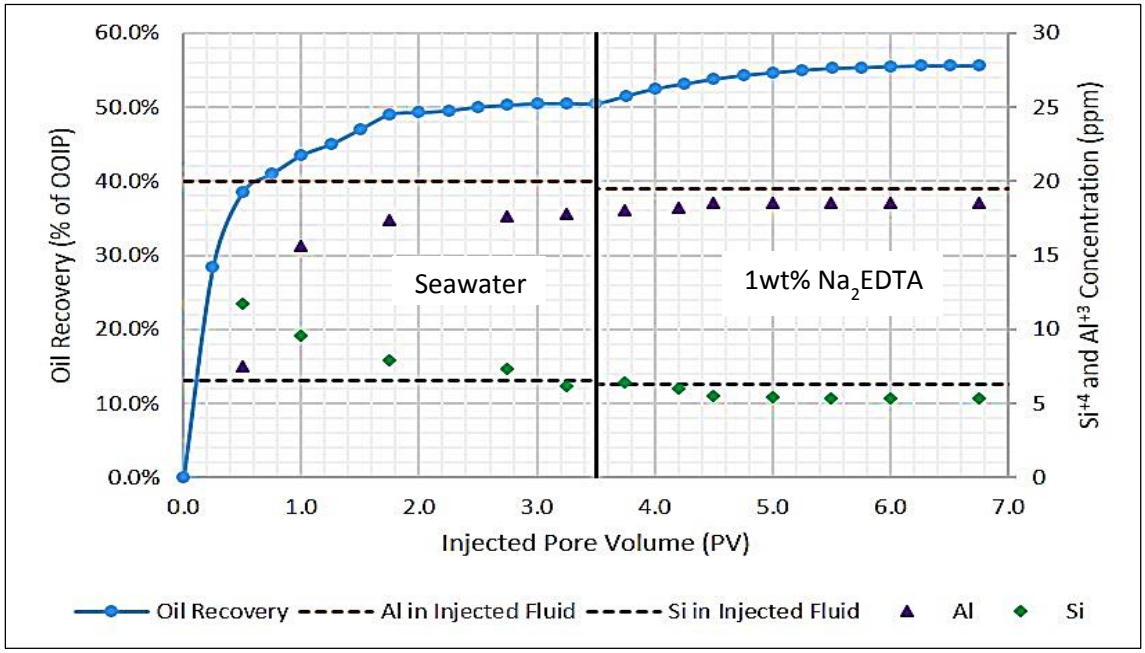

Figure 4.12: Si^{+4} and Al^{+3} Concentration in the Produced Effluents during Seawater and 1wt% Na_2EDTA Injection into Gray Berea Sandstone and Oil Recovery, Experiment #1.

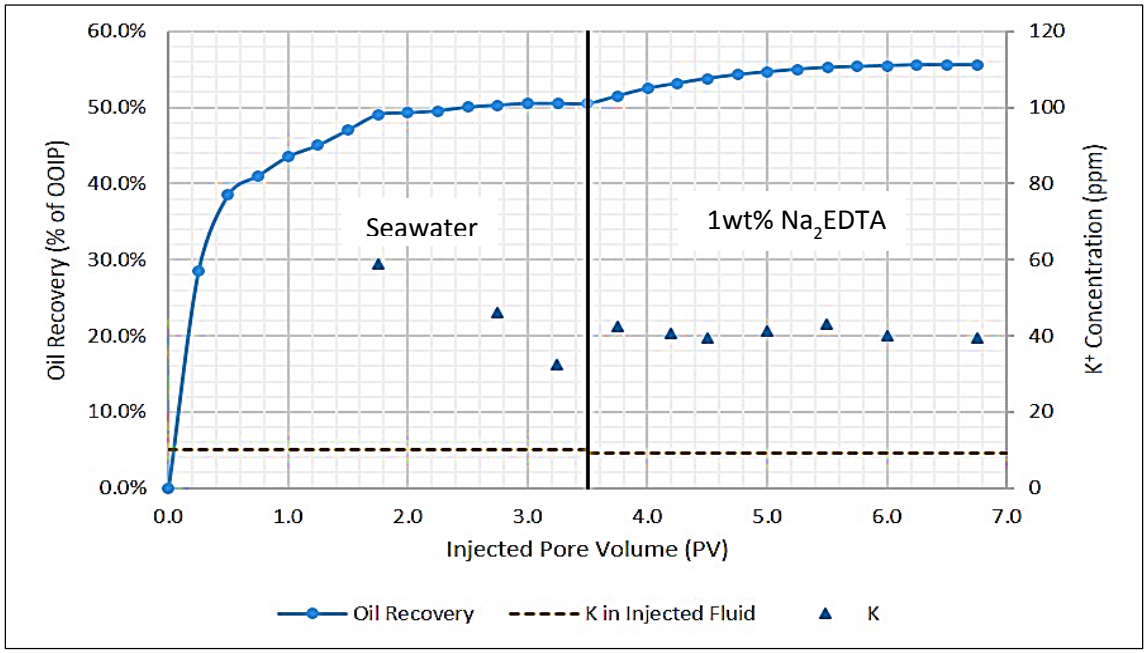

Figure 4.13: K^+ Concentration in the Produced Effluents during Seawater and 1wt% Na_2EDTA Injection into Gray Berea Sandstone and Oil Recovery, Experiment #1.

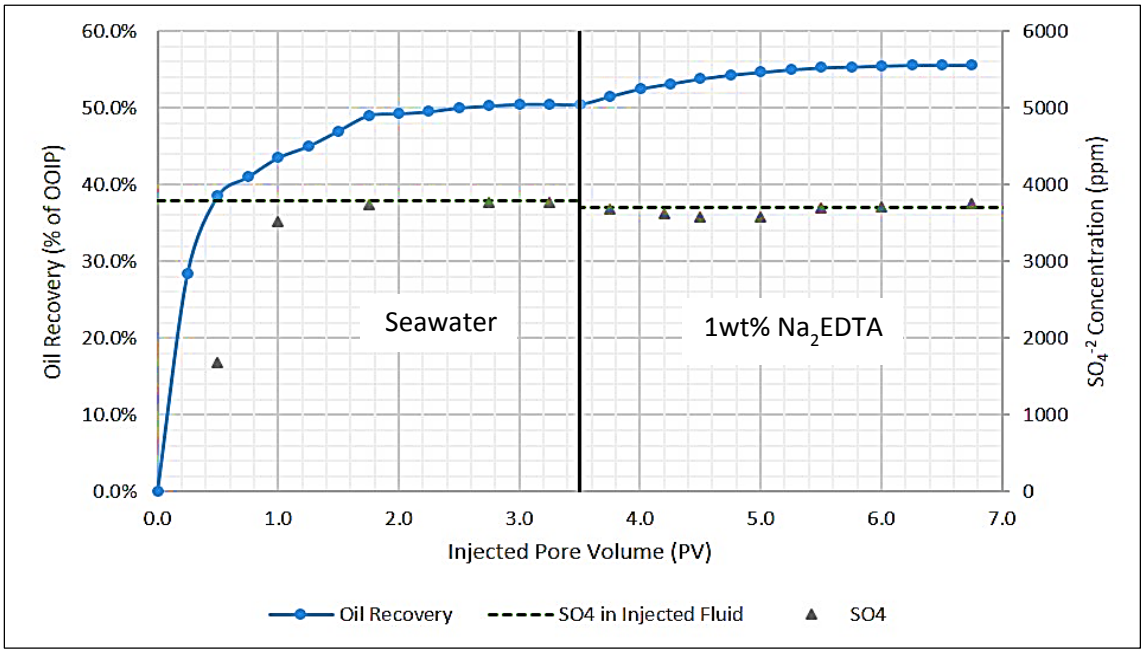

Figure 4.14: SO_4^{-2} Concentration in the Produced Effluents during Seawater and 1wt% Na_2EDTA Injection into Gray Berea Sandstone and Oil Recovery, Experiment #1.

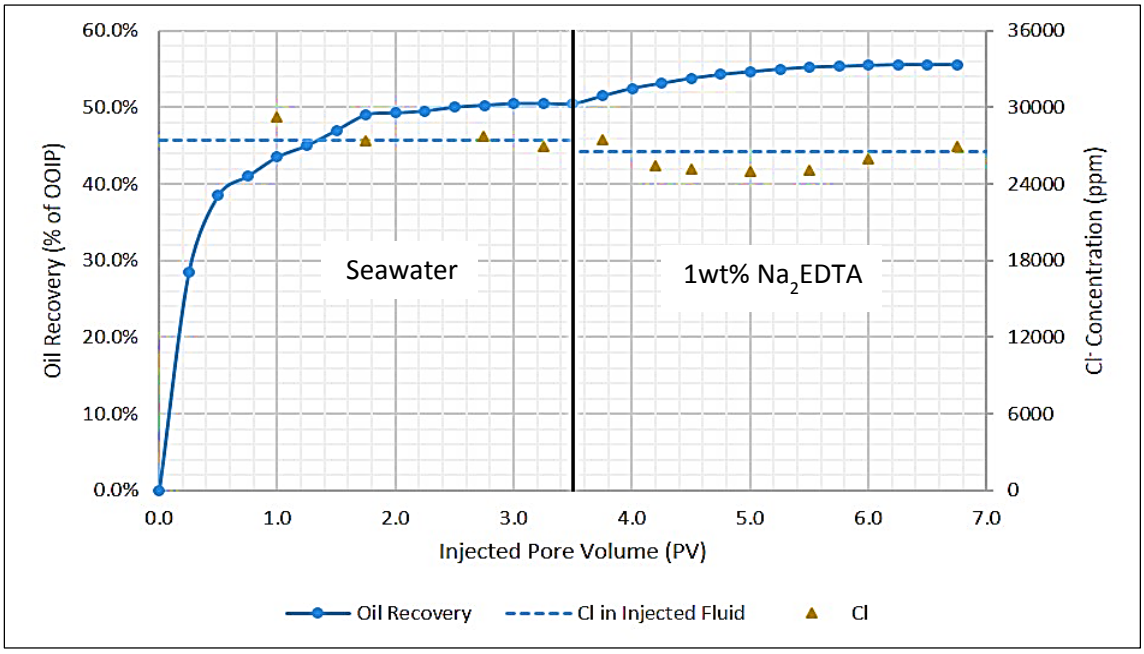

Figure 4.15: Cl^- Concentration in the Produced Effluents during Seawater and 1wt% Na_2EDTA Injection into Gray Berea Sandstone and Oil Recovery, Experiment #1.

In the second coreflood experiment (Experiment #2) conducted on Gray Berea sandstone samples, higher concentrations of EDTA solutions (3wt%, 5wt%, and 7wt% of EDTA) followed the seawater injection in an attempt to find the optimum concentration of the EDTA that will recover the maximum amount of the remaining oil. The oil recovery and pressure drop during the experiment as well as the pH change of the produced effluent from this experiment are summarized in Figures 4.16 and 4.17. The results show that more 16.96 % of OOIP could be produced with larger volumes of those higher concentrations of the chelating agent solutions compared with 15.36% obtained in experiment #1 with lower concentrations and less amount of Na_2EDTA.

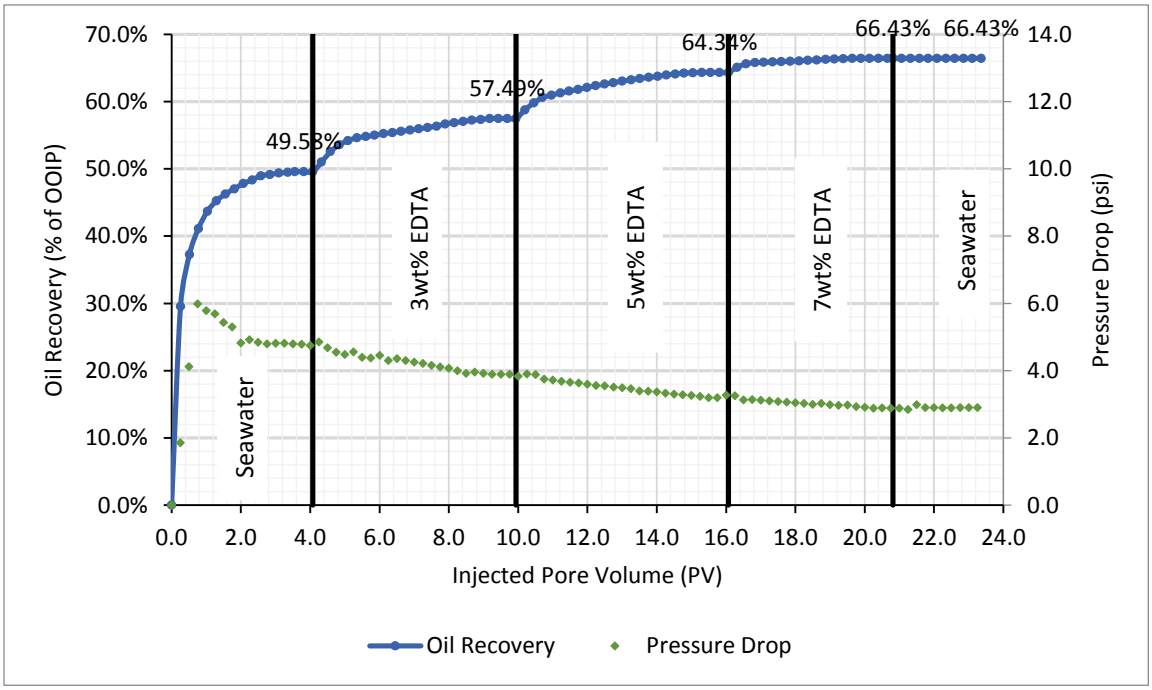

Figure 4.16: Recovery and Pressure Drop during Experiment #2 as a Function of Injected Pore Volume.

Switching from seawater injection to 3wt% increased the pH of the effluent from 7.5 to 8.14, the pH kept increasing with the increase of the concentration of the injected chelating

agent solutions as shown in Figure 4.17. This increase in the pH is due to the increase of the injected fluid pH, the produced fluids during the chelating agents flooding have lower pH than the injected fluids; indicating the increase in the alkalinity of the system near to the clays surfaces which is believed to be the main reason for increasing the oil recovery as suggested for the oil recovery mechanism by low salinity water injection by Rezaeidoust et al., (2011) and Aksulu et al., (2012).

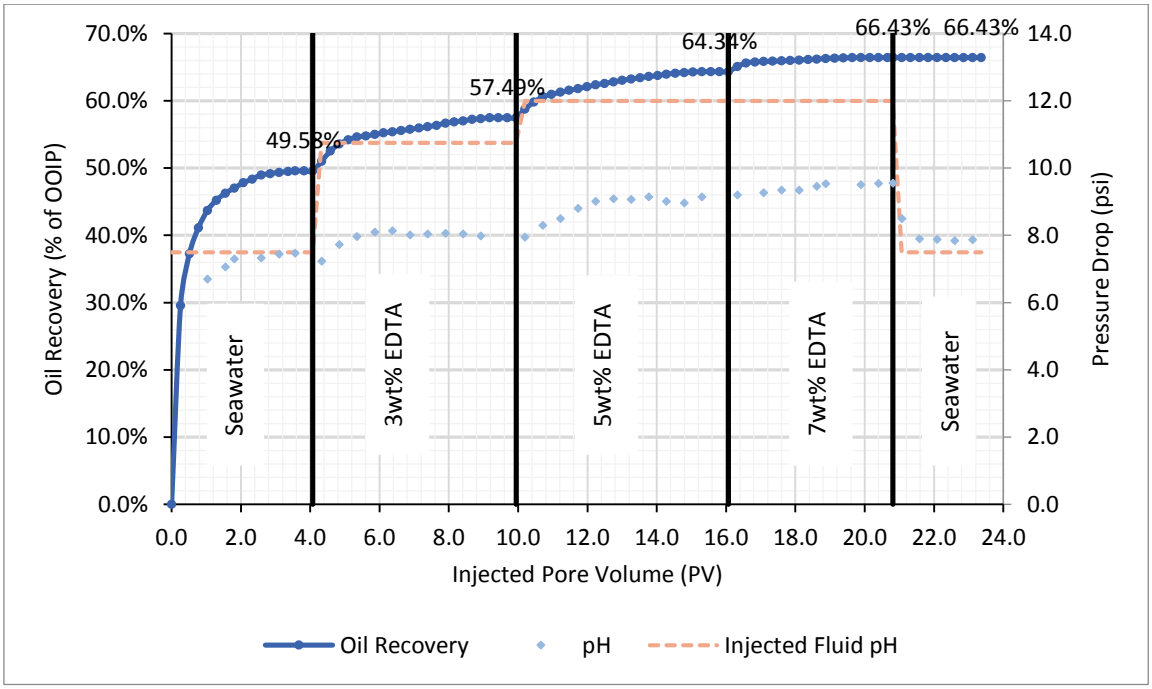

Figure 4.17: The Change of the pH with the Change of EDTA Concentration during Experiment #2.

Figures C.1 to C.14 in Appendix C summarize the results of the ICP and IC analyses for the produced effluents during the seawater and the 3wt% Na_2EDTA injection periods; from those figures the same observations noticed in the first experiment (during the injection of 1wt% EDTA) are observed again with higher amount of the chelated Ca^{+2} and Fe^{+3} and the precipitated Mg^{+2} and SO_4^{-2} in this case. This could be attributed to the increase in the

concentration of the chelating agent as well as the injected fluid pH which increased the alkalinity of the region adjacent to the clays surfaces, a good correlation between the increase of oil recovery, pH, and the chelation of the Ca^{+2} and Fe^{+3} initially adsorbed onto the surface of clay minerals.

In the third experiment carried out on Gray Berea sandstone rock 5wt%, 7wt%, and 10wt% of EDTA solutions were followed the seawater injection, which resulted in an additional recovery of 16.47% of OOIP (88.4% of this additional oil was recovered by injecting 4.50 PV of the 5wt% of EDTA) as shown in Figure 4.18, only 1.73% of OOIP was recovered by injecting the 7wt% EDTA solution and 0.21% of OOIP was produced by the 10wt% EDTA. The pressure drop showed an increase of 0.25 psi during the injection of the first half pore volume after shifting from seawater to the 5wt% EDTA which is higher than the increase in the previous two experiments; this increase is due to the higher viscosity of the injected fluid after the end of the seawater flushing compared to those used in the first two experiments as well as mobilization of the residual oil.

As indicated in Figure 4.19 the effluent pH was also increasing throughout the experiment when shifting from lower to higher concentration. Since the injected chelating agent in this experiment have the same pH of 12.00; the increase in the pH of the system in this experiment when shifting from a lower to a higher concentration is attributed to the exchange of the cations and anions between the injected fluids and the rock system.

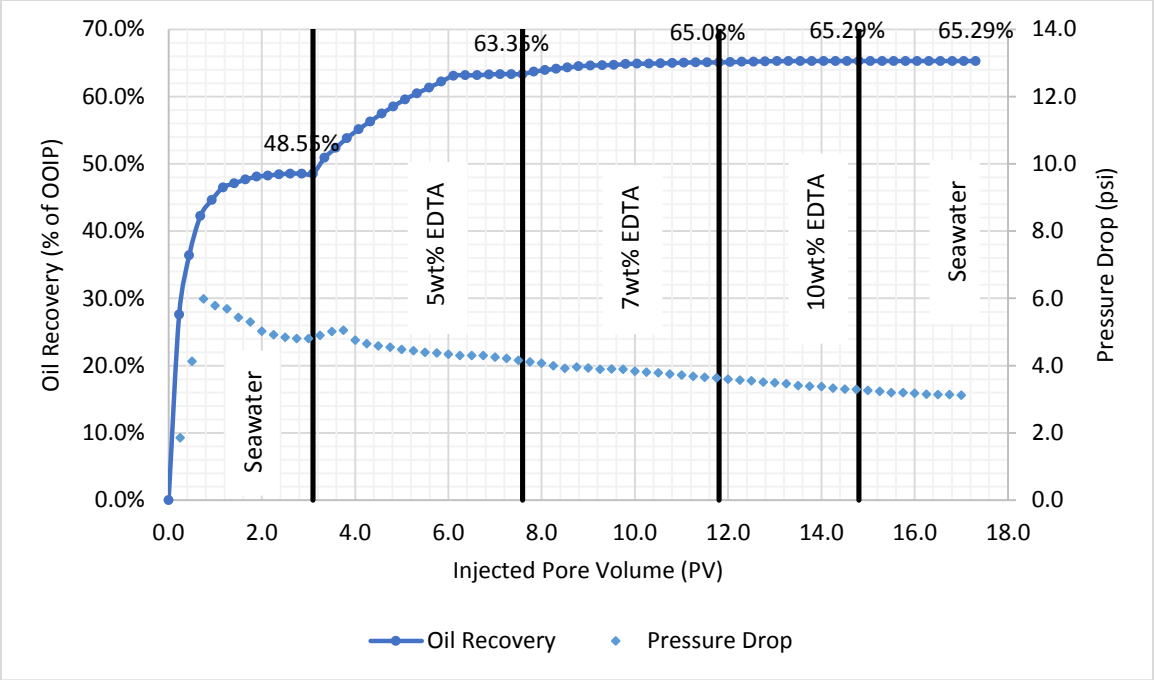

Figure 4.18: Recovery and Pressure Drop during Experiment #3 as a Function of Injected Pore Volume.

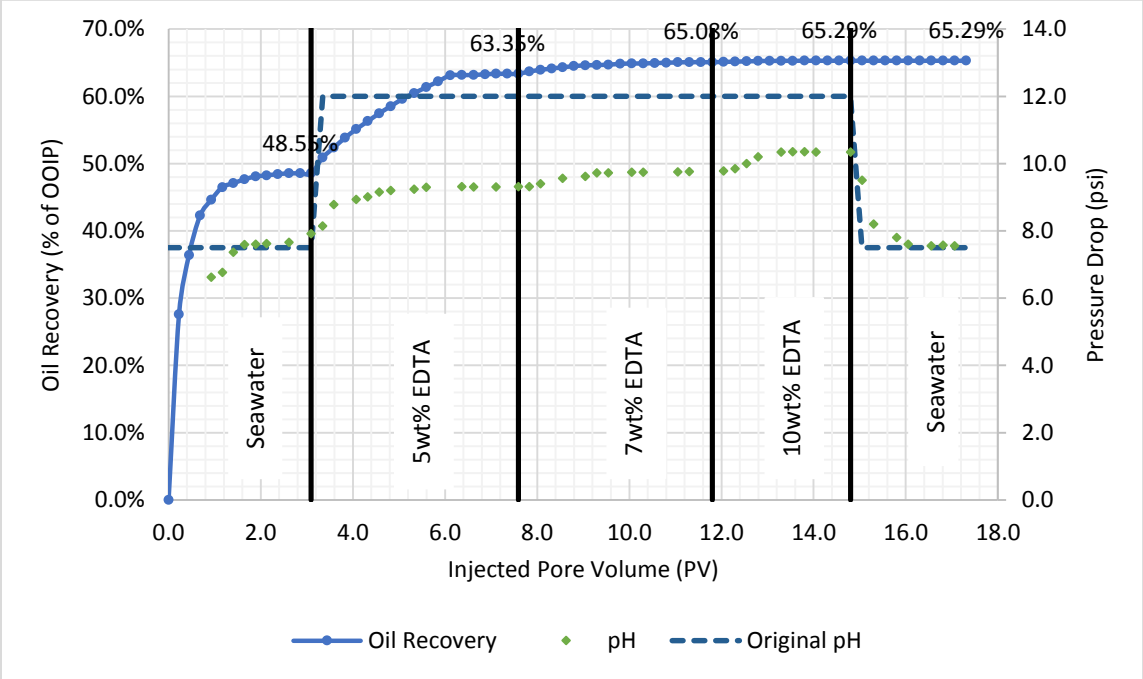

Figure 4.19: The Change of the pH with the Change of EDTA Concentration during Experiment #3.

The ICP and IC results of experiment #3 are shown in Figures C.15 to C.28. These data followed the same trend of the first two experiments but the rate of the increase in the concentrations of the produced Ca^{+2} and Fe^{+3} are higher in this case due to injection of higher concentration of the EDTA. Again there was a good correlation between the oil recovery, pH, and the chelated Ca^{+2}.

The results of the previous three coreflood experiments show that to recover about 65.00% of OOIP injection of around 16.0 PV of fluids was required in the first and second experiments, as indicated by Figures C.6 and C.16, respectively, while only about 7.6 PV of fluids injected in the third experiment when higher concentrations of the EDTA were used, as showed in Figure 4.18.

Table 4.2 compares the amount of oil recovered in the three experiments conducted on Gray Berea sandstone core samples with the amount of the Na_2EDTA required to produce that oil. This table shows that 17.0030 grams of this chelate were needed in experiment#3 to recover an additional amount of 16.74% of OOIP, 16.7658 grams of Na_2EDTA were required in experiment #2 to recover 16.96% of OOIP while only 9.8264 grams of this chemical were used to produce almost the same amount of oil in experiment #1 (15.36% of OOIP).

Table 4.2: Oil Recovery and the Amount of Chemicals Used in Experiments #1, #2 and #3 in Grams.

EDTA Concentration	Experiment #1		Experiment #2		Experiment #3	
	Na_2EDTA Weight (grams)	Recovery (% of OOIP)	Na_2EDTA Weight (grams)	Recovery (% of OOIP)	Na_2EDTA Weight (grams)	Recovery (% of OOIP)
1wt%	0.7384	5.09	-	-	-	-
3wt%	2.5560	5.34	3.4056	8.02	-	-
5wt%	6.5320	4.46	5.9640	6.85	4.6650	14.80
7wt%	-	-	7.3962	2.09	6.1180	1.73
10wt%	-	-	-	-	6.2200	0.21
Total	**9.8264**	**15.36**	**16.7658**	**16.96**	**17.0030**	**16.74**

The results of the previous experiments indicated that increasing the chelating agent concentration higher than the 5wt% EDTA did not show a promising increase in the oil recovery. Figure 4.20 compares the oil recovery after flooding the core samples with the 5wt% EDTA in the experiments #1, #2 and #3, where the 5wt% EDTA was used in the third, second, and first stages respectively, the oil recovery up to those stages are 61.64%, 63.36%, and 65.39% of OOIP, respectively; this result indicates that the 5wt% EDTA will produce the same amount of the oil whenever the stage in injected; the slightly difference in the produced oil was found to be well correlated with the samples permeability as indicated in Figure 4.21 which shows that the amount of the produced oil increases with the increase of the rock sample permeability.

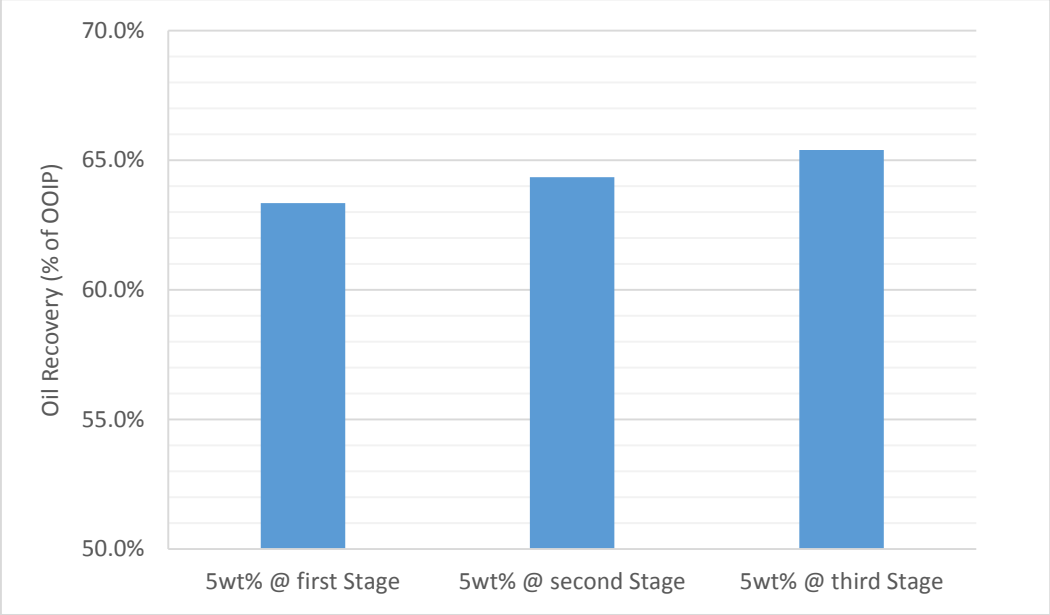

Figure 4.20: Comparison between the Oil Recovered at the end of injecting the 5wt% EDTA Solution for the Three Experiments Conducted on Gray Berea.

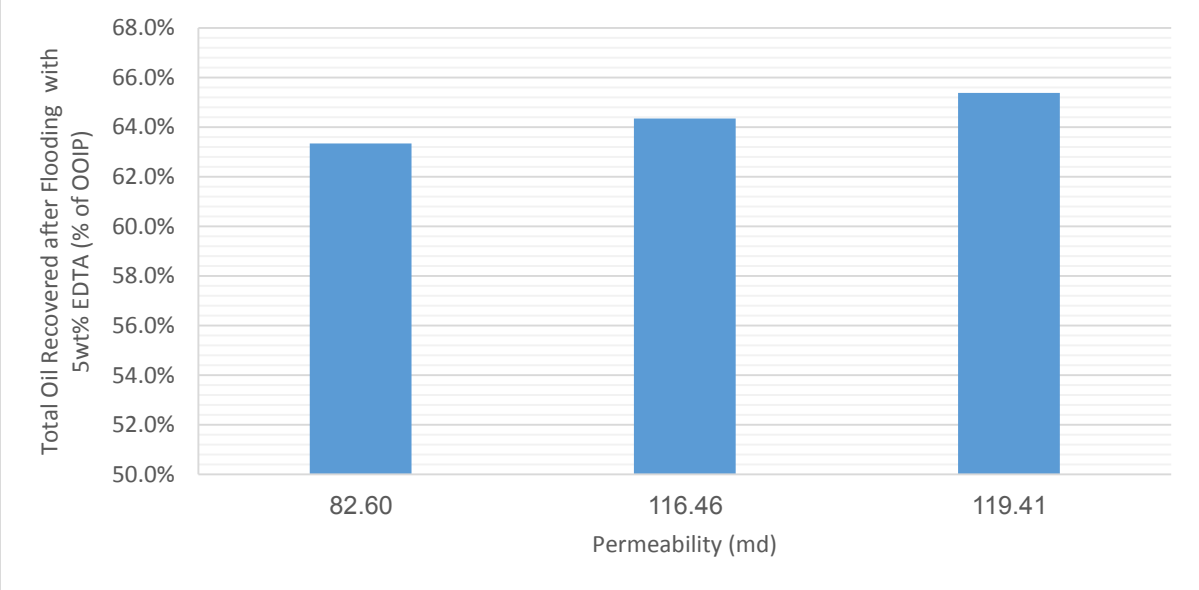

Figure 4.21: The Effect of Core Samples Permeability on Oil Recovery.

4.3.2 Coreflood Experiments for Gray Bandera Sandstone Samples

Two coreflood experiments were conducted on Gray Bandera sandstone samples. Figure 4.22 shows the increase in oil recovery and the pressure drop changes as a function of the pore volume injected during the first experiment (experiment #4). The oil recovered after injection of seawater was slightly lower than 40% compared to around 50% recovered from Gray Berea sandstone. This is due to the very low permeability of Gray Bandera samples as compared to Gray Berea samples permeability.

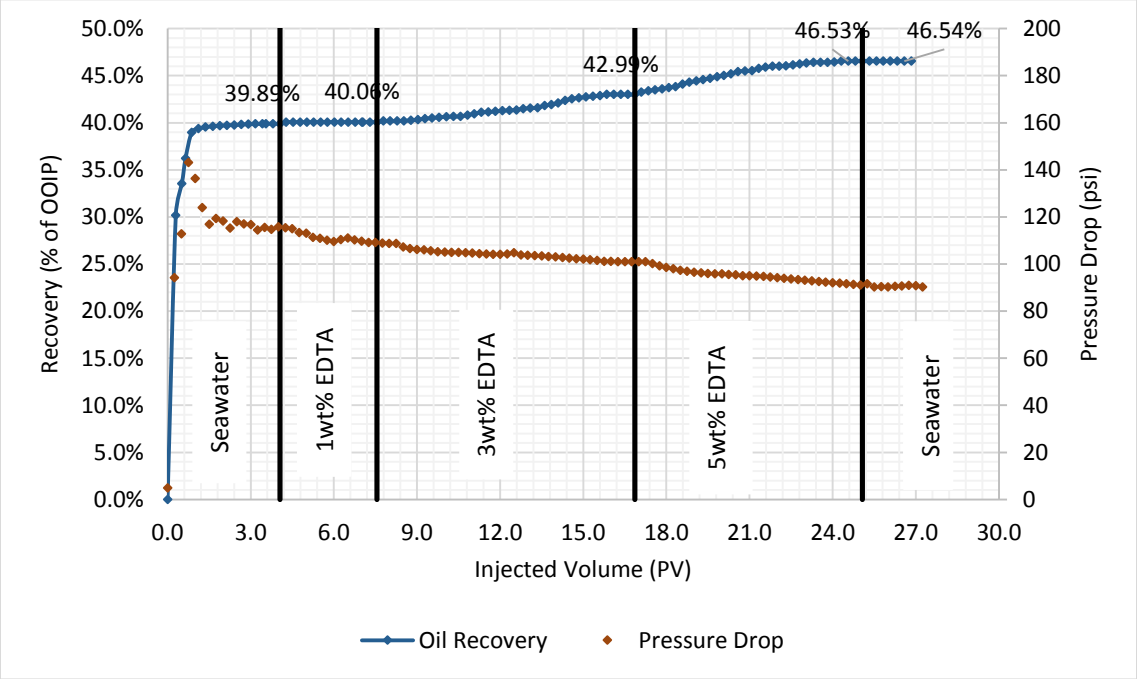

Figure 4.22: Recovery and Pressure Drop of Experiment #4 as a Function of Injected Pore Volume.

Injection of 1wt% EDTA did not show a promising recovery (only 0.16% of OOIP) and the increase in the pH of the produced effluent was only about 0.30 pH unit as shown in Figure 4.23. Injection of 3wt% increased the produced effluent pH to around 8.00 and

results in producing additional 2.93% of OOIP. When shifting to 5wt% the pH was increased to about 8.75 and the recovery was increased by 3.55%. This result shows that the increase in the concentration of the chemical will result in increasing the oil recovery as expected; and this increase is mainly due to the chelation of most of those cations originally surrounding the oil particles that are highly concentrated in Gray Bandera sandstone samples.

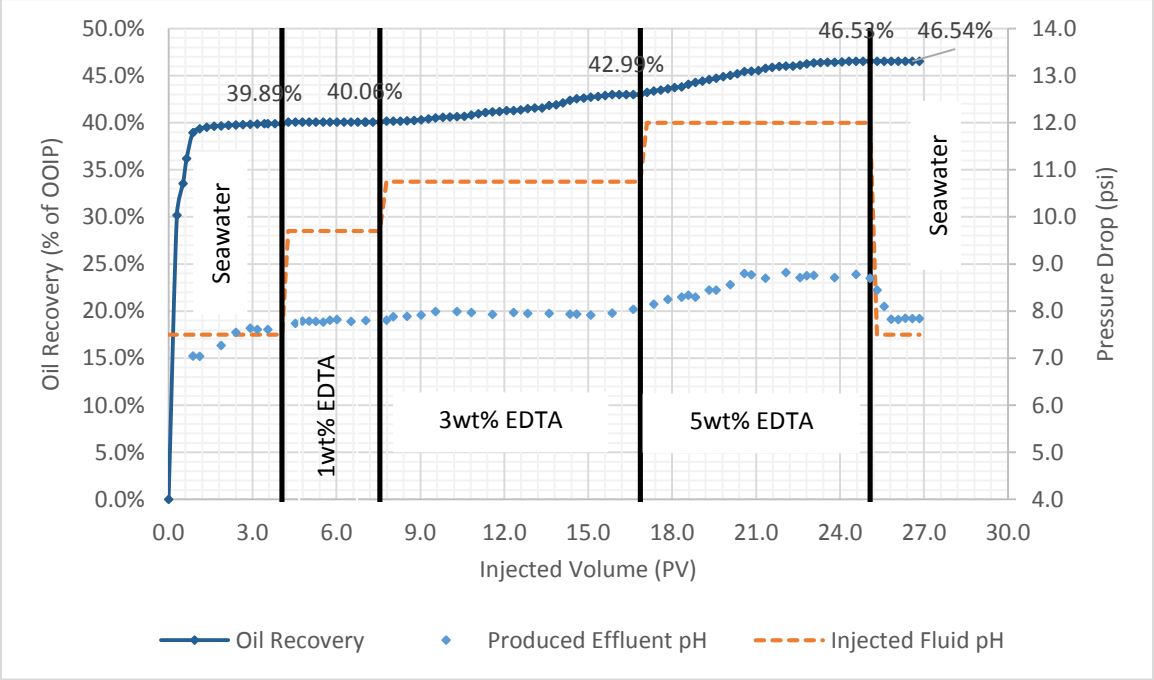

Figure 4.23: The Change of the pH with the Change of EDTA Concentration for Experiment #4.

The results of the ICP and IC analyses shown in Figures C.29 to C.42 follows the same trend of Gray Berea sandstone and the same conclusions are noticed. The increase in oil recovery and the produced Ca^{+2} and Fe^{+3} are well correlated, with the start of producing the Ca^{+2} and the Fe^{+3}, the concentration of Mg^{+2} in the produced effluent started decreasing to compensate for the produced positive cations already adsorbed onto the surfaces of the

clay minerals. The chelating agent at the concentrations used in this experiment do not tend to attach the clay minerals as indicated by the concentrations of Si^{+4} and Al^{+3}, as can be seen from Figure C.37, Appendix C.

In the last coreflood experiment in this study (experiment #5) conducted on Gray Bandera sandstone 5wt%, 7wt%, and 10wt% of the chelate were used, 39.02% of the OOIP was recovered by the seawater, additional 6.34% of OOIP was recovered by injecting the 5wt% Na_4EDTA solution, additional 0.63% was recovered by the 7wt%, and the 10wt% was able to recover only 0.53% of OOIP as shown in Figure 4.24. The total additional oil recovery from this experiment by using different chelating agent solutions is 6.64% of OOIP.

Although all the solutions used in this study have constant pH of 12.00, the produced effluent pH was increasing from about 7.60 to almost 9.00 when shifting to the 5wt% EDTA, then to about 9.40 after injecting to 7wt% solution and to around 9.80 with the injection of the 10 wt% EDTA as indicated in Figure 4.25. Production of fluids with lower pH than the injected pH indicated the increase of the alkalinity of the rock fluid system and the increase of the pH in the vicinity to the clays surfaces.

The results of the ICP and IC analyses for this experiment are shown in Figures C.43 to C.56, Appendix C. Those results follow the same trend of the previous experiments, and there was a good correlation between the increase in the oil recovery, pH, and the produced Ca^{+2}. The produced Fe^{+3} is kept increasing even when no more oil was produced which indicates that for this sample and the used chemical concentrations the relationship between the presence of the Fe^{+3} and the increase in the oil production is not a direct relationship.

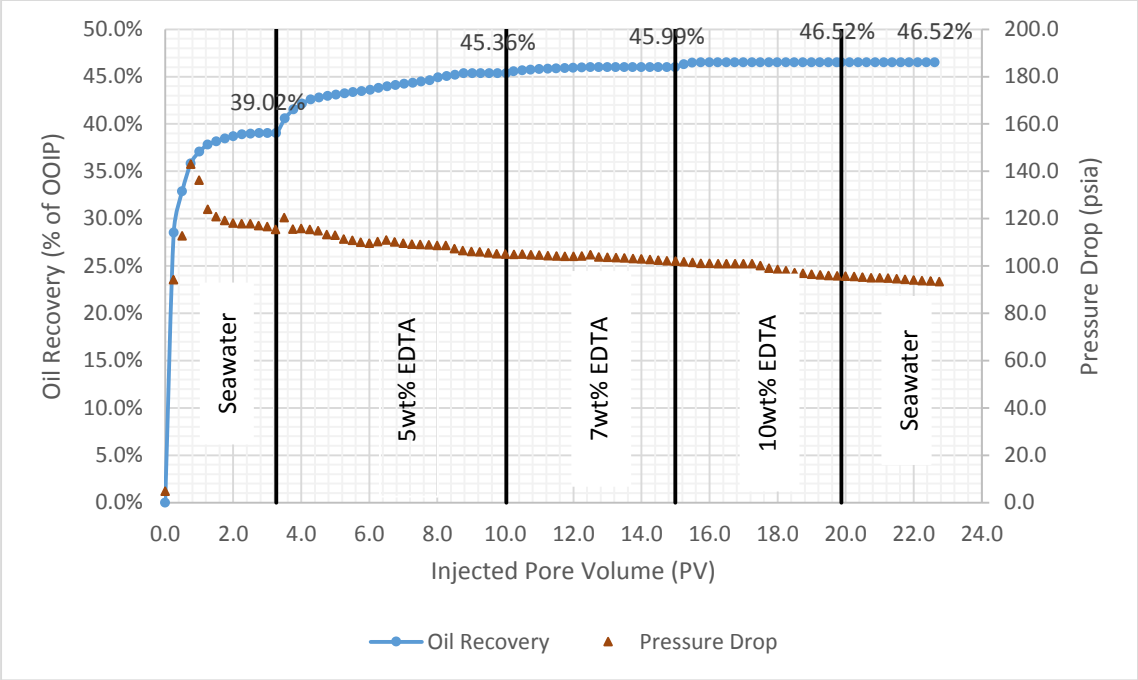

Figure 4.24: Recovery and Pressure Drop of Experiment #5 as a Function of Injected Pore Volume.

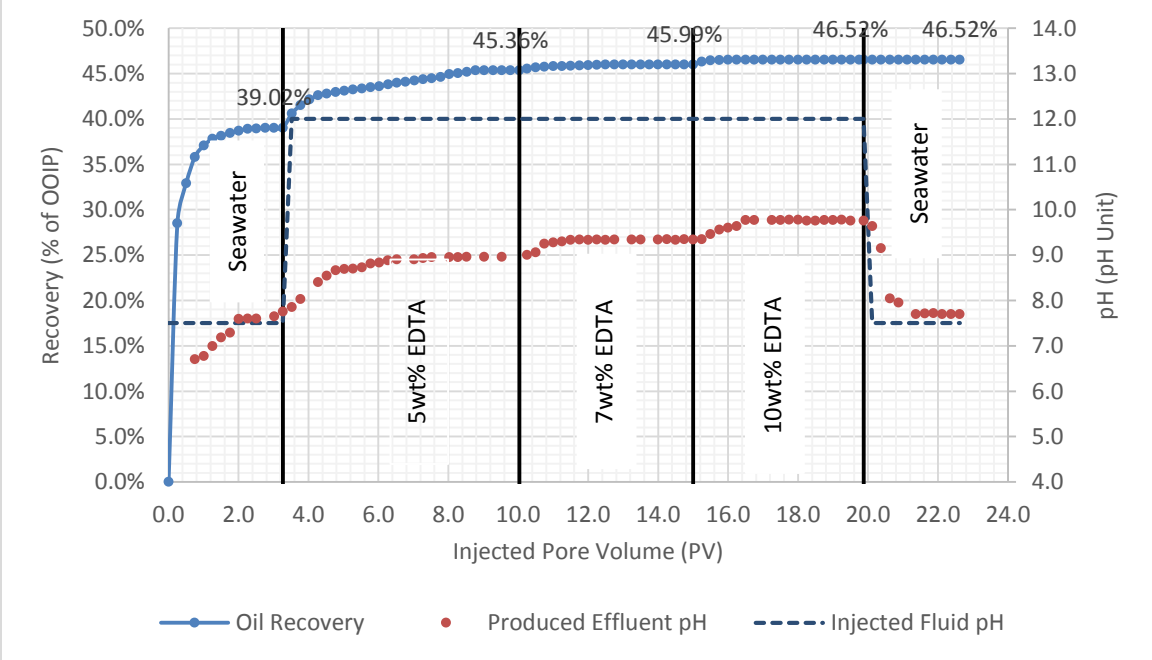

Figure 4.25: The Change of the pH with the Change of EDTA Concentration for Experiment #5.

The results of the coreflood experiments conducted on Gray Bandera sandstone show that to recover around 46.00% of OOIP 24.0 PV of fluids were injected in experiment #4, as indicated by Figure 4.22, while only 10.0 PV of the fluids were required in experiment #5 where higher concentrations of EDTA solutions used, as shown in Figure 4.24.

4.4 The effect of EDTA Solutions on Rock Integrity

The permeability of the different core samples used in the coreflood experiments was measured after flooding with different concentrations of EDTA solutions, Figure 4.26 compares the permeability enhancement for the ten core samples.

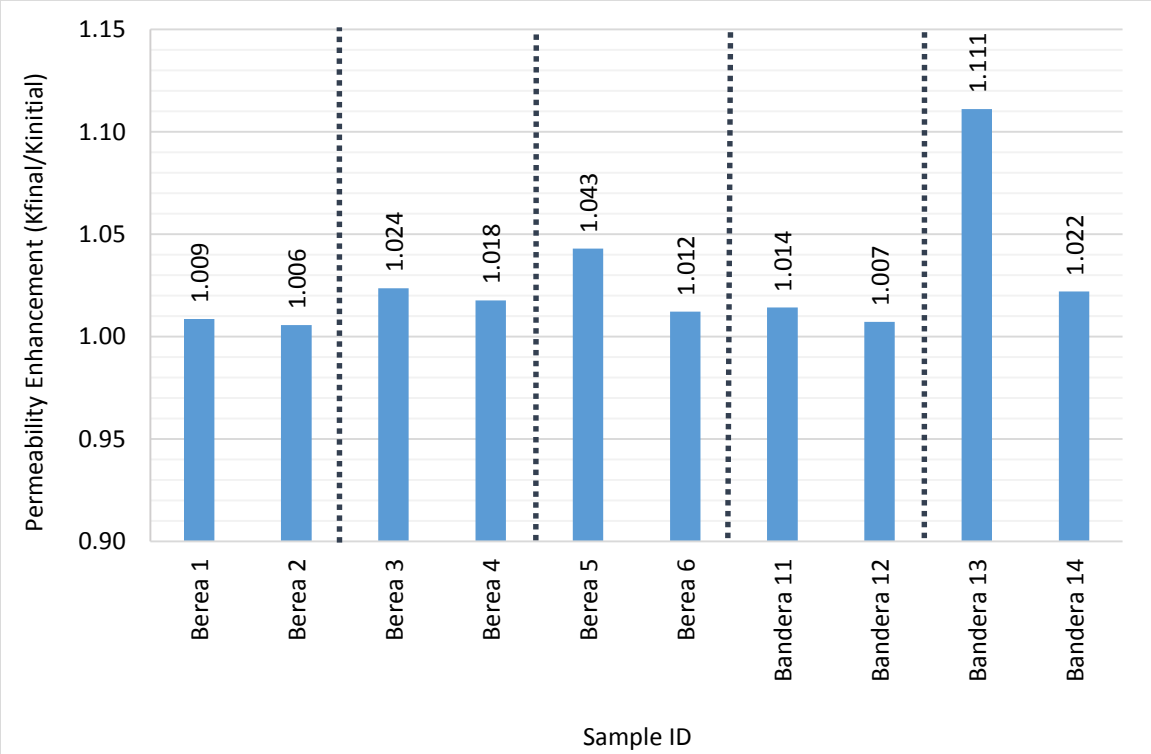

Figure 4.26: Permeability Enhancement for the Different Core Samples Used in this Study.

Figure 4.26 shows clearly that the enhancement for the core samples used in experiment#1 and experiment#4 conducted on Gray Berea and Gray Bandera sandstones, respectively, where the maximum EDTA concentration used was 5wt% was less than 1.5%, compared with 1.5 to 26 times permeability enhancement reported by Ali et al. (2005) for stimulation job at high temperature sandstone formation from West Africa with chelating agent based fluids at 20wt% and pH of 4.0.

4.5 The Impact of Reservoir Quality on Chelating Agents Flooding Performance

Winland's empirical equation (Equation 4.2) was used to calculate the pore throat radius for all core samples to determine the rock type (flow units).

$$\log(R35) = 0.732 + 0.588\log(k) - 0.864\log(\emptyset) \qquad \text{Equation 4.2}$$

Where R35 is the pore throat radius at 35% Hg saturation from a mercury injection capillary pressure test in microns, k is the permeability in md and ∅ is the porosity in percentage.

Table 4.3 summarizes the pore throats diameters in microns for the different core samples used in this study and the rock types which were classified according to (Martin et al., 1997) classification, the pore through of Gray Bandera is less than 2µm; since the EDTA solutions chelate Ca^{+2} from the rock surface and precipitate the SO_4^{-2} this will prevent $CaSO_4$ precipitation which has crystal size of about 5µm; so it can block the pore system.

The $CaSO_4$ sometimes precipitate from the seawater or low salinity water flooding. Equation 4.2 was used to develop the crossplot shown in Figure 4.27.

Table 4.3: The Summary of the Rock Types for the Sandstone Samples Used in this Study.

Core ID	R35 (microns)	Rock Type
Berea 1	6.660	Macro-Porous
Berea 2	6.799	Macro-Porous
Berea 3	6.938	Macro-Porous
Berea 4	6.850	Macro-Porous
Berea 5	6.094	Macro-Porous
Berea 6	5.869	Macro-Porous
Bandera 11	1.968	Meso-Porous
Bandera 12	1.848	Meso-Porous
Bandera 13	1.240	Meso-Porous
Bandera 14	1.414	Meso-Porous

The crossplot shown in Figure 4.27 indicates that the Gray Berea and Gray Bandera sandstone samples have totally different flow systems. Although the rock composition effects oil recovery, the pore system type of course will have a considerable effect on recovery mechanism and total possible oil recovery, the lower porosity and permeability of Gray Bandera sandstone could be attributed to the higher concentration of illite and kaolinite types clay minerals inside the same pore system, as showed earlier in Table 3.5.

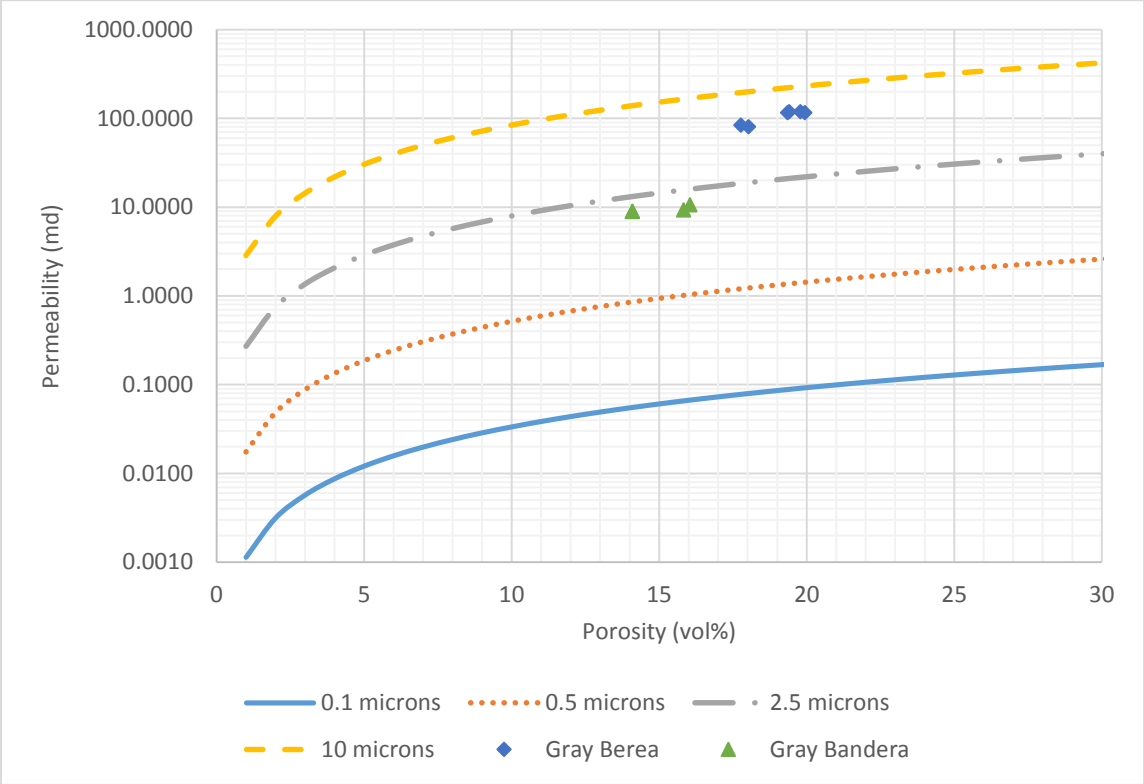

Figure 4.27: The Crossplot of the Permeability Variation versus Porosity for Sandstone Cores Used in this Study.

CHAPTER 5

CONCLUSIONS AND RECOMMENDATIONS

5.1 Conclusions

Based on the results of this study, the following conclusions can be drawn:

- The EDTA solutions are compatible with seawater.
- Addition of 5wt% of EDTA in seawater reduced the IFT from 20.58mN/m in case of seawater to 5.29mN/m in case of 5wt% EDTA solution.
- Zeta potential at solid/5wt% EDTA solution interface at pH of 12.00 were -21.07mV and -28.02mV for Gray Berea and Gray Bandera respectively, compared to those of -5.87mV and -3.72mV at the interface of Gray Berea and Gray Bandera with seawater.
- The optimum concentration of EDTA solution to maximize the oil recovery without effect on the rock integrity is the 5wt% EDTA in the seawater.
- The maximum oil recovered from Gray Berea sandstone with the 5wt% EDTA solution was slightly higher than 15.00% of OOIP compared to about 6.30% of OOIP recovered from Gray Bandera sandstone samples.
- The low permeability of Gray Bandera sandstone samples is one of the main reason for effected oil recovery from those samples.
- The presence of higher concentration of illite in Gray Bandera than Gray Berea with the presence of considerable amount of kaolinite is one of the main reasons for the high difference in the permeability between Gray Berea and Gray Bandera.

- Kaolinite type clay mineral with its large surface area was considered as one of the main crude oil adsorbent at pH higher than 5.5 through Ca^{+2} (Brady et al., 2012). Chelating of Ca^{+2} from Gray Berea with 4.8 % of kaolinite attributed to the increase in oil recovery.
- The effluent analyses results showed very low concentrations of the Si^{+4} and Al^{+3} indicating that Na_4EDTA chelating agent solutions with the concentration of 5wt% and less do not tend to attack the basic sheets of clay minerals (tetrahedral and octahedral sheets) since the concentration of those cations did not increase with the injection of those chemicals.
- Chelating agents deactivation chemistry introduced the possibility of increasing the seawater pH without dilution, this increase in the pH also enhance the oil recovery.
- The effluent analyses results also indicate that those Na_4EDTA solutions will exchange some of their cations with the cations already adsorbed onto the clay minerals surfaces (especially the Ca^{+2} and Fe^{+3} adsorbed from the formation brine).
- The elemental analysis showed that the recovery mechanism of the EDTA chelating agent depends on chelation of Ca^{+2} and Fe^{+3} those are initially adsorbed onto the clay minerals and they represent bridges to adsorb the crude oil particles to clays.
- The Mg^{+2} will be adsorbed onto the clay minerals to compensate for its negative charge and for the chelated positive cations (Ca^{+2} and Fe^{+3}).
- The decrease in the concentration of the SO_4^{-2} is well correlated to the increase in oil recovery which indicate that those anions will compensate for the negatively charged oil particles produced from the reservoir to keep the reservoir charges in balance.

5.2 Recommendations

- Uses of sandstone core samples with higher concentrations of clay minerals especially the swellable clay minerals group (smectite group) is recommended in the future works.
- Long core samples at least 12' in length could be used to clearly quantify the effect of clay minerals migration on the system permeability, especially in the case of Gray Bandera sandstone samples with the high concentration of illite and the presence of considerable amount of highly dispersible kaolinite.
- Firing both Gray Berea and Gray Bandera sandstone samples could be used to deactivate the presence of kaolinite clay mineral and study the effect of this deactivation on the oil recovery mechanism.

APPENDIX A: TABULATED DATA OF OIL RECOVERY, PRESSURE DROP AND pH

Table A.1: Data for Recovery, Pressure Drop and pH Curves Shown in Figures 4.6 and 4.7, Experiment #1.

Injected Fluid	Cumulative PV Injected (PV)	Cumulative Recovery (%OOIP)	Pressure Drop (psi)	pH (pH Unit)
Seawater	0.0000	00.00	0.000	-
	0.2501	28.47	1.855	-
	0.5002	38.49	4.126	6.40
	0.7503	41.00	6.280	6.91
	1.0004	43.51	5.923	-
	1.2506	45.01	5.688	7.36
	1.5007	47.02	5.438	-
	1.7508	49.02	5.304	7.41
	2.0009	49.27	4.828	-
	2.2510	49.52	4.919	7.31
	2.5011	50.02	4.846	-
	2.7512	50.27	4.802	-
	3.0013	50.50	4.812	7.40
	3.2514	50.50	4.813	-
	3.5015	50.50	4.801	-
1wt% EDTA	3.7517	51.50	4.767	7.30
	4.0018	52.50	4.718	-
	4.2519	53.16	4.694	7.66
	4.5020	53.81	4.523	-
	4.7521	54.31	4.500	8.01
	5.0022	54.66	4.499	-
	5.2523	55.01	4.520	8.02
	5.5024	55.26	4.468	-
	5.7525	55.36	4.444	8.02
	6.0026	55.49	4.350	-
	6.2528	55.59	4.312	8.03
	6.5029	55.59	4.290	-
	6.7530	55.59	4.320	-
3wt% EDTA	7.0031	57.09	4.352	8.03
	7.2532	57.84	4.235	-
	7.5033	58.14	4.200	8.10
	7.7534	58.44	4.123	-
	8.0035	58.74	4.113	8.25
	8.2536	59.37	4.022	-
	8.5037	59.67	4.000	8.21

Table A.2: Cont. Data for Recovery, Pressure Drop and pH Curves Shown in Figures 4.6 and 4.7, Experiment #1.

Injected Fluid	Cumulative PV Injected (PV)	Cumulative Recovery (%OOIP)	Pressure Drop (psi)	pH (pH Unit)
3wt% EDTA	8.7539	59.82	3.995	-
	9.0040	60.07	4.061	8.27
	9.2541	60.32	3.957	-
	9.5042	60.50	3.832	8.30
	9.7543	60.67	3.822	-
	10.0044	60.93	3.811	8.26
	10.2545	60.93	3.801	-
	10.5046	60.93	3.755	-
5wt% EDTA	10.7547	61.68	3.710	8.24
	11.0048	62.18	3.726	-
	11.2550	62.53	3.735	8.70
	11.5051	62.70	3.721	-
	11.7552	62.88	3.692	8.91
	12.0053	63.01	3.687	-
	12.2554	63.28	3.641	8.99
	12.5055	63.68	3.602	-
	12.7556	63.81	3.586	9.08
	13.0057	64.21	3.565	-
	13.2558	64.46	3.531	9.19
	13.5059	64.58	3.512	-
	13.7561	64.68	3.495	9.15
	14.0062	64.71	3.486	-
	14.2563	64.76	3.421	9.19
	14.5064	64.91	3.367	-
	14.7565	65.06	3.375	9.10
	15.0066	65.14	3.333	-
	15.2567	65.31	3.311	9.08
	15.5068	65.36	3.302	-
	15.7569	65.39	3.285	9.19
	16.0070	65.39	3.246	-
	16.2572	65.39	3.201	-
Seawater	16.5073	65.49	3.211	8.10
	16.7574	65.54	3.201	-
	17.0075	65.64	3.266	7.88
	17.2576	65.69	3.215	-
	17.5077	65.79	3.199	7.77
	17.7578	65.84	3.199	-
	18.0079	65.86	3.202	7.74
	18.2580	65.86	3.199	-
	18.5081	65.86	3.199	7.75
	18.7583	65.86	3.202	-

Table A.3: Data for Recovery, Pressure Drop and pH Curves Shown Figures 4.16 and 4.17, Experiment #2.

Injected Fluid	Cumulative PV Injected (PV)	Cumulative Recovery (%OOIP)	Pressure Drop (psi)	pH (pH Unit)
Seawater	0.0000	00.00	0.000	-
	0.2583	29.56	1.855	-
	0.5166	37.27	4.126	-
	0.7749	43.69	5.985	-
	1.0332	46.26	5.785	6.70
	1.2916	47.24	5.688	-
	1.5499	47.29	5.438	7.06
	1.8082	47.55	5.304	7.30
	2.0665	48.57	4.828	-
	2.3248	48.83	4.919	-
	2.5831	48.98	4.846	7.33
	2.8414	49.16	4.802	-
	3.0997	49.37	4.812	7.44
	3.3580	49.47	4.813	-
	3.5602	49.58	4.801	7.47
	3.8185	49.58	4.785	-
	4.0768	49.58	4.754	-
3wt% EDTA	4.3284	50.76	4.624	7.23
	4.5836	52.04	4.587	-
	4.8387	52.81	4.551	7.73
	5.0939	53.17	4.487	-
	5.3491	53.38	4.555	7.97
	5.6042	53.56	4.401	-
	5.8594	53.76	4.376	8.10
	6.1146	53.92	4.456	-
	6.3697	54.10	4.302	8.14
	7.1352	54.72	4.257	-
	7.3904	54.92	4.215	8.04
	7.6456	55.13	4.158	-
	7.9007	55.46	4.112	8.16
	8.1559	55.64	4.075	-
	8.4111	55.79	4.000	8.20
	8.6662	56.00	3.925	-
	8.9214	56.10	3.959	7.99
	9.1765	56.26	3.926	-
	9.6869	56.26	3.898	-
	9.9420	56.26	3.895	-

Table A.4: Cont. Data for Recovery, Pressure Drop and pH Curves Shown in Figures 4.16 and 4.17, Experiment #2.

Injected Fluid	Cumulative PV Injected (PV)	Cumulative Recovery (%OOIP)	Pressure Drop (psi)	pH (pH Unit)
5wt% EDTA	10.1972	57.54	3.837	7.95
	10.4524	58.57	3.809	-
	10.7075	59.37	3.786	8.30
	10.9627	59.73	3.754	-
	11.2179	60.04	3.722	8.50
	11.4730	60.32	3.688	-
	11.7282	60.57	3.659	8.80
	11.9834	60.86	3.635	-
	12.2385	61.13	3.599	9.01
	12.4937	61.36	3.565	-
	12.7489	61.59	3.549	9.09
	13.0040	61.80	3.512	-
	13.2592	62.00	3.491	9.07
	13.5144	62.21	3.462	-
	13.7695	62.36	3.403	9.15
	14.0247	62.52	3.391	-
	14.2799	62.72	3.375	9.01
	14.5350	62.88	3.330	-
	14.7902	62.98	3.301	8.97
	15.0454	63.06	3.288	-
	15.3005	63.11	3.265	9.15
	15.5557	63.11	3.235	-
	15.8109	63.11	3.202	-
	16.0660	63.11	3.202	-
7wt% EDTA	16.3212	63.88	3.180	9.20
	16.5764	64.39	3.155	-
	16.8315	64.55	3.137	-
	17.0867	64.60	3.141	9.27
	17.3419	64.65	3.124	-
	17.5970	64.70	3.104	9.35
	17.8522	64.75	3.085	-
	18.1074	64.83	3.065	9.35
	18.3625	64.91	3.046	-
	18.6177	64.96	3.025	9.46
	18.8729	65.06	3.000	-
	19.1280	65.11	3.032	-
	19.3832	65.14	2.987	-
	19.6384	65.19	2.968	-

Table A.5: Cont. Data for Recovery, Pressure Drop and pH Curves Shown in Figures 4.16 and 4.17, Experiment #2.

Injected Fluid	Cumulative PV Injected (PV)	Cumulative Recovery (%OOIP)	Pressure Drop (psi)	pH (pH Unit)
7wt% EDTA	19.8899	65.20	2.979	9.51
	20.1451	65.20	2.929	-
	20.4003	65.20	2.912	9.55
	20.6554	65.20	2.890	-
	20.8127	65.20	2.897	9.56
Seawater	21.0678	65.20	2.887	8.50
	21.3230	65.20	2.889	-
	21.5782	65.20	2.847	7.90
	21.8333	65.20	2.988	-
	22.0885	65.20	2.902	7.88
	22.3437	65.20	2.904	-
	22.5988	65.20	2.895	7.84
	22.8540	65.20	2.899	-
	23.1092	65.20	2.903	7.87
	23.3643	65.20	2.901	-

Table A.6: Data for Recovery, Pressure Drop and pH Curves Shown in Figures 4.18 and 4.19, Experiment #3.

Injected Fluid	Cumulative PV Injected (PV)	Cumulative Recovery (%OOIP)	Pressure Drop (psi)	pH (pH Unit)
Seawater	0.0000	0.00	0.000	-
	0.2265	27.59	1.855	-
	0.4434	36.40	4.126	-
	0.6844	42.27	5.985	-
	0.9254	44.61	5.785	6.62
	1.1664	46.49	5.688	6.76
	1.4074	47.08	5.438	7.36
	1.6484	47.67	5.304	7.59
	1.8893	48.08	5.028	7.60
	2.1303	48.25	4.919	7.62
	2.3713	48.43	4.846	-
	2.6123	48.55	4.802	7.66
	2.8533	48.55	4.801	-
	3.0943	48.55	4.901	7.91
5wt% EDTA	3.3449	50.90	5.011	8.14
	3.5859	52.36	5.055	8.78
	3.8269	53.83	4.754	-
	4.0751	55.12	4.654	8.93
	4.3233	56.30	4.587	9.01
	4.5715	57.47	4.551	9.15
	4.8197	58.53	4.487	9.20
	5.0704	59.58	4.443	-
	5.3258	60.46	4.401	9.24
	5.5909	61.34	4.376	9.29
	5.8512	62.23	4.342	-
	6.1114	63.11	4.302	-
	6.3669	63.16	4.301	9.31
	6.6175	63.17	4.303	9.30
	6.8681	63.29	4.255	-
	7.1091	63.35	4.215	9.30
	7.3501	63.35	4.162	-
	7.5911	63.35	4.112	9.31

Table A.7: Cont. Data for Recovery, Pressure Drop and pH Curves Shown in Figures 4.18 and 4.19, Experiment #3.

Injected Fluid	Cumulative PV Injected (PV)	Cumulative Recovery (%OOIP)	Pressure Drop (psi)	pH (pH Unit)
7wt% EDTA	7.8321	63.70	4.075	9.31
	8.0731	63.93	4.000	9.40
	8.3141	64.14	3.925	-
	8.5550	64.32	3.959	9.56
	8.7960	64.49	3.926	-
	9.0467	64.61	3.895	9.62
	9.2973	64.65	3.898	9.72
	9.5479	64.71	3.895	9.72
	9.7985	64.83	3.837	-
	10.0492	64.88	3.808	9.74
	10.2998	64.89	3.786	9.74
	10.5504	64.95	3.754	-
	10.8010	64.99	3.722	-
	11.0517	65.05	3.688	9.75
	11.3023	65.08	3.659	9.76
	11.5529	65.08	3.635	-
	11.8035	65.08	3.599	-
10wt% EDTA	12.0445	65.12	3.565	9.78
	12.2952	65.16	3.549	9.85
	12.5458	65.20	3.512	10.00
	12.7964	65.24	3.491	10.20
	13.0470	65.27	3.462	-
	13.2977	65.28	3.403	10.34
	13.5483	65.28	3.391	10.35
	13.7989	65.29	3.375	10.35
	14.0495	65.29	3.330	10.34
	14.3002	65.29	3.301	-
	14.5508	65.29	3.288	-
	14.8014	65.29	3.265	10.34
Seawater	15.0521	65.29	3.235	9.50
	15.3027	65.29	3.202	8.20
	15.5533	65.29	3.202	7.80
	15.8039	65.29	3.180	7.60
	16.0546	65.29	3.155	-
	16.3052	65.29	3.137	-
	16.5558	65.29	3.140	7.55
	16.8064	65.29	3.124	7.57
	17.0571	65.29	3.099	7.55
	17.3077	65.29	3.074	7.55

Table A.8: Data for Recovery, Pressure Drop and pH Curves Shown in Figures 4.22 and 4.23. Experiment #4.

Injected Fluid	Cumulative PV Injected (PV)	Cumulative Recovery (%OOIP)	Pressure Drop (psi)	pH (pH Unit)
Seawater	0.0000	00.00	004.854	-
	0.2964	30.18	094.136	-
	0.5159	33.53	112.727	-
	0.6476	36.22	143.074	-
	0.8672	38.96	136.287	7.05
	1.1175	39.37	123.903	7.04
	1.3677	39.54	116.835	-
	1.6257	39.62	119.242	-
	1.8836	39.67	118.159	7.27
	2.1416	39.73	115.230	-
	2.3996	39.76	117.879	7.55
	2.6575	39.81	116.996	-
	2.9155	39.84	116.713	7.64
	3.1679	39.87	114.418	-
	3.4204	39.89	115.443	7.61
	3.5521	39.90	114.619	-
	4.0571	39.90	115.409	-
1wt% EDTA	4.2766	40.06	114.900	-
	4.5346	40.06	113.254	7.74
	4.7816	40.06	112.987	7.79
	5.0231	40.06	111.325	7.79
	5.2700	40.06	110.870	7.78
	5.5225	40.06	110.003	7.77
	5.7695	40.06	109.547	7.81
	6.0192	40.06	110.321	7.82
	6.2662	40.06	110.954	-
	6.5187	40.06	110.125	7.78
	6.7656	40.06	109.587	-
	7.0181	40.06	109.152	-
	7.0456	40.06	109.126	7.80
	7.2980	40.06	108.897	-
	7.5505	40.06	108.654	-
3wt% EDTA	7.7865	40.17	108.654	7.81
	8.0335	40.17	107.254	7.88
	8.2805	40.17	106.548	-
	8.5274	40.20	106.125	7.89
	8.7772	40.26	105.954	-
	9.0324	40.33	105.547	7.92
	9.2876	40.42	105.123	-
	9.5428	40.50	105.015	7.99
	9.8008	40.57	104.856	-
	10.3139	40.65	104.759	7.99

Table A.9: Cont. Data for Recovery, Pressure Drop and pH Curves Shown in Figures 4.22 and 4.23, Experiment #4.

Injected Fluid	Cumulative PV Injected (PV)	Cumulative Recovery (%OOIP)	Pressure Drop (psi)	pH (pH Unit)
3wt% EDTA	10.5664	40.68	104.587	-
	10.8189	40.82	104.365	7.97
	11.0714	40.95	104.235	-
	11.3238	41.09	104.012	-
	11.5763	41.15	104.099	7.93
	11.8288	41.20	104.235	-
	12.0812	41.28	104.775	-
	12.3337	41.31	103.854	7.97
	12.5862	41.35	103.699	-
	12.8386	41.49	103.565	7.95
	13.0911	41.56	103.356	-
	13.6070	41.83	102.987	7.95
	13.8485	41.91	102.752	-
	14.0955	42.11	102.424	-
	14.3425	42.38	102.124	7.94
	14.5895	42.54	101.987	7.94
	14.8419	42.64	101.785	-
	15.0944	42.72	101.542	7.92
	15.3469	42.80	101.123	-
	15.5993	42.88	101.032	-
	15.8518	42.99	101.000	7.96
	16.1043	42.99	100.895	-
	16.6092	42.99	100.923	8.04
	16.8617	42.99	100.897	-
5wt% EDTA	17.0977	43.24	100.123	-
	17.3474	43.38	99.125	8.15
	17.5944	43.49	98.542	-
	17.8414	43.60	97.954	8.25
	18.0884	43.74	97.235	-
	18.3353	43.82	96.853	8.30
	18.5823	44.09	96.523	8.34
	18.8293	44.28	96.214	8.30
	19.0763	44.42	95.932	-
	19.3233	44.59	95.755	8.45
	19.5757	44.72	95.721	8.45
	19.8255	44.89	95.562	-
	20.0779	45.03	95.322	8.56
	20.3304	45.19	95.000	-
	20.5829	45.44	95.012	8.80
	20.8326	45.49	94.846	8.77
	21.0851	45.53	94.652	-

Table A.10: Cont. Data for Recovery, Pressure Drop and pH Curves Shown in Figures 4.22 and 4.23, Experiment #4.

Injected Fluid	Cumulative PV Injected (PV)	Cumulative Recovery (%OOIP)	Pressure Drop (psi)	pH (pH Unit)
5wt% EDTA	21.3321	45.78	94.365	8.70
	21.5790	45.89	94.123	-
	21.8233	46.00	93.852	-
	22.0703	46.01	93.655	8.82
	22.3172	46.02	93.321	-
	22.5642	46.13	93.022	8.71
	22.8112	46.24	92.856	8.75
	23.0582	46.35	92.549	8.76
	23.3052	46.41	92.237	-
	23.5576	46.41	92.013	-
	23.8101	46.42	91.790	8.71
	24.0626	46.45	91.532	-
	24.3150	46.53	91.365	-
	24.5675	46.53	91.033	8.78
	24.8200	46.54	91.546	-
	25.0724	46.54	90.200	8.70
Seawater	25.3249	46.54	90.351	8.45
	25.5774	46.54	90.147	8.10
	25.8299	46.54	90.546	7.83
	26.0823	46.54	90.616	7.82
	26.3348	46.54	90.937	7.85
	26.5873	46.54	90.795	7.84
	26.8397	46.54	90.165	7.84

Table A.11: Data for Recovery, Pressure Drop and pH Curves Shown in Figures 4.24 and 4.25, Experiment #5.

Injected Fluid	Cumulative PV Injected (PV)	Cumulative Recovery (%OOIP)	Pressure Drop (psi)	pH (pH Unit)
Seawater	0.0000	0.00	4.854	-
	0.2512	28.51	94.136	-
	0.5024	32.89	112.727	
	0.7536	35.82	143.074	6.70
	1.0047	37.07	136.287	6.77
	1.2559	37.83	123.903	6.99
	1.5071	38.14	120.835	7.18
	1.7583	38.45	119.242	7.29
	2.0095	38.70	118.159	7.59
	2.2607	38.89	117.830	7.60
	2.5118	38.96	117.879	7.60
	2.7630	39.02	116.996	-
	3.0142	39.02	116.713	7.65
	3.2654	39.02	115.418	7.75
5wt% EDTA	3.5228	40.59	120.443	7.85
	3.7728	41.53	115.619	8.03
	4.0272	42.16	115.797	-
	4.2772	42.60	115.409	8.40
	4.5272	42.79	114.900	8.54
	4.7772	42.94	113.254	8.66
	5.0272	43.10	112.987	8.69
	5.2772	43.23	111.325	8.70
	5.5272	43.35	110.870	8.73
	5.7772	43.48	110.003	8.81
	6.0272	43.60	109.547	8.83
	6.2772	43.79	110.321	8.88
	6.5272	43.98	110.954	8.90
	6.7772	44.11	110.125	-
	7.0272	44.23	109.587	8.90
	7.2772	44.36	109.152	8.93
	7.5272	44.48	109.126	8.95
	7.7772	44.61	108.897	8.95
	8.0272	44.92	108.654	-
	8.2772	45.05	108.654	8.95
	8.5272	45.17	107.254	8.96
	8.7772	45.36	106.548	-
	9.0272	45.36	106.125	8.96
	9.2772	45.36	105.954	-
	9.5272	45.36	105.547	8.96
	9.7772	45.36	105.123	-
	10.0272	45.36	105.015	-

Table A.12: Cont. Data for Recovery, Pressure Drop and pH Curves Shown in Figures 4.24 and 4.25, Experiment #5.

Injected Fluid	Cumulative PV Injected (PV)	Cumulative Recovery (%OOIP)	Pressure Drop (psi)	pH (pH Unit)
7wt% EDTA	10.2470	45.55	104.856	9.00
	10.4970	45.68	104.958	9.06
	10.7470	45.74	104.759	9.25
	10.9970	45.80	104.587	9.28
	11.2470	45.83	104.365	9.30
	11.4970	45.86	104.235	9.33
	11.7470	45.90	104.012	9.34
	11.9970	45.93	104.099	9.33
	12.2470	45.96	104.235	9.34
	12.4970	45.99	104.775	9.33
	12.7470	45.99	103.854	9.34
	12.9970	45.99	103.699	-
	13.2470	45.99	103.565	9.34
	13.4970	45.99	103.356	9.34
	13.7470	45.99	103.125	-
	13.9970	45.99	102.987	9.34
	14.2470	45.99	102.752	9.35
	14.4970	45.99	102.424	9.33
	14.7470	45.99	102.124	9.35
	14.9970	45.99	101.987	9.34
10wt% EDTA	15.2470	46.30	101.785	9.35
	15.4970	46.46	101.542	9.46
	15.7470	46.49	101.123	9.56
	15.9970	46.52	101.032	9.60
	16.2470	46.52	101.000	9.64
	16.4970	46.52	100.895	9.77
	16.7470	46.52	100.901	9.77
	16.9970	46.52	100.923	-
	17.2470	46.52	100.897	9.77
	17.4970	46.52	100.123	9.77
	17.7470	46.52	99.125	9.78
	17.9970	46.52	98.542	9.78
	18.2470	46.52	97.954	9.76
	18.4970	46.52	97.235	9.76
	18.7470	46.52	96.853	9.77
	18.9970	46.52	96.523	9.77
	19.2470	46.52	96.214	9.78
	19.4970	46.52	95.932	9.76
	19.7470	46.52	95.755	-
	19.8725	46.52	95.721	9.76

Table A.13: Cont. Data for Recovery, Pressure Drop and pH Curves Shown in Figures 4.24 and 4.25, Experiment #5.

Injected Fluid	Cumulative PV Injected (PV)	Cumulative Recovery (%OOIP)	Pressure Drop (psi)	pH (pH Unit)
Seawater	20.1225	46.52	95.562	9.64
	20.3725	46.52	95.322	9.15
	20.6225	46.52	95.000	8.04
	20.8725	46.52	95.012	7.95
	21.1225	46.52	94.846	7.70
	21.3725	46.52	94.652	7.70
	21.6225	46.52	94.365	7.71
	21.8725	46.52	94.123	7.72
	22.1225	46.52	93.852	7.70
	22.3725	46.52	93.655	7.70
	22.6225	46.52	93.321	7.70

APPENDIX B: PERMEABILITY CALCULATION PLOTS

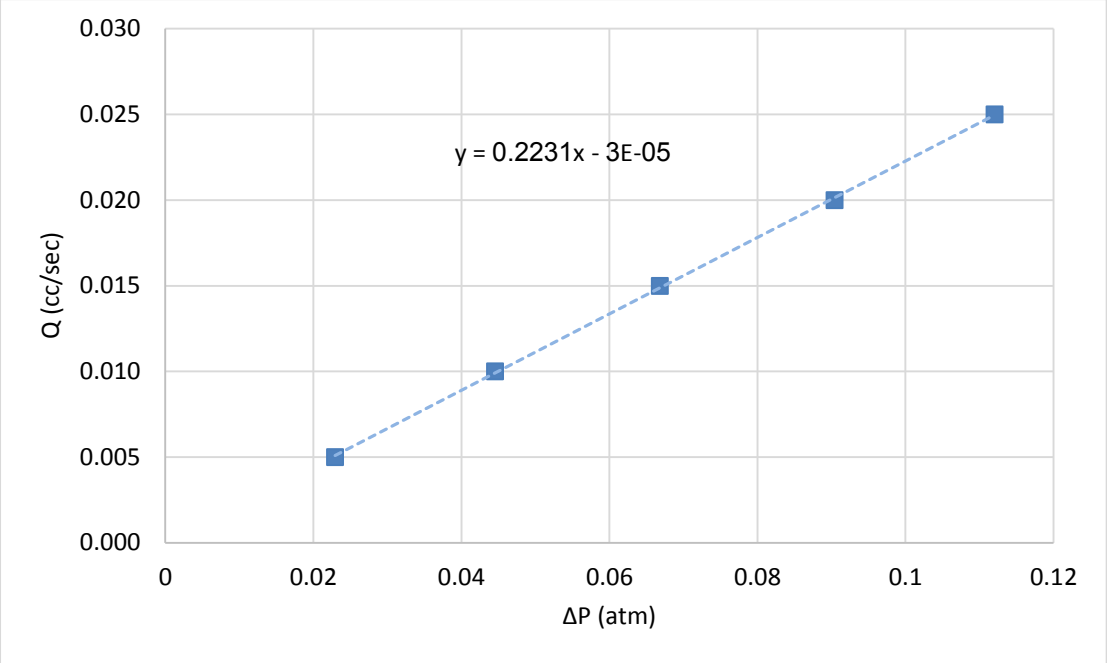

Figure B.1: Initial Absolute Permeability Measurement for Core Sample Gray Berea 1 @ 25°C.

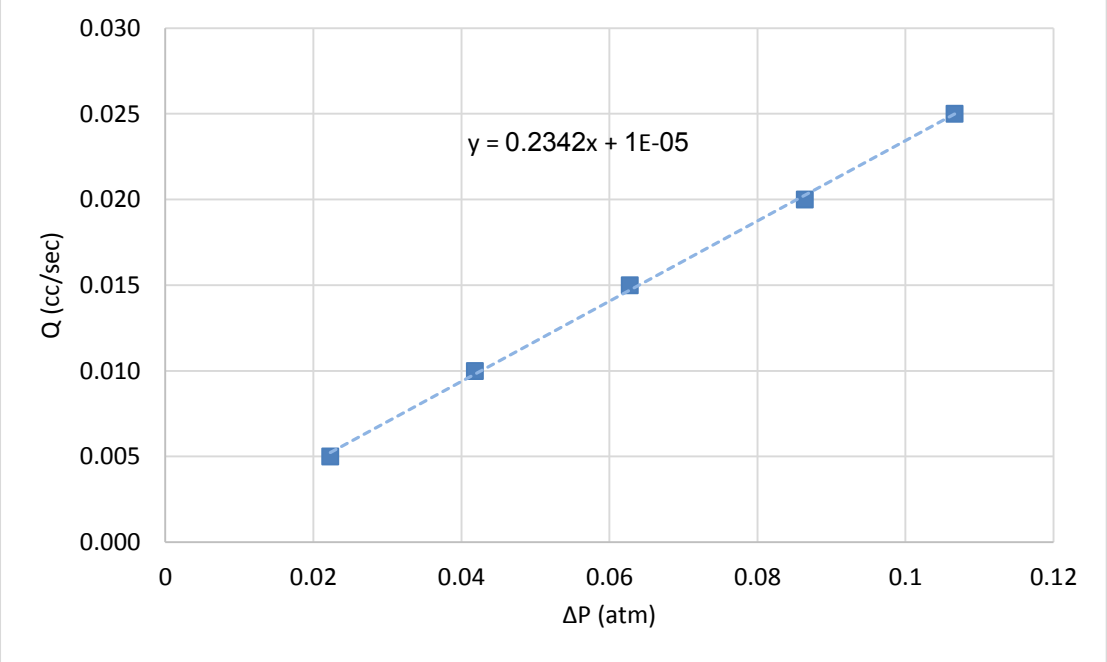

Figure B.2: Initial Absolute Permeability Measurement for Core Sample Gray Berea 2 @ 25°C.

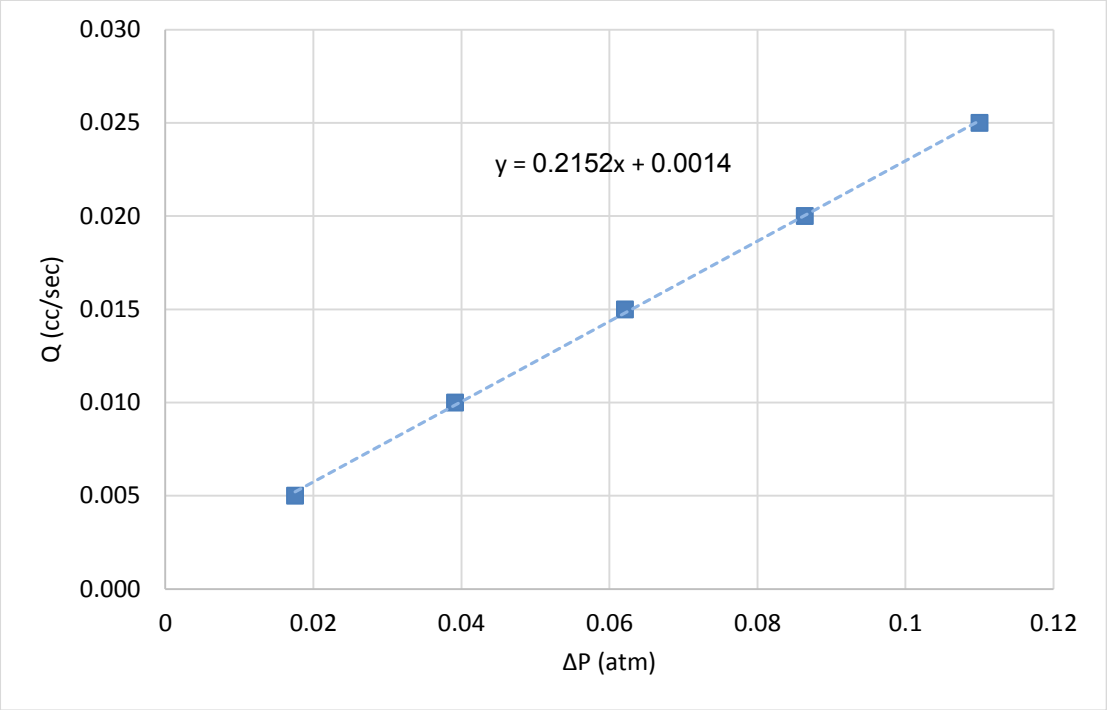

Figure B.3: Initial Absolute Permeability Measurement for Core Sample Gray Berea 3 @ 25°C.

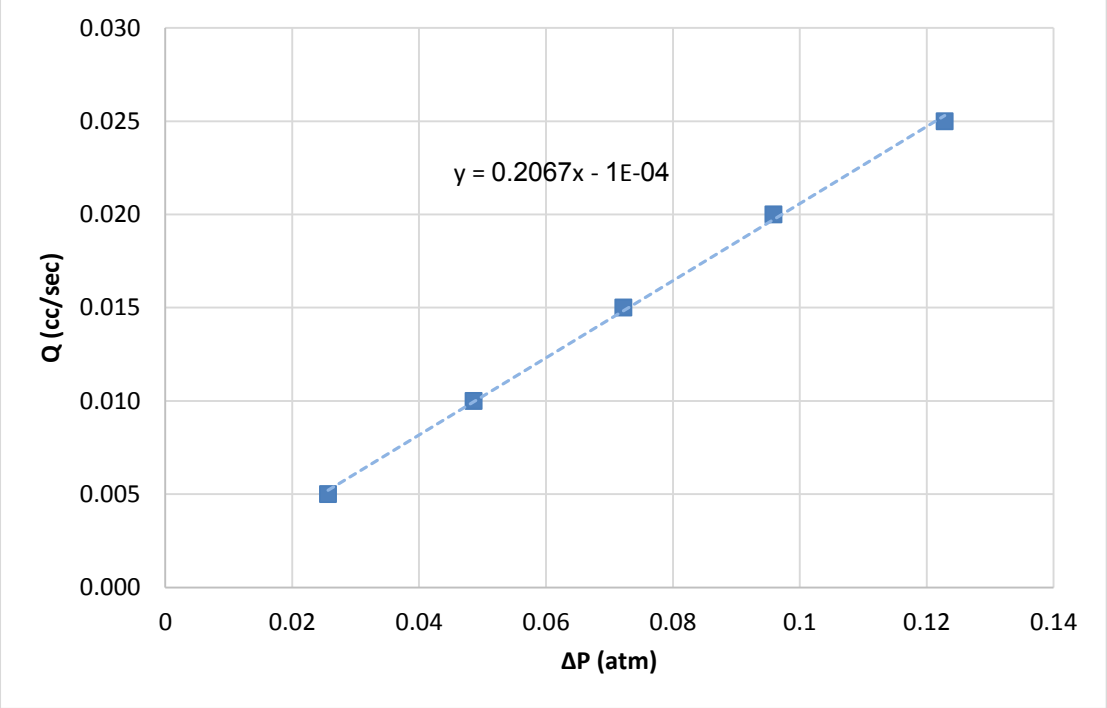

Figure B.4: Initial Absolute Permeability Measurement for Core Sample Gray Berea 4 @ 25°C.

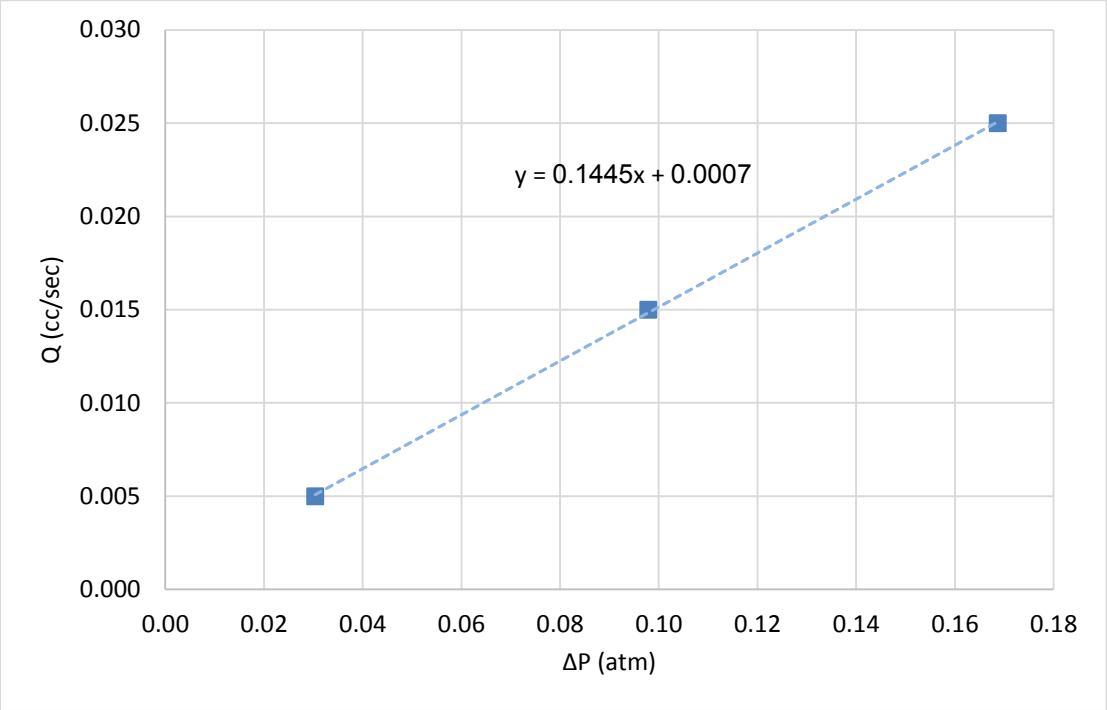

Figure B.5: Initial Absolute Permeability Measurement for Core Sample Gray Berea 5 @ 25°C.

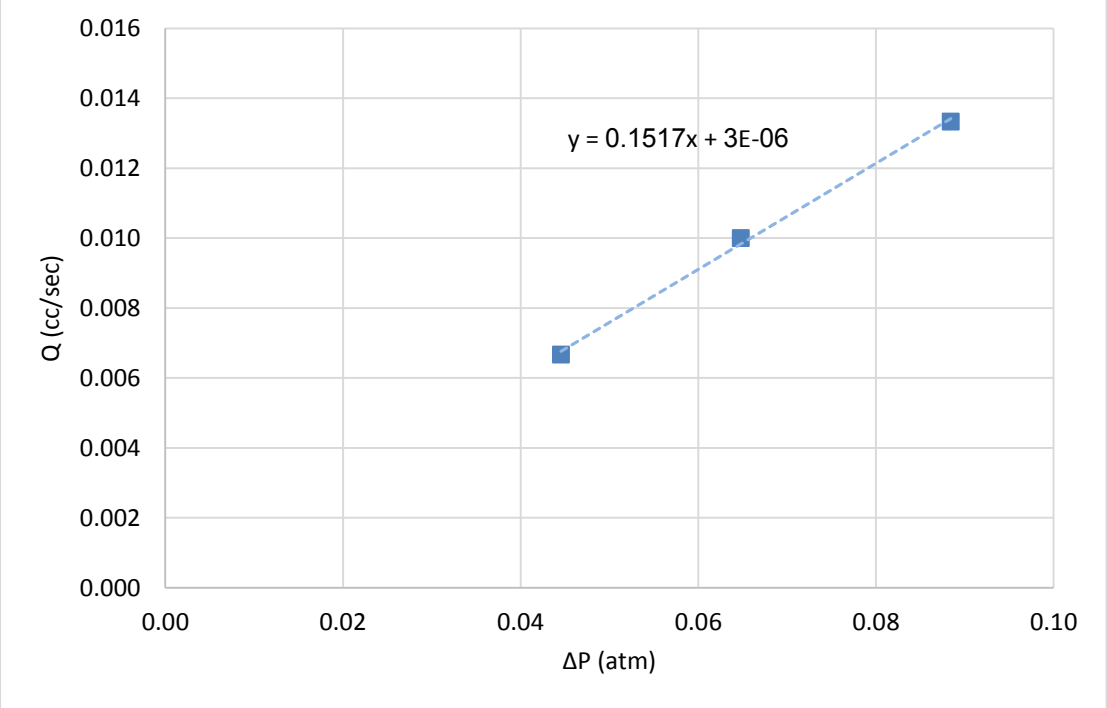

Figure B.6: Initial Absolute Permeability Measurement for Core Sample Gray Berea 6 @ 25°C.

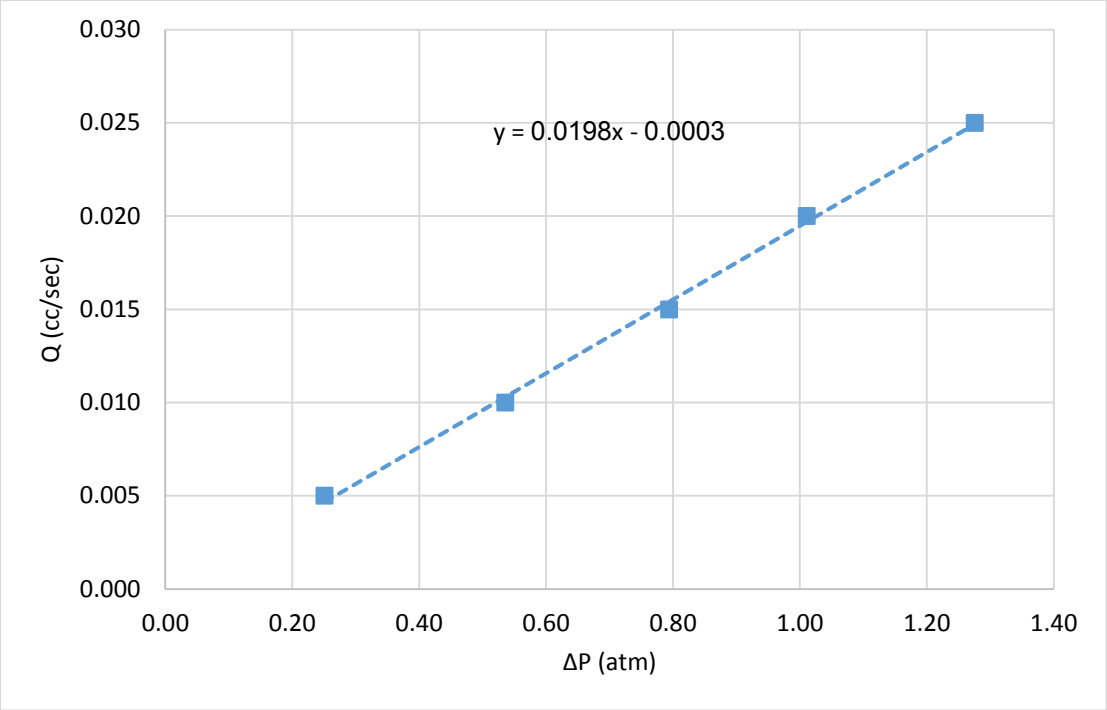

Figure B.7: Initial Absolute Permeability Measurement for Core Sample Gray Bandera 11 @ 25°C.

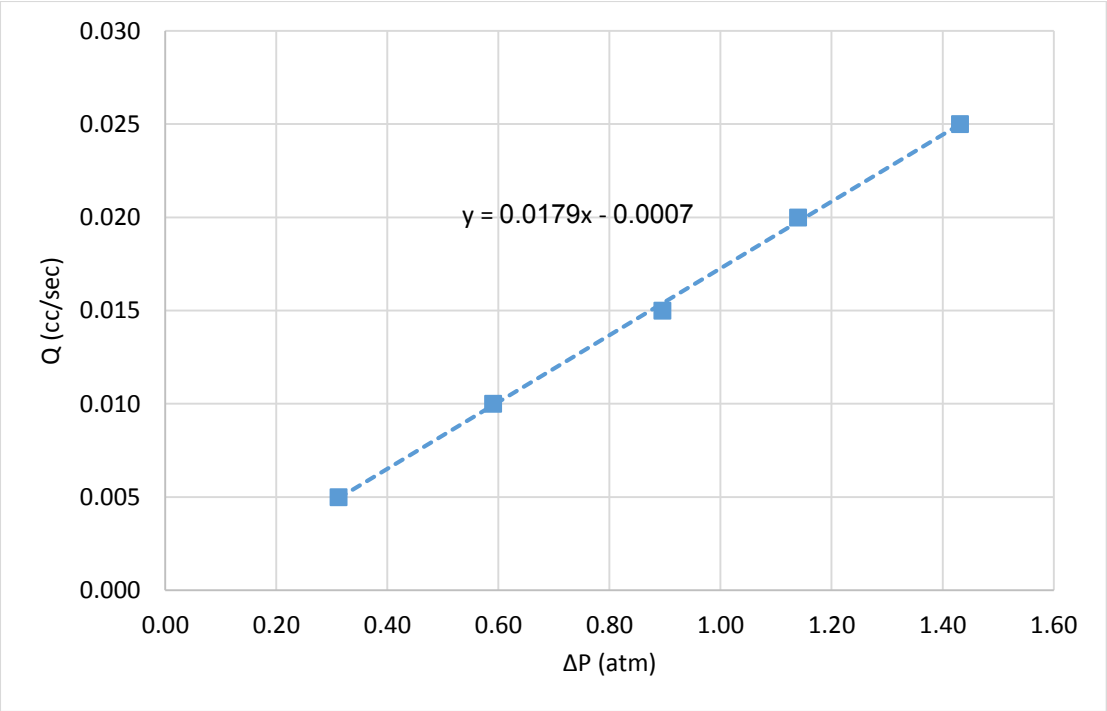

Figure B.8: Initial Absolute Permeability Measurement for Core Sample Gray Bandera 12 @ 25°C.

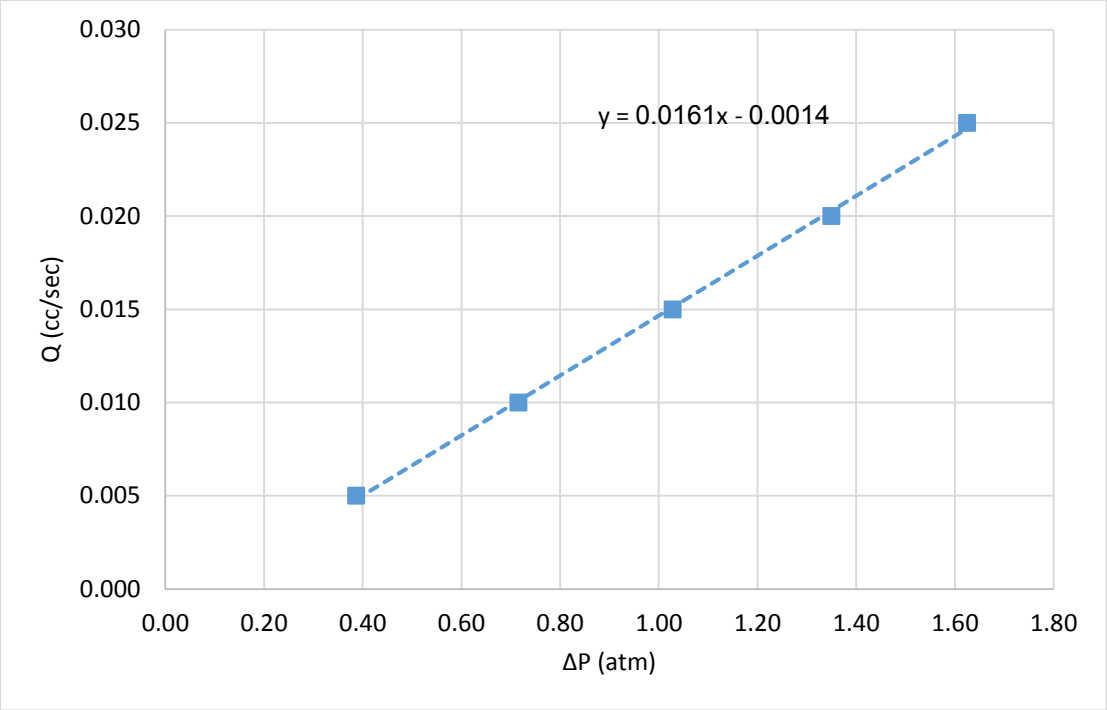

Figure B.9: Initial Absolute Permeability Measurement for Core Sample Gray Bandera 13 @ 25°C.

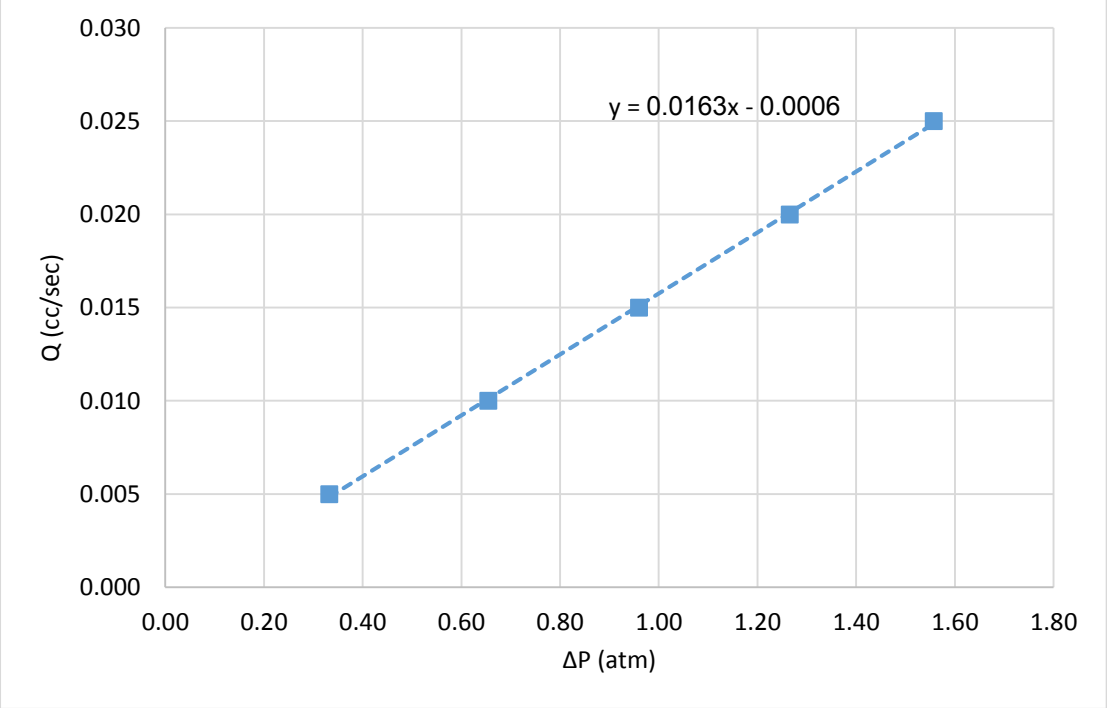

Figure B.10: Initial Absolute Permeability Measurement for Core Sample Gray Bandera 14 @ 25°C.

APPENDIX C: THE ELEMENTAL ANALYSES RESULTS

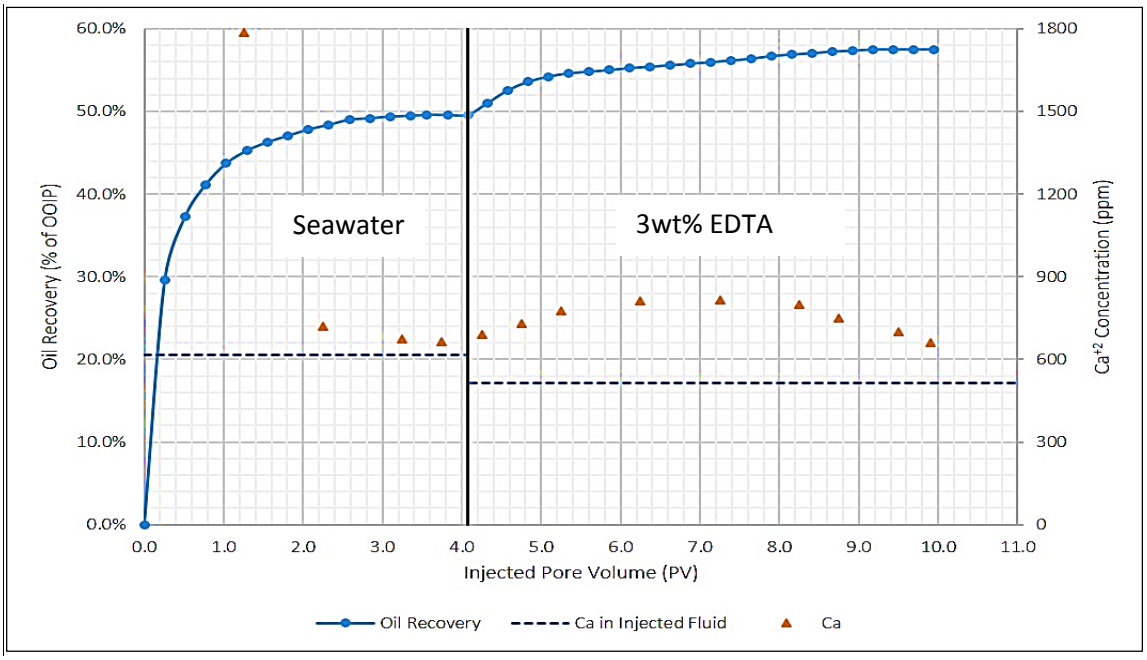

Figure C.1: Ca^{+2} Concentration in the Produced Effluents from Seawater and 3wt% EDTA Injection into Gray Berea Sandstone and Oil Recovery, Experiment #2.

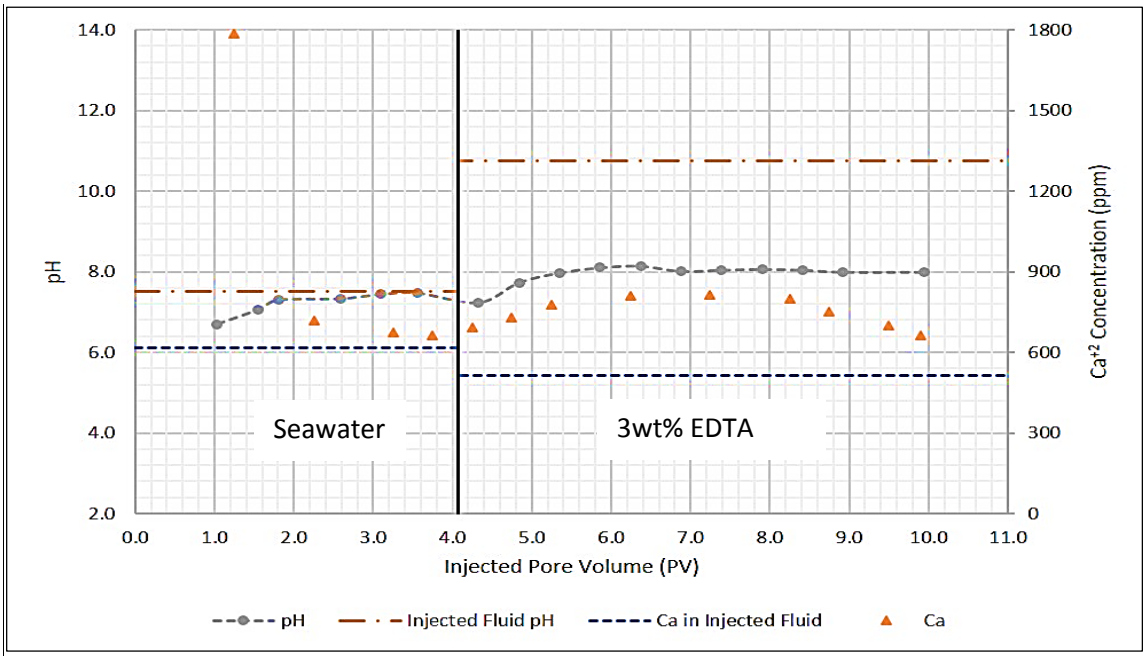

Figure C.2: Ca^{+2} Concentration in the Produced Effluents from Seawater and 3wt% EDTA Injection into Gray Berea Sandstone and the pH, Experiment #2.

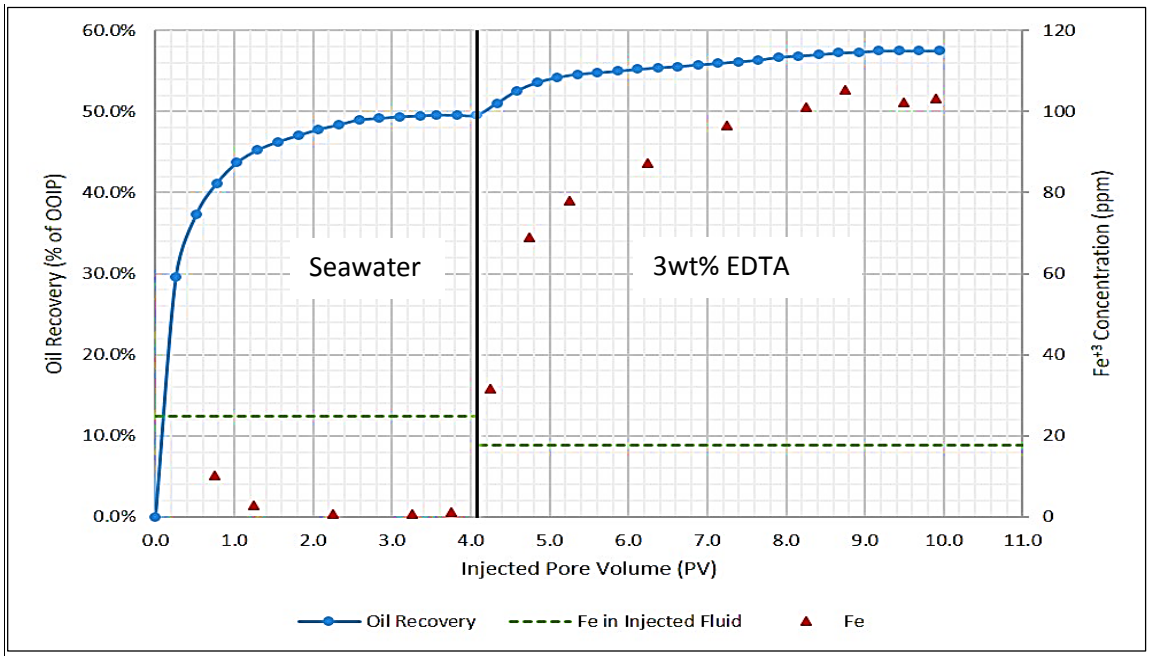

Figure C.3: Fe^{+3} Concentration in the Produced Effluents from Seawater and 3wt% EDTA Injection into Gray Berea Sandstone and Oil Recovery, Experiment #2.

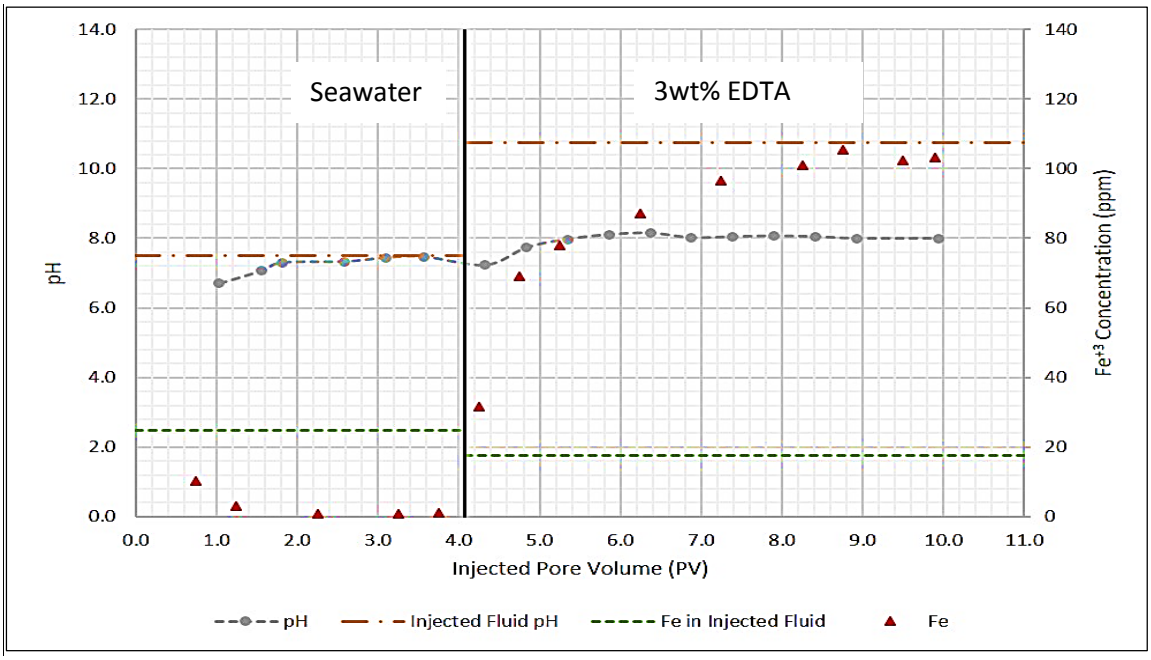

Figure C.4: Fe^{+3} Concentration in the Produced Effluents from Seawater and 3wt% EDTA Injection into Gray Berea Sandstone and the pH, Experiment #2.

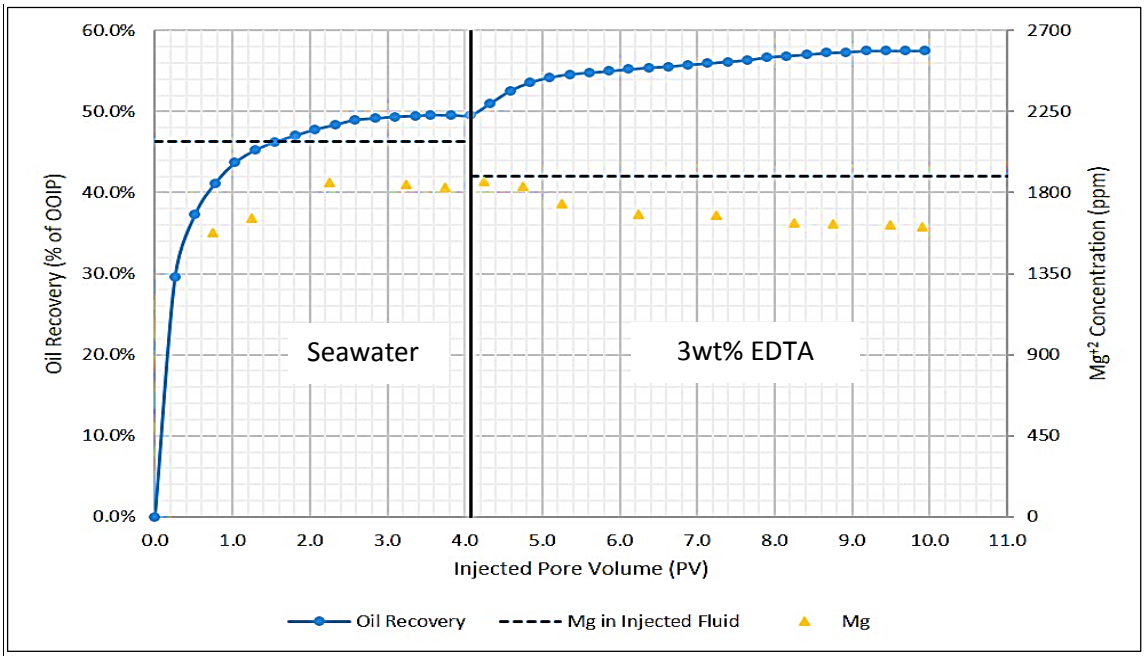

Figure C.5: Mg^{+2} Concentration in the Produced Effluents from Seawater and 3wt% EDTA Injection into Gray Berea Sandstone and Oil Recovery, Experiment #2.

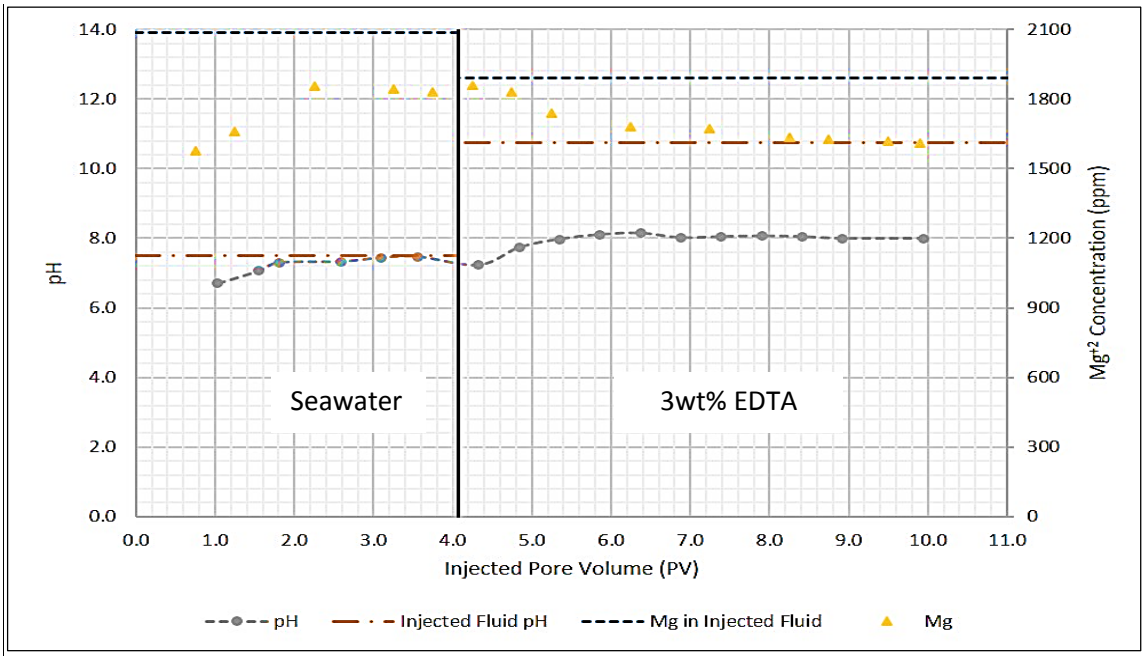

Figure C.6: Mg^{+2} Concentration in the Produced Effluents from Seawater and 3wt% EDTA Injection into Gray Berea Sandstone and the pH, Experiment #2.

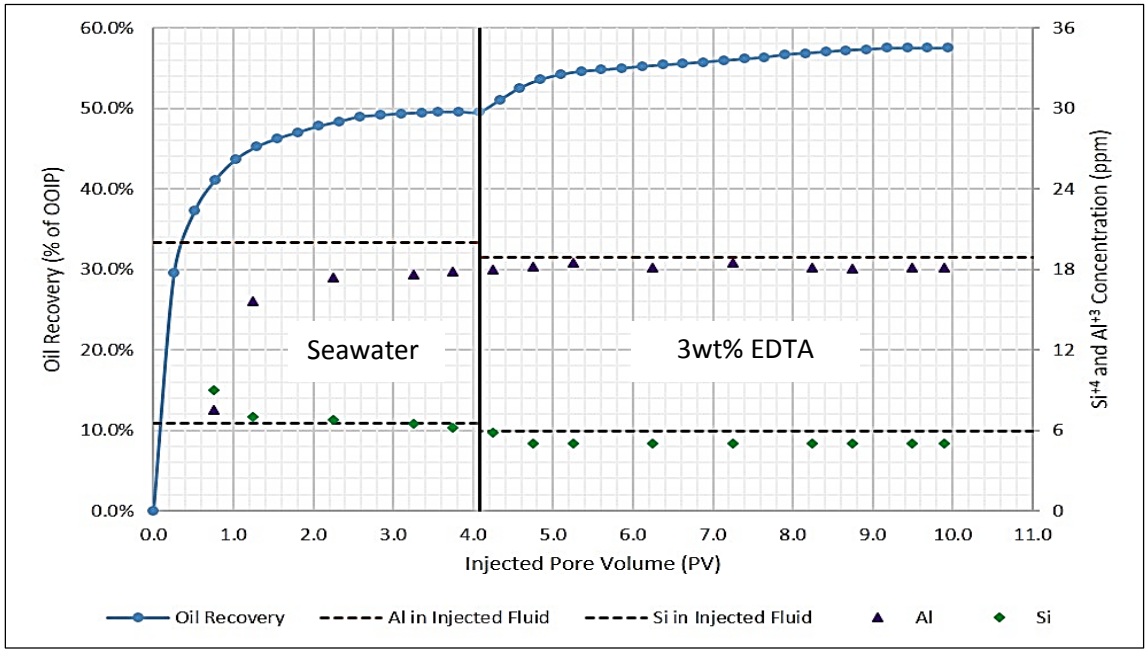

Figure C.7: Si^{+4} and Al^{+3} Concentration in the Produced Effluents from Seawater and 3wt% EDTA Injection into Gray Berea Sandstone and Oil Recovery, Experiment #2.

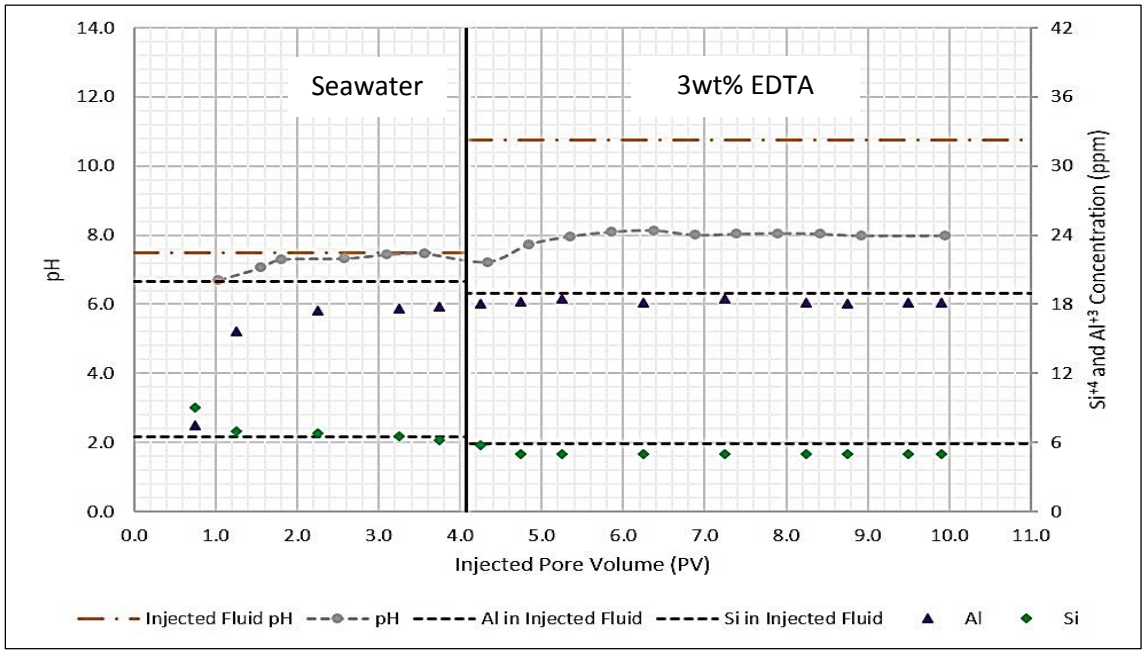

Figure C.8: Si^{+4} and Al^{+3} Concentration in the Produced Effluents from Seawater and 3wt% EDTA Injection into Gray Berea Sandstone and the pH, Experiment #2.

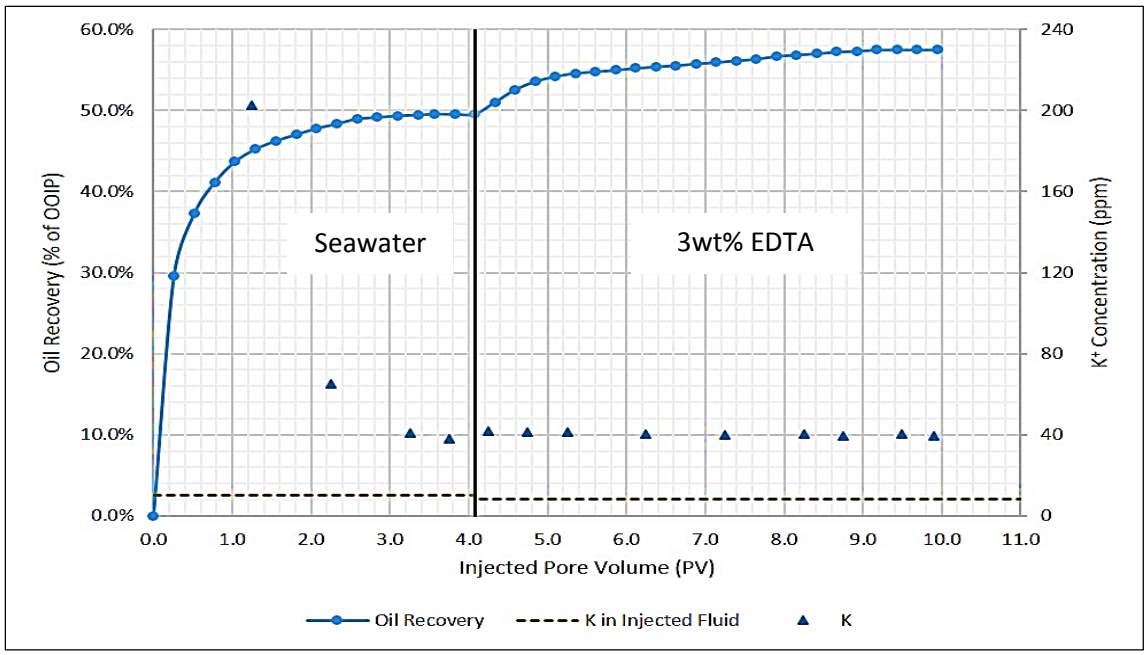

Figure C.9: K^+ Concentration in the Produced Effluents from Seawater and 3wt% EDTA Injection into Gray Berea Sandstone and Oil Recovery, Experiment #2.

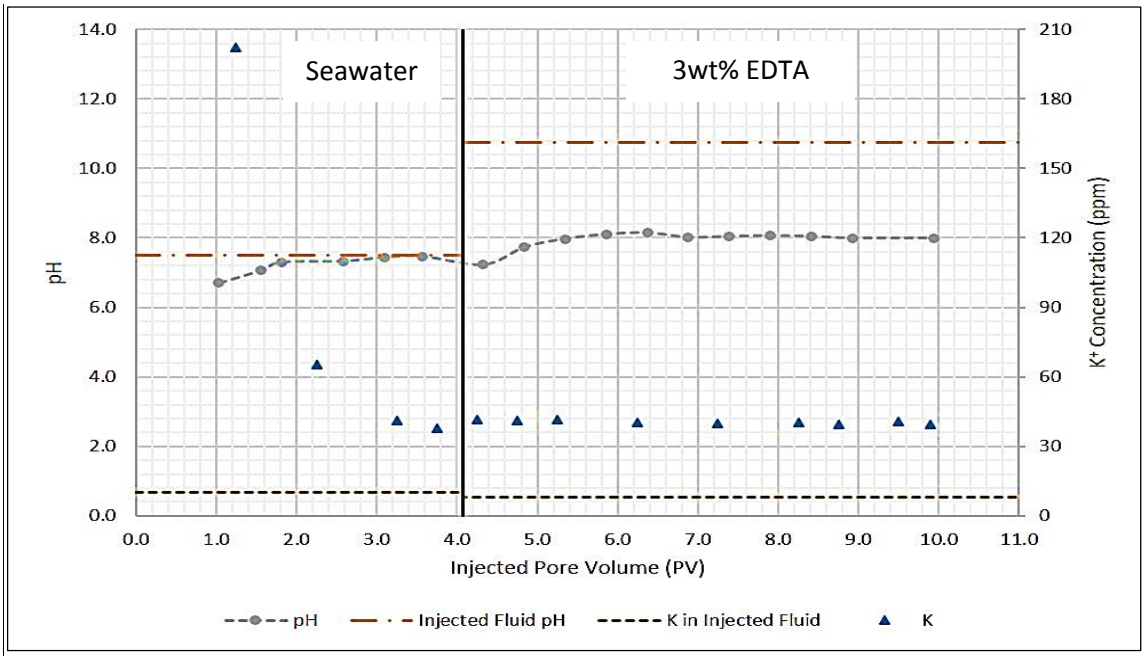

Figure C.10: K^+ Concentration in the Produced Effluents from Seawater and 3wt% EDTA Injection into Gray Berea Sandstone and the pH, Experiment #2.

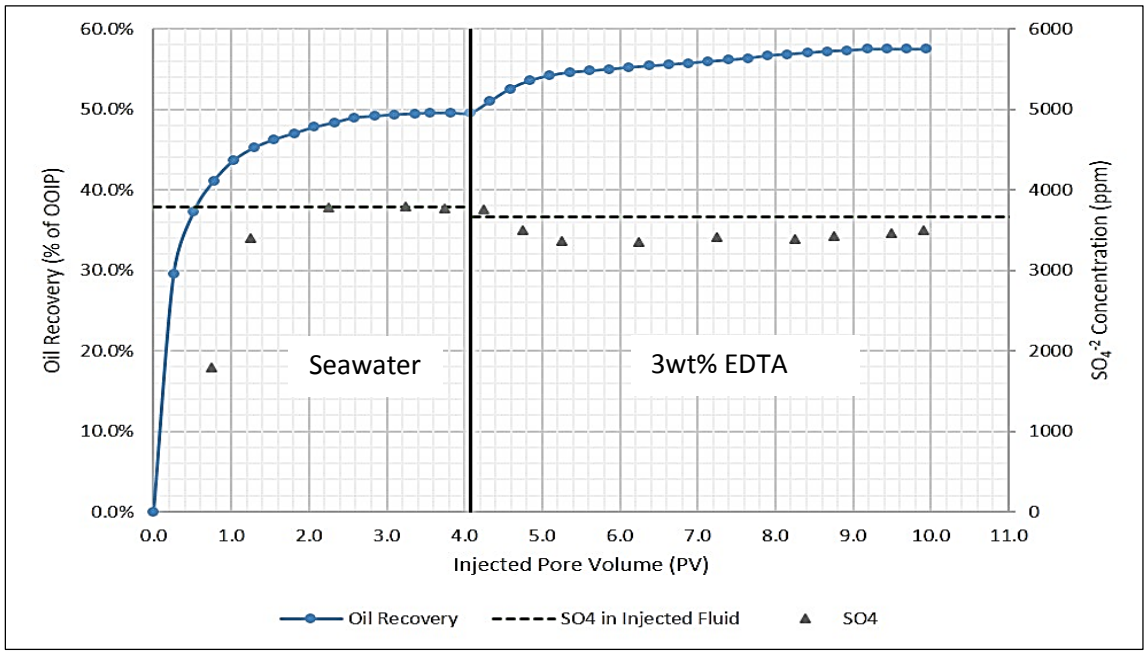

Figure C.11: SO_4^{-2} Concentration in the Produced Effluents from Seawater and 3wt% EDTA Injection into Gray Berea Sandstone and Oil Recovery, Experiment #2.

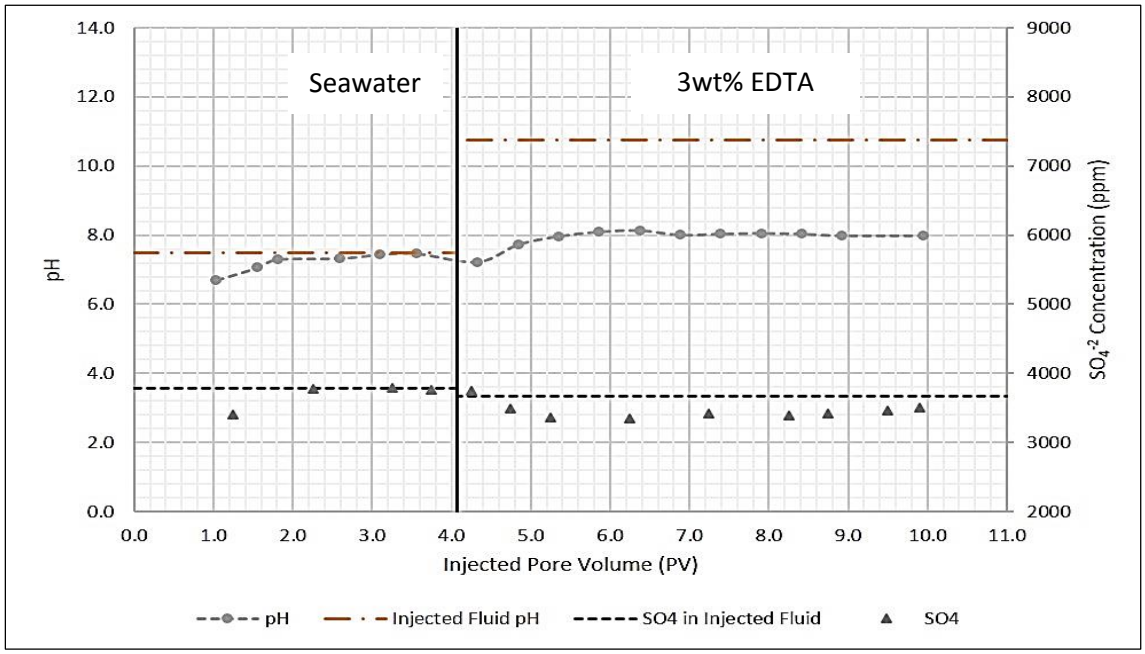

Figure C.12: SO_4^{-2} Concentration in the Produced Effluents from Seawater and 3wt% EDTA Injection into Gray Berea Sandstone and the pH, Experiment #2.

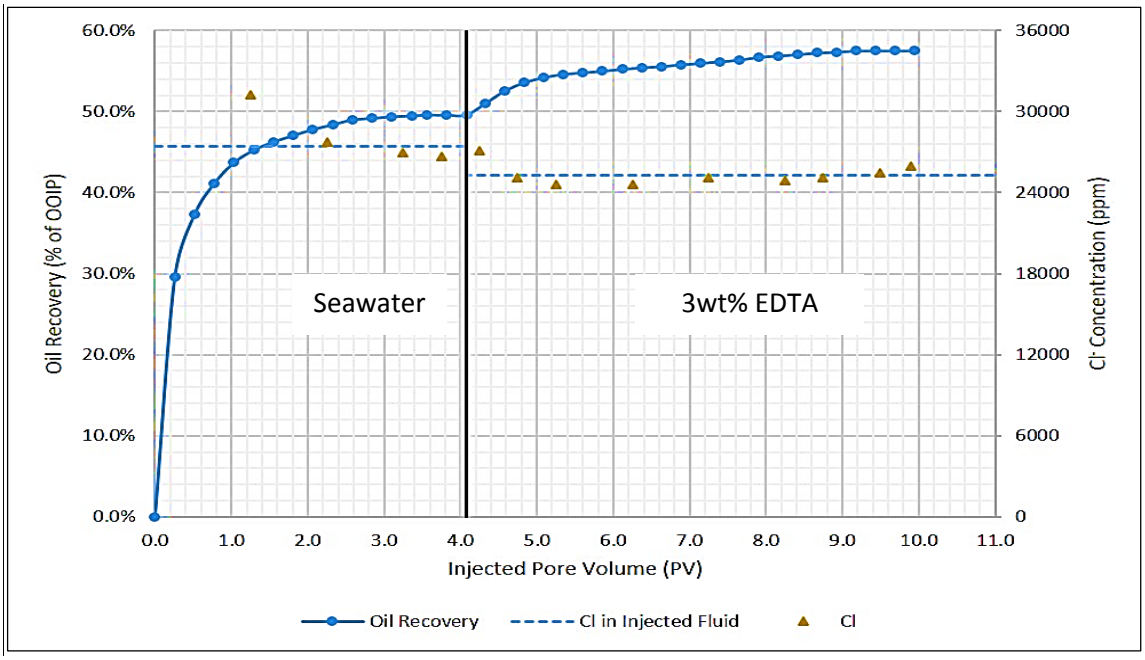

Figure C.13: Cl^- Concentration in the Produced Effluents from Seawater and 3wt% EDTA Injection into Gray Berea Sandstone and Oil Recovery, Experiment #2.

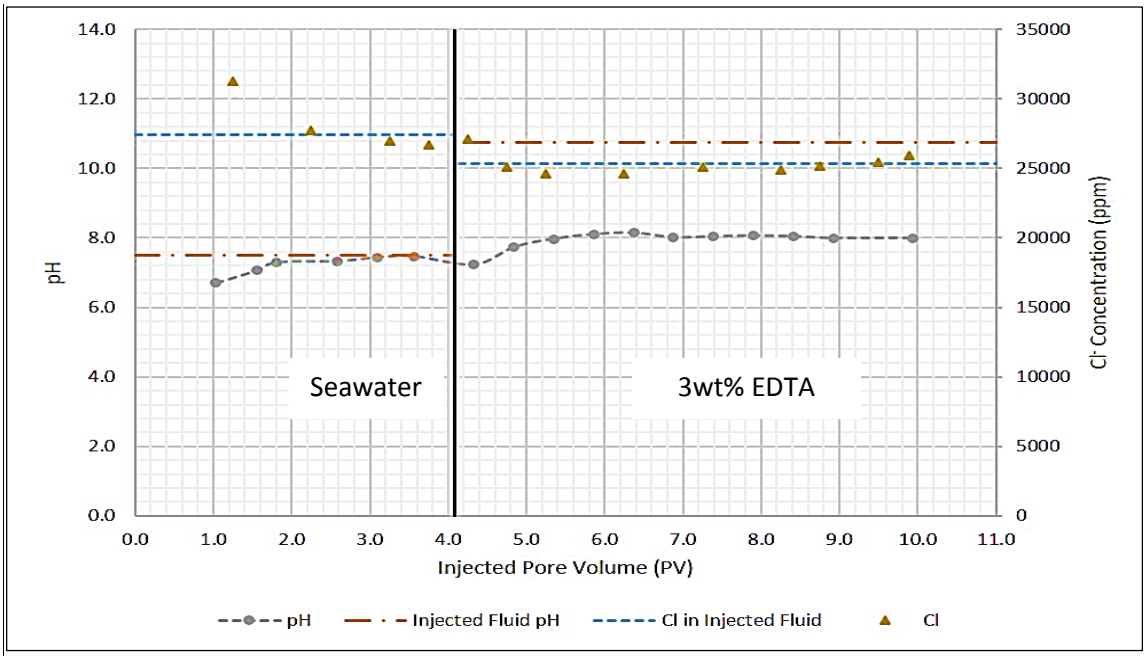

Figure C.14: Cl^- Concentration in the Produced Effluents from Seawater and 3wt% EDTA Injection into Gray Berea Sandstone and the pH, Experiment #2.

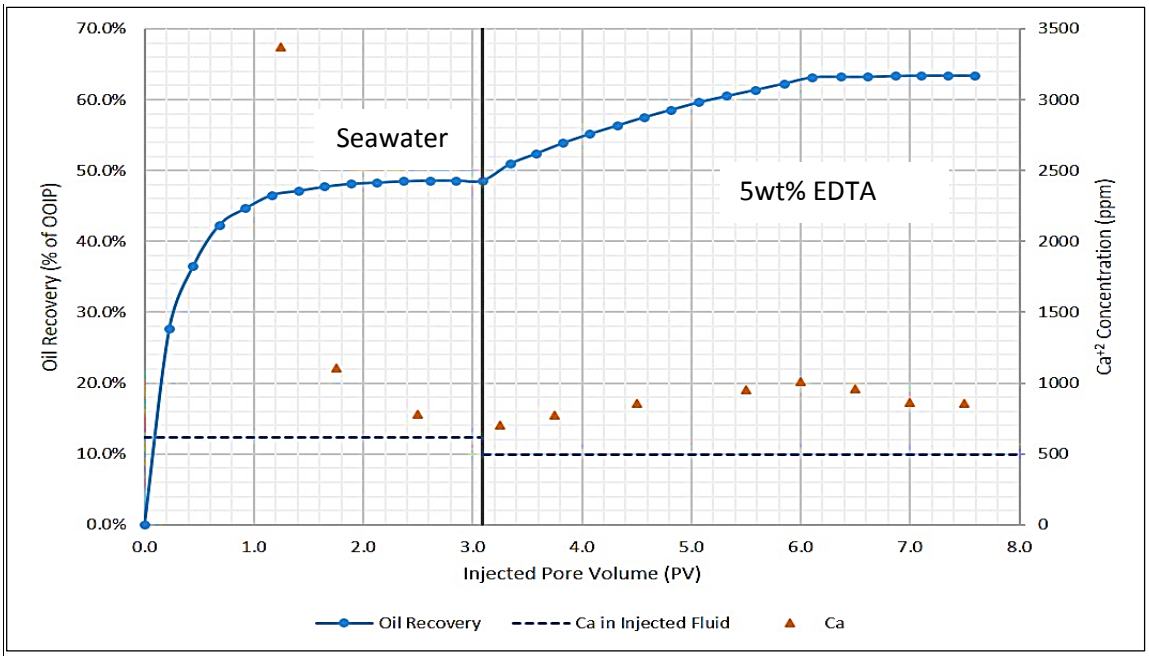

Figure C.15: Ca^{+2} Concentration in the Produced Effluents from Seawater and 5wt% EDTA Injection into Gray Berea Sandstone and Oil Recovery, Experiment #3.

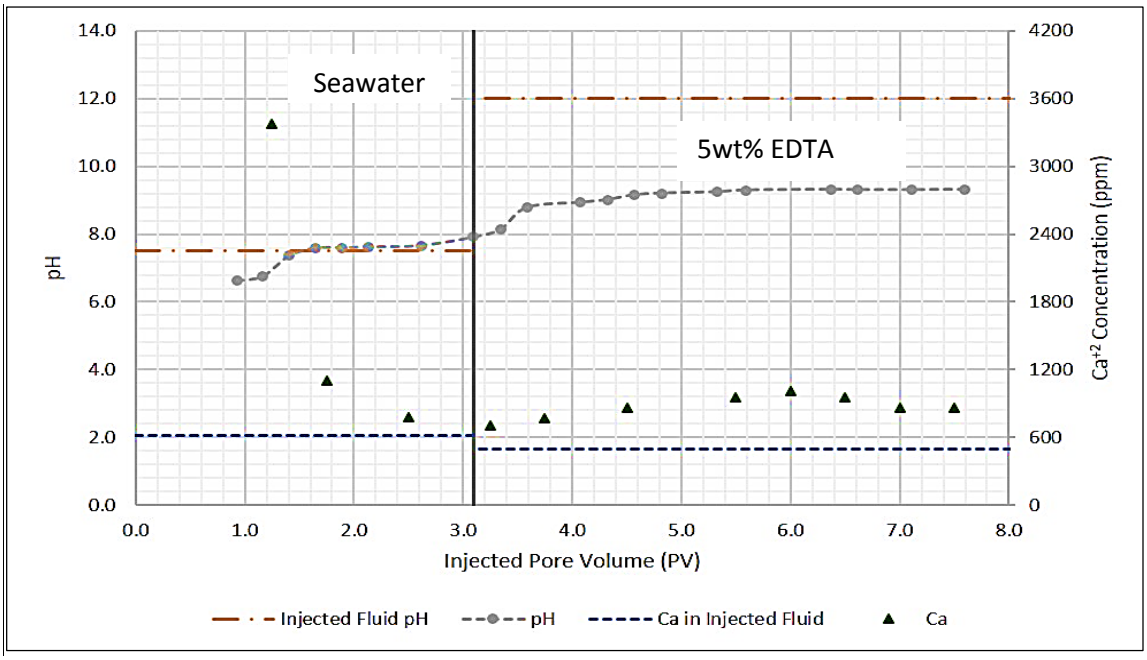

Figure C.16: Ca^{+2} Concentration in the Produced Effluents from Seawater and 5wt% EDTA Injection into Gray Berea Sandstone and the pH, Experiment #3.

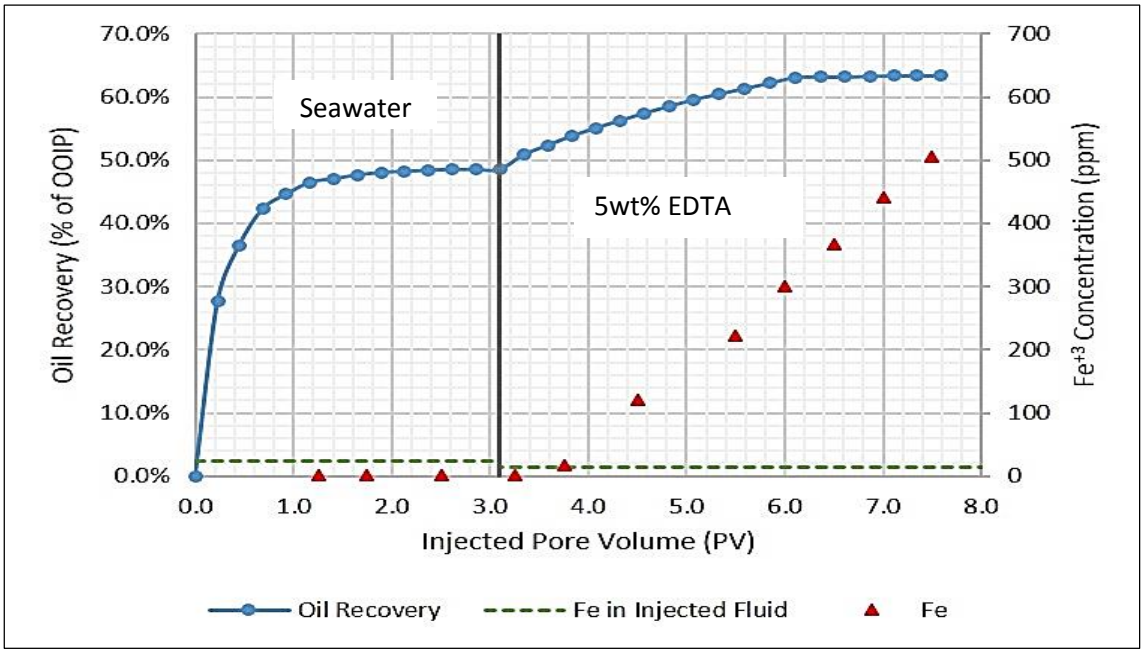

Figure C.17: Fe^{+3} Concentration in the Produced Effluents from Seawater and 5wt% EDTA Injection into Gray Berea Sandstone and Oil Recovery, Experiment #3.

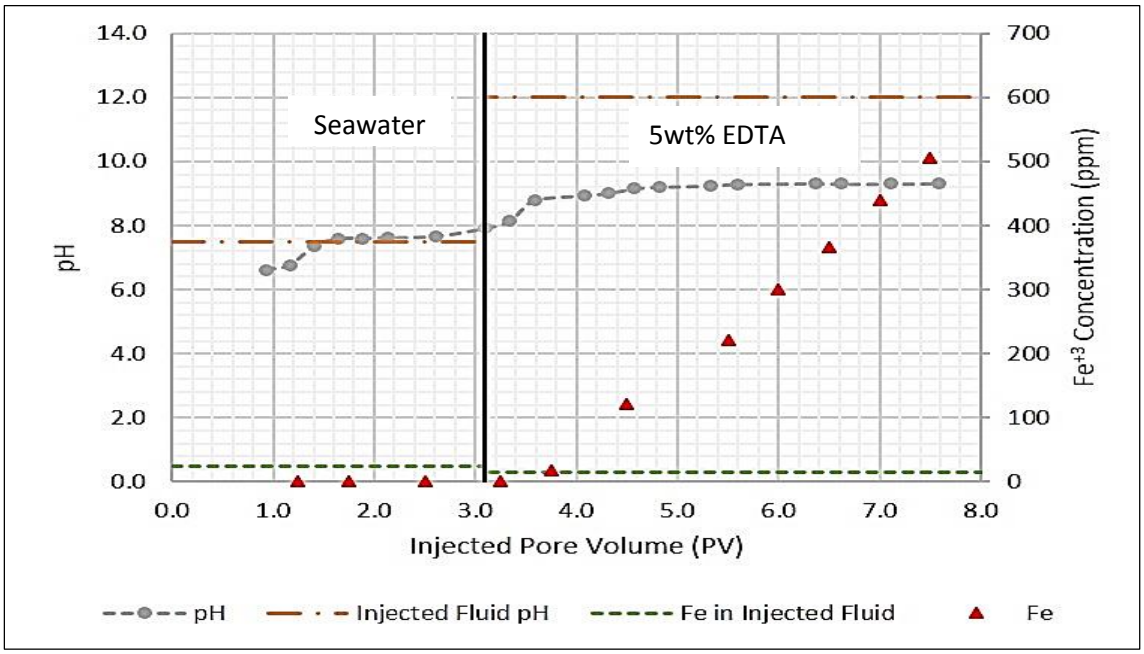

Figure C.18: Fe^{+3} Concentration in the Produced Effluents from Seawater and 5wt% EDTA Injection into Gray Berea Sandstone and the pH, Experiment #3.

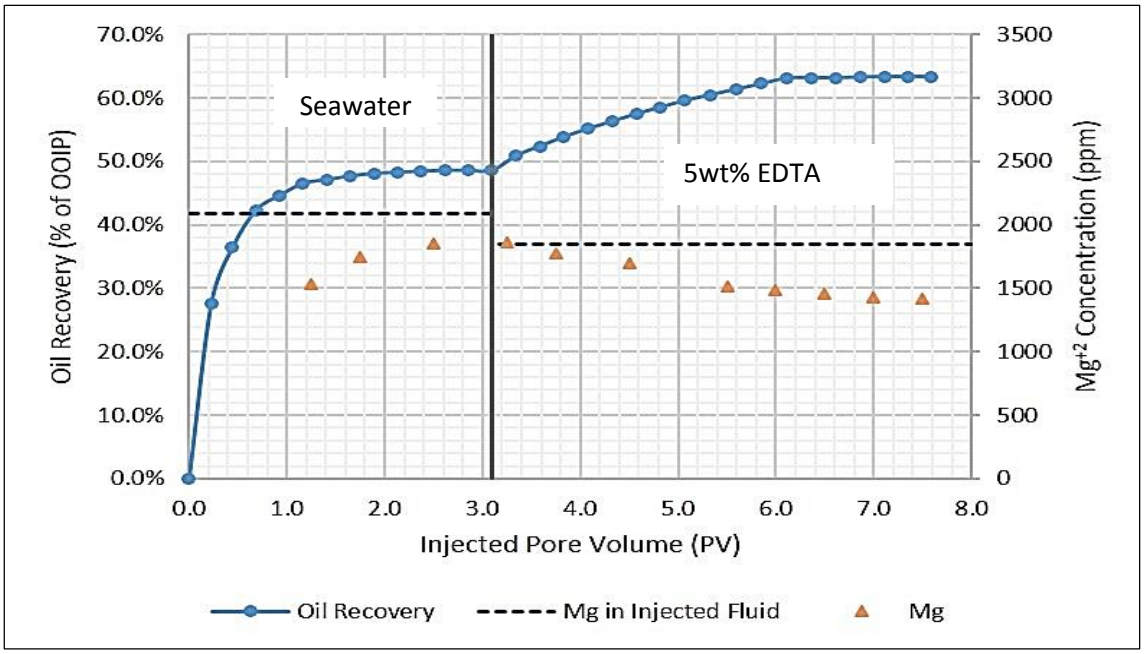

Figure C.19: Mg^{+2} Concentration in the Produced Effluents from Seawater and 5wt% EDTA Injection into Gray Berea Sandstone and Oil Recovery, Experiment #3.

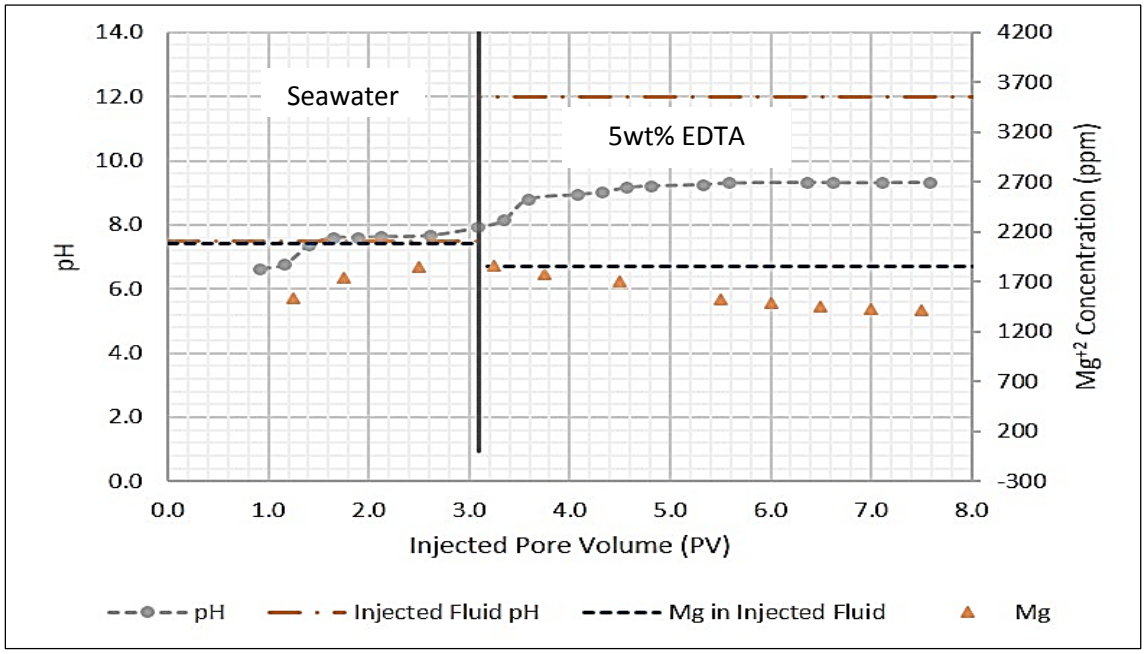

Figure C.20: Mg^{+2} Concentration in the Produced Effluents from Seawater and 5wt% EDTA Injection into Gray Berea Sandstone and the pH, Experiment #3.

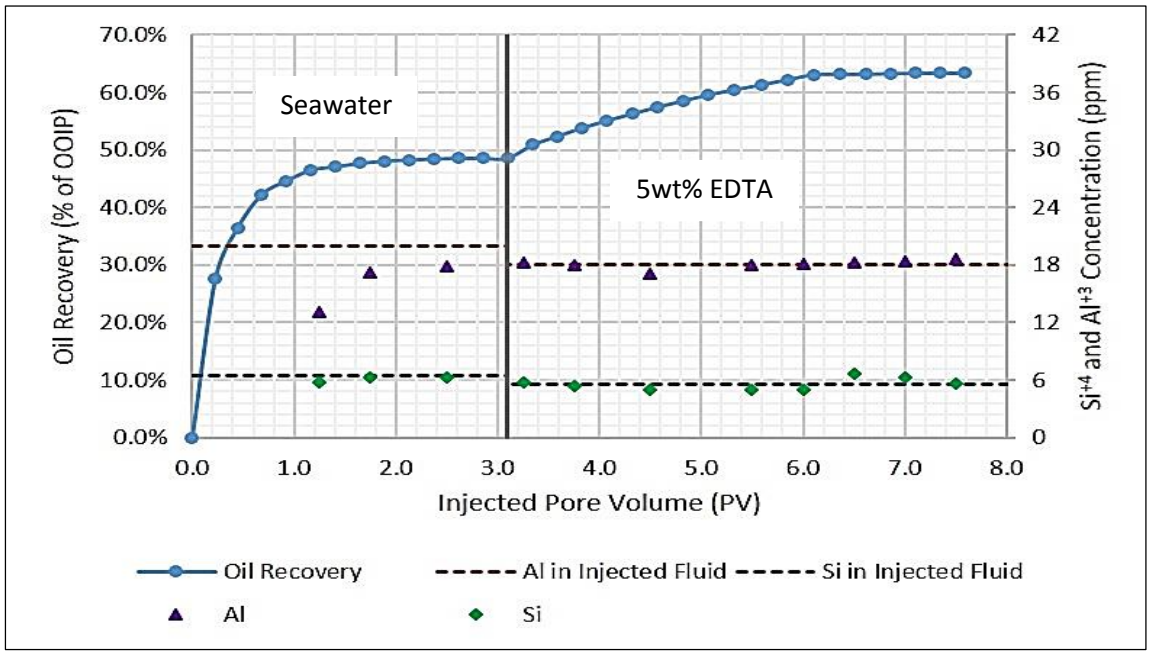

Figure C.21: Si^{+4} and Al^{+3} Concentration in the Produced Effluents from Seawater and 5wt% EDTA Injection into Gray Berea Sandstone and Oil Recovery, Experiment #3.

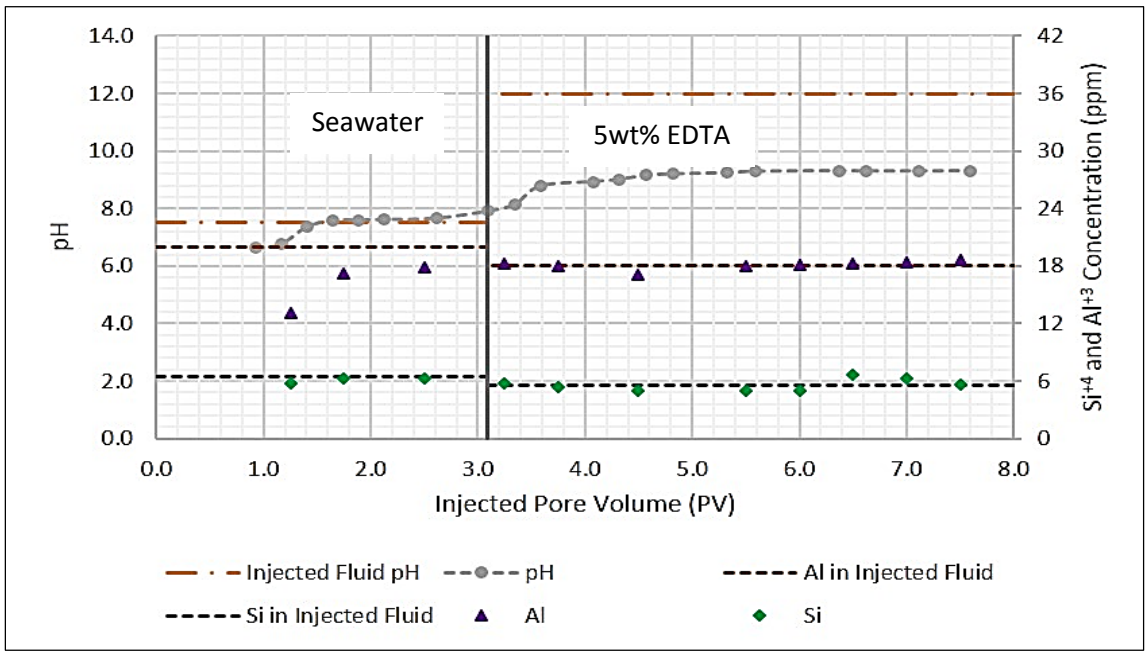

Figure C.22: Si^{+4} and Al^{+3} Concentration in the Produced Effluents from Seawater and 5wt% EDTA Injection into Gray Berea Sandstone and the pH, Experiment #3.

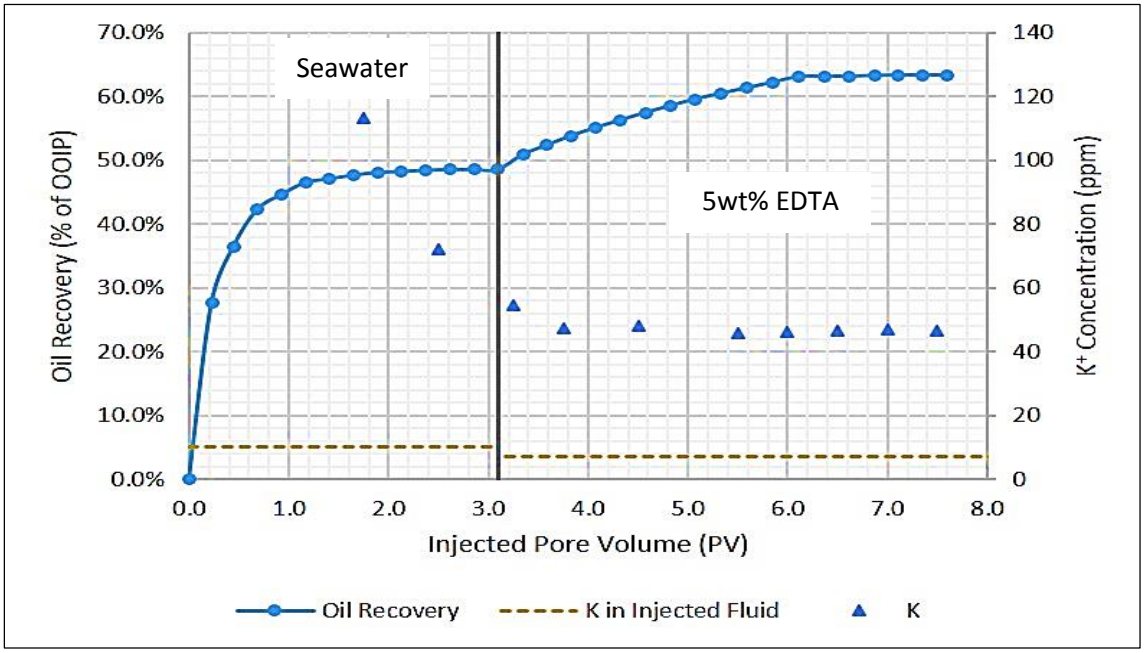

Figure C.23: K^+ Concentration in the Produced Effluents from Seawater and 5wt% EDTA Injection into Gray Berea Sandstone and Oil Recovery, Experiment #3.

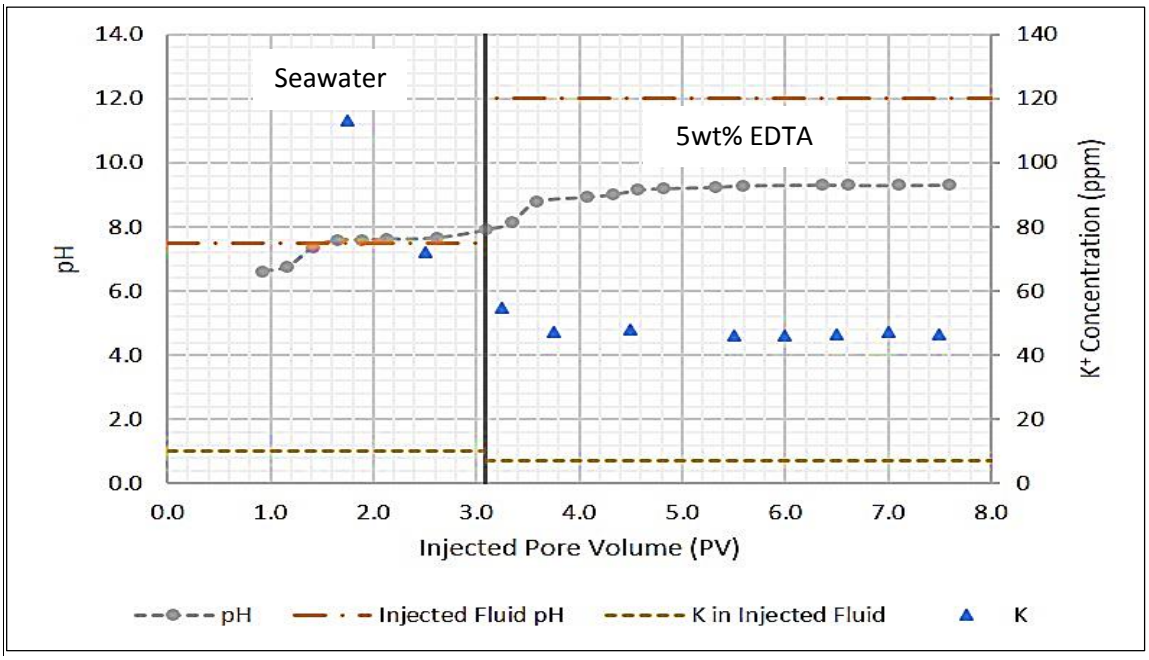

Figure C.24: K^+ Concentration in the Produced Effluents from Seawater and 5wt% EDTA Injection into Gray Berea Sandstone and the pH, Experiment #3.

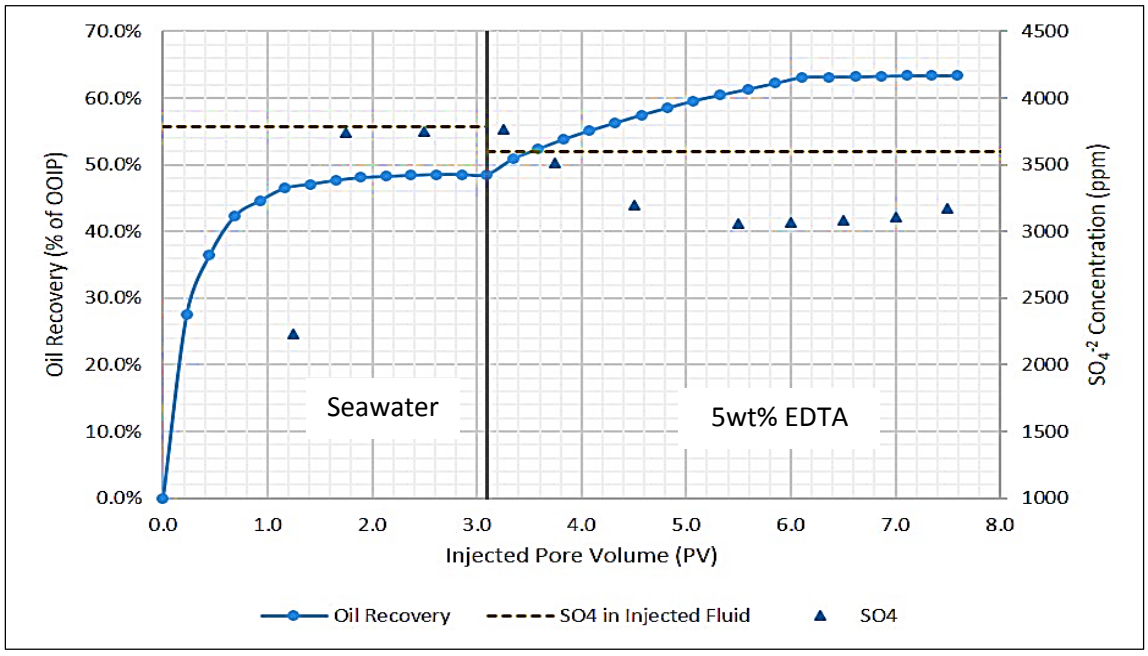

Figure C.25: SO_4^{-2} Concentration in the Produced Effluents from Seawater and 5wt% EDTA Injection into Gray Berea Sandstone and Oil Recovery, Experiment #3.

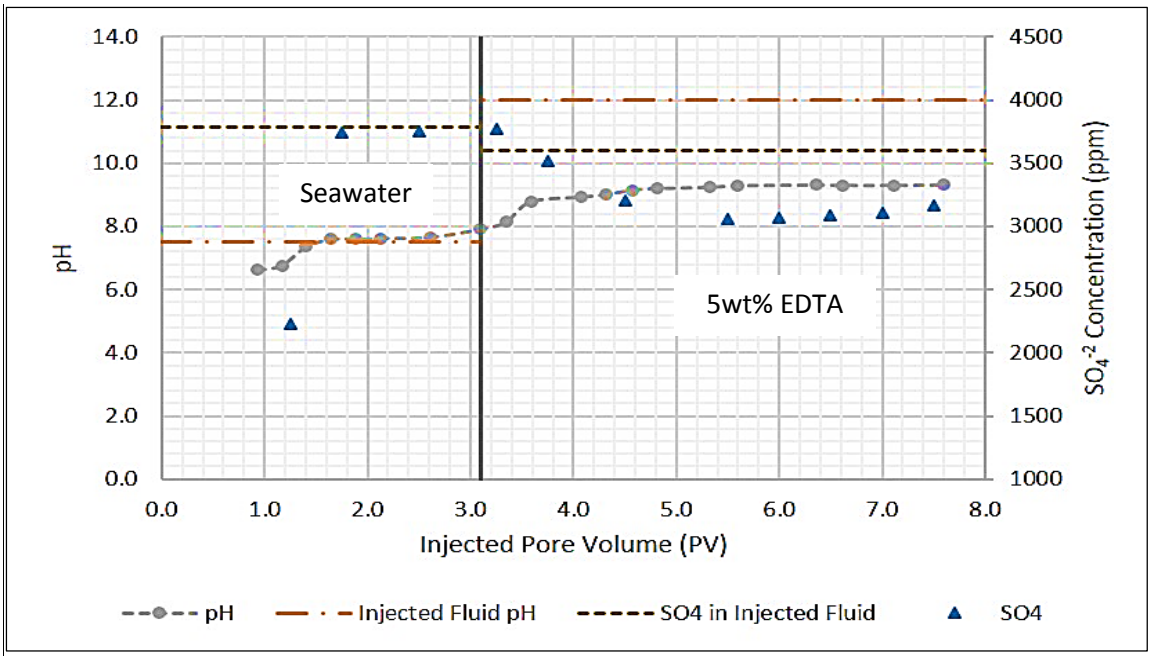

Figure C.26: SO_4^{-2} Concentration in the Produced Effluents from Seawater and 5wt% EDTA Injection into Gray Berea Sandstone and the pH, Experiment #3.

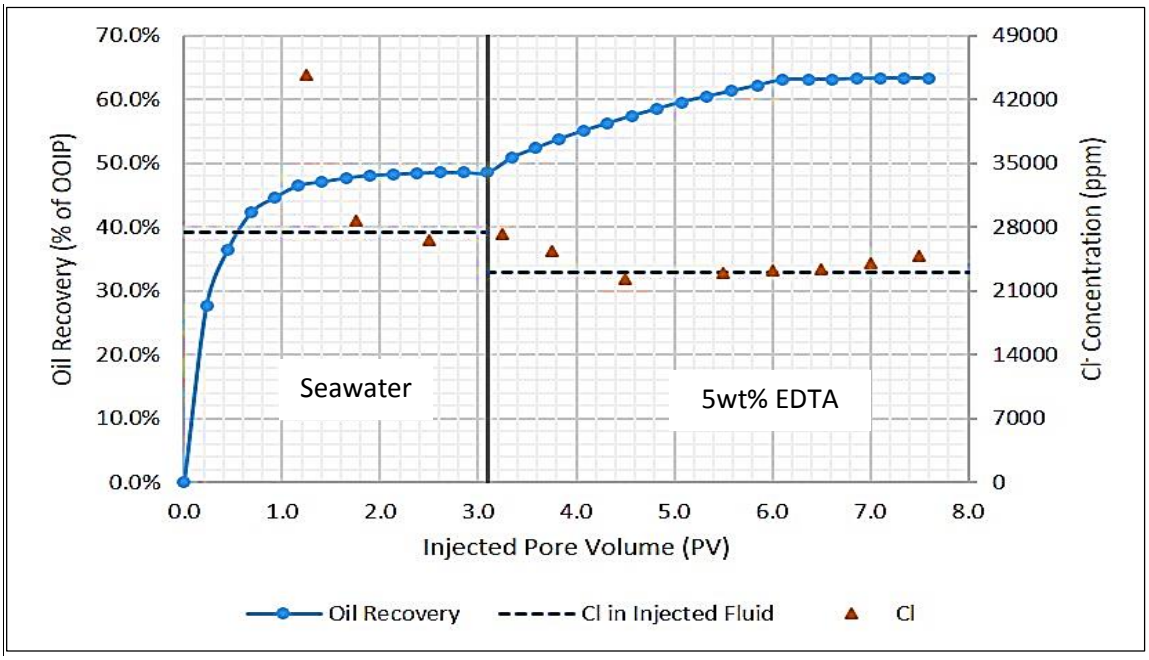

Figure C.27: Cl^- Concentration in the Produced Effluents from Seawater and 5wt% EDTA Injection into Gray Berea Sandstone and Oil Recovery, Experiment #3.

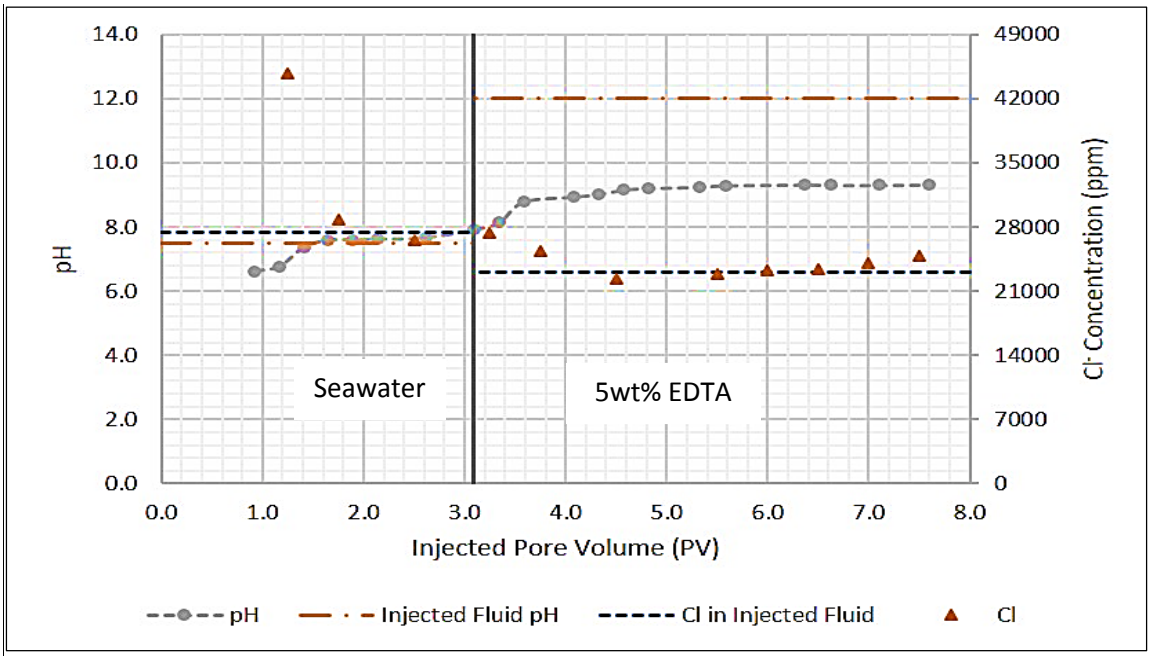

Figure C.28: Cl^- Concentration in the Produced Effluents from Seawater and 5wt% EDTA Injection into Gray Berea Sandstone and the pH, Experiment #3.

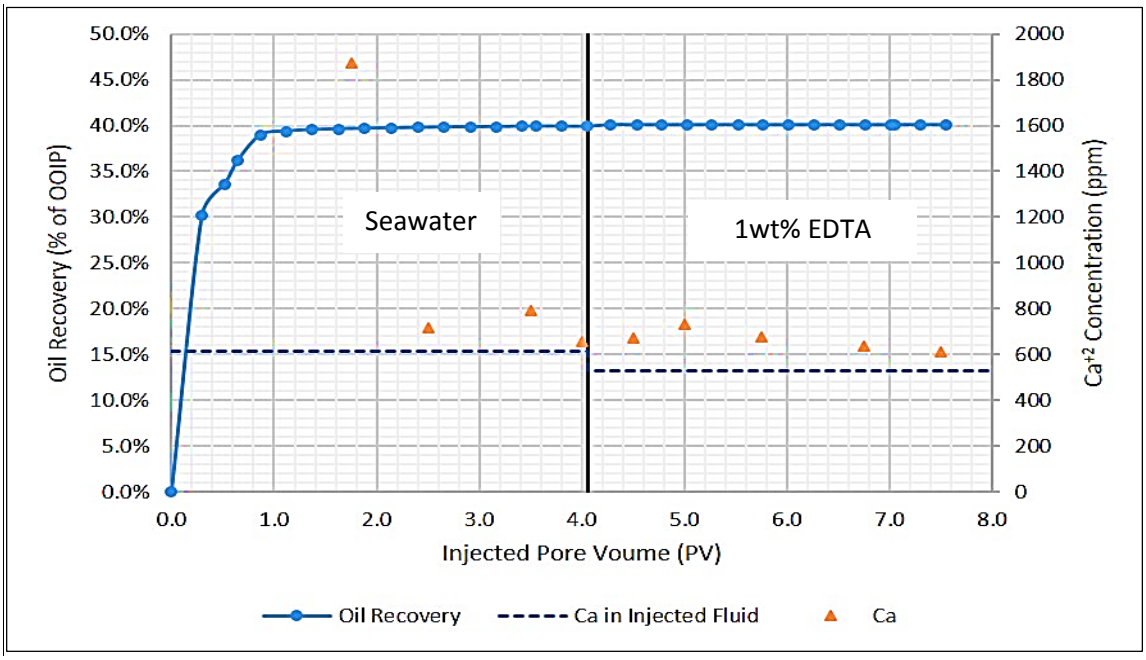

Figure C.29: Ca^{+2} Concentration in the Produced Effluents from Seawater and 1wt% EDTA Injection into Gray Bandera Sandstone and Oil Recovery, Experiment #4.

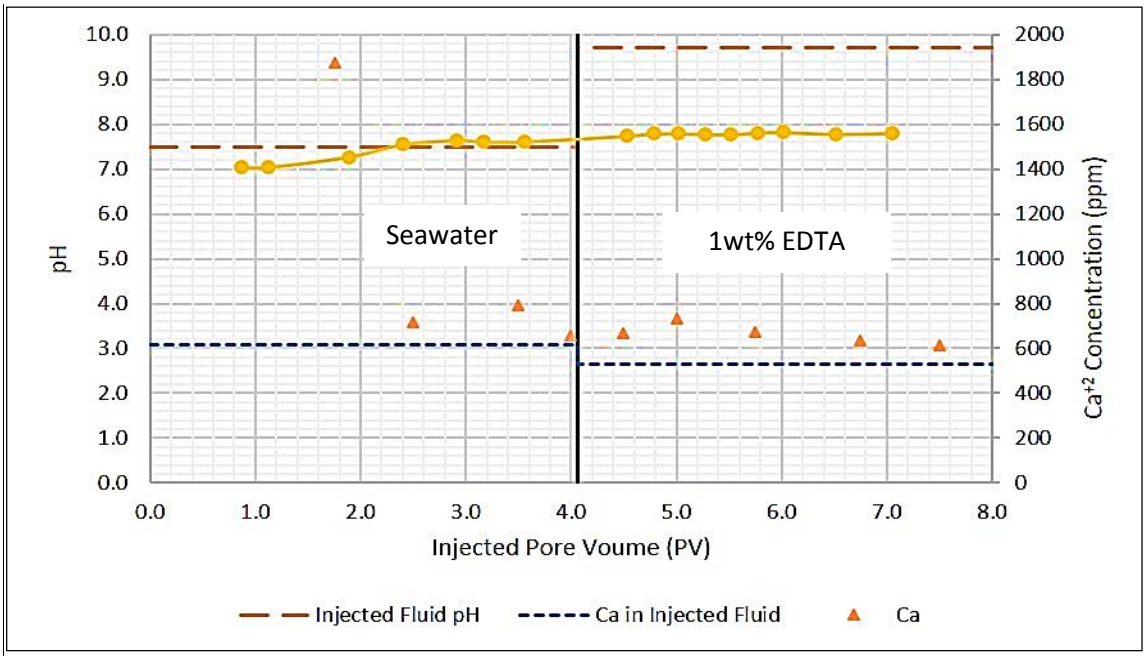

Figure C.30: Ca^{+2} Concentration in the Produced Effluents from Seawater and 1wt% EDTA Injection into Gray Bandera Sandstone and the pH, Experiment #4.

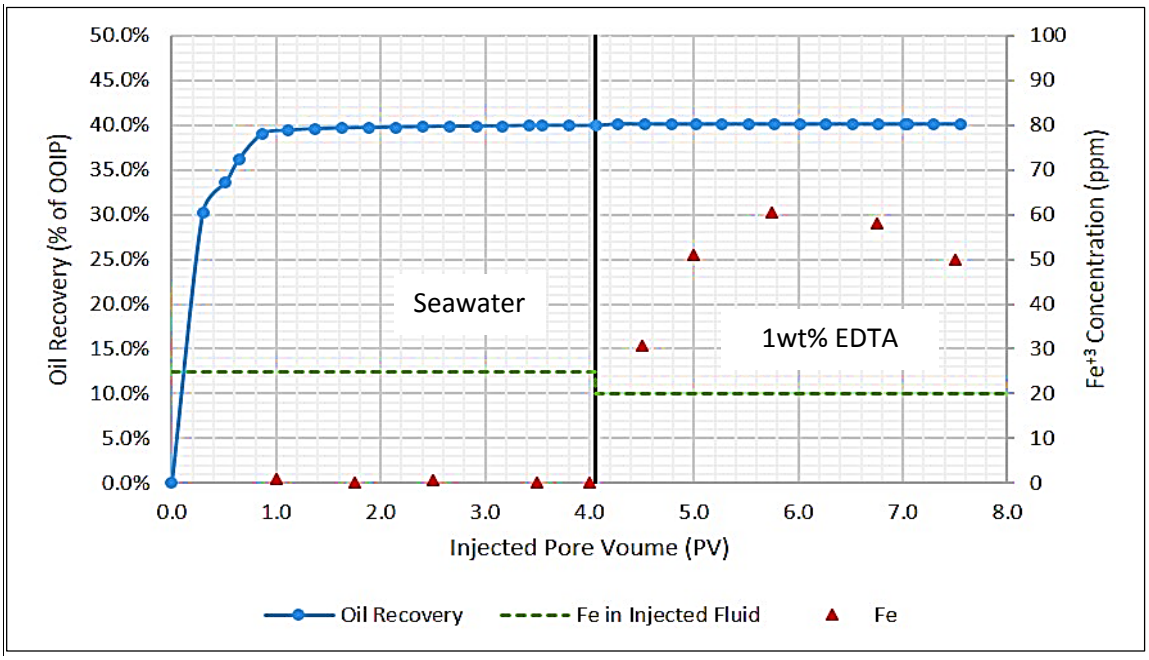

Figure C.31: Fe^{+3} Concentration in the Produced Effluents from Seawater and 1wt% EDTA Injection into Gray Bandera Sandstone and Oil Recovery, Experiment #4.

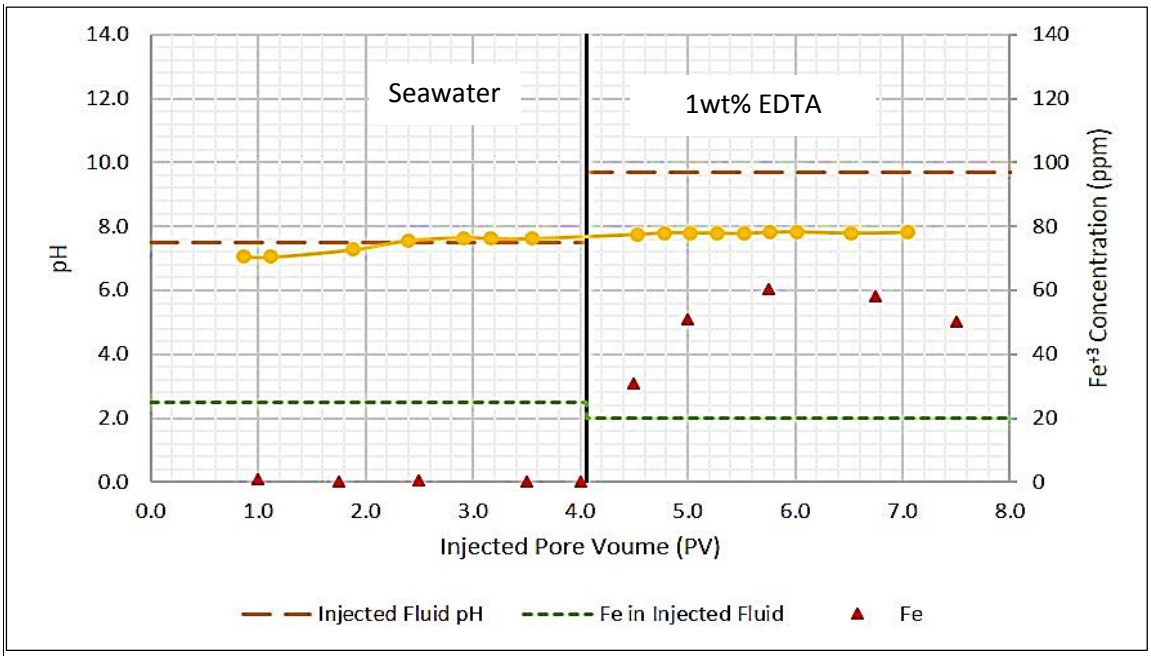

Figure C.32: Fe^{+3} Concentration in the Produced Effluents from Seawater and 1wt% EDTA Injection into Gray Bandera Sandstone and the pH, Experiment #4.

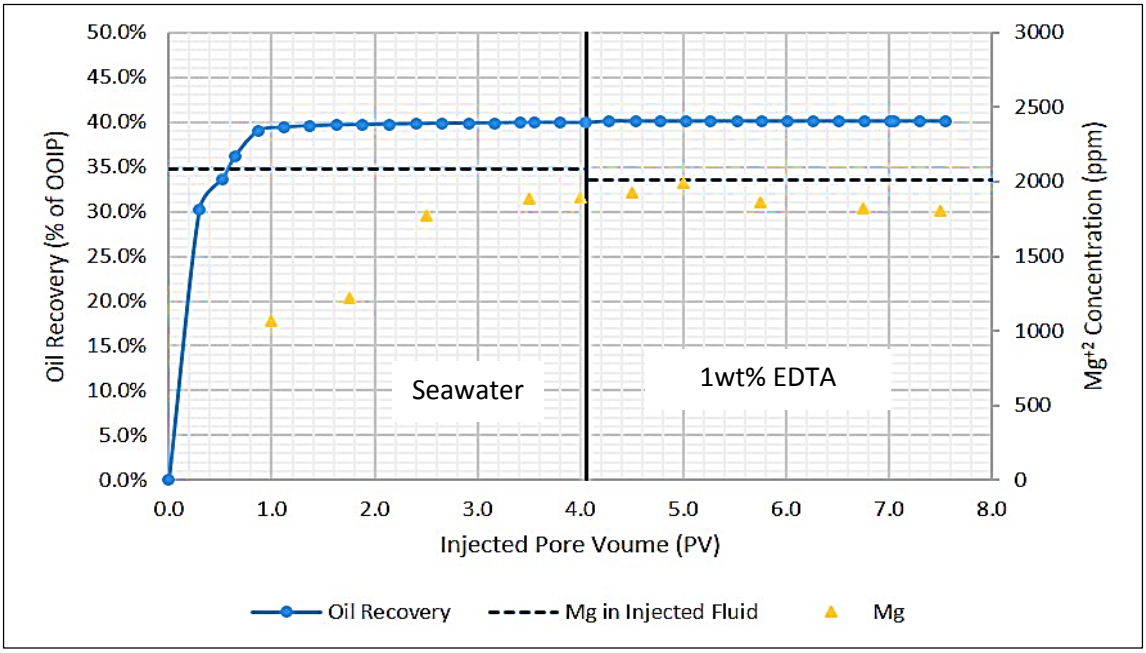

Figure C.33: Mg^{+2} Concentration in the Produced Effluents from Seawater and 1wt% EDTA Injection into Gray Bandera Sandstone and Oil Recovery, Experiment #4.

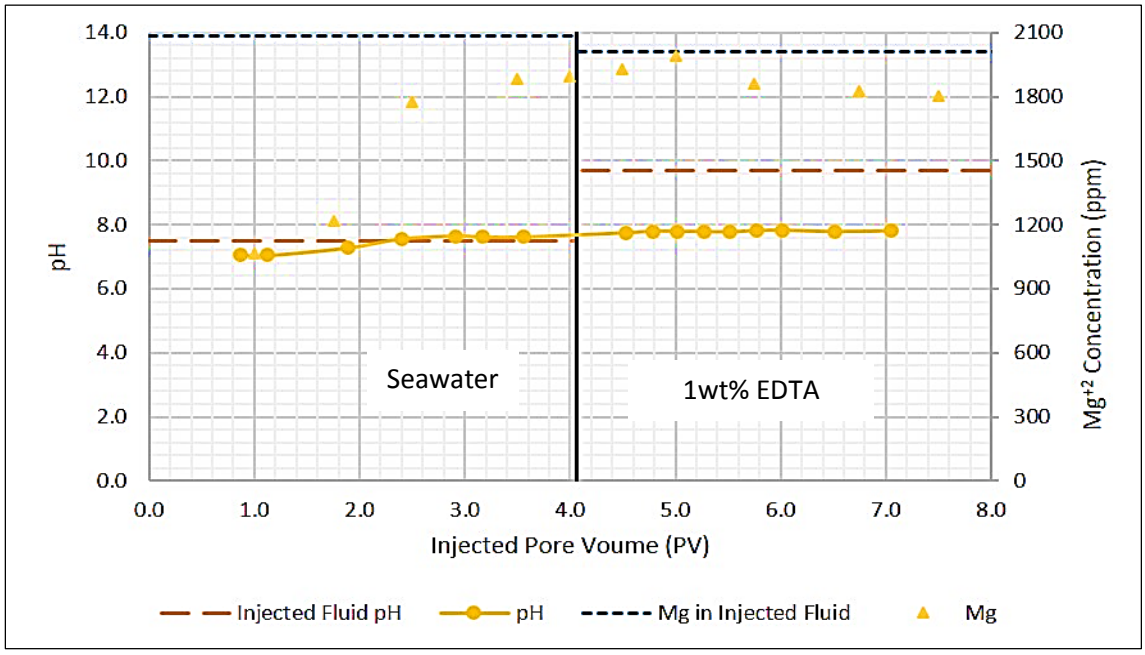

Figure C.34: Mg^{+2} Concentration in the Produced Effluents from Seawater and 1wt% EDTA Injection into Gray Bandera Sandstone and the pH, Experiment #4.

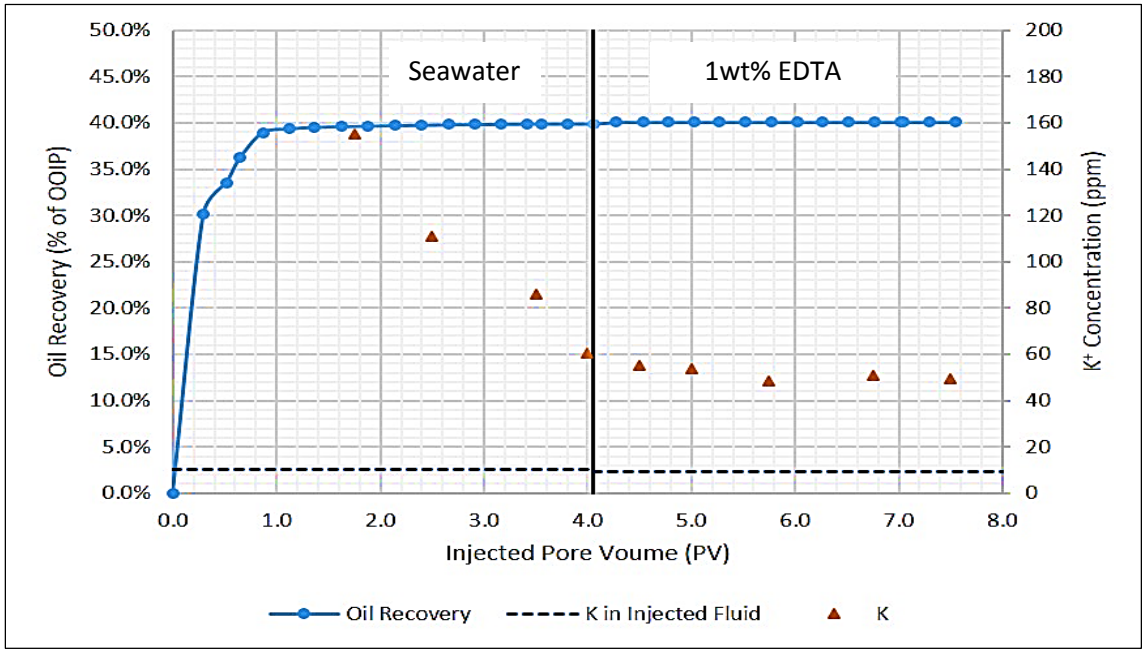

Figure C.35: K^+ Concentration in the Produced Effluents from Seawater and 1wt% EDTA Injection into Gray Bandera Sandstone and Oil Recovery, Experiment #4.

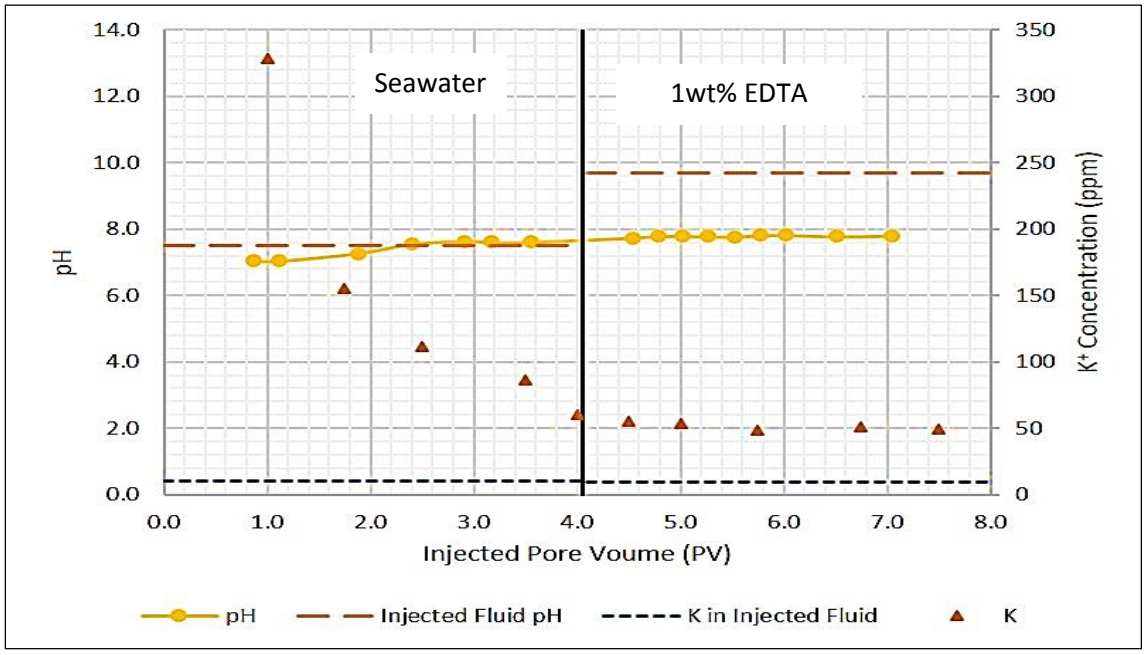

Figure C.36: K^+ Concentration in the Produced Effluents from Seawater and 1wt% EDTA Injection into Gray Bandera Sandstone and the pH, Experiment #4.

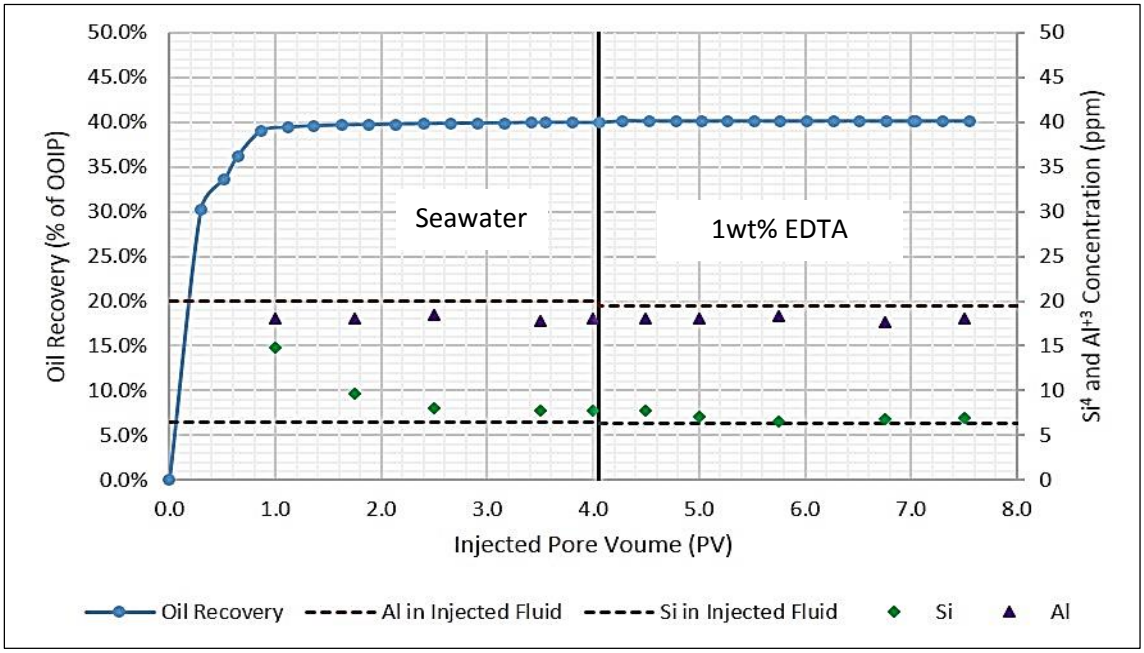

Figure C.37: Si^{+4} and Al^{+3} Concentration in the Produced Effluents from Seawater and 1wt% EDTA Injection into Gray Bandera Sandstone and Oil Recovery, Experiment #4.

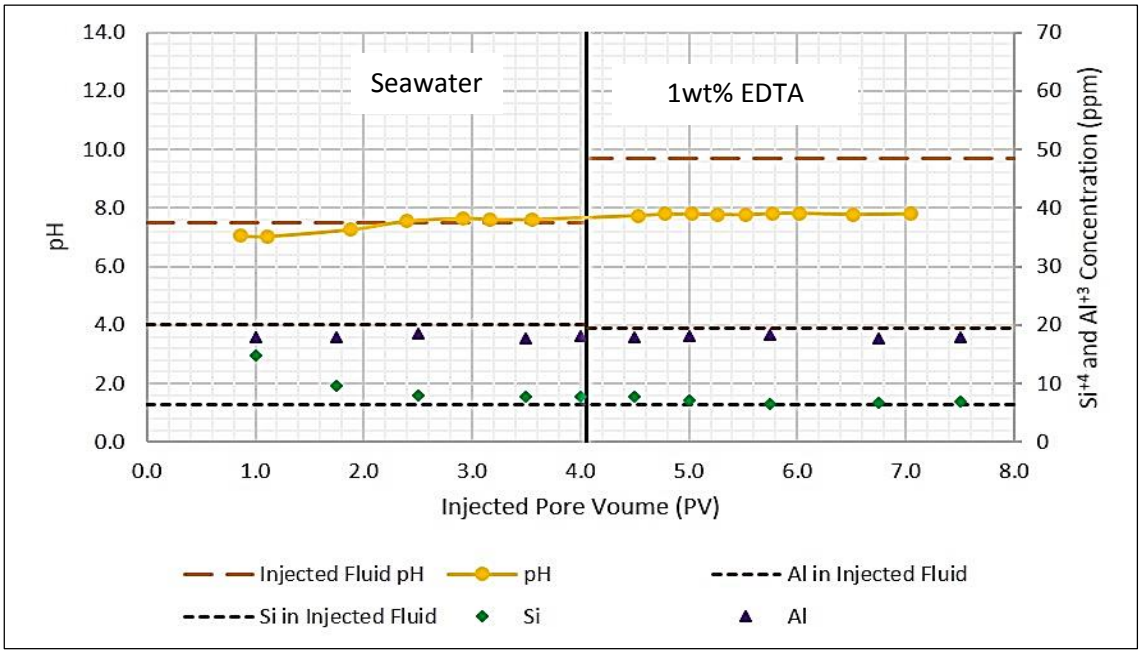

Figure C.38: Si^{+4} and Al^{+3} Concentration in the Produced Effluents from Seawater and 1wt% EDTA Injection into Gray Bandera Sandstone and the pH Recovery, Experiment #4.

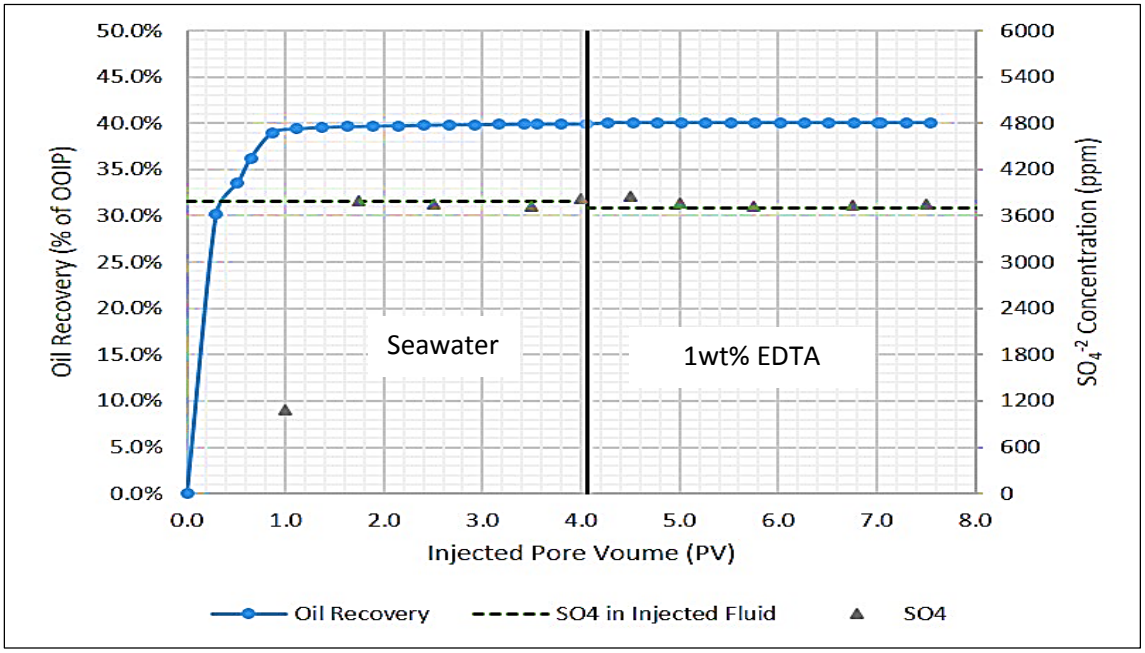

Figure C.39: SO_4^{-2} Concentration in the Produced Effluents from Seawater and 1wt% EDTA Injection into Gray Bandera Sandstone and Oil Recovery, Experiment #4.

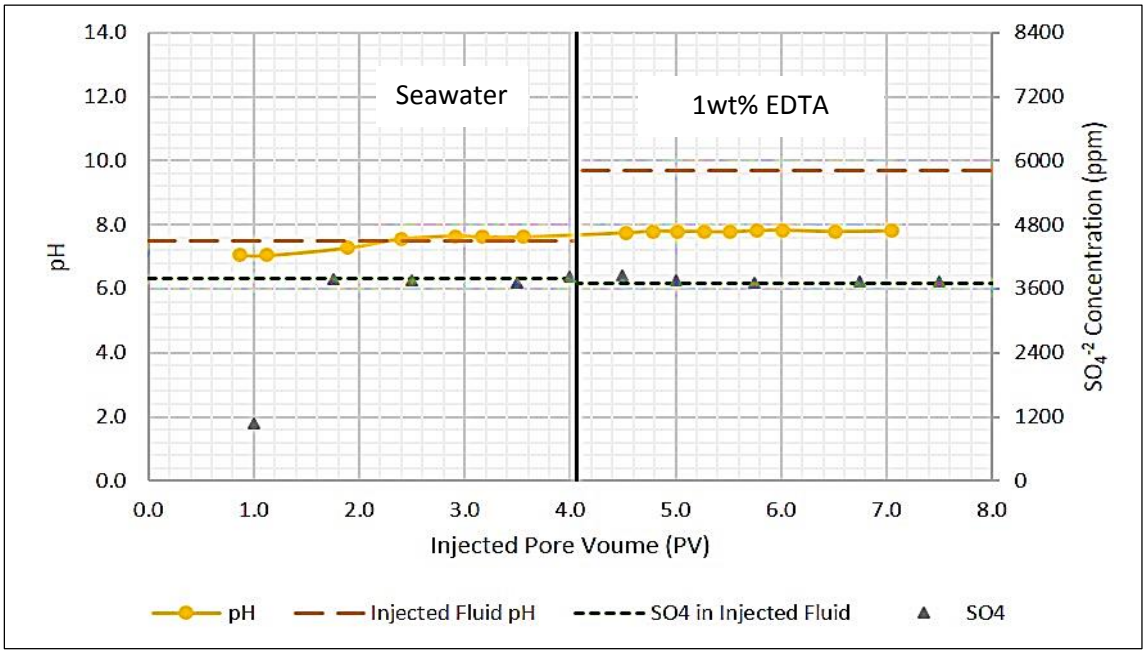

Figure C.40: SO_4^{-2} Concentration in the Produced Effluents from Seawater and 1wt% EDTA Injection into Gray Bandera Sandstone and the pH, Experiment #4.

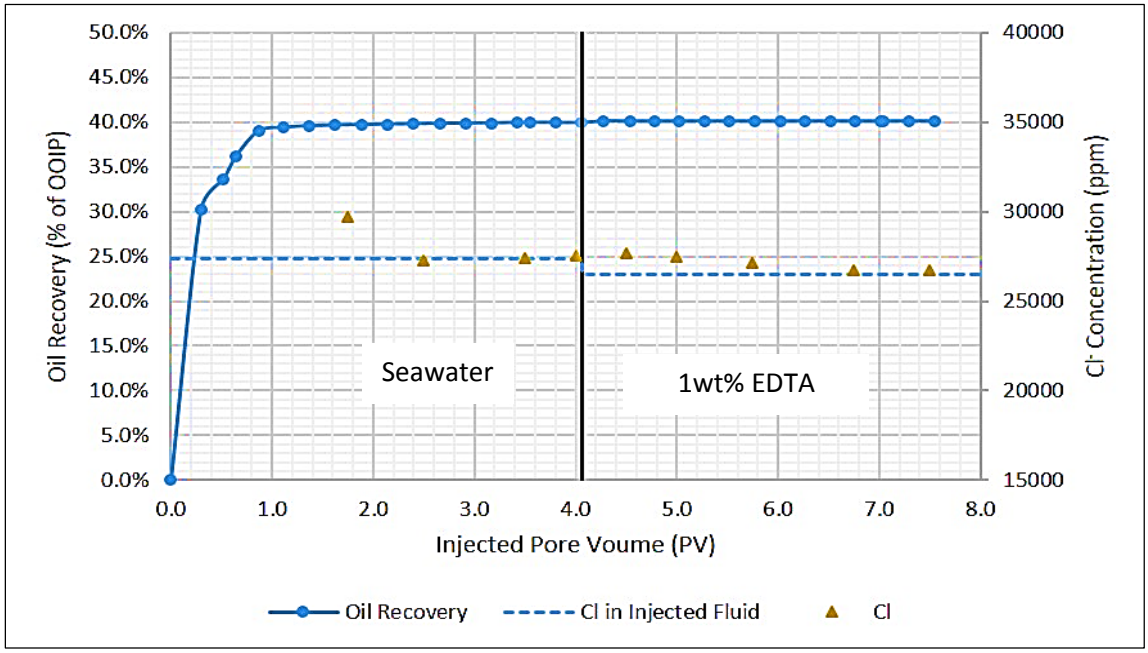

Figure C.41: Cl^- Concentration in the Produced Effluents from Seawater and 1wt% EDTA Injection into Gray Bandera Sandstone and Oil Recovery, Experiment #4.

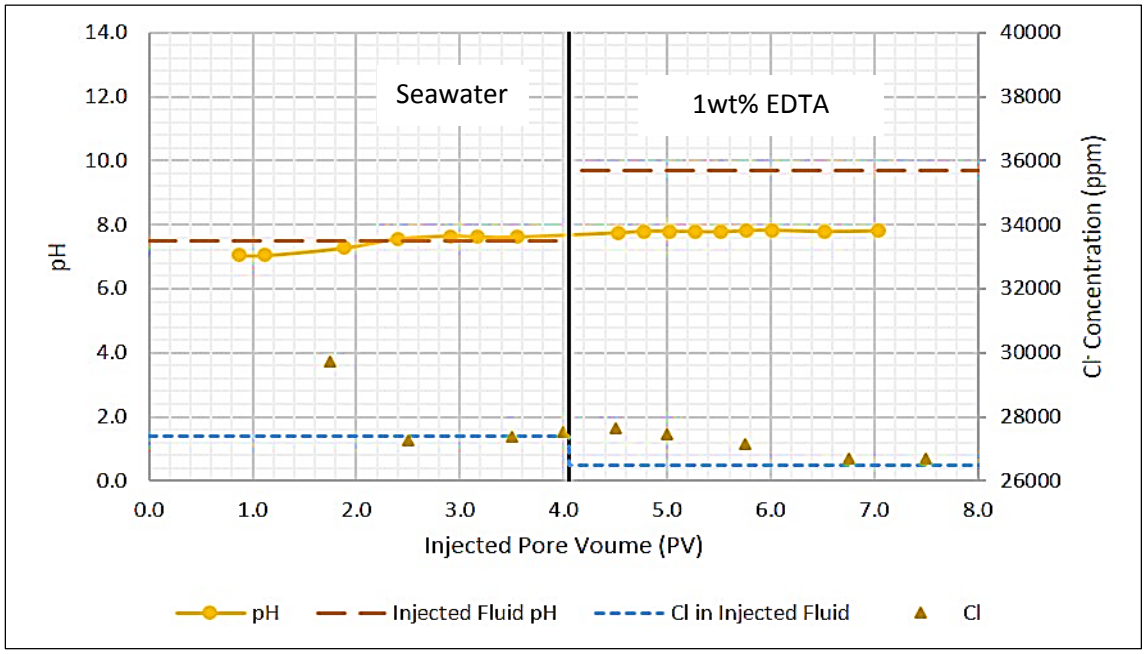

Figure C.42: Cl^- Concentration in the Produced Effluents from Seawater and 1wt% EDTA Injection into Gray Bandera Sandstone and the pH, Experiment #4.

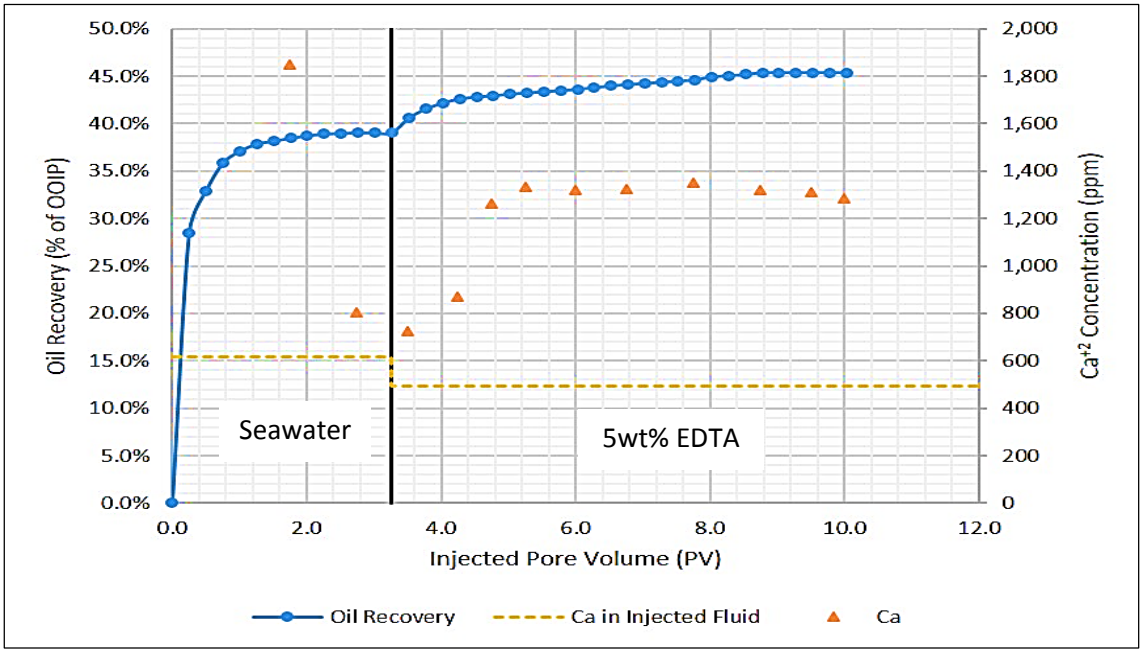

Figure C.43: Ca^{+2} Concentration in the Produced Effluents from Seawater and 5wt% EDTA Injection into Gray Bandera Sandstone and Oil Recovery, Experiment #5.

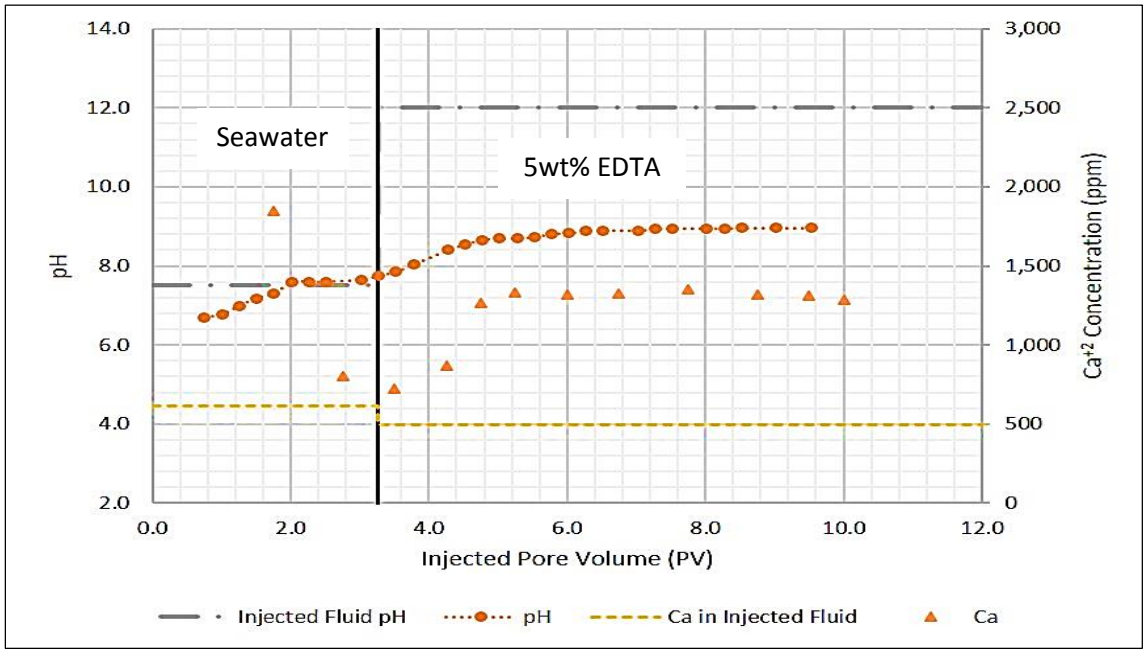

Figure C.44: Ca^{+2} Concentration in the Produced Effluents from Seawater and 5wt% EDTA Injection into Gray Bandera Sandstone and the pH, Experiment #5.

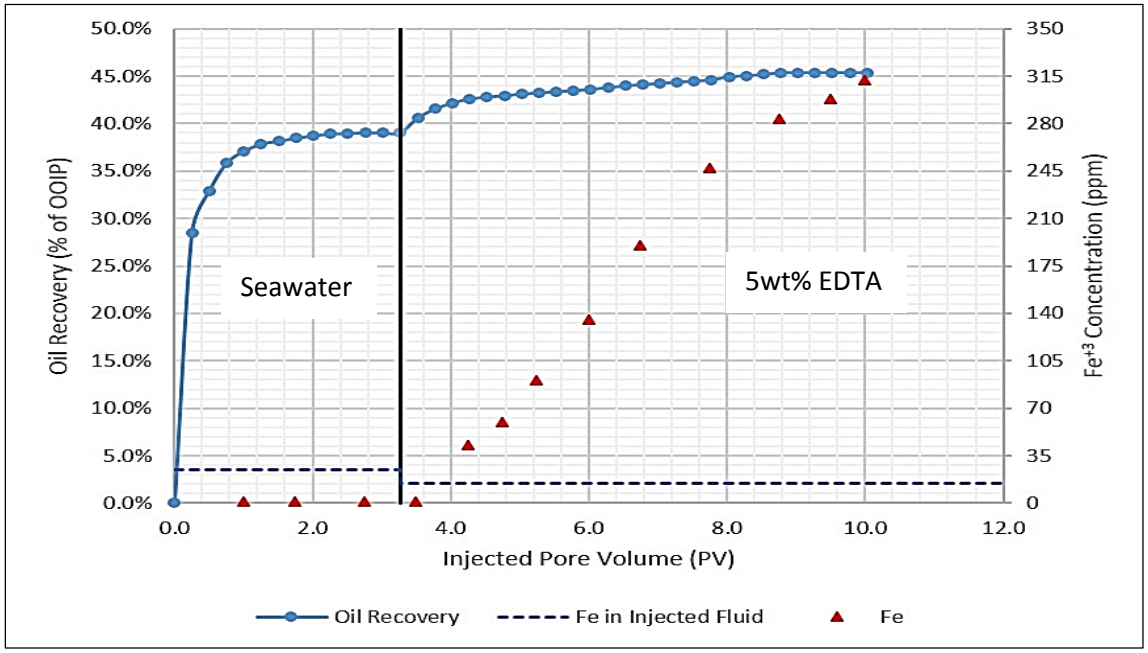

Figure C.45: Fe^{+3} Concentration in the Produced Effluents from Seawater and 5wt% EDTA Injection into Gray Bandera Sandstone and Oil Recovery, Experiment #5.

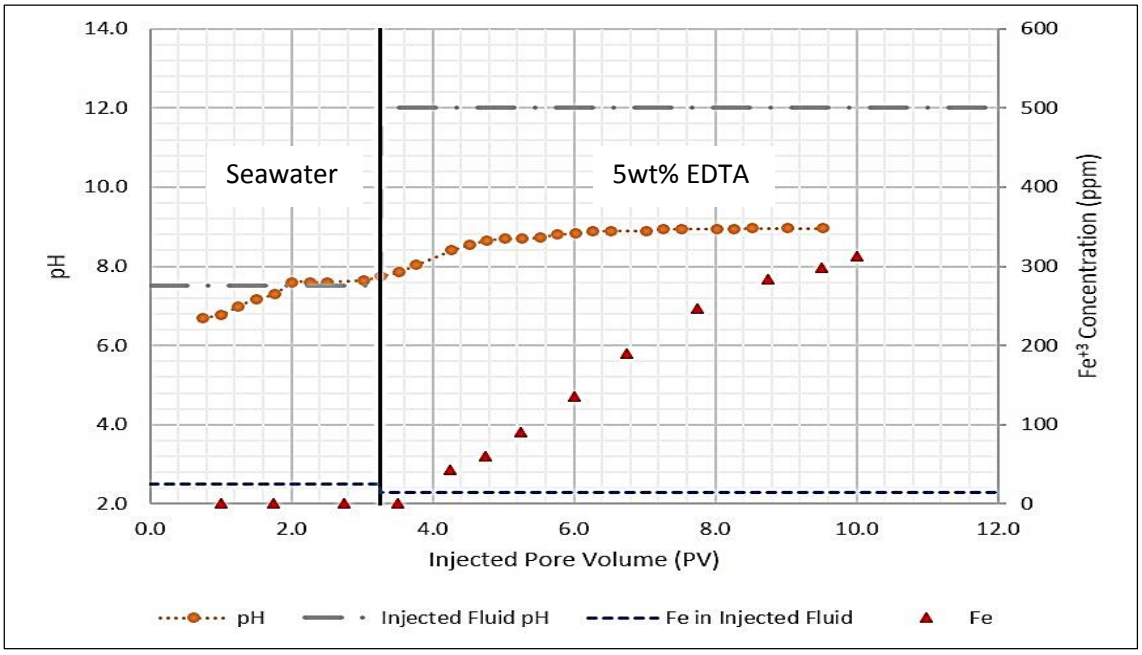

Figure C.46: Fe^{+3} Concentration in the Produced Effluents from Seawater and 5wt% EDTA Injection into Gray Bandera Sandstone and the pH, Experiment #5.

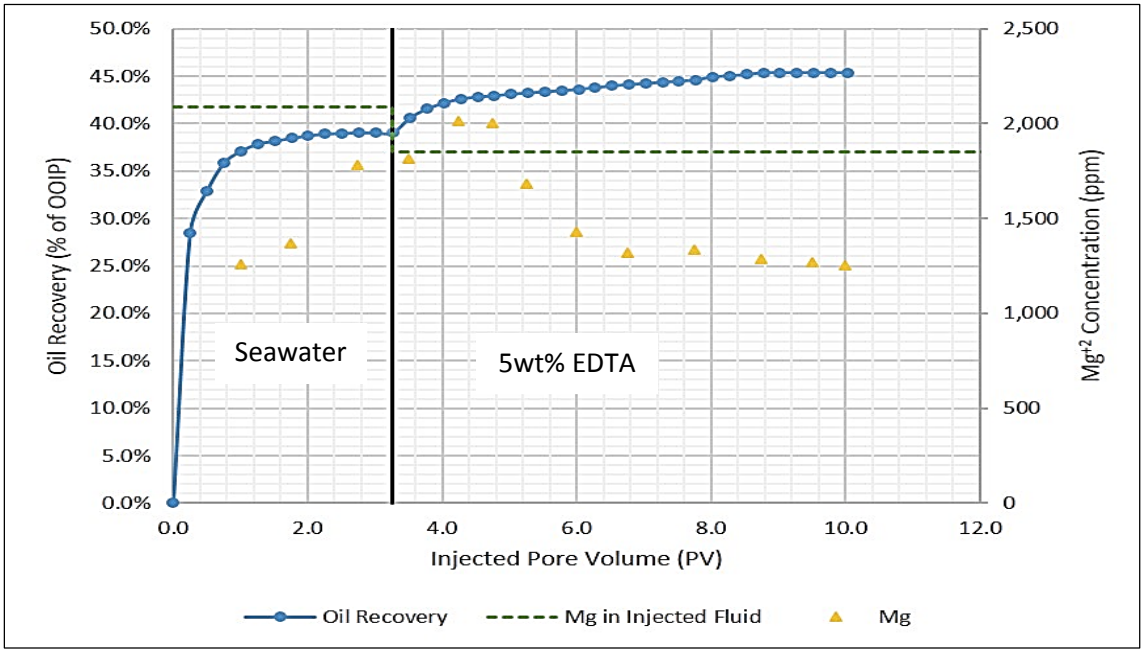

Figure C.47: Mg^{+2} Concentration in the Produced Effluents from Seawater and 5wt% EDTA Injection into Gray Bandera Sandstone and Oil Recovery, Experiment #5.

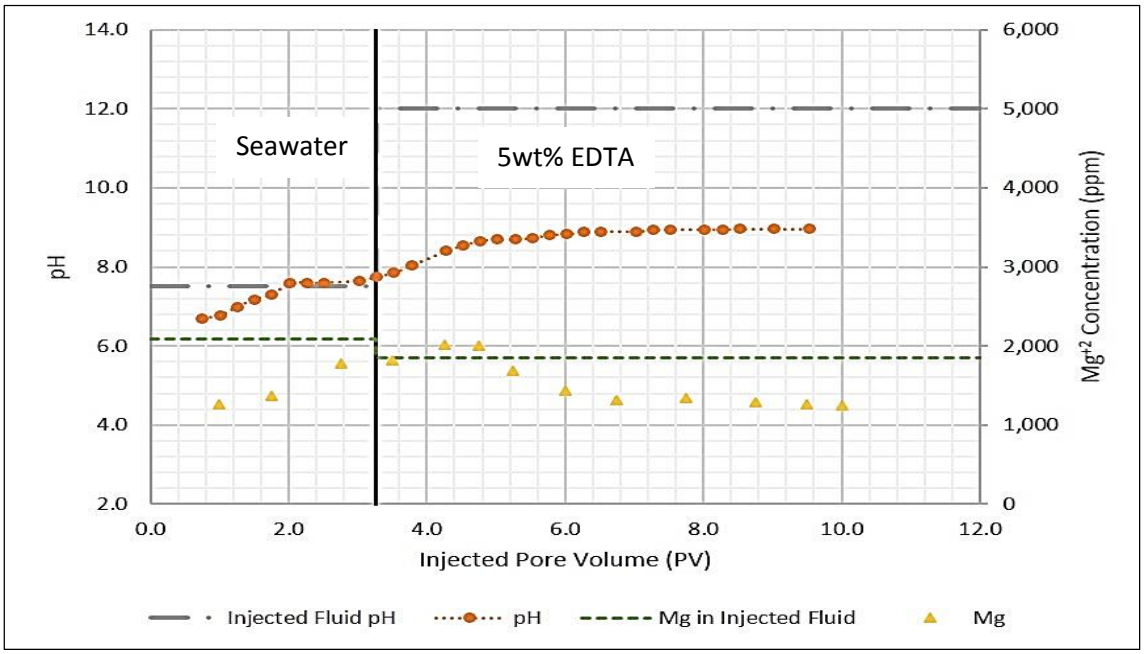

Figure C.48: Mg^{+2} Concentration in the Produced Effluents from Seawater and 5wt% EDTA Injection into Gray Bandera Sandstone and the pH, Experiment #5.

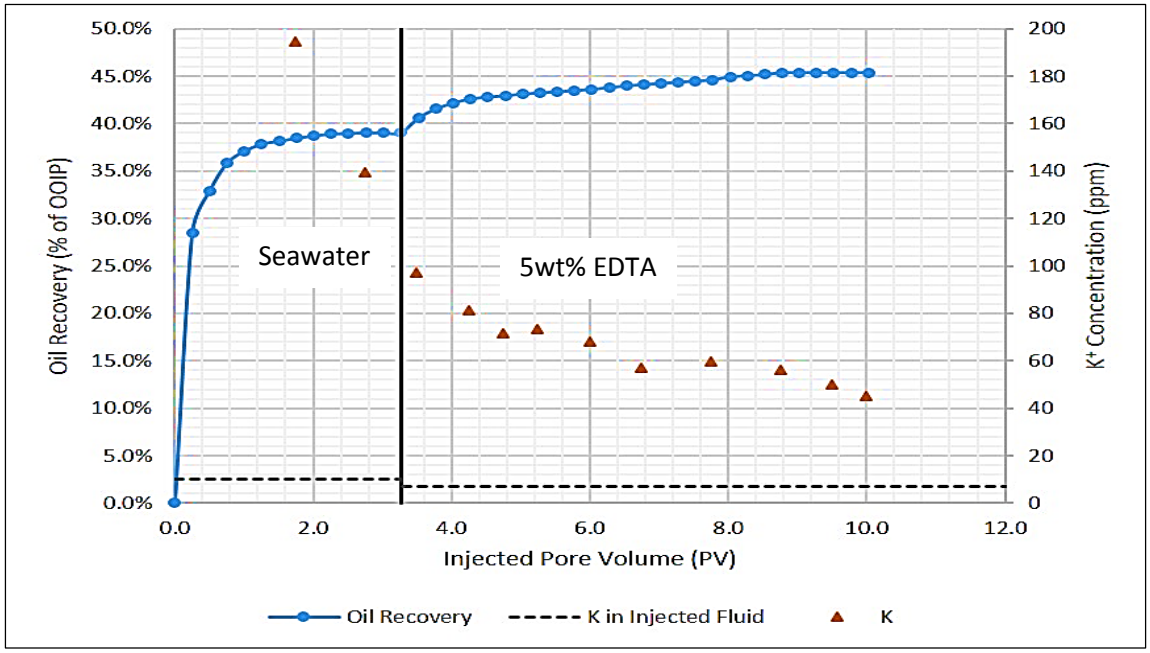

Figure C.49: K^+ Concentration in the Produced Effluents from Seawater and 5wt% EDTA Injection into Gray Bandera Sandstone and Oil Recovery, Experiment #5.

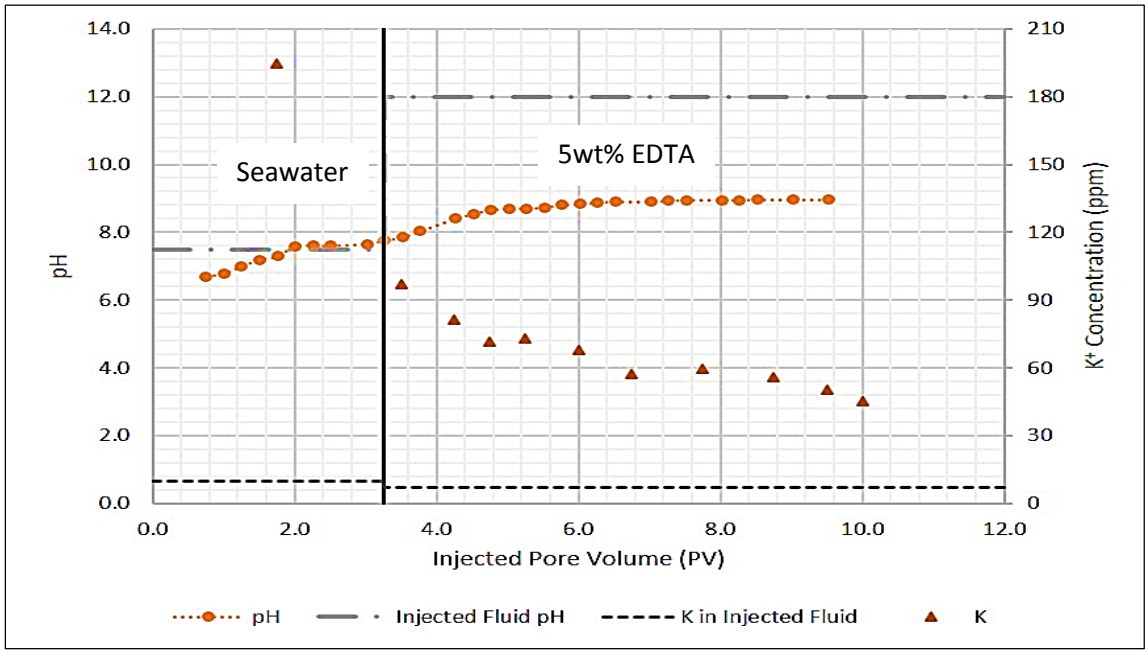

Figure C.50: K^+ Concentration in the Produced Effluents from Seawater and 5wt% EDTA Injection into Gray Bandera Sandstone and the pH, Experiment #5.

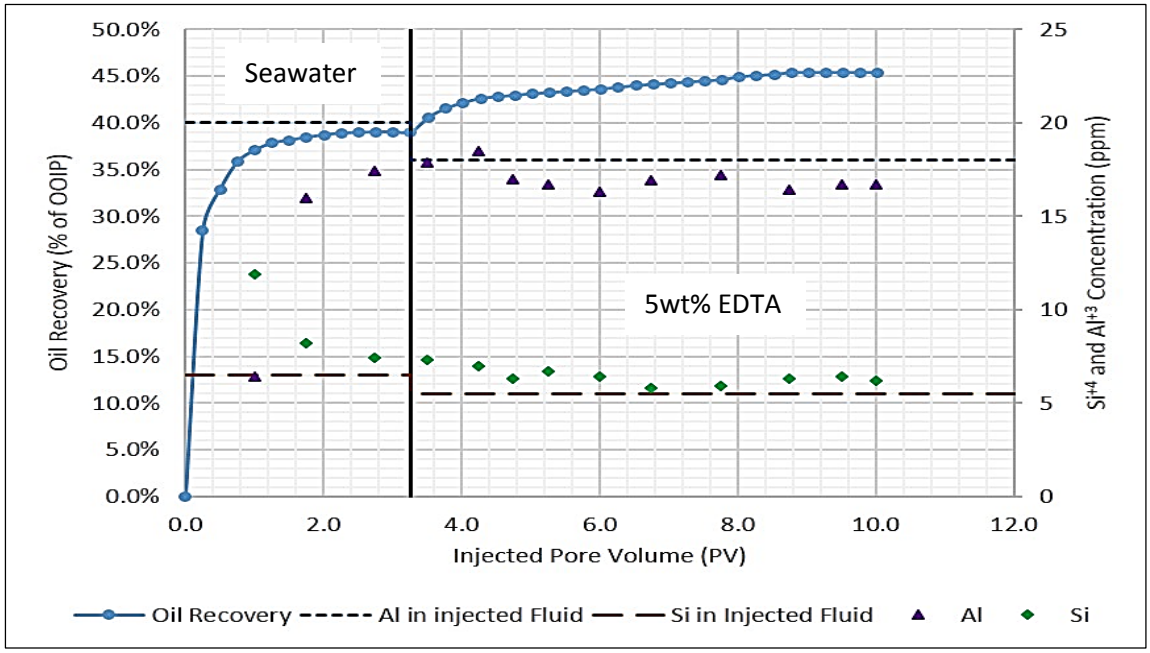

Figure C.51: Si^{+4} and Al^{+3} Concentration in the Produced Effluents from Seawater and 5wt% EDTA Injection into Gray Bandera Sandstone and Oil Recovery, Experiment #5.

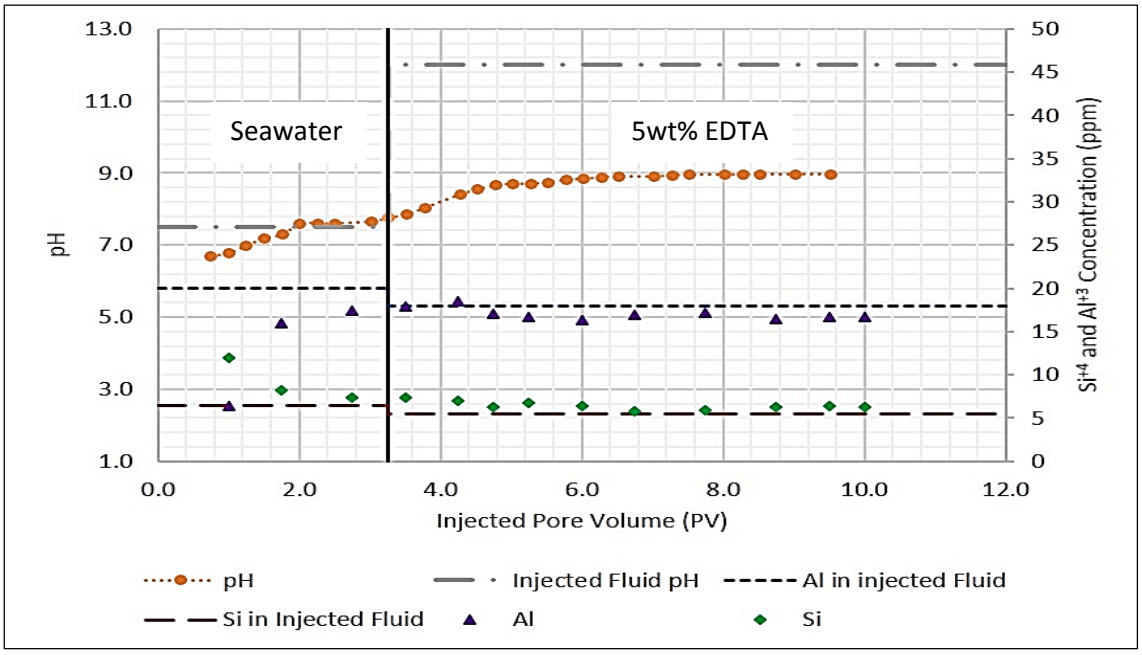

Figure C.52: Si^{+4} and Al^{+3} Concentration in the Produced Effluents from Seawater and 5wt% EDTA Injection into Gray Bandera Sandstone and the pH, Experiment #5.

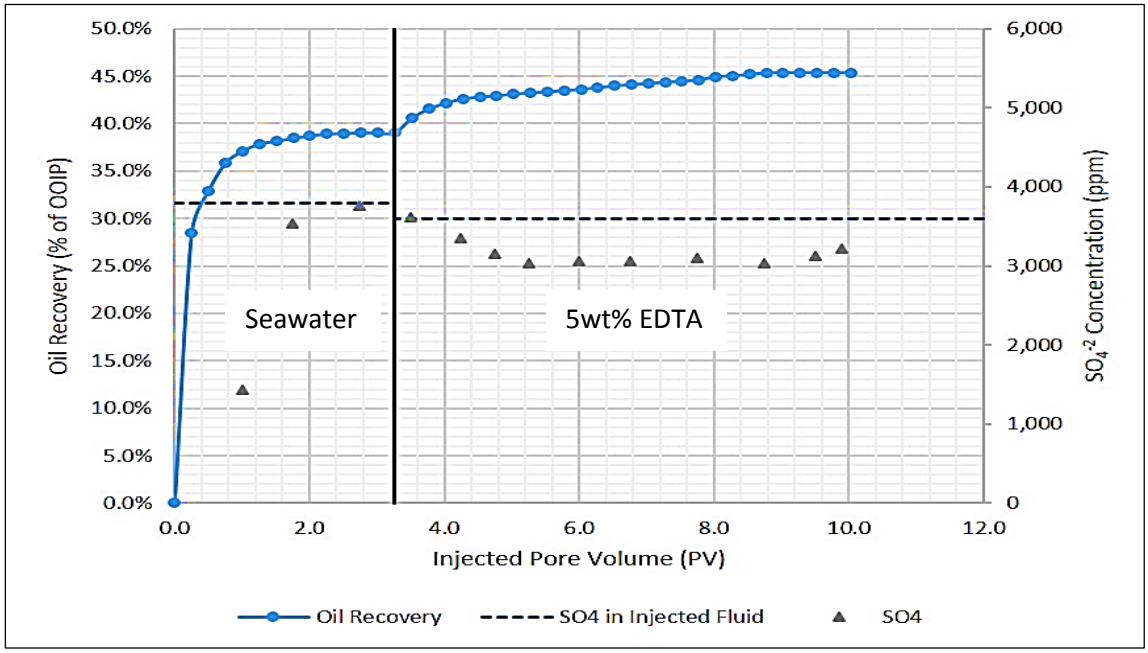

Figure C.53: SO_4^{-2} Concentration in the Produced Effluents from Seawater and 5wt% EDTA Injection into Gray Bandera Sandstone and Oil Recovery, Experiment #5.

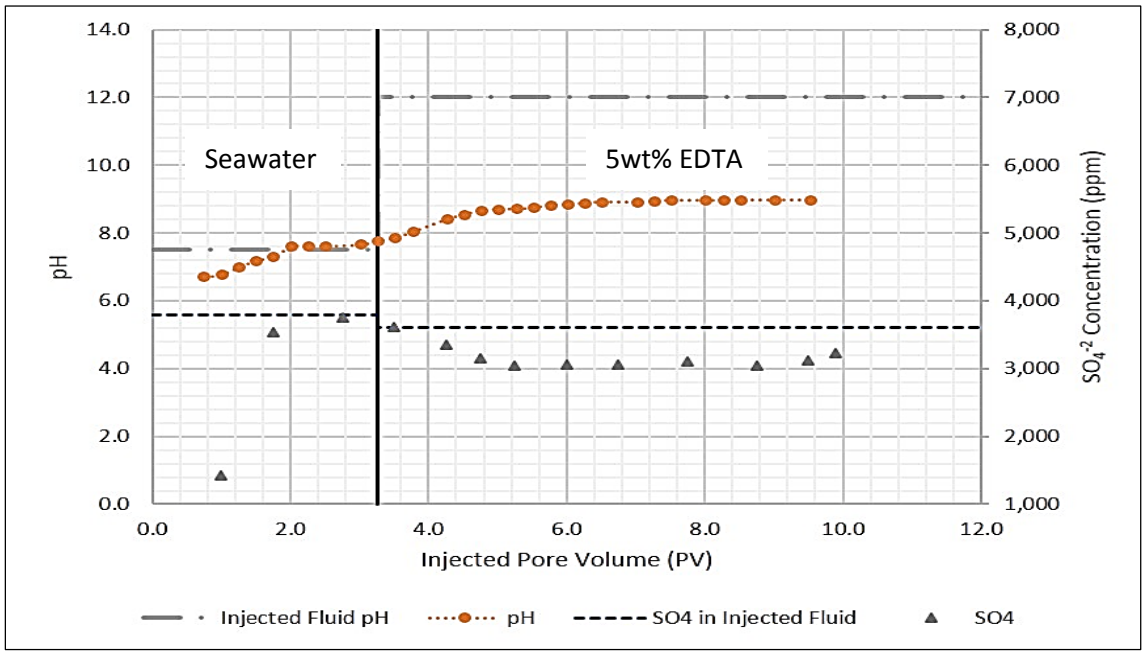

Figure C.54: SO_4^{-2} Concentration in the Produced Effluents from Seawater and 5wt% EDTA Injection into Gray Bandera Sandstone and the pH, Experiment #5.

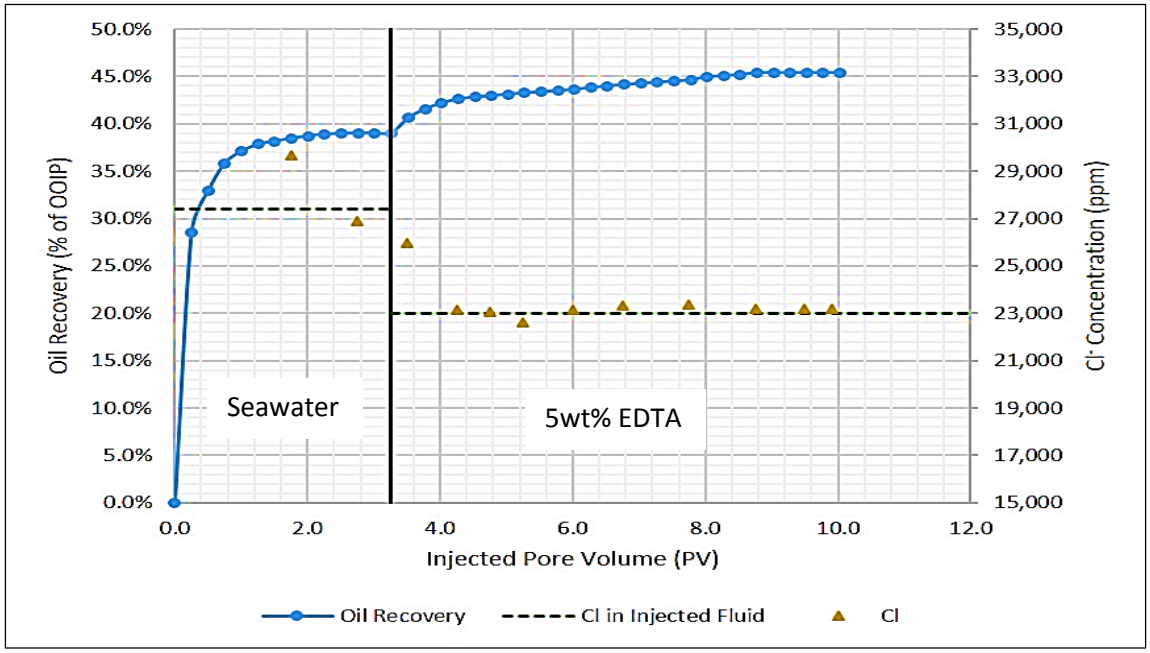

Figure C.55: Cl^- Concentration in the Produced Effluents from Seawater and 5wt% EDTA Injection into Gray Bandera Sandstone and Oil Recovery, Experiment #5.

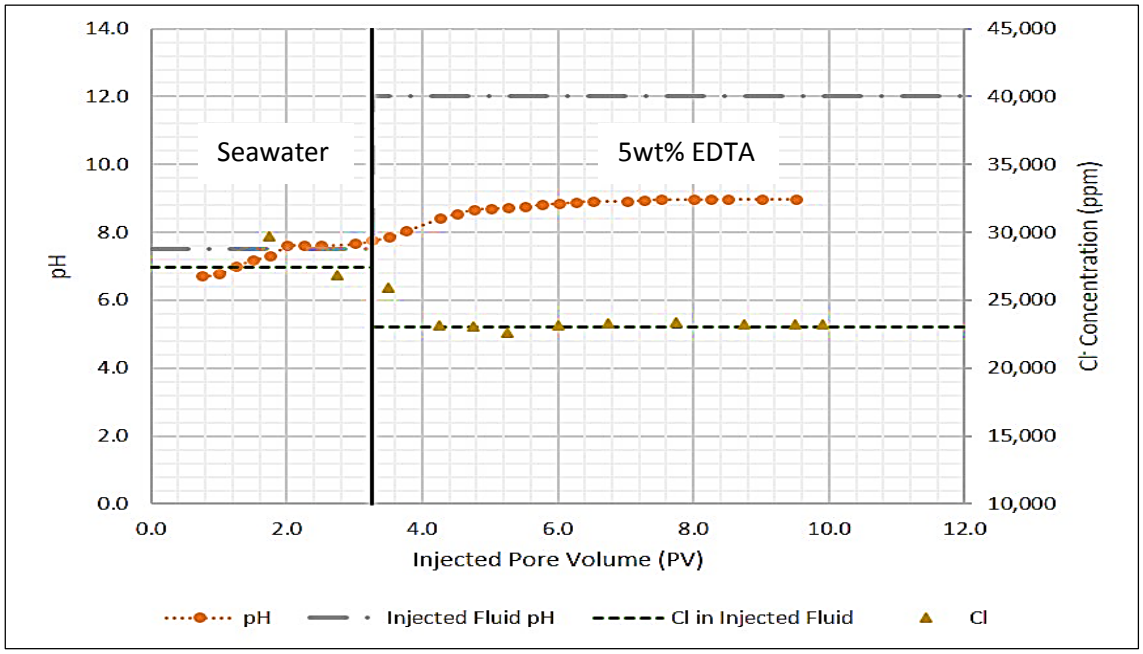

Figure C.56: Cl^- Concentration in the Produced Effluents from Seawater and 5wt% EDTA Injection into Gray Bandera Sandstone and the pH, Experiment #5.

References

[1] Abbasi, Saeed, Abbas Shahrabadi, and Hassan Golghanddashti. 2011. "Experimental Investigation of Clay Minerals' Effects on the Permeability Reduction in Water Injection Process in the Oil Fields." *Paper "SPE 144248" presented at the SPE European Formation Damage Conferenece Hold in Noordwijk, The Netherland*.

[2] Abdallah, W., Buckley, J. S., Edwards, J., Fordham, E., Carnegie, A., Herold, B., Graue, A., Habashy, T., Seleznev, N., Signer, C., Hussain, H., M. Bernard, Ziauddin, Murtaza 2007. "Fundamentals of Wettability." 44–61.

[3] Abdelgawd, K. Z. 2013. "AN INNOVATIVE APPLICATION OF CHELATING AGENTS FOR EOR IN CARBONATE RESERVOIRS.", M.S Thesis, King Fahd University of Petroleum & Minerals, Saudi Arabia.

[4] Aksulu, Hakan, Dagny Hamso, Skule Strand, Tina Puntervold, and Tor Austad. 2012. "Evaluation of Low-Salinity Enhanced Oil Recovery Effects in Sandstone: Effects of the Temperature and pH Gradient." *Energy & Fuels* 26:3497–3503.

[5] Ali, S., Ermel, E., Clarke, J., Fuller, M. J., Xiao, Z., Malone, B., 2005. "Stimulation of High-Temperature Sandstone Formations From West Africa With Chelating Agent-Based Fluids." *"SPE 93805" paper presented at the SPE European Formation Damage Conference, 25-27 May, Sheveningen, The Netherlands*.

[6] Ali, S., Ermel, E., Clarke, J., Fuller, M. J., Xiao, Z., Malone, B., 2008. "Stimulation of High-Temperature Sandstone Formations From West Africa With Chelating Agent-Based Fluids." *SPE 93805 "SPE Production & Operations."*

[7] Alkan, Mahir, Özkan Demirbaş, and Mehmet Doğan. 2005. "Electrokinetic Properties of Kaolinite in Mono- and Multivalent Electrolyte Solutions." *Microporous and Mesoporous Materials* 83(1-3):51–59.

[8] Alotaibi, M. B., and H. A. Naser-El-Din. 2009. "Chemistry of Injection Water and Its Impact on Oil Recovery in Carbonate and Clastic Formations." *paper SPE 121565 Presented at the 2009 SPE International Symposium on Oilfield Chemistry Held in the Woodlands, Texas, USA, 20-22 April 2009*.

[9] Alotaibi, M. B., R. A. Nasralla, and H. A. Naser-El-Din. 2011. "Wettability Studies Using Low-Salinity Water in Sandstone Reservoirs." *Paper SPE 149942 Presented at the Offshore Technology Conference, Houston, USA, 3-6 May*.

[10] Anderson, William G. 1986. "Wettability Literature Survey — Part 1 : Rock/Oil/Brine Interactions and the Effects of Core Handling on Wettabiiity." *SPE 13932 (Journal of Petroleum Technology)*.

[11] Attia, M. 2013. “A New EOR Method for Sandstone Reservoirs Using High pH Chelating Agents.”, M.S Thesis,King Fahd University of Petroleum & Minerals, Saudi Arabia.

[12] Attia, M., M. A. Mahmoud, H. S. Al-Hashim, and A. S. Sultan. 2014. “Shifting to a New EOR Area for Sandstone Reservoirs with High Recovery , No Damage , and Low Cost.” *paper SPE-169670 presented at the SPE Enhanced Oil Recovery Conference at Oil and Gas West Asia, 31 March-2 April, Muscat, Oman*.

[13] Austad, Tor, Alireza Rezaeidoust, and Tina Puntervold. 2010. “Chemical Mechanism of Low Salinity Water Flooding in Sandstone Reservoirs.” *SPE 129767 Presented at the 2010 SPE Improved Oil Recovery Symposium held in Tulsa, Oklahoma, USA, 24-28 April 2010*.

[14] Bernard, George G. 1967. “Effect Of Floodwater Salinity on Recovery of Oil from Cores Containing Clays.” *paper SPE 1725 presented at the 38th Annual California Regional Meeting of the Society of Petroleum Engineers AIME, Oct 26-27.*

[15] Brady, Patrick V., James L. Krumhansl, and Paul E. Mariner. 2012. “Surface Complexation Modeling for Improved Oil Recovery.” in *Paper SPE 153744 Presented at the Eighteenth SPE Improved Oil Recovery Symposium held in Tulsa, Oklahoma, USA, 14-18 April 2012*.

[16] Cissokho, M., S. Boussour, P. Cordier, H. Bertin, and G. Hamon. 2010. “Low Salinity Oil Recovery on Clayey Sandstone : Experimental Study.” *PETROPHYSICS* 51(5):305–13.

[17] Craig, Forrest F. 1971. *The Reservoir Engineering Aspects of Waterflooding*. Second Edi. Society of Petroleum Engineers of AIME.

[18] Dubey, S. T., and P. H. Doe. 1993. “Base Number and Wetting Properties of Crude Oils.” *SPE Reservoir Engineering* (August):195–200.

[19] Fogden, Andrew. 2012. “Removal of Crude Oil from Kaolinite by Water Flushing at Varying Salinity and pH.” *Colloids and Surfaces A: Physicochemical and Engineering Aspects* 402:13–23.

[20] Fredd, C. N., and H. S. Foglar. 1997. “Chelating Agents as Effective Matrix Stimulation Fluids for Carbonate Formations.” *paper SPE37212 presented at the International Symposium on Oilfield Chemistry Houston, Texas, February 18-21*.

[21] Green, Don W., and G. Paul Willhite. 1998. *Enhanced Oil Recovery*.

[22] Hematfar, Vahid, Brij B. Maini, and Zhangxin John Chen. 2013. “Influence of Clay Minerals and Water Film Properties on In-Situ Adsorption of Asphaltene.” *SPE Heavy Oil Conference - Canada, 2013* 1–7.

[23] Hirasaki, G. J. 1991. "Wettability : Fundamentals and Surface Forces." *paper SPE 17367, SPE Formation Evaluation Journal* (June 1991).

[24] Kassim, Moshood Oluwaseun. 2012. "The Role of Potential Determining Ions in Carbonate Rock - Seawater Interactions.", M.S. Thesis, King Fahd University of Petroleum & Minerals, Saudi Arabia.

[25] Lager, A., K. J. Webb, C. J. J. Black, M. Singleton, and K. S. Sorbie. 2006. "Low Salinity Oil Recovery - an Experimental Investigation." *Paper SCA2006-36 presented at the International Symposium of the Society of Core Analysis held in Trondheim, Norway 12-16 September,*.

[26] Lager, A., K. J. Webb, R. I. Collins, and D. M. Richmond. 2008. "LoSal Enhanced Oil Recovery : Evidence of Enhanced Oil Recovery at the Reservoir Scale." *Paper SPE 113976 Presented at the 2008 SPE/DOE Improved Oil Recovery Symposium held in Tulsa, Oklahoma, U.S.A., 19-23 April*.

[27] Lebedeva, Evgenia V., and Andrew Fogden. 2011. "Wettability Alteration of Kaolinite Exposed to Crude Oil in Salt Solutions." *Colloids and Surfaces A: Physicochemical and Engineering Aspects* 377(1-3):115–22.

[28] Loahardjo, Nina, Xina Xie, Peigui Yin, and Norman R. Morrow. 2007. "Low Salinity Waterflooding of a Reservoir." *Papaer SCA2007-29 presented at the International Symposium of the Scoiety of Core Analysts*.

[29] Mahmoud, M. A., H. A. Naser-El-Din, and C. A. De Wolf. 2011a. "Novel Environmentally Friendly Fluids to Remove Carbonate Minerals from Deep Sandstone Formations." *Paper SPE 143301 Presented at SPE European Formation Damage Conference, 7-10 June, Noordwijk, The Netherlands*.

[30] Mahmoud, M. A., H. A. Naser-El-Din, and C. A. De Wolf. 2011b. "Removing Formation Damage and Stimulation of Deep Illitic-Sandstone Reservoirs Using Green Fluids." *Paper SPE 147395 Presented at the SPE Annual Technical Conference and Exhibition, 30 October-2 November, Denver, Colorado, USA*.

[31] Mahmoud, M. A., H. A. Naser-El-Din, C. A. De Wolf, J. N. Lepage, and J. H. Bemelaar. 2010. "Evaluation of a New Environmentally Friendly Chelating Agent for High-Temperature Applications." *Paper SPE 127923 Presented at the SPE International Symposium and Exhibiton on Formation Damage Control, 10-12 February, Lafayette, Louisiana, USA*.

[32] Martin, Alden J., Stephen T. Solomon, and Dan J. Hartmann. 1997. "Characterization of Petrophysical Flow Units in Carbonate Reservoirs." *AAPG Bulletin* 81(5):734–59.

[33] McGuire, P. L., J. R. Chatham, F. K. Paskvan, D. M. Sommer, and F. H. Carini. 2005. "Low Salinity Oil Recovery : An Exciting New EOR Opportunity for Alaska's North Slope." *Paper SPE 93903 Presented at the SPE Western Regional Meeting, 30 March-1 April, Irvine, California*.

[34] Moore, Duane M., and Robert C. Reynolds. 1986. *X-Ray Diffraction and the Identification and Analysis of Clay Minerals*. First Edition.

[35] Moore, Duane M., and Robert C. Reynolds. 1997. *X-Ray Diffraction and the Identification and Analysis of Clay Minerals*. Second Edition.

[36] Morrow, Norman R., Guo Qing Tang, Marc Valat, and Xina Xie. 1998. "Prospects of Improved Oil Recovery Related to Wettability and Brine Composition." *Journal of Petroleum Science and Engineering* 20(3):267–76.

[37] Nasralla, Ramez A., Mohammed A. Bataweel, and Hisham A. Nasr-el-din. 2011. "Investigation of Wettability Alteration by Low Salinity Water in Sandstone Rock." *Paper SPE 146322 Presented at the SPE Offshore Europe Oil and Gas Conference and Exhibition held in Aberdeen, UK, 6-8 September*.

[38] Nasralla, Ramez A., and Hisham A. Nasr-El-Din. 2011. "Impact of Electrical Surface Charges and Cation Exchange on Oil Recovery by Low Salinity Water." *Paper SPE 147937 Presented at the SPE Asia Pacific Oil and Gas Conference and Exhibition held in Jakarta, Indonisia, 20-22 September*.

[39] Nasralla, Ramez A., and Hisham A. Nasr-El-Din. 2012. "Double-Layer Expansion : Is It A Primary Mechanism of Improved Oil Recovery by Low-Salinity Waterflooding ?" *Paper SPE 154334 Presented at the Eighteenth SPE Improved Oil Recovery Symposium held in Tulsa, Oklahoma, USA, 14-18 April*.

[40] Nasr-El-Din, H. A., H. Dana, V. Tomos, T. Stanitzek, and C. A. De Wolf. 2014. "Field Treatment to Stimulate an Oil Well in an Offshore Sandstone Reservoir Using a Novel , Low Corrosive , Environmentally Friendly Fluid." *Paper SPE 168163 Presented at the SPE International Symposium and Exhibition on Formation Damage Control, 26-28 February, Lafayette, Louisiana, USA*.

[41] Neasham, JohnW. 1977. "The Morphology of Dispersed Clay in Sandstone Reservoirs and Its Effect on Sandstone Shaliness, Pore Space and Fluid Flow Properties." *SPE 6858*.

[42] Rezaeidoust, Alireza, Tina Puntervold, and Tor Austad. 2010. "A Discussion of the Low Salinity EOR Potential for a North Sea Sandstone Field." *Paper SPE 134459 Presented at the SPE Annual Techincal Conference and Exibition held in Florence, Italy, 19-22 September*.

[43] Rezaeidoust, Alireza, Tina Puntervold, and Tor Austad. 2011. "Chemical Verification of the EOR Mechanism by Using Low Saline/Smart Water in Sandstone." *Energy & Fuels* 25:2151–62.

[44] Shaughnessy, C. M., and W. E. Kline. 1983. "EDTA Removes Fomation Damage at Prudhoe Bay." *Paper SPE-11188-PA, Journal of Petroleum Technology* 1783–91.

[45] Shaw, Jerry C., Peter L. Churcher, and Blaine F. Hawkins. 1991. "The Effect of Firing on Berea Sandstone." *SPE Formation Evaluation* 72–78.

[46] Shehata, Ahmed M., and Hisham A. Nasr-el-din. 2014. "Role of Sandstone Mineral Compositions and Rock Quality on the Performance of Low-Salinity Waterflooding." 1–24.

[47] Strand, Skule, Eli J. Høgnesen, and Tor Austad. 2006. "Wettability Alteration of Carbonates - Effects of Potential Determining Ions (Ca2+ and SO42-) and Temperature." *Colloids and Surfaces A: Physicochemical and Engineering Aspects* 275:1–10.

[48] Szilágyi, Petra Ágota. 2007. "Study of Iron-Chelates in Solid State and Aqueous Solutions Using Mössbauer Spectroscopy." *Doctorate Thesis, Submitted for the degree of PhD*.

[49] Tang, G. Q., and N. R. Morrow. 1997. "Salinity, Temperature, Oil Composition, and Oil Recovery by Waterflooding." *SPE Reservoir Engineering* 12(November):269–76.

[50] Tang, Guo-Qing, and Norman R. Morrow. 1999. "Influence of Brine Composition and Fines Migration on Crude Oil/brine/rock Interactions and Oil Recovery." *Journal of Petroleum Science and Engineering* 24(2-4):99–111.

[51] Willhite, G. Paul. 1986. *Waterflooding*. Society of Petroleum Engineers.

[52] De Wolf, C. A., Bang, E., Bouwman, A., Braun, W., De Oliveira, E., and Nasr-El-Din, H.,. 2014. "Evaluation of Environmentally Friendly Chelating Agents for Applications in the Oil and Gas Industry." *Paper SPE 168145 presented at the SPE International Symposium and Exhibition on Formation Damage Control, 26-28 February, Lafayette, Louisiana, USA*.

Vitae

Name : Ahmed Abdulhamid Ahmed Mahmoud

Nationality : Sudanese

Date of Birth : March 16, 1989

Email : ahmed_petra06@hotmail.com,

eng.ahmedmahmoud@rocketmail.com

Address : Alfyhaa Area-Umbadda-Omdurman-Sudan

Academic Background : B.S. in Petroleum Engineering, (2011)

Department of Petroleum and Natural Gas Engineering

Faculty of Engineering

University of Khartoum

Khartoum, Sudan

: M.S. in Petroleum Engineering, expected in May 2015

Department of Petroleum Engineering

College of Engineering

KFUPM

Dhahran, Saudi Arabia